Steel Bridge Design Handbook

APPENDIX

Design Example 5: Three-Span Continuous Horizontally Curved Composite Steel Tub-Girder Bridge

February 2022

Smarter.
Stronger.
Steel.

by

American Institute of Steel Construction

Printed in the United States of America

Foreword

The Steel Bridge Design Handbook covers a full range of topics and design examples to provide bridge engineers with the information needed to make knowledgeable decisions regarding the selection, design, fabrication, and construction of steel bridges. The Handbook has a long history, dating back to the 1970s in various forms and publications. The more recent editions of the Handbook were developed and maintained by the Federal Highway Administration (FHWA) Office of Bridges and Structures as FHWA Report No. FHWA-IF-12-052 published in November 2012, and FHWA Report No. FHWA-HIF-16-002 published in December 2015. The previous development and maintenance of the Handbook by the FHWA, their consultants, and their technical reviewers is gratefully appreciated and acknowledged.

This current edition of the Handbook is maintained by the National Steel Bridge Alliance (NSBA), a division of the American Institute of Steel Construction (AISC). This Handbook, published in 2021, has been updated and revised to be consistent with the 9th edition of the AASHTO LRFD Bridge Design Specifications which was released in 2020. The updates and revisions to various chapters and design examples have been performed, as noted, by HDR, M.A. Grubb & Associates, Don White, Ph.D., and NSBA. Furthermore, the updates and revisions have been reviewed independently by Francesco Russo, Ph.D., P.E., Brandon Chavel, Ph.D., P.E., and NSBA.

The Handbook consists of 19 chapters and 6 design examples. The chapters and design examples of the Handbook are published separately for ease of use, and available for free download at the NSBA website, www.aisc.org/nsba.

The users of the Steel Bridge Design Handbook are encouraged to submit ideas and suggestions for enhancements that can be implemented in future editions to the NSBA and AISC at solutions@aisc.org.

TECHNICAL REPORT DOCUMENTATION PAGE

1. Title and Subtitle Steel Bridge Design Handbook, Appendix Design Example 5: Three-Span Continuous Horizontally Curved Composite Steel Tub-Girder Bridge	**2. Report Date** February 2022
3. Original Author(s) Brandon Chavel, Ph.D., P.E. (HDR) and Julie Rivera, P.E. (HDR)	**4. Revision Author(s)** Michael A. Grubb, P.E (M.A. Grubb & Associates, LLC)
5. Sponsoring Agency Name and Address National Steel Bridge Alliance, a division of the American Institute of Steel Construction 130 E. Randolph, Suite 2000 Chicago, IL 60601	**6. Revision Performing Organization Name and Address** HDR, Inc. 301 Grant Street, Suite 1700 Pittsburgh, PA 15219
7. Supplementary Notes The previous edition of this Handbook was published as FHWA-HIF-16-002 and was developed to be current with the 7th edition of the AASHTO LRFD Bridge Design Specifications. This edition of the Handbook was updated to be current with the 9th edition of the AASHTO LRFD Bridge Design Specifications, released in 2020.	
8. Abstract Tub girders, as closed-section structures, provide a more efficient cross-section for resisting torsion than I-girders, which is especially important in horizontally curved highway bridges. The increased torsional resistance of a closed composite steel tub girder also results in an improved lateral distribution of live loads. For curved bridges, warping, or flange lateral bending stresses, are lower in tub girders when compared to I-girders, since tub girders carry torsion primarily by means of St. Venant torsional shear flow around the perimeter of the closed section, whereas I-girders have low St. Venant torsional stiffness and carry torsion primarily by means of warping. This design example illustrates the design calculations for a curved steel tub girder bridge with a span arrangement of 160.0 ft – 210.0 ft – 160.0 ft, considering the strength, service, fatigue and constructability limit states in accordance with the AASHTO LRFD Bridge Design specifications. This example illustrates the flexural design of a section in positive flexure, the flexural design of a section in negative flexure, the shear design of the web, computation of distortional stresses, the design of a bottom flange longitudinal stiffener, a bolted field splice design, an internal pier diaphragm design, the bearing stiffener design at an interior pier, and a top flange lateral bracing member design.	
9. Keywords Steel Tub Girder Bridge, Steel Box Girder Bridge, LRFD, Bolted Field Splice, Top Flange Lateral Bracing, Box Girder Distortional Stresses	**10. AISC Publication No.** B956-22

Steel Bridge Design Handbook
Design Example 5: Three-Span Continuous Curved Composite Tub-Girder Bridge

Table of Contents

LIST OF FIGURES

LIST OF TABLES

1.0 INTRODUCTION

Steel boxes may either be tub sections or closed-box sections, with either inclined or vertical webs. Most composite box girders built in the U.S. are tub girders having a solid bottom flange, two solid webs, and an open top with two separate top flanges on each web connected with top lateral bracing to form a pseudo-box to resist the torsion prior to hardening of the concrete deck. Narrow noncomposite closed steel boxes are often employed as straddle beams to provide support and necessary underclearance.

Tub girders are sometimes selected over I-girders where aesthetic considerations are a significant factor because of their pleasing appearance offering a smooth, uninterrupted, cross section. Bracing, web stiffeners, utilities, and other structural and nonstructural components are typically hidden from view within the steel tub girder, leading to a clean, uncluttered appearance. Additionally, steel tub girder bridges offer some distinct advantages over other superstructure types in terms of span range, stiffness, durability and future maintenance.

Steel tub girders can potentially be more economical than steel plate I-girders in long-span applications due to the increased bending strength offered by their wide bottom flanges, and because they require less field work due to the handling of fewer pieces. Steel tub girders can also be suitable in short span ranges as well, especially when aesthetic preferences or constructability considerations preclude the use of other structure types. However, tub girders should be no less than 5 feet deep to allow access for inspection, thus limiting the efficiency of conventional steel tub girders in short-span applications.

Tub girders, as closed-section structures, provide a more efficient cross section for resisting torsion than I-girders. The increased torsional resistance of a closed composite steel tub girder also results in an improved lateral distribution of live loads. Tub girders offer some distinct advantages over I-girders for horizontally curved bridges since the torsional stiffness of a tub girder is much larger than the torsional stiffness of an I-girder. The high torsional resistance of individual tub-girder sections permits the tub girder to carry more of the load applied to it rather than shifting the load to the adjacent tub girder with greater radius, as is the case for torsionally weaker I-girders. The tendency to share gravity loads more uniformly reduces the relatively large deflection of the girder on the outside of the curve. Also less material needs to be added to tub girders to resist the torsional effects. Torsion in tub sections is resisted mainly by St. Venant torsional shear flow, rather than by warping torsion (which is the primary torsional response mechanism in I-shaped girders). Thus, warping shear and normal stresses due to warping torsion are typically quite small and Article C6.11.1.1 recommends that these stresses be neglected.. However, warping associated with distortion of the cross-section should be considered when evaluating the fatigue performance of tub girders in certain cases, as discussed further in Section 7.9.1 of this design example.

The exterior surfaces of tub girders are less susceptible to corrosion since there are fewer details for debris to accumulate, in comparison to an I-girder structure. For tub girders, stiffeners and most diaphragms are located within the tub girder and are protected from the environment. Additionally, the interior surface of the tub girder is protected from the environment, further reducing the likelihood of deterioration. Tub girder bridges tend to be easier to inspect and maintain since much of the inspection can occur from inside the tub girder, with the tub serving as a protected walkway.

Erection costs for tub girders may be lower than that of I-girders because the erection of a single tub girder, in a single lift, is equivalent to the placement and connection of two I-girders. However, a single tub girder will typically require the use of a larger crane than an I-girder of the same length. Tub girders are also inherently more stable during erection, due to the presence of lateral bracing between the top flanges. Overall, the erection of a tub girder bridge may be completed in less time than that of an I-girder counterpart because there are fewer pieces to erect, a fewer number of external cross-frames or diaphragms to be placed in the field, and subsequently fewer field connections to be made. This is a significant factor to consider when available time for bridge erection is limited by schedule or site access.

In many instances, these advantages are not well reflected in engineering cost estimates based solely on material quantity comparisons. Consequently, tub girder bridges have historically been considered more economical than I-girder bridges only if their use resulted in a reduction in the total number of webs in cross section, particularly for straight bridges. However, if regional fabricators have the experience and equipment to produce tub girders efficiently, the competitiveness of tub girders in a particular application can be enhanced. Therefore, the comparative economies of I- and tub girder systems should be evaluated on a case-by-case basis, and the comparisons should reflect the appropriate costs of shipping, erection, and future inspection and maintenance, as well as fabrication. A more in-depth discussion on the relative advantages of steel tub girders and on steel tub girder design and construction may be found in the NSBA Publication *Practical Steel Tub Girder Design* [1], which is available on the NSBA website (www.aisc.org/nsba).

Furthermore, designers should not feel limited by an overly strict interpretation of the AASHTO design provisions for tub girders in some cases. For example, there are currently cross-sectional restrictions placed on the use of approximate live load distribution factors for straight tub girders in the *AASHTO LRFD Bridge Design Specifications* [2], referred to hereafter as the *AASHTO LRFD BDS*. Limiting the proportions of tub girder cross-sections solely to allow for the use of these approximate live load distribution factors and more simplified analysis methods may reduce the efficiency and competitiveness of a tub-girder cross-section. However, these cross-section proportion restrictions do not apply when a refined analysis is employed; thus the use of a refined analysis method allows the designer to explore additional, and perhaps more economical, design options.

This design example demonstrates the design of a horizontally curved three-span continuous composite tub girder bridge with a span arrangement of 160′-0″ – 210′-0″ – 160′-0″. This example illustrates the flexural design of a section in positive flexure, the flexural design of a section in negative flexure, computation of distortional stresses, the shear design of the web, the design of the bottom flange longitudinal stiffener, the design of an internal diaphragm, the design of a top flange lateral bracing member, the design of a bolted field splice, as well as other design and analysis related topics.

The bridge cross-section consists of two trapezoidal tub girders with the top flanges of each tub spaced at 10′-0″ on centers, 12′-6″ between the centerline of adjacent top tub flanges, and 4′-0″ overhangs for a deck width of 40′-6″ out-to-out. For the sake of brevity, only the Strength I, Service

II, and Fatigue load combinations are examined for dead- and live-load force effects in this design example. The effects of wind loads, design permit loads, and other loads (braking forces, seismic forces, etc.) are not considered. It is recommended that the reader refer to NSBA's *Steel Bridge Design Handbook: Example 1: Three-Span Continuous Straight Composite Steel I-Girder Bridge* [3] for information regarding additional load combination cases and design for wind-load force effects both during construction and in the final constructed condition.

The example calculations provided herein comply with the provisions of the current *AASHTO LRFD BDS*, but the analysis described herein was not performed as part of this design example. The analysis results and general superstructure details contained within this design example were taken from the design example published as part of the National Cooperative Highway Research Program (NCHRP) Project 12-52 published in 2005, titled "AASHTO-LRFD Design Example: Horizontally Curved Steel Box Girder Bridge, Final Report" [4].

2.0 OVERVIEW OF LRFD ARTICLE 6.11

The design of composite tub girder flexural members is contained within Article 6.11 of the 9th Edition of the *AASHTO LRFD BDS*. The provisions of Article 6.11 are organized to correspond to the general flow of the calculations necessary for the design of tub girder flexural members. Most of the provisions are written such that they are largely self-contained, however to avoid repetition, some portions of Article 6.11 refer to provisions contained in Article 6.10 for the design of I-section flexural members when applicable (particularly those pertaining to tub girder top flange design, which is fundamentally similar to I-girder design). The provisions of Article 6.11 are organized as follows:

6.11.1 General
6.11.2 Cross-Section Proportion Limits
6.11.3 Constructability
6.11.4 Service Limit State
6.11.5 Fatigue and Fracture Limit State
6.11.6 Strength Limit State
6.11.7 Flexural Resistance - Sections in Positive Flexure
6.11.8 Flexural Resistance - Sections in Negative Flexure
6.11.9 Shear Resistance
6.11.10 Shear Connectors
6.11.11 Stiffeners

It should be noted that Article 6.11, and specifically Article 6.11.6.2, does not permit the use of Appendices A6 and B6 because the applicability of these provisions to tub girders has not been demonstrated; however, Appendices C6 and D6 are generally applicable. Flow charts for flexural design of steel girders according to the LRFD provisions, along with an outline giving the basic steps for steel-bridge superstructure design, are provided in Appendix C6. Appendix C6 may also prove to be a useful reference for tub girder design. Fundamental calculations for flexural members are contained within Appendix D6.

Example calculations demonstrating the provisions of Article 6.10, pertaining to straight and horizontally curved I-girder design and straight rolled-beam design, are provided in NSBA's *Steel Bridge Design Handbook: Examples 1, 2A, 2B* and *3*. [3, 5-7] This design example will demonstrate the application of the provisions of Article 6.11 of the *AASHTO LRFD BDS* as they relate to horizontally curved tub girder design. NSBA's *Steel Bridge Design Handbook: Example 4: Three-Span Continuous Straight Composite Steel Tub-Girder Bridge* [8] demonstrates the application of these provisions to a straight tub girder design.

The provisions of Articles 6.10 and 6.11 provide a unified approach for consideration of major-axis bending and flange lateral bending for both straight and horizontally curved bridges. Bottom flange lateral bending stresses in tub girders tend to be quite small since (as explained earlier) torsion in a tub girder is carried primarily by St. Venant torsional shear flow, rather than by warping torsion. Top flange lateral bending is caused by the outward thrust induced by the inclination of the webs, by wind loads, by eccentric loading of temporary support brackets for deck overhangs, curvature, and from loads introduced by the lateral bracing system.

In addition to providing adequate strength, the constructability provisions of Article 6.11.3 verify that nominal yielding does not occur and that there is no reliance on post-buckling resistance for main load-carrying members during critical stages of construction. The *AASHTO LRFD BDS* specifies that for critical stages of construction, both compression and tension flanges must be investigated, and the effects of top flange lateral bending should be considered. For noncomposite top flanges in compression, constructability design checks verify that the maximum combined stresses in the flange will not exceed the specified minimum yield strength, the compression flanges have sufficient strength to resist lateral torsional and flange local buckling, and that theoretical web bend-buckling and web shear buckling will not occur during construction. For noncomposite bottom flanges in compression during critical stages of construction, local buckling of the flange is checked in addition to the web bend-buckling and shear buckling resistance. For noncomposite top and bottom flanges in tension, constructability design checks verify that the maximum combined stress will not exceed the specified minimum yield strength of the flanges during construction. At the strength limit state, the top flanges are continuously braced by the hardened concrete deck and flange lateral bending stresses along with lateral torsional and flange local buckling of the flanges is not a concern. Also, due to the inherent torsional stiffness and strength of the closed section represented by the tub girder with the hardened composite concrete deck, global lateral torsional buckling of the composite tub girder is also not a concern.

One additional requirement specified for tub-girder sections relates to the consideration of longitudinal warping and transverse bending stresses due to cross-section distortion. When tub girders are subjected to torsion, their cross-sections become distorted, resulting in secondary bending stresses. Therefore, as specified in Article 6.11.5, longitudinal warping stresses and transverse bending stresses due to cross-section distortion are to be considered for:

- Single tub girders in straight or horizontally curved bridges;
- Multiple tub girders in straight bridges that do not satisfy requirements of Article 6.11.2.3;
- Multiple tub girders in horizontally curved bridges; or
- Any single or multiple tub girder with a bottom flange that is not fully effective according to the provisions of Article 6.11.1.1.

In accordance with Article 6.11.1.1, transverse bending stresses due to cross section distortion are to be considered for fatigue as specified in Article 6.11.5, and at the strength limit state. Transverse bending stresses at the strength limit state are not to exceed 20.0 ksi. Longitudinal warping stresses due to cross-section distortion are to be considered for fatigue as specified in Article 6.11.5, but may be ignored at the strength limit state. Article C6.11.1.1 allows the use of the beam-on-elastic-foundation (BEF) analogy developed by Wright and Abdel-Samad [9] for determining the transverse bending stresses and the longitudinal warping stresses due to cross-section distortion. The application of the BEF analogy for the calculation of these stresses is demonstrated in Section 7.9.1 of this design example.

Even though the longitudinal warping stresses and transverse stresses due to cross-section distortion are generally small and may often be neglected, there are cases where such an assumption may not be warranted. For example, these stresses may be of particular concern in

boxes that are subjected to large torques; e.g., single box sections, sharply curved boxes, and boxes resting on skewed supports.

3.0 DESIGN PARAMETERS

The following data apply to this design example:

Specifications:	2020 AASHTO LRFD Bridge Design Specifications, Customary U.S. Units, Ninth Edition
Structural Steel:	ASTM A709, Grade 50 with F_y = 50 ksi, and F_u = 65 ksi
Concrete:	f'_c = 4.0 ksi, γ = 150 pcf
Slab Reinforcing Steel:	ASTM A615, Grade 60 with F_y = 60 ksi

The bridge has spans of 160′-0″ – 210′-0″ – 160′-0″ measured along the centerline of the bridge. Span lengths are arranged to give relatively equal positive dead load moments in the end spans and center span. The radius of the bridge is 700 ft at the centerline of the bridge.

The out-to-out deck width is 40.5 feet, and the bridge is to be designed for three 12-foot-wide traffic lanes. The roadway is superelevated at 5 percent. All supports are radial to the roadway. The framing consists of two trapezoidal tub girders with the top of the webs in each tub spaced 10 feet apart at the top of the tub and with a deck span of 12.5 feet between the top of the interior webs of the two adjacent tubs.

Structural steel having a specified minimum yield stress of 50 ksi is used throughout the bridge. The deck is a conventional cast-in-place concrete deck, with a specified minimum 28-day compressive strength of 4,000 psi. The structural deck thickness is 9.5 inches, and there is no integral wearing surface assumed. The deck haunch is 4.0 inches thick, measured from the top of the web to the bottom of the deck, and is constant throughout the structure. The width of the haunch is assumed to be 20.0 inches for weight computations.

Shear connectors are provided along the entire length of each top flange; therefore, the tub girders in this example are composite throughout the entire span, including in regions of negative flexure as required in Article 6.11.10. The shear connectors are 7/8 inch diameter by 6 inches in length. All tub girders (whether straight or curved) are subject to torsional loading, and the use of shear connectors along the entire length of a tub girder bridge (in both the positive and negative flexure regions) is required to provide an adequate and continuous load path for the St. Venant torsional shear flow along the entire length of the girder.

Permanent steel stay-in-place deck forms are used between the girders; the forms are assumed to weigh 15.0 psf since it is assumed concrete will be in the flutes of the deck forms. In this example, the steel stay-in-place deck forms are used between the top flanges of individual tub girders and between the top flanges of adjacent girders. Sequential placement of the concrete deck is considered in this design example.

An allowance for a future wearing surface of 30.0 psf is incorporated in the design. Parapets are each assumed to weigh 495 lbs/ft.

The bridge is designed for HL-93 live load, in accordance with Article 3.6.1.2. Multiple presence factors are accounted for in the analysis, as specified in Article 3.6.1.1.2. Live load for fatigue is

taken as defined in Article 3.6.1.4. The bridge is designed for a 75-year fatigue life, and the projected single lane Average Daily Truck Traffic $(ADTT)_{SL}$ in one direction is assumed to be 1,000 trucks per day.

The bridge site is assumed to be located in Seismic Zone 1, and so seismic effects are not considered in this design example.

Composite tub girder bridges fabricated using uncoated weathering steel have performed successfully without any interior corrosion protection. However, the interior of tub girders should always be coated in a light color to aid visibility during girder inspection. Without Owner-agency direction towards a specific coating and preparation, the girder interior should receive a light brush blast and be painted with a white or light-colored coating capable of telegraphing cracks in the steel section. Specified interior coatings should be tolerant of minimal surface preparation. At the Engineer's discretion, for painted tub girders, an allowance may be made for the weight of the paint as discussed in Article C6.11.3.1.

Provisions for adequate draining and ventilation of the interior of the tub are essential. As suggested in the NSBA Publication *Practical Steel Tub Girder Design* [1], bottom flange drain holes should be 1 ½ inches in diameter and spaced along the low side of the bottom flange every 50 feet, and be placed 4 inches away from the web plate. Access holes must be provided to allow for periodic structural inspection of the interior of the tub. The access holes should provide easy access for authorized inspectors. Solid doors can be used to close the access holes, however they should be light in weight, and they should be hinged and locked, but not bolted. Wire-mesh screens should always be place over copes and clips in end plates, and over the bottom flange drain holes to prevent entry of wildlife and insects. Wire mesh should be 10 gage to withstand welding and blasting and have a weave of approximately ½ inch by ½ inch.

Additional detailing guidelines can be found on the NSBA website (www.aisc.org/nsba), with particular attention given to document AASHTO/NSBA Steel Bridge Collaboration document G1.4, *Guidelines for Design Details* [10]. Four other detailing references offering guidance include the NSBA Publication *Practical Steel Tub Girder Design* [1], the Texas Steel Quality Council's *Preferred Practices for Steel Bridge Design, Fabrication, and Erection* [11], the Mid-Atlantic States Structural Committee for Economic Fabrication (SCEF) Standards, and the AASHTO/NSBA Steel Bridge Collaboration document G12.1, *Guidelines to Design for Constructability and Fabrication* [12].

4.0 GENERAL STEEL FRAMING CONSIDERATIONS

4.1 Span Arrangement

Often, site-specific features will influence the span arrangement required. Careful consideration of the layout of the steel framing is an important part of the design process and involves the investigation of alternative span arrangements based on the superstructure and substructure costs to arrive at the most economical solution. In the absence of site constraints, choosing a balanced span arrangement for continuous steel bridges (end spans approximately 80% of the length of the center spans) will typically provide an efficient design. The span arrangement for this example bridge has spans of 160′-0″ – 210′-0″ – 160′-0″. Refer NSBA's *Steel Bridge Design Handbook: Example 1: Three-Span Continuous Straight Composite Steel I-Girder Bridge* [3] for further discussion on span arrangement considerations. The framing plan of the bridge for this example is shown in Figure 1.

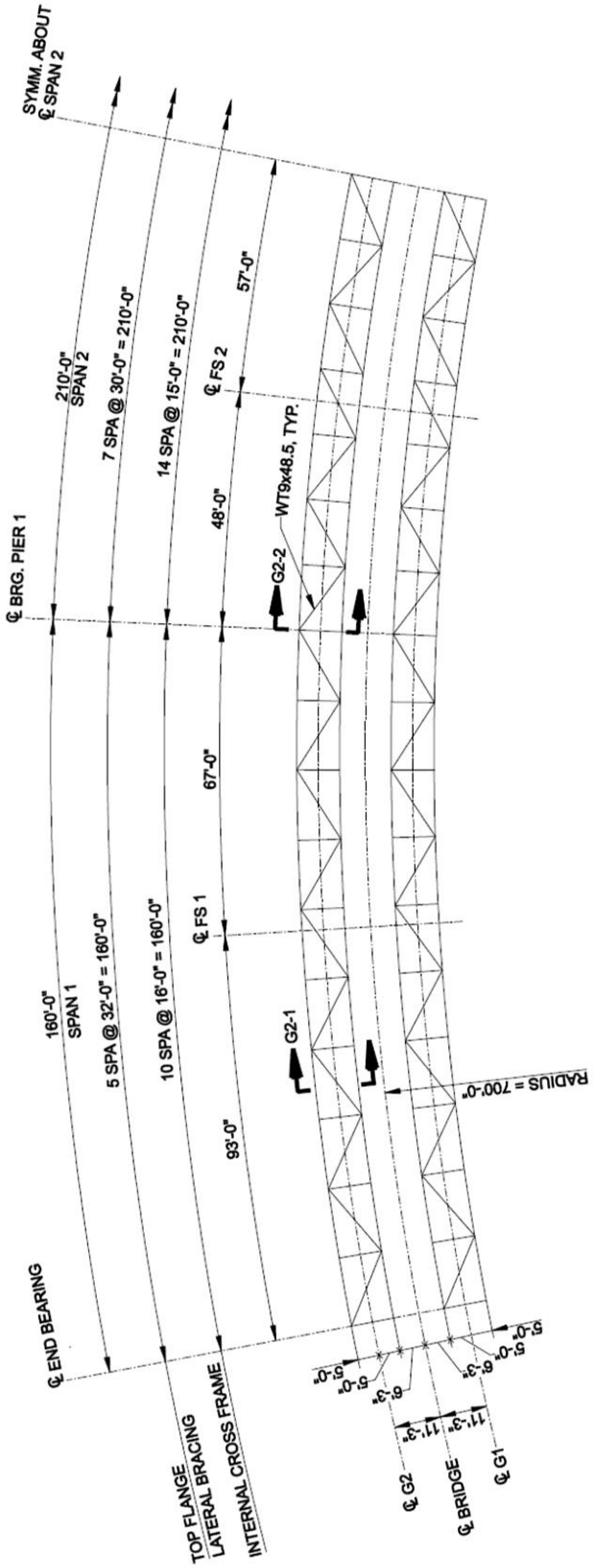

Figure 1 Framing Plan of the Example Tub Girder Bridge (all lengths shown are taken along the centerline of the bridge)

4.2 Field Section Sizes

The lengths of field sections are generally dictated by shipping (weight and length) restrictions. Generally, the weight of a single shipping piece is restricted to 200,000 lbs, while the piece length is limited to a maximum of 140 feet, with an ideal piece length of 120 feet. However, shipping requirements are typically dictated by state or local authorities, in which additional restrictions may be placed on piece weight and length. Handling issues during erection and in the fabrication shop also need to be considered in the determination of field section lengths, as they may govern the length of field sections. Therefore, the Engineer should consult with contractors and fabricators regarding any specific restrictions that might influence the field section lengths.

Field section lengths should also be determined with consideration given to the number of field splices required, as well as the locations of the field splices. It is desirable to locate field splices as close as possible to dead load inflection points, so as to reduce the forces that must be carried by the field splice. Field splices located in higher moment regions can become quite large, with cost increasing proportionally to their size. The Engineer should determine an economical solution for the given span arrangement. For complex and longer span bridges, the fabricator's input can be helpful in reaching an economical solution.

The final girder field section lengths are shown on the framing plan in Figure 1. The longest field section is the field section of Girder G2 over the pier, and has a length of approximately 116.75 feet. This field section is also the heaviest field section, with a total approximate weight of 99,000 pounds (including internal cross-frames, top flange lateral bracing, and other steel details).

In curved girder bridges, the Engineer must also consider the girder sweep and the subsequent total width when determining the lengths of the field sections. The curvature combined with the girder length can cause the field section to be too wide to transport, depending on shipping routes and local requirements. In the case of the field section of Girder G2 over the pier, the total width of the tub girder including girder sweep and the width of the top flanges is approximately 13.90 feet.

4.3 Bridge Cross-Section and Girder Spacing

When developing the bridge cross-section, the designer will evaluate the number of girder lines required, relative to the overall cost. Specifically, the total cost of the superstructure is a function of steel quantity, details and erection costs. Developing an efficient bridge cross-section should also consider the provision of an efficient deck design, which is generally influenced by girder spacing and overhang dimensions. Specifically, with the exception of an empirical deck design, girder spacing significantly affects the design moments in the deck slab. . Larger deck overhangs result in a greater load on the exterior web of the tub girder. Larger overhangs will increase the bending moment in the deck, caused by the cantilever action of the overhang, resulting in additional deck slab reinforcing for the overhang region of the deck.

In addition, wider deck spans between top flanges can become problematic for several reasons. Some owners have economical deck detail standards for cast-in-place decks that may not be suited, or even permitted, for wider deck spans. At the same time, wider deck spans are progressively more difficult to form and construct.

Special attention should be paid to the design of decks for steel tub girder bridges in the area near the girder top flanges between adjacent girders. The inherent torsional stiffness of tub girders can produce a situation where the deck is subjected to a racking effect when there is differential vertical displacement between adjacent girders. This phenomenon is illustrated in Figure C9.7.2.4-1 of the *AASHTO LRFD BDS* [2]. This effect is not directly addressed in the empirical deck design method (as noted in the *AASHTO LRFD BDS* Commentary C9.7.4.2). When the traditional deck design method is used, the effects of this phenomenon should be addressed either by approximate calculation methods (when a line girder analysis method is being used) or by evaluating deck stresses (when a refined analysis model is being used).

As shown in Figure 2, the example bridge cross-section consists of two trapezoidal tub girders with top flanges spaced at 10.0 feet within each tub girder, 12.5 feet between the centerline of adjacent top flanges, with 4.0 foot-wide deck overhangs, and an out-to-out deck width of 40.5 feet. The 37.5 feet roadway width can accommodate up to three 12-foot-wide design traffic lanes. The total thickness of the cast-in-place concrete deck is 9.5 inches with no integral wearing surface. The concrete deck haunch is 4.0 inches deep measured from the top of the web to the bottom of the deck.

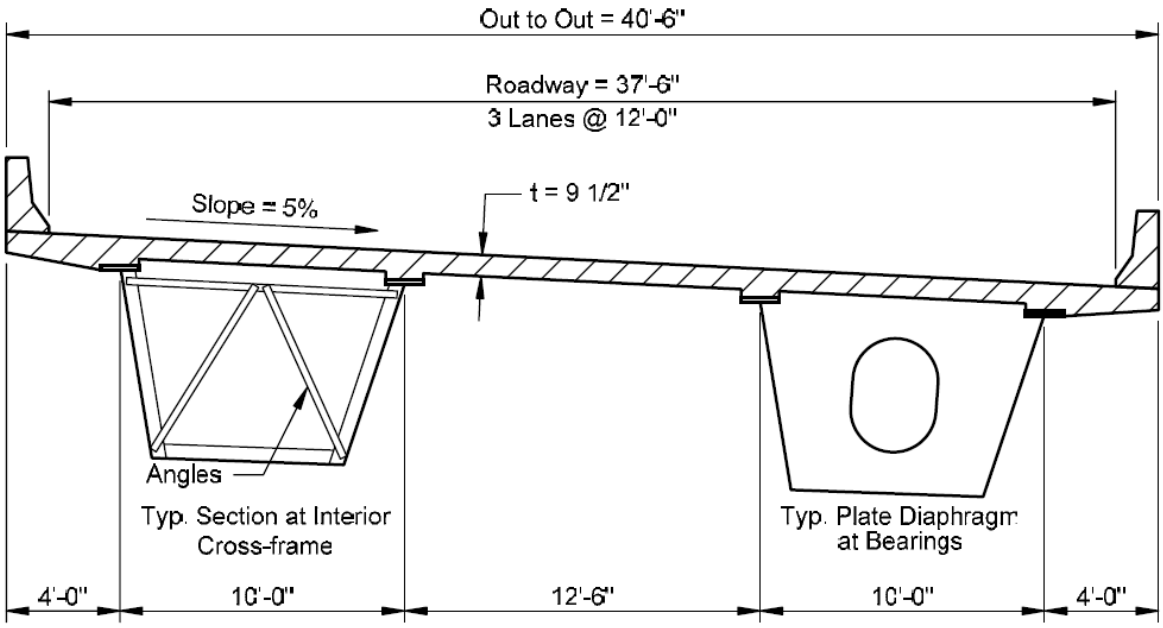

Figure 2 Cross Section of the Tub Girder Bridge [4]

4.4 Intermediate Internal and External Cross-Frames

Internal intermediate cross-frames are provided in tub girders to control cross-sectional distortion. Cross-sectional distortion results due to the St. Venant torsion shear flow changing direction at the corners of the tub. Cross-sectional distortion introduces additional stresses in the tub girder and, therefore, should be minimized. The distortion stresses basically occur because the section is not perfectly round. The shear flow must change direction at the corners, which tends to distort the cross-section. Adequate internal cross-bracing usually controls the magnitude of these stresses in

tub girders of typical proportion such that they are not critical to the ultimate resistance of the tub section at the strength limit state. As a minimum, internal cross-frames should be placed at points of maximum moment within a span and at points adjacent to field splices in straight bridges. Spacing of internal diaphragms, considered during development of the framing plan, should be influenced by factors such as the angle and length of the lateral bracing members.

Most internal cross-frames in modern tub girder bridges are K-frames, often without a bottom strut, which allow for better access during construction and inspection. Slenderness requirements (KL/r) generally govern the design of cross-frame members, however handling and strength requirements should always be considered. When refined analysis methods are used and the cross-frame members are included in the structural model to determine force effects, the cross-frame members are to be designed for the calculated force effects. Consideration should be given to the cross-frame member forces during construction. When simplified analysis methods are used, such cross-frame forces due to dead and live loads are typically difficult to calculate. Therefore, the cross-frame members should at least be designed to transfer wind loads, carry any construction loads due to deck overhang brackets, control tub girder cross- section distortion, and satisfy appropriate slenderness requirements.

External intermediate cross-frames may be incorporated to control the differential displacements and rotations between individual tub girders during deck placement. In a finished bridge, when the tub girders are fully closed and the concrete deck effectively attaches the girders together, twist rotation is expected to be small and the contribution of the external cross-frames is typically less significant. However, during construction the rotational rigidity of the tub girder is not nearly as large and, since the two top flanges of a single tub girder are spaced apart but rotate together, the resulting differential deflections may be large even with a small girder rotation. Helwig et al. [13] present an approximate method for estimating these differential deflections that can be very helpful in evaluating the possible need for external intermediate cross-frames early in the design process.
a
External intermediate cross-frames typically utilize a K-frame configuration, with the depth closely matching the girder depth for efficiency and simplification of supporting details. Solid web (plate girder) diaphragms have been successfully used as well. At locations of external intermediate cross-frames, there should be bracing inside the tub girder to receive the forces of the external bracing. In some cases, for aesthetic reasons, it may be desirable to remove the external intermediate cross-frames after the deck has hardened. However, extreme care should be taken in evaluating the effects that the removal of external intermediate cross-frames has on the structure. The NSBA Publication *Practical Steel Tub Girder Design* [1] offers further discussion on this topic.

Based on the preceding considerations, the internal cross-frame spacings shown on the framing plan in Figure 1 were chosen for this example. The tub girders are braced internally at intermediate locations with K-type cross-frames, where the diagonals intersect the top strut at the top flange level. The internal cross-frames are uniformly spaced in the end span and center span field sections. Internal cross-frame spacing in the center span positive flexure region is 15 feet. The top struts, both the individual struts and the ones that are part of internal cross-frames, also serve as part of the top flange lateral bracing system. Article C6.11.3.2 allows top lateral bracing attached to the flanges at points where only struts exist between the flanges to be considered as brace points at the

discretion of the Engineer. In the case of this design example, which features a full-length top flange lateral bracing system, it is reasonable to consider both the struts with internal cross-frames and the alternating struts without internal cross-frames as brace points for the top flanges.

The design of the internal cross-frame members is not shown in this example. Internal cross-frames were modeled as truss members in the three-dimensional analysis, with a cross-sectional area of 5.0 square inches. There are no intermediate external cross-frames provided between the tub girders in this design example as the differential rotations and rotations between the individual tub girders during the deck placement were not anticipated to be significant in this case.

4.5 Support Diaphragms

Internal diaphragms at points of support are typically full-depth plates with a top flange. These diaphragms are subjected to bending moments which result from the shear forces in the inclined girder webs. If a single bearing is employed at the support, and the bearing sole plate does not span the full width of the girder bottom flange, bending of the internal diaphragm over the support will result, causing bending stresses in the top flange of the diaphragm and the bottom flange of the tub girder. Additionally, a torsional moment reaction in the tub girder at the support will induce a shear flow along the circumference of the internal diaphragm. To provide the necessary force transfer between the tub girder and the internal diaphragms, the internal diaphragms should be connected to the web and top flanges of the tub girder.

Inspection access through the internal diaphragms at interior supports must be provided with access holes at least 18 inches wide and 24 inches high; however, if feasible, a larger hole at least 36.0 in. deep is preferable. In addition to restraining distortion of the box section, the internal diaphragms at supports also transfer load from the girder webs to the bearing(s). If a single centered bearing is used, the diaphragm must be stout enough to resist the reaction and transfer the load around any access hole. Bearing stiffeners are usually attached to the diaphragms. If a single centered bearing is employed, two stiffeners are generally used. A bearing stiffener on each side of the access hole generally removes the shear from the diaphragm before it is engaged by the hole. Torsion generally causes a different magnitude of shear in the webs of the box on the two sides of the diaphragm. Reinforcement around the hole may be required, particularly if the access hole requires a large portion of the diaphragm or if a single bearing is located under the diaphragm. Auxiliary stiffeners on the diaphragm or webs may be employed to spread out the reaction. Sample design calculations for an internal diaphragm are provided in Section 7.2.

As discussed in Article C6.7.4.3, external plate diaphragms with aspect ratios, or ratios of length to depth, less than 4.0 and internal plate diaphragms act as deep beams and should be evaluated by considering principal stresses rather than by simple beam theory. Fatigue-sensitive details on these diaphragms and at the connection of the diaphragms to the flanges should be investigated by considering the principal tensile stresses.

Similar to internal support diaphragms, external support diaphragms are typically full-depth plate sections, but with top and bottom flanges. As acknowledged in the NSBA publication *Practical Steel Tub Girder Design* [1], the behavior of an external diaphragm at a point of support is highly dependent on the bearing arrangement at that location. If dual bearings used at each girder

sufficiently prevent transverse rotation, external diaphragms at the point of support should theoretically be stress free. The force couple behavior of a dual bearing system resists the torsion that would otherwise be resisted by the external diaphragm and, in turn, minimizes the bending moments applied to the external diaphragm.

If a single bearing under each tub girder is employed, torsional moments must be resisted by the external diaphragm through vertical bending. In a single bearing arrangement, the internal diaphragms of adjacent girders function with the external diaphragms to form a system (or beam) which resists the girder torsional moments. The total torque is resisted by differential reactions at the bearings of adjacent girders. The diaphragms then are subjected to bending and shear forces. Torsional moments resisted by the external diaphragm often require the use of a moment connection to the tub girder in which the flanges and webs of the external diaphragm are connected. The largest torsional moment will typically occur during the construction stage and can be quite large, particularly in horizontally curved structures. Torsional moments in straight bridges are typically smaller but should still be considered in the design.

In accordance with Article 6.7.4.3, full-depth internal and external diaphragms are provided at the support lines in this design example. The web plates for the internal and external diaphragms in the three-dimensional analysis are assumed to have a thickness of 0.5 inches. The external diaphragm top and bottom flanges are assumed to have an area of 8.0 square inches for each flange.

4.6 Top Flange Lateral Bracing

Lateral bracing between common top flanges of a tub girder is required to provide proper shear flow in the individual tub girders. Without lateral bracing, the section acts as an open section and is much less stable under torsional loading. The bracing acts to enhance the global lateral torsional buckling stability of the section. Top lateral bracing raises the shear center to the inside of the tub section resulting in a pseudo-box section and significantly increasing the torsional stiffness. A single tub girder with a properly designed top flange lateral bracing system has substantially greater stability than an equivalent pair of I-shaped girders without lateral bracing, even if the pair of I-shaped girders has the same net major-axis bending section modulus as the single tub girder.

In accordance with Article 6.7.5.3, for horizontally curved tub girders, a full-length lateral bracing system between common flanges of individual tub sections is to be provided, and the stability of compression flanges between panel points of the lateral bracing system is to be investigated during the deck placement. Generally, lateral bracing will not be required between adjacent tub girders. A full-length lateral bracing system is particularly important when the torques on the noncomposite section are large; e.g., in tub-section members on which the deck weight is applied unsymmetrically, or in members resting on skewed supports. A full-length lateral bracing system also helps to limit distortions that may result from temperature changes occurring prior to deck placement, and to resist the torsion and twist resulting from any eccentric loads that may act on the steel section during construction, including the effects of deck overhang brackets.

Top lateral bracing is to be designed to resist shear flow in the pseudo-box section due to factored loads before the concrete deck has hardened or is made composite. Forces in the bracing due to flexure of the tub girder should also be considered during construction based on the Engineer's

assumed construction sequence. The top lateral bracing member forces can be determined using a refined three-dimensional analysis where the bracing members are explicitly modeled. Or, in the absence of a refined analysis, design equations have been developed to evaluate the bracing member forces due to tub girder major-axis bending [13].

The lateral bracing is typically comprised of WT or angle sections and is often configured in a single diagonal arrangement, such as a Warren-type or Pratt-type truss system. The diagonal bracing members commonly frame into the work point of the girder top flange and internal diaphragm or strut connection. Alternatively, the length between internal cross-frames can be divided into multiple lateral bracing panels. Such framing arrangements usually include a single transverse strut at intermediate brace locations. The plane of the top flange lateral bracing system should be detailed to be as close as possible to the plane of the girder top flanges so as to increase the torsional stiffness of the section, while at the same time reducing connection eccentricities and excessive out-of-plane bending in the web. In most cases, the top flange lateral bracing is often attached directly to the top flange of the tub girders. Although not checked in this example, wherever the bracing members are bolted to a top flange subject to tension, *AASHTO LRFD BDS* Equation 6.10.1.8-1 must be satisfied at cross-sections of flexural members containing holes in the tension flange at the strength limit state and when checking constructability.

Single diagonal top lateral bracing systems are preferred over X-type systems because there are fewer pieces to fabricate and erect, and fewer connections. Warren-type and Pratt-type systems offer some advantages with regard to the behavior of each top flange lateral bracing system. In a Warren-type system, the bracing members alternate directions along the length of the bridge (see Figure 3). In most cases, the bracing forces will alternate from tension to compression along the length of the bridge. The tension and compression forces result from a combination of girder major-axis bending and girder torsion. If necessary, the flange lateral bending stresses and forces in the lateral bracing members can often be effectively mitigated by the judicious placement of parallel single-diagonal members in a Pratt-type configuration. In a Pratt-type system, the bracing members should be oriented based on the sign of the torque so that the forces induced in these members due to torsion resulting from the non-composite dead load offset the compressive or tensile forces induced in the same members due to major-axis bending of the tub section, thus allowing for smaller brace sizes (see Figure 4). NSBA's *Steel Bridge Design Handbook: Bracing System Design* [14] discusses issues related to the selection of the lateral bracing configuration in greater detail.

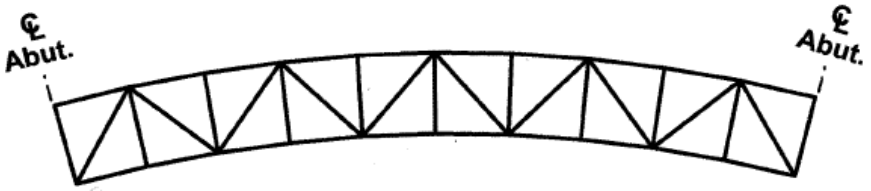

Figure 3 Plan View of a Warren-type truss lateral bracing system

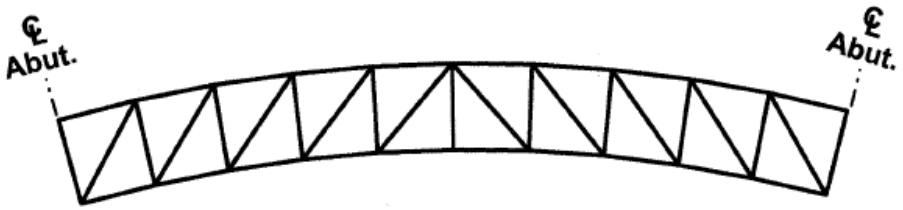

Figure 4 Plan View of a Pratt-type truss lateral bracing system

As shown in Figure 1, a Warren-type single diagonal top lateral bracing system is used in this design example. The bracing is assumed to be directly connected to the flanges at each internal cross-frame and internal top strut; thus the bracing is assumed to lie in the plane of the top flange in the design calculations. The connection of the top flange lateral bracing directly to the flanges may require wider flanges than might otherwise be required, however, this approach may still be more economical considering the high fabrication cost associated with the use of gusset plates for the connections.

Truss members with an area of 8.0 square inches were assumed for the top flange lateral bracing members in the three-dimensional analysis. However, design calculations show that a WT9x48.5 is required, which has a cross-sectional area of 14.3 square inches (Section 7.13). Although not done in this example, the designer should perform a second iteration of the analysis with this larger cross-sectional area, as the larger cross-sectional area will affect the load distribution in the bracing system in the noncomposite condition.

5.0 FINAL DESIGN

5.1 Limit States

The *AASHTO LRFD BDS* requires that bridges be designed for specified limit states to achieve the objectives of constructability, safety, and serviceability. These objectives are met through the strength, service, fatigue and fracture, and extreme-event limit states. These limit states are intended to provide a safe, constructible, and serviceable bridge capable of carrying the appropriate design loads for a specified service life. A brief discussion of these limit states is provided herein, but the reader can refer to NSBA's *Steel Bridge Design Handbook: Limit States* [15] for a more detailed discussion.

5.1.1 Strength Limit State

At the strength limit state, it must be verified that adequate strength and stability are provided to resist the statistically significant load combinations the bridge is expected to experience over its design life. The strength limit state is not based upon durability or serviceability. Extensive structural damage may occur, but overall structural integrity is maintained. There are five different strength limit state load combinations that must be considered by the Engineer.

In general, Strength I is the load combination used for checking the strength of a member or component under normal loading in the absence of wind. To check the strength of a member or component under Owner-specified special design vehicles and/or evaluation permit vehicles in the absence of wind, the Strength II load combination is used. The Strength III load combination is used for checking the strength of a member or component assuming the bridge is exposed to the design wind speed at the location of the bridge in the absence of live load. The Strength IV load combination basically relates to bridges with very high dead-to-live load force effect ratios. This load combination controls over Strength I for components with a ratio of dead load to live load force effects exceeding 7.0. The Strength IV load combination is not applicable to the investigation of construction stages. The Strength V load combination is used to check the strength of a member or component assuming the bridge is exposed to a wind velocity equal to 80 miles per hour in combination with normal vehicular use.

5.1.2 Service Limit State

To satisfy the service limit state, restrictions on stress and deformation under regular service conditions are specified to provide satisfactory performance of the bridge over its service life. As specified in Article 6.10.4.1, optional live load deflection criteria and span-to-depth ratios (Article 2.5.2.6) may be invoked to control deformations.

The *AASHTO LRFD BDS* includes four service limit state load combinations of which only two are applicable to steel bridges. The Service I load combination relates to normal operational use of the bridge and is used primarily for crack control in reinforced concrete structures. However, the live load portion of the Service I load combination is used for checking live load deflection in steel bridges. The Service II load combination only applies to steel superstructures, and is intended to be used to satisfy the requirements of Article 6.10.4.2, which are intended to prevent objectionable

permanent deformations, caused by localized yielding and potential web bend-buckling under expected severe traffic loadings, which might impair rideability. The live-load portion of the Service II load combination is intended to be the HL-93 design live load specified in Article 3.6.1.1 (Section 5.2.3). For evaluation of the Service II load combination under Owner-specified special design vehicles and/or evaluation permit vehicles, a reduction in the specified load factor for live load should be considered for this limit-state check. The Service II load combination is also used to check for slip in bolted slip-critical connections..

5.1.3 Fatigue and Fracture Limit State

To satisfy the fatigue limit state, restrictions on stress range under regular service conditions are specified to control crack growth under repetitive loads (Article 6.6.1). Material toughness requirements are specified to satisfy the fracture limit state (Article 6.6.2).

For checking fatigue in steel structures, the fatigue load and fatigue load combinations apply. The Fatigue I load combination is related to infinite load-induced fatigue life, and the Fatigue II load combination is related to finite load-induced fatigue life. Fatigue resistance of details is discussed in Article 6.6. A special fatigue requirement for webs (Article 6.10.5.3) is also specified to control out-of-plane flexing of the web that might potentially lead to fatigue cracking under repeated live loading.

5.1.4 Extreme Event Limit State

Structural survival of the bridge must be verified during an extreme event, such as an earthquake, flood, vessel collision, vehicle collision, or ice flow. The Extreme Event I load combination is related to earthquake loading, while the Extreme Event II load combination relates to the other possible extreme events.

5.1.5 Constructability

Although not a specific limit state, the bridge must be safely erected and have adequate strength and stability during all phases of construction, as constructability is one the basic objectives of the *AASHTO LRFD BDS*. Specific constructability design provisions are given in Articles 6.10.3 and 6.11.3 for I- and tub-girders, respectively. The constructability checks are typically performed on the steel section only under the factored noncomposite dead loads using appropriate strength load combinations, especially when considering the deck placement sequence. Article 3.4.2 provides further guidance on the specific strength load combinations to be considered in the constructability checks, and on the load factors to use for construction loads.

5.2 Loads

5.2.1 Dead Load

As defined in Article 3.5.1, dead loads are permanent loads that include the weight of all components of the structure, appurtenances and utilities attached to the structure, earth cover, wearing surfaces, future overlays and planned widenings.

The component dead load (DC) consists of all the structure dead load except for non-integral wearing surfaces, if anticipated, and any specified utility loads. For composite steel-girder design, DC is further divided into:

- Noncomposite dead load (DC_1) is the portion of loading resisted by the noncomposite section. DC_1 represents the permanent component load that is applied before the concrete deck has hardened or is made composite.
- Composite dead load (DC_2) is the portion of loading resisted by the long-term composite section. DC_2 represents the permanent component load that is applied after the concrete deck has hardened or is made composite.

The self-weight of the steel girders, cross-frames, diaphragms, lateral bracing and other attachments is applied to the fully erected steel structure in the three-dimensional model through the use of body forces in the various finite elements used to model the structure. The weight of the detail steel such as stiffeners and splices, which were not included in the analysis model, was accounted for in the analysis by increasing the density of the steel (490 pounds per cubic foot) by approximately 7 percent. The steel self-weight is a noncomposite dead load (DC_1).

The concrete deck weight is assumed to be placed at one time on the non-composite steel structure for the strength limit state checks. The concrete deck weight, haunch weight, and permanent metal deck form weight are all considered to be non-composite dead loads (DC_1). The weight of the wet concrete of the deck was applied to the non-composite 3D model with concentrated loads at the nodes representing the top flanges of the girders. The wet concrete was assumed to have no stiffness. The concentrated loads applied to each top flange node were determined by the tributary area of deck associated with the distance between the adjacent top flange nodes. The deck overhang tapers (Figure 1) were considered in computing the concentrated loads applied to the top flange nodes on the fascia webs. The weight of the wet concrete in the deck haunches was included in the concentrated loads applied to each top flange node. An average deck haunch width of 20 inches and deck haunch thickness of 4 inches was assumed (the reduction in weight due to the concrete displaced by the top flanges was ignored). The unit weight of the concrete was taken equal to 0.150 kcf, which includes an additional 0.005 kcf to account for the weight of the rebars.

The assumed weight of the SIP deck forms (15 psf) was applied directly to the girders of the non-composite 3D model as concentrated loads to each top-flange node as was done for the deck. The forms exist only between flange edges inside the tub girders and between the two tub girders; thus, the weight of the forms and the concrete in the forms was based on the associated clear span between the top flanges.

The composite dead load (DC_2), also referred to as a superimposed dead load, includes the weight of the parapets. The parapets are assumed to weigh 495 pounds per linear foot. The parapet weight was applied as line loads along the edges of the deck elements in the three-dimensional analysis.

The component dead load (DW) consists of the dead load of any non-integral wearing surfaces and any utilities, which can also be considered as superimposed dead loads. For this example, a

future wearing surface of 30 pounds per square foot of roadway is assumed, but no utilities are included. DW was applied as a surface load on the deck in the 3D analysis.

For computing flexural stresses from composite dead loads DC_2 and DW, the stiffness of the long-term composite section in regions of positive flexure is calculated by transforming the concrete deck using a modular ratio of 3*n* (Article 6.10.1.1.1b). In regions of negative flexure, the long-term composite section is typically assumed to consist of the steel section plus the longitudinal reinforcement within the effective width of the concrete deck (Article 6.10.1.1.1c).

5.2.2 Deck Placement Sequence

The deck is considered to be placed in the following sequence for the constructability limit state design checks (Figure 5) The concrete is first cast from the left abutment to a location near the dead load inflection point in Span 1. The concrete between approximate dead load inflection points in Span 2 is cast second. The concrete beyond the approximate dead load inflection point to the abutment in Span 3 is cast third. Finally, the concrete over the two piers is cast. In the analysis, earlier concrete casts are assumed fully composite for each subsequent cast. The modular ratio for the deck is assumed to be *3n* to account for creep. A smaller modular ratio may be desirable for the staging analyses since full creep usually takes approximately three years to occur (note that one State DOT has found a composite stiffness calculated using 1.4n to be appropriate). A modular ratio of *n* should be used to check the deck stresses.

For the constructability limit state design checks, the noncomposite section is checked for the moments resulting from the deck placement sequence or the moments computed assuming the entire deck is cast at one time, whichever is larger.

The weight of the fresh concrete on the overhang brackets, along with other loads applied to the brackets, produces lateral forces on the outermost top flange of G2 and the innermost top flange of G1. This eccentric loading and subsequent lateral forces on the top flanges must be considered in the constructability limit state design checks.

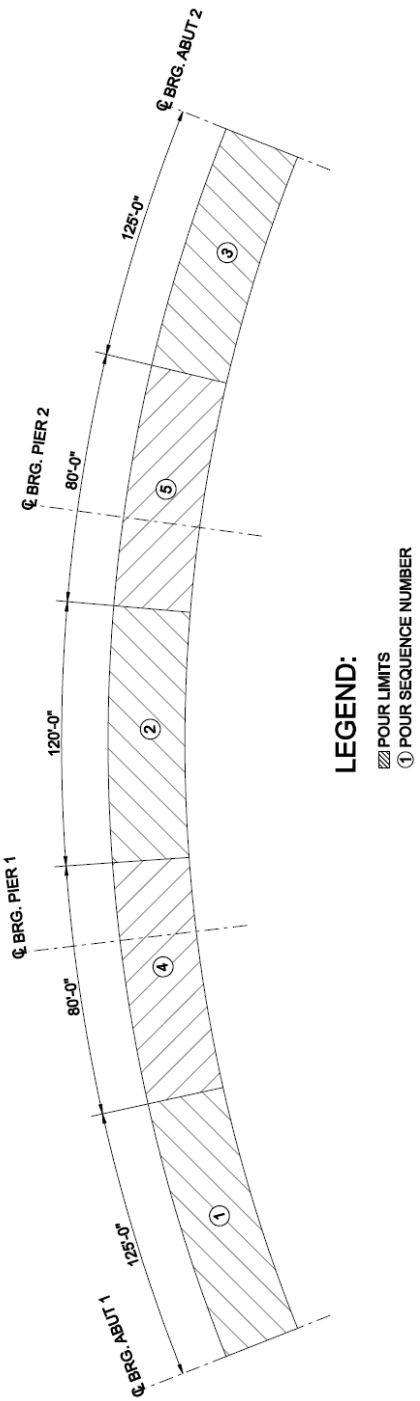

Figure 5 Assumed Deck Placement Sequence

5.2.3 Live Load

Live loads are assumed to consist of gravity loads (vehicular live loads, rail transit loads and pedestrian loads), the dynamic load allowance, centrifugal forces, and braking forces. Live loads illustrated in this example include the HL-93 vehicular live load and a fatigue load, with the appropriate dynamic load allowance and centrifugal force (see Section 5.3) effects included.

Influence surfaces are utilized to determine the live load force effects in this design example. More details regarding influence surfaces and the live load analysis associated with the 3D analysis model are provided in Section 6.1.2 of this example.

Live loads are considered to be transient loads applied to the short-term composite (*n*) section. For computing flexural stresses from transient loading, the short-term composite (*n*) section in regions of positive flexure is calculated by transforming the concrete deck using a modular ratio of *n* (Article 6.10.1.1.1b). In regions of negative flexure, the short-term composite (*n*) section is assumed to consist of the steel section plus the longitudinal reinforcement within the effective width of the concrete deck (Article 6.10.1.1.1c), except as permitted otherwise for the fatigue and service limit states (see Articles 6.6.1.2.1 and 6.10.4.2.1).

When computing longitudinal flexural stresses in the concrete deck due to permanent and transient loads, the short-term composite section should be used (see Article 6.10.1.1.1d).

Design Vehicular Live Load (Article 3.6.1.2)

The design vehicular live load is designated as the HL-93 and consists of a combination of the following placed within each design lane:

- a design truck *or* design tandem.
- a design lane load.

The design vehicular live load is discussed in greater detail in NSBA's *Steel Bridge Design Handbook: Example 1: Three-Span Continuous Straight Composite Steel I-Girder Bridge* [3].

Fatigue Load (Article 3.6.1.4)

The vehicular live load for checking fatigue consists of a single design truck (without the lane load) with a constant rear-axle spacing of 30 feet (Article 3.6.1.4.1). The fatigue live load is discussed in greater detail in NSBA's *Steel Bridge Design Handbook: Example 1: Three-Span Continuous Straight Composite Steel I-Girder Bridge* [3].

5.3 Centrifugal Force Computation

The centrifugal force is determined according to Article 3.6.3. The centrifugal force has two components, the radial force and the overturning force. The radial component of the centrifugal force is assumed to be transmitted from the deck through the end cross-frames or diaphragms and to the bearings and the substructure.

The overturning component of centrifugal force occurs because the radial force is applied at a distance above the top of the deck. The center of gravity of the design truck is assumed to be 6 feet above the roadway surface according to the provisions of Article 3.6.3. The transverse spacing of the wheels is 6 feet per Figure 3.6.1.2.2-1. The overturning component causes the exterior (with respect to curvature) wheel line to be more than half the weight of the truck and the interior wheel line to be less than half the weight of the truck by the same amount. Thus, the outside of the bridge is more heavily loaded. The effect of superelevation, which reduces the overturning effect of centrifugal force, is considered as permitted by Article 3.6.3. Figure 6 shows the centrifugal force wheel-load reactions. The dimensions denoted by s and h in Figure 6 are both equal to 6 feet.

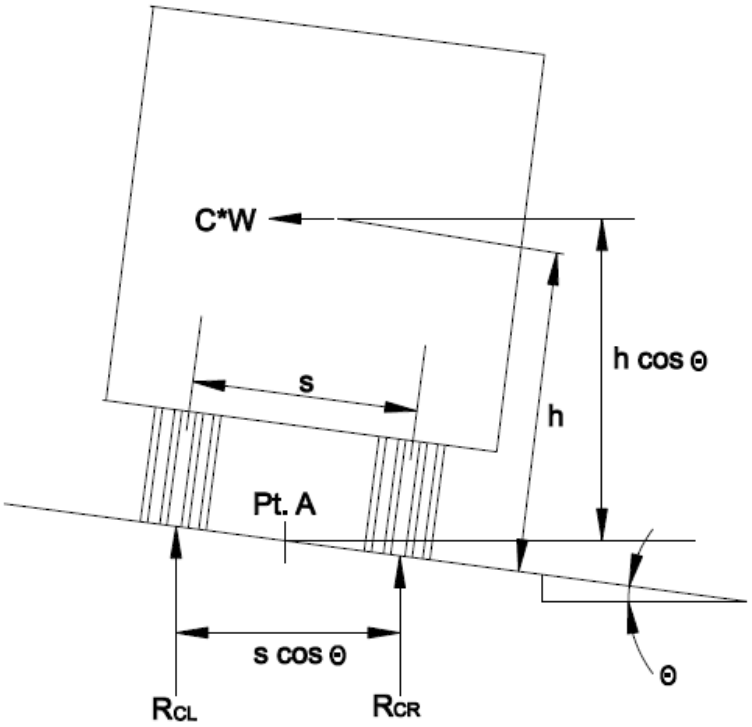

Figure 6 Vehicular Centrifugal Force Wheel-Load Reactions

Article 3.6.3 states that the centrifugal force is to be taken as the product of the axle weights of the design truck or tandem and the factor C, taken as:

$$C = f\,\frac{v^2}{g\,R} \qquad \text{Eq. (3.6.3-1)}$$

where:

f = 4/3 for load combinations other than fatigue and 1.0 for fatigue
v = highway design speed (ft/sec)
g = gravitational acceleration = 32.2 ft/sec^2
R = radius of curvature (ft)

Use the average bridge radius, R = 700 ft, in this case. For the purpose of this design example, the design speed is assumed to be 35 mph = 51.3 ft/s. Therefore, for the HL-93 design truck:

$$C = \frac{4}{3}\left[\frac{51.3^2}{(32.2)(700)}\right] = 0.156$$

The next step is to compute the wheel load reactions, R_{CL} and R_{CR}, due to centrifugal force effects, as shown in Figure 6. In the case of the design truck, the wheel spacing, s, and the height of the radial force, h, are both equal to 6.0 feet. Therefore, summing moments about Point A (Figure 6) and enforcing equilibrium, the wheel load reactions, R_{CL} and $-R_{CR}$ are simply equal to C multiplied by W, as follows:

$$R_{CL} = -R_{CR} = (C * W)\frac{h\cos(\theta)}{2\left(\frac{s}{2}\cos(\theta)\right)} = C * W = 0.156W$$

where:

W = axle weight (kips)

R_{CL} is an upward reaction for the left wheel, and R_{CR} is an equal but opposite downward reaction for the right wheel.

As permitted by Article 3.6.3, the effects of superelevation on the individual wheel load reactions can be computed and combined with the centrifugal force effects. For the 5% deck cross slope, the angle θ is equal to:

$\theta = \tan^{-1}(0.05) = 2.86°$

The wheel-load reactions due to superelevation, R_{SL} and R_{SR}, as shown in Figure 7, are computed by summing the moments about the left wheel and enforcing equilibrium, as follows:

$$R_{SR} = \frac{\left[\frac{s}{2}\cos(\theta) + h\sin(\theta)\right]W}{s\cos(\theta)} = \frac{\left[\left(\frac{6}{2}\right)\cos(2.86°) + (6)\sin(2.86°)\right]W}{(6)\cos(2.86°)} = 0.550W$$

$R_{SL} = 1.0W - R_{SR} = 1.0W - 0.550W = 0.450W$

If the superelevation is significant, the Engineer may wish to consider its effect for the case with no centrifugal force effects included (that is, a stationary vehicle), since the superelevation will cause an increase in the vertical wheel loads toward the inside of the bridge and an unloading of the vertical wheel loads toward the outside of the bridge, which may potentially be a more critical case for the interior girder.

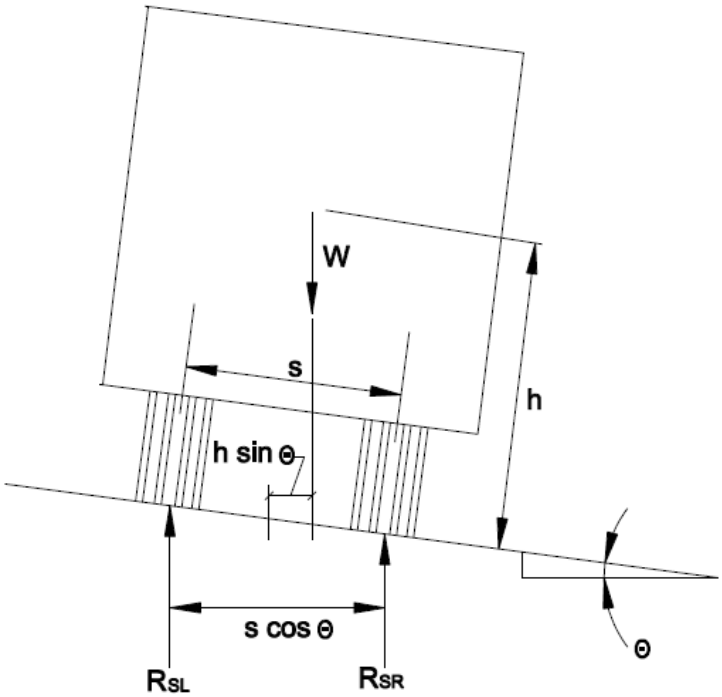

Figure 7 Effects of Superelevation of the Wheel-Load Reactions

For a refined analysis, as employed in this design example, unit wheel load factors can be computed based on the sum of the wheel load reactions due to the centrifugal force and superelevation effects. The unit wheel load factors are applied to the appropriate wheels in the analysis. Unit wheel load factors due to the combined effects of centrifugal force and superelevation can be computed for the left wheels, F_L, and the right wheels, F_R. The sum of F_L and F_R must equal 2.0, as there are two wheel loads per one axle. The left and right unit wheel load factors, F_L and F_R, are computed as follows:

$$F_L = 2.0\frac{R_{CL} + R_{SL}}{W} = 2.0\frac{0.156W + 0.450W}{W} = 1.212$$

$$F_R = 2.0\frac{R_{CR} + R_{RL}}{W} = 2.0\frac{-0.156W + 0.550W}{W} = 0.788$$

As shown in Figure 8, F_L and F_R represent the factors that must be multiplied by the left wheel and right wheel load, respectively, in the analysis to take into account the combined effects of both centrifugal force and superelevation. In this case, since F_L is greater than F_R, the outermost wheel of the design truck will receive a slightly higher load and the innermost wheel will receive a slightly lower load in the analysis. It is also necessary to compute the condition with no centrifugal force and no superelevation effects considered and select the worst case. In the live load analysis performed for this design example, strength and service limit state force effects from an analysis due to live load cases with centrifugal force effects included (F_L equals 1.212 and F_R equals 0.788) are compared to force effects due to cases with no centrifugal force and superelevation effects included (i.e., F_L and F_R equal 1.0), and the maximum/minimum force effect is selected.

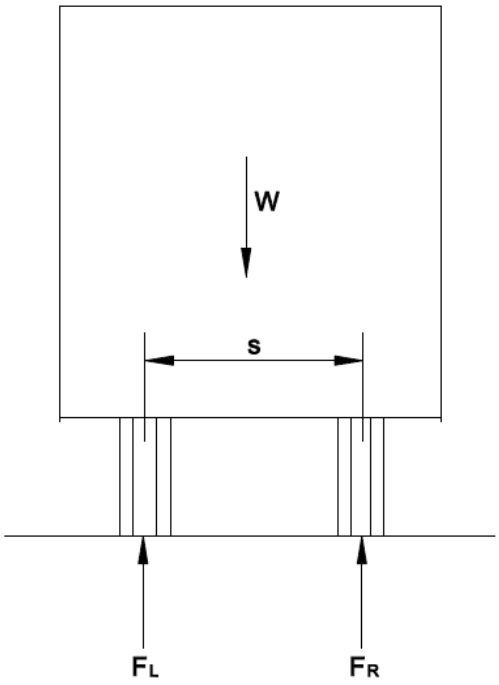

Figure 8 Unit Wheel Load Factors due to Combined Effects of Centrifugal Force and Superelevation

In accordance with Article C3.6.3, centrifugal force is not required to be applied to the design lane load, as the spacing of vehicles at high speed is assumed to be large, resulting in a low density of vehicles following and/or preceding the design truck. The design lane load is still considered, as applicable, even though the centrifugal force is not applied to the load.

From separate calculations for the fatigue limit state, similar to those shown previously, the centrifugal force factor C is equal to 0.117, and the unit wheel load factors, F_L and F_R, are 1.134 and 0.866, respectively.

5.4 Load Combinations

For each limit state described previously in Section 5.1, the following basic equation (Article 1.3.2.1) must be satisfied:

$$\Sigma\eta_i\gamma_i Q_i \leq \phi R_n = R_r \qquad \text{Eq. (1.3.2.1-1)}$$

where:

η_i = load modifier related to ductility, redundancy and operational importance
γ_i = load factor, a statistically based multiplier applied to force effects
ϕ = resistance factor, a statistically based multiplier applied to nominal resistance
Q_i = force effect

R_n = nominal resistance
R_r = factored resistance

The load factors are specified in Tables 3.4.1-1 and 3.4.1-2 of the specifications. For steel structures, the resistance factors are specified in Article 6.5.4.2.

As evident from the above equation, in the LRFD specifications, redundancy, ductility, and operational importance are considered more explicitly in the design. Ductility and redundancy relate directly to the strength of the bridge, while the operational importance relates directly to the consequences of the bridge being out of service. The grouping of these three effects on the load side of the above equation through the use of the load modifier η_i represents an initial attempt at their codification. Improved quantification of these effects may be possible in the future. For loads for which a maximum value of γ_i is appropriate:

$$\eta_i = \eta_D \eta_R \eta_I \geq 0.95 \qquad \text{Eq. (1.3.2.1-2)}$$

where:

η_D = ductility factor specified in Article 1.3.3
η_R = redundancy factor specified in Article 1.3.4
η_I = operational importance factor specified in Article 1.3.5

For loads for which a minimum value of γ_i is appropriate:

$$\eta_i = \frac{1}{\eta_D \eta_R \eta_I} \leq 1.0 \qquad \text{Eq. (1.3.2.1-3)}$$

Eq. (1.3.2.1-3) is only applicable for the calculation of the load modifier when dead- and live-load force effects are of opposite sign and the minimum load factor specified in Table 3.4.1-2 is applied to the dead-load force effects (e.g., when investigating for uplift at a support or when designing bolted field splices located near points of permanent load contraflexure); otherwise, Eq. (1.3.2.1-2) is to be used.

For typical bridges for which additional ductility-enhancing measures have not been provided beyond those required by the specifications, and/or for which exceptional levels of redundancy are not provided, the η_D and η_R factors have default values of 1.0 specified at the strength limit state. Note that some owner-agencies specify redundancy factors greater than 1.0 for certain types of steel tub girder bridges depending on the number of girders in the cross-section and the existence and number of external intermediate diaphragms. The value of the load modifier for operational importance η_I should be chosen with input from the Owner-agency. In the absence of such input, the load modifier for operational importance at the strength limit state should be taken as 1.0. At all other limit states, all three η factors must be taken equal to 1.0. For this example, η_i will be taken equal to 1.0 at all limit states.

Table 3.4.1-1 is used to determine load combinations for strength. The Strength I load combination is to be used for checking the strength of a member or component under normal use in the absence of wind. Load Combinations Strength III and V from Table 3.4.1-1 are checked for temperature and wind loadings in combination with vertical loading.

As described previously, Service I relates to normal operational use of the bridge in combination with a 70-mph wind with all loads taken at their nominal values and would be used primarily for crack control in reinforced concrete structures. However, the live-load portion of the Service I load combination is used for checking live-load deflection in steel bridges. Service II is used only for steel structures to control permanent deformations due to local yielding and slip of slip-critical connections under vehicular live load.

Two Fatigue load combinations are given in Table 3.4.1-1. The Fatigue I load combination is to be used when designing a detail or component for infinite fatigue life, and the Fatigue II load combination is to be used when designing a detail or component for finite fatigue life.

The following load combinations and load factors are typically checked in girder designs similar to this design example. For this example, it has been assumed that the Strength I load combination governs for the strength limit state, so only Strength I loads are checked in the sample calculations for the strength limit state included herein. In some design instances, other load cases may be critical, but for this example, these other load cases are assumed not to apply. Refer to NSBA's *Steel Bridge Design Handbook: Example 1 Three-Span Continuous Straight Composite Steel I-Girder Bridge* [3] for further detail on all of the load combinations specified in Table 3.4.1-1.

From Table 3.4.1-1 (minimum load factors of Table 3.4.1-2 are not considered here):

Strength I	$\eta \times [1.25(DC) + 1.5(DW) + 1.75((LL + IM) + CE + BR) + 1.2(TU)]$
Strength III	$\eta \times [1.25(DC) + 1.5(DW) + 1.0(WS) + 1.2(TU)]$
Strength V	$\eta \times [1.25(DC) + 1.5(DW) + 1.35((LL + IM) + CE + BR) + 1.0(WS) + 1.0(WL) + 1.2(TU)]$
Service I	$\eta \times [DC + DW + ((LL + IM) + CE + BR) + 1.0(WS) + 1.0(WL) + 1.2(TU)]$
Service II	$\eta \times [DC + DW + 1.3((LL + IM) + CE + BR) + 1.2(TU)]$
Fatigue I	$\eta \times [1.75((LL + IM) + CE)]$
Fatigue II	$\eta \times [0.80((LL + IM) + CE)]$

where:

η	=	Load modifier specified in Article 1.3.2
DC	=	Dead load: components and attachments
DW	=	Dead load: wearing surface and utilities
LL	=	Vehicular live load
IM	=	Vehicular dynamic load allowance
CE	=	Vehicular centrifugal force
WS	=	Wind load on structure
WL	=	Wind on live load
TU	=	Uniform temperature

BR = Vehicular braking force

When evaluating the strength of the structure for the maximum force effects during construction, the load factor for construction loads, for equipment and for dynamic effects (i.e., temporary dead and/or live loads that act on the structure only during construction) is not to be taken less than 1.5 in the Strength I load combination (Article 3.4.2.1). Also, the load factors for the weight of the structure and appurtenances, DC and DW, are not to be taken less than 1.25 when evaluating the construction condition. The load factor for wind load when evaluating the Strength III load combination during construction is to be specified by the Owner-agency (Article 3.4.2.1). Any applicable construction loads are to be included with a load factor not less than 1.25. Also, the load factors for the weight of the structure and appurtenances, DC and DW, are not to be taken less than 1.25 when evaluating the construction condition. The Strength II, IV, and V load combinations are not applicable to the investigation of construction stages.

Article 3.4.2.1 further states that unless otherwise specified by the Owner, primary steel superstructure components are to be investigated for maximum force effects during construction for an additional load combination consisting of the applicable DC loads and any construction loads that are applied to the fully erected steelwork. For this additional load combination, the load factor for DC and construction loads including dynamic effects (if applicable) is not to be taken less than 1.4. For steel superstructures, the use of higher-strength steels, composite construction, and limit-states design approaches in which smaller factors are applied to dead load force effects than in previous service-load design approaches, have generally resulted in lighter members overall. To provide adequate stability and strength of primary steel superstructure components during construction, an additional strength limit state load combination is specified for the investigation of loads applied to the fully erected steelwork (i.e., for investigation of the deck placement sequence and deck overhang effects).

Construction:	Strength I:	η x [1.25(D) + 1.5(C)]
	Strength III:	η x [1.25D + Owner-specified load factor * (WC)]
	Special Load Combination:	η x [1.4(D + C)]

where:

D = Dead load
C = Construction loads
WC = Wind load for construction conditions

In this design example, it has been assumed that there is no equipment on the bridge during construction and wind load is not considered during construction or in the final condition. Refer to NSBA's *Steel Bridge Design Handbook: Example 1: Three-Span Continuous Straight Composite Steel I-Girder Bridge* [3]. for an illustration of these wind-load checks. Thermal loads and vehicular braking forces are also not considered.

6.0 ANALYSIS

Article 4.4 of the *AASHTO LRFD BDS* requires that the analysis be performed using a method that satisfies the requirements of equilibrium and compatibility and utilizes stress-strain relationships for the proposed materials. Article 4.6.1.2 provides additional guidelines for structures that are curved in plan. The moments, shears, and other force effects required to proportion the superstructure components are to be based on a rational analysis of the entire superstructure. Equilibrium of horizontally curved I-girders is developed by the transfer of load between the girders, thus the analysis must recognize the integrated behavior of structural components. Equilibrium of horizontally curved tub girders can be somewhat less dependent on the interaction between girders, as there are typically fewer external bracing members between adjacent tub girders as compared to I-girder bridges, but the analysis should still recognize the integrated behavior of the structural components.

Furthermore, in accordance with Article 4.6.1.2, the entire superstructure, including bearings, is to be considered as an integral structural unit in the analysis. Boundary conditions should represent the articulations provided by the bearings and/or integral connections used in the design.

In most cases, small deflection elastic theory is acceptable for the analysis of horizontally curved steel girder bridges. However, curved girders, especially I-girders, are prone to deflect laterally when the girders are insufficiently braced during erection, and this behavior may not be appropriately recognized by small deflection theory. In most all curved tub-girder bridge construction, there is typically sufficient bracing provided during steel erection so that deflections do not invalidate the use of small deflection elastic theory.

In general, three levels of analysis exist for horizontally curved girder bridges: approximate methods of analysis, 2D (two-dimensional) methods of analysis, and 3D (three-dimensional) methods of analysis. The V-load method and the M/R methods are approximate analysis method that may be used to analyze curved I-girder bridges and curved tub girder bridges, respectively. Both methods are developed based on the understanding of the distribution of forces through the curved bridge system. The two primary types of 2D analysis models are the traditional grid (or grillage) model and the plate and eccentric beam model. In a traditional 2D analysis model, the girders and external cross-frames and diaphragms are modeled using beam elements, with the nodes for the grid representing the steel superstructure in a single horizontal plane. In a plate and eccentric beam model, the girders and cross-frames are modeled using beam elements, with nodes in a single horizontal plane, and the deck is modeled with shell elements offset a vertical distance from the steel superstructure elements. A 3D model recognizes the depth of the superstructure. Two planes of nodes are typically used for each girder, one in the plane of the top flanges and the second in the plane of the bottom flange. The deck in a 3D model is typically modeled with shell elements or solid elements. Further details regarding these methods of analysis can be found in NSBA's *Steel Bridge Design Handbook: Structural Analysis* [16] and in the FHWA *Manual for Refined Analysis in Bridge Design and Evaluation* [17].

It should be noted that when a tub-girder bridge satisfies the requirements of Article 4.6.1.2.4c, the effects of curvature may be ignored in the analysis for determining the major-axis bending moments and bending shears. If the requirements of Article 4.6.1.2.4c are satisfied, the tub girders

may be analyzed as individual straight girders with span lengths equal to the arc lengths. Internal cross-frame or diaphragm spacing is to be set to limit flange lateral bending effects in the top flanges before the deck hardens, which may be determined from an appropriate approximation [**Error! Reference source not found.**]. The internal cross-frame or diaphragm spacing must not e xceed 40 feet. Transverse bending and longitudinal warping stresses due to cross-section distortion may be neglected. Cross-frames or diaphragms and their connections are to be designed in accordance with the applicable provisions of Articles 6.7.4.3 and 6.13. At a minimum, cross-frame or diaphragms are to meet all applicable slenderness requirements specified in Articles 6.8.4 or 6.9.3, as applicable. Lateral bracing members are to be designed in accordance with Articles 6.7.5 and 6.13 for forces computed by rational means.

6.1 Three-Dimensional Finite Element Analysis

A three-dimensional finite element analysis was used to analyze the superstructure in this design example. The girder webs and bottom flanges were modeled using plate elements. The top flanges of each tub girder were modeled with beam elements. The girder elements were connected to nodes that were placed in two horizontal planes; one plane at the top flange level and one plane at the bottom flange level. The horizontal curvature of the girders was represented by a series of straight elements connected at the nodes, rather than by curved elements. Nodes were placed on all flanges along the girder at each internal cross-frame and top flange lateral bracing location, and typically at the middle of each top flange lateral bracing bay.

The composite deck was modeled using a series of eight-node solid elements attached to the girder top flanges with rigid beam elements, which represented the shear studs.

Bearings were modeled with dimensionless elements called “foundation elements.” These dimensionless elements can provide six different stiffnesses, with three for translation and three for rotation. If a guided bearing is to be modeled and is to be orientated along the tangential axis of a girder, a translational stiffness of zero is assigned to the stiffness in the tangential direction. The translational stiffness of the bearing, and supporting structure if not explicitly modeled, is assigned to the direction orthogonal to the tangential axis.

Internal cross-frame members were modeled with individual truss elements connected to the nodes at the top and bottom flange of the girders. Internal solid-plate diaphragms at the supports were modeled with a single plate element. External solid-plate diaphragms at the supports were modeled using three full-depth plate elements along the length of the diaphragm, and three beam elements placed at the top and bottom of the web representing the top and bottom flanges of the diaphragm. Since the plate and beam elements are isoparametric, three sets of elements were used to model the web and flanges of the external diaphragm to allow for the possibility of reverse curvature.

Top flange lateral bracing members were modeled with individual truss elements connected to nodes at the top flanges of the tub girders.

Article 4.6.3.3.4 specifies that the influence of end-connection eccentricities is to be considered in the calculation of the equivalent axial stiffness of single-angle and flange-connected tee-section cross-frame members in the analysis. In lieu of a more accurate analysis, Article C4.6.3.3.4

recommends that a stiffness reduction factor of 0.65 be applied to the axial stiffness, AE, of the cross-frame members in a 3D analysis, or when computing the equivalent beam stiffness of the cross-frame members in a 2D analysis, to account for the influence of the end-connection eccentricities. Although this reduction factor was not applied in the analysis for this design example, the use of this stiffness reduction factor is strongly encouraged.

6.1.1 Bearing Orientation and Arrangement

The orientation and horizontal restraint of the bearings affects the behavior of most girder bridges for most load conditions, and is particularly true for curved and skewed girder bridges. Furthermore, in tub girder bridges, one or two bearings can be used under each tub girder at each support.

The use of two bearings to support an individual girder at a support allows the girder torsion to be directly removed through the force couple provided by the bearings, and reduces the reaction demand in the bearings. Two-bearing systems typically work well with radial supports, but are impractical with supports skewed more than a few degrees where the tub girder and/or diaphragm stiffnesses work against the achievement of uniform bearing contact during various stages of girder erection and deck slab construction [1].

The use of one bearing to support an individual girder at a support optimizes contact between the girder and the bearing. One-bearing systems also tend to be more forgiving of construction tolerances, and at skewed supports, one-bearing systems are demonstrably better than two-bearing systems [1]. A disadvantage of one-bearing systems is that stiff cross-frames or diaphragms between girders are required to resolve the girder torsion into the bearings.

Although one-bearing systems are commonly used in modern tub-girder designs, in this example, two bearings are used at each girder support location. The centerline of each bearing is located 28.5 inches from the girder centerline at the support. Furthermore, the bearings at Pier 1 are assumed fixed against translation in both the radial and longitudinal directions (Fixed Bearings). The bearings at the abutments and at Pier 2 are assumed fixed against radial movement but free in the longitudinal direction (Guided Bearings). The longitudinal direction at each support varies, as in this case the longitudinal direction is taken along a straight line chord line between the fixed support (Pier 1) and each expansion bearing. Curved girder bridges do not expand and contract along the girder line, but more so along the aforementioned chord lines. Orientating the bearings in the manner discussed significantly reduces the longitudinal stresses in the girders horizontal reactions at the bearings that can occur due to thermal loading. Therefore, due to the bearing orientation and from a separate analysis, the girder demands due to thermal loading are determined to be quite small, and are neglected throughout these computations. In all designs, the thermal demands must be considered and properly addressed.

6.1.2 Live Load Analysis

The use of live load distribution factors is typically not appropriate for curved steel tub girder bridges because these structures are ideally analyzed as a system. Therefore, influence surfaces are most often utilized to more accurately determine the live load force effects in curved girder bridges.

Influence surfaces are an extension of influence lines, in that an influence surface not only considers the longitudinal position of the live loads but the transverse position as well.

Influence surfaces provide influence ordinates over the entire deck. The influence ordinates are determined by applying a series of unit vertical loads, one at a time, at selected longitudinal and transverse positions on the bridge deck surface. The magnitude of the response for the unit vertical load is the magnitude of the ordinate of the influence surface for the particular response at the point on the deck where the load is applied. The entire influence surface is created by curve fitting between calculated ordinates. Specified live loads are then placed on the surface, mathematically, at the critical locations, as allowed by the governing specification, to determine the maximum and minimum effects. The actual live load effect is determined by multiplying the live load by the corresponding ordinate. In the case of an HL-93 truck or tandem load, a different ordinate will exist for each wheel load. The total HL-93 truck or tandem live load effect is the summation of all the wheel loads times their respective ordinates. For the design lane load, the effect is determined by integrating the area of the influence surface under the load and multiplying it by the intensity of the load.

The fatigue load, which consists of a single design truck without a lane load, is analyzed in a similar manner as the HL-93 truck load.

In curved girder bridges, influence surfaces are generally needed for all live load force results, such as major-axis bending moments, flange lateral bending moments, girder shear, reactions, torques, deflections, cross-frame forces, diaphragm forces, lateral bracing forces, etc.

Unless noted otherwise, all live load force effects in this example were computed using influence surfaces developed using the three-dimensional analysis. The dynamic load allowance (impact) was included in the analysis, and was applied to the live-load force effects in accordance with Article 3.6.2 for strength, service, and fatigue as required. Multiple presence factors were also appropriately applied to the force effects from the analysis. Also, as appropriate, centrifugal force effects were considered in the analysis by applying adjustment factors to the wheel loads as described in Section 5.3 of this design example.

6.2 Analysis Results

This section shows the results from the three-dimensional analysis of the superstructure. Analysis results are provided for the moments, shears, and torques for girders G1 and G2. All analysis results are unfactored. The reported live load results included multiple presence factors, dynamic load allowance (impact), and centrifugal force effects.

Specific analysis results for design Section G2-1, which is located approximately 57 feet from the centerline of the bearings at Abutment 1, are provided in Table 7. These analysis results are used in the design computations associated with Section G2-1, provided later within this design example.

NOTE: *The analysis results shown herein apply to an example girder designed using earlier versions of the AASHTO LRFD (i.e., prior to the 8th Edition). Revisions to some of the plate sizes*

in this example design were necessary to provide a more reasonable b/t ratio for the bottom (tension) flange in regions of positive flexure and to provide a constant top-flange width within the interior-pier field section. While it is nearly always desirable to perform a new analysis whenever plate sizes are revised, the effect on the analysis results in this case was felt to be relatively minor and so new analyses were not performed. The primary intent of this example is to illustrate the proper application of the AASHTO LRFD provisions to the design of a continuous horizontally curved steel tub-girder bridge. However, this also illustrates that a designer should always be aware of specification changes and how they may affect a design and perhaps future load ratings.

Table 1 Girder G1 Unfactored Shears by Tenth Point

Girder G1 Unfactored Shears									
10th Point	Span Length	Dead Load				LL+I		Fatigue LL+I	
		$DC1_{STEEL}$	$DC1_{CONC}$	DC2	DW	Pos.	Neg.	Pos.	Neg.
	(ft)	(kip)	(kip)	(kip)	(kip)	(kip)	(kip)	(kip)	(kip)
0	0.00	27	114	25	33	139	-24	52	-4
1	15.74	19	80	12	15	115	-29	41	-6
2	31.49	10	45	8	10	94	-35	34	-9
3	47.23	5	23	5	6	78	-41	28	-12
4	62.97	-6	-25	-3	-4	53	-52	22	-16
5	78.71	-11	-44	-6	-7	40	-63	16	-22
6	94.46	-16	-69	-8	-11	31	-83	13	-27
7	110.20	-23	-98	-13	-17	25	-101	10	-34
8	125.94	-28	-116	-18	-23	21	-116	7	-40
9	141.69	-34	-137	-24	-32	19	-127	7	-43
10	157.43	-44	-171	-40	-54	14	-163	4	-53
10	0.00	45	175	41	55	171	-15	58	-4
11	20.66	31	128	23	31	140	-23	44	-6
12	41.33	25	110	16	21	124	-26	39	-7
13	61.99	17	72	10	13	101	-37	31	-12
14	82.65	11	47	5	6	78	-45	27	-15
15	103.31	0	0	0	0	58	-57	22	-22
16	123.98	-11	-47	-5	-6	43	-78	15	-27
17	144.64	-17	-72	-10	-14	36	-101	12	-31
18	165.30	-25	-110	-16	-21	26	-124	6	-39
19	185.96	-31	-127	-23	-31	23	-140	6	-46
20	206.63	-45	-175	-41	-55	14	-166	4	-55
20	0.00	44	171	40	54	167	-15	56	-4
21	15.74	34	137	24	32	128	-19	43	-7
22	31.49	28	116	18	23	116	-21	40	-7
23	47.23	23	98	13	17	101	-25	34	-10
24	62.97	16	69	8	11	83	-31	27	-13
25	78.71	11	44	6	7	64	-38	22	-16
26	94.46	6	25	3	4	51	-52	16	-22
27	110.20	-5	-23	-5	-6	41	-77	12	-28
28	125.94	-10	-45	-8	-10	32	-92	9	-34
29	141.69	-19	-80	-12	-16	27	-113	6	-41
30	157.43	-27	-114	-25	-34	24	-139	4	-52

Note: Reported shears are the vertical shears and are for major-axis bending plus torsion in the critical tub girder web.

Table 2 Girder G2 Unfactored Shears by Tenth Point

Girder G2 Unfactored Shears									
10th Point	Span Length	Dead Load				LL+I		Fatigue LL+I	
		$DC1_{STEEL}$	$DC1_{CONC}$	DC2	DW	Pos.	Neg.	Pos.	Neg.
	(ft)	(kip)	(kip)	(kip)	(kip)	(kip)	(kip)	(kip)	(kip)
0	0.00	31	110	39	52	128	-26	61	-12
1	16.26	19	74	17	22	110	-29	52	-12
2	32.51	11	44	11	15	93	-35	44	-12
3	48.77	5	21	6	8	75	-44	36	-12
4	65.03	-7	-26	-3	-5	54	-52	25	-18
5	81.29	-11	-45	-6	-8	40	-67	18	-27
6	97.54	-17	-69	-12	-16	36	-85	13	-34
7	113.80	-24	-97	-17	-23	33	-102	12	-43
8	130.06	-29	-117	-22	-29	26	-114	7	-49
9	146.31	-35	-137	-27	-35	16	-127	4	-53
10	162.57	-46	-185	-41	-55	13	-155	4	-61
10	0.00	47	185	44	58	160	-14	65	-4
11	21.34	32	130	28	37	135	-22	55	-4
12	42.68	26	105	22	29	120	-33	49	-9
13	64.01	17	69	15	20	100	-42	41	-13
14	85.35	12	46	7	10	78	-46	33	-16
15	106.69	0	0	0	0	57	-57	24	-24
16	128.03	-12	-46	-7	-10	46	-78	16	-33
17	149.36	-17	-69	-15	-20	41	-99	13	-41
18	170.70	-26	-105	-22	-29	33	-120	9	-50
19	192.04	-32	-130	-28	-37	22	-135	4	-55
20	213.38	-47	-185	-44	-58	14	-159	4	-64
20	0.00	46	185	41	55	158	-14	64	-4
21	16.26	35	137	27	35	128	-15	53	-4
22	32.51	29	117	22	29	115	-26	49	-7
23	48.77	24	97	17	23	102	-33	41	-12
24	65.03	17	69	12	16	85	-36	33	-13
25	81.29	11	45	6	8	67	-40	27	-18
26	97.54	7	26	3	5	52	-54	18	-25
27	113.80	-5	-21	-6	-8	44	-75	12	-36
28	130.06	-11	-44	-11	-15	34	-93	12	-44
29	146.31	-19	-74	-17	-22	28	-111	12	-52
30	162.57	-31	-110	-39	-52	26	-129	12	-61

Note: Reported shears are the vertical shears and are for major-axis bending plus torsion in the critical tub girder web.

Table 3 Girder G1 Unfactored Major-Axis Bending Moments by Tenth Point

Girder G1 Unfactored Major-Axis Bending Moments									
10th Point	Span Length	Dead Load				LL+I		Fatigue LL+I	
		$DC1_{STEEL}$	$DC1_{CONC}$	DC2	DW	Pos.	Neg.	Pos.	Neg.
	(ft)	(kip-ft)	(kip-ft)	(kip-ft)	(kip-ft)	(kip-ft)	(kip-ft)	(kip-ft)	(kip-ft)
0	0.00	0	0	0	0	0	0	0	0
1	15.74	521	2191	340	450	2472	-469	748	-98
2	31.49	882	3666	592	785	4330	-938	1252	-196
3	47.23	1049	4321	724	960	5412	-1408	1477	-293
4	62.97	1047	4320	734	972	5863	-1878	1545	-385
5	78.71	851	3503	620	821	5777	-2338	1502	-471
6	94.46	493	2043	387	514	5189	-2795	1367	-553
7	110.20	-75	-315	36	47	4109	-3915	1108	-667
8	125.94	-837	-3461	-434	-576	2602	-4547	714	-813
9	141.69	-1781	-7206	-1014	-1343	1252	-5559	270	-991
10	157.43	-2969	-11629	-1762	-2335	1061	-7784	231	-1249
10	0.00	-2969	-11629	-1762	-2335	1061	-7784	231	-1249
11	20.66	-1422	-5845	-802	-1062	1310	-4411	363	-810
12	41.33	-326	-1516	-95	-125	2993	-3033	924	-618
13	61.99	493	1881	425	563	4784	-2275	1324	-470
14	82.65	977	3900	733	972	5926	-2008	1556	-367
15	103.31	1118	4442	836	1108	6304	-1749	1616	-279
16	123.98	976	3900	733	972	5928	-2013	1556	-369
17	144.64	492	1880	424	562	4775	-2279	1326	-471
18	165.30	-327	-1519	-95	-127	3000	-3021	923	-616
19	185.96	-1422	-5848	-803	-1064	1315	-4421	381	-810
20	206.63	-2969	-11633	-1762	-2336	1062	-7788	233	-1230
20	0.00	-2969	-11633	-1762	-2336	1062	-7788	233	-1230
21	15.74	-1780	-7203	-1014	-1345	1248	-5556	270	-997
22	31.49	-837	-3459	-436	-577	2591	-4532	714	-810
23	47.23	-74	-312	34	46	4099	-3900	1107	-665
24	62.97	493	2044	386	511	5181	-2783	1367	-551
25	78.71	851	3504	618	819	5769	-2328	1502	-462
26	94.46	1047	4320	732	971	5855	-1868	1544	-378
27	110.20	1048	4321	723	958	5405	-1402	1477	-286
28	125.94	882	3666	591	784	4326	-993	1252	-191
29	141.69	521	2189	339	449	2470	-466	748	-96
30	157.43	0	0	0	0	0	0	0	0

Table 4 Girder G2 Unfactored Major-Axis Bending Moments by Tenth Point

Girder G2 Unfactored Major-Axis Bending Moments									
10th Point	Span Length	Dead Load				LL+I		Fatigue LL+I	
		$DC1_{STEEL}$	$DC1_{CONC}$	DC2	DW	Pos.	Neg.	Pos.	Neg.
	(ft)	(kip-ft)	(kip-ft)	(kip-ft)	(kip-ft)	(kip-ft)	(kip-ft)	(kip-ft)	(kip-ft)
0	0.00	0	0	0	0	0	0	0	0
1	16.26	555	2268	351	465	2606	-484	796	-95
2	32.51	938	3868	610	808	4559	-967	1330	-191
3	48.77	1116	4632	742	984	5687	-1446	1564	-289
4	65.03	1115	4633	745	988	6152	-1931	1630	-390
5	81.29	905	3780	622	824	6059	-2416	1579	-498
6	97.54	525	2207	373	494	5434	-2907	1427	-616
7	113.80	-79	-256	-1	-1	4308	-4097	1148	-757
8	130.06	-892	-3579	-501	-665	2751	-4768	750	-917
9	146.31	-1896	-7599	-1122	-1488	1305	-5836	287	-1110
10	162.57	-3154	-12272	-1923	-2550	1114	-8127	256	-1384
10	0.00	-3154	-12272	-1923	-2550	1114	-8127	256	-1384
11	21.34	-1513	-6169	-906	-1201	1401	-4629	388	-902
12	42.68	-348	-1473	-160	-211	3176	-3197	933	-692
13	64.01	525	2077	384	509	5018	-2366	1345	-527
14	85.35	1040	4196	704	934	6205	-2070	1587	-393
15	106.69	1190	4826	813	1077	6598	-1786	1655	-277
16	128.03	1039	4195	704	934	6204	-2065	1585	-391
17	149.36	525	2075	384	509	5001	-2355	1344	-524
18	170.70	-348	-1476	-159	-211	3166	-3165	932	-690
19	192.04	-1514	-6173	-906	-1200	1393	-4627	399	-901
20	213.38	-3155	-12275	-1922	-2547	1114	-8128	255	-1378
20	0.00	-3155	-12275	-1922	-2547	1114	-8128	255	-1378
21	16.26	-1895	-7595	-1121	-1485	1312	-5843	289	-1113
22	32.51	-891	-3577	-500	-662	2762	-4778	751	-923
23	48.77	-79	-253	1	2	4320	-4106	1151	-760
24	65.03	525	2208	375	496	5445	-2917	1430	-621
25	81.29	906	3781	624	827	6068	-2424	1581	-495
26	97.54	1115	4634	747	990	6160	-1936	1631	-387
27	113.80	1116	4632	743	986	5689	-1451	1564	-287
28	130.06	938	3867	611	810	4560	-971	1330	-190
29	146.31	555	2266	351	465	2607	-487	797	-95
30	162.57	0	0	0	0	0	0	0	0

Table 5 Girder G1 Unfactored Torques by Tenth Point

Girder G1 Unfactored Torques							
10th Point	Span Length	Dead Load				LL+I	
		$DC1_{STEEL}$	$DC1_{CONC}$	DC2	DW	Pos.	Neg.
	(ft)	(kip-ft)	(kip-ft)	(kip-ft)	(kip-ft)	(kip-ft)	(kip-ft)
0	0.00	42	286	-62	-83	660	-398
1	15.74	82	398	-54	-71	775	-448
2	31.49	34	189	-40	-53	756	-482
3	47.23	30	153	-40	-52	597	-389
4	62.97	-1	9	-23	-31	389	-307
5	78.71	-29	-125	-13	-17	309	-354
6	94.46	-33	-158	0	0	360	-479
7	110.20	-54	-262	21	28	462	-636
8	125.94	-25	-165	46	62	569	-766
9	141.69	-10	-135	83	110	668	-866
10	157.43	-22	-231	126	168	1049	-922
10	0.00	36	294	-144	-191	1049	-922
11	20.66	4	105	-89	-117	995	-702
12	41.33	60	309	-52	-68	919	-598
13	61.99	39	205	-22	-30	716	-464
14	82.65	61	261	-9	-11	555	-383
15	103.31	0	0	0	0	446	-430
16	123.98	-64	-261	9	11	413	-540
17	144.64	-39	-205	22	29	500	-724
18	165.30	-60	-309	52	68	625	-906
19	185.96	-4	-105	89	117	713	-991
20	206.63	-36	-294	144	190	928	-1046
20	0.00	22	231	-127	-169	928	-1046
21	15.74	10	134	-85	-112	874	-657
22	31.49	25	166	-47	-62	770	-549
23	47.23	54	262	-22	-29	640	-434
24	62.97	33	158	0	-1	482	-319
25	78.71	30	125	12	17	375	-281
26	94.46	1	-10	23	30	346	-378
27	110.20	-30	-153	39	51	434	-591
28	125.94	-34	-190	39	52	512	-751
29	141.69	-82	-398	57	75	503	-772
30	157.43	-42	-285	75	99	399	-662

Table 6 Girder G2 Unfactored Torques by Tenth Point

Girder G2 Unfactored Torques							
10th Point	Span Length	Dead Load				LL+I	
		$DC1_{STEEL}$	$DC1_{CONC}$	DC2	DW	Pos.	Neg.
	(ft)	(kip-ft)	(kip-ft)	(kip-ft)	(kip-ft)	(kip-ft)	(kip-ft)
0	0.00	43	98	180	238	621	-533
1	16.26	87	276	139	184	774	-503
2	32.51	35	92	104	137	785	-469
3	48.77	32	88	64	84	638	-427
4	65.03	-2	-22	21	28	412	-391
5	81.29	-32	-129	-19	-26	348	-439
6	97.54	-36	-125	-58	-76	333	-535
7	113.80	-59	-203	-87	-114	433	-676
8	130.06	-28	-53	-107	-140	552	-793
9	146.31	-10	63	-118	-155	687	-848
10	162.57	-22	48	-149	-197	980	-863
10	0.00	36	-33	193	254	980	-863
11	21.34	3	-101	160	212	978	-709
12	42.68	64	183	144	189	925	-569
13	64.01	40	118	105	138	754	-433
14	85.35	68	237	54	72	580	-425
15	106.69	0	0	0	0	477	-491
16	128.03	-68	-237	-55	-72	391	-596
17	149.36	-40	-118	-105	-138	456	-746
18	170.70	-64	-183	-144	-191	603	-915
19	192.04	-3	102	-161	-212	725	-974
20	213.38	-36	33	-193	-255	878	-976
20	0.00	22	-48	149	197	878	-976
21	21.34	10	-63	118	155	853	-674
22	42.68	28	53	107	140	799	-536
23	64.01	59	203	87	114	685	-430
24	85.35	36	125	58	76	542	-321
25	106.69	32	129	19	26	415	-360
26	128.03	1	22	-21	-28	385	-440
27	149.36	-32	-88	-64	-84	433	-626
28	170.70	-35	-92	-104	-137	502	-782
29	192.04	-87	-276	-139	-184	533	-783
30	213.38	-43	-98	-180	-237	533	-621

Table 7 Section G2-1 Unfactored Major-Axis Bending Moments and Torques

Unfactored Demands at Section G2-1 (10th Point = 3.5)									
Demand	Dead Load					LL+I		Fatigue LL+I	
	$DC1_{STEEL}$	$DC1_{CONC}$	$DC1_{CAST1}$	DC2	DW	Pos.	Neg.	Pos.	Neg.
Moment (kip-ft)	1144	4747	2979	765	1006	5920	-1689	-290	1525
Torque (kip-ft)	59	205	464	41	54	525	-409	-113	232

7.0 DESIGN

Sample design calculations at selected critical locations of Girder G2 are provided within this section. The calculations are intended to illustrate the application of some of the more significant provisions of the *AASHTO LRFD BDS*. As such, complete calculations for each girder section and all bridge components are not shown. Two critical girder section checks are provided: Section G2-1 represents a girder section checked for positive moment, and Section G2-2 represents a girder section at an interior pier and the maximum negative moment location. The sample girder design calculations illustrate provisions that need to be checked at the strength, service, fatigue, and constructability limit states. Also, sample calculations for determining tub girder distortional stresses based on the beam-on-elastic-foundation (BEF) analogy are provided.

Sample design calculations are also provided for the longitudinal bottom flange stiffener design, internal full-depth diaphragm design, bearing stiffener design, top flange lateral bracing member design, and a bolted field splice design. The sample design calculations make use of the moments, shears, and torques provided in the tables shown in Section 6.2 of this design example, and the section properties that are computed in the sections that follow. In the calculation of major-axis bending stresses throughout the sample calculations, compressive stresses are always shown as negative values and tensile stresses are always shown as positive values.

7.1 Girder Section Proportioning

Figure 9 illustrates the Girder G2 elevation, showing the flange and web sizes employed in this design example. The same flange and web sizes of Girder G2 are used on Girder G1, but with plate lengths radially proportional to the plate lengths for Girder G2.

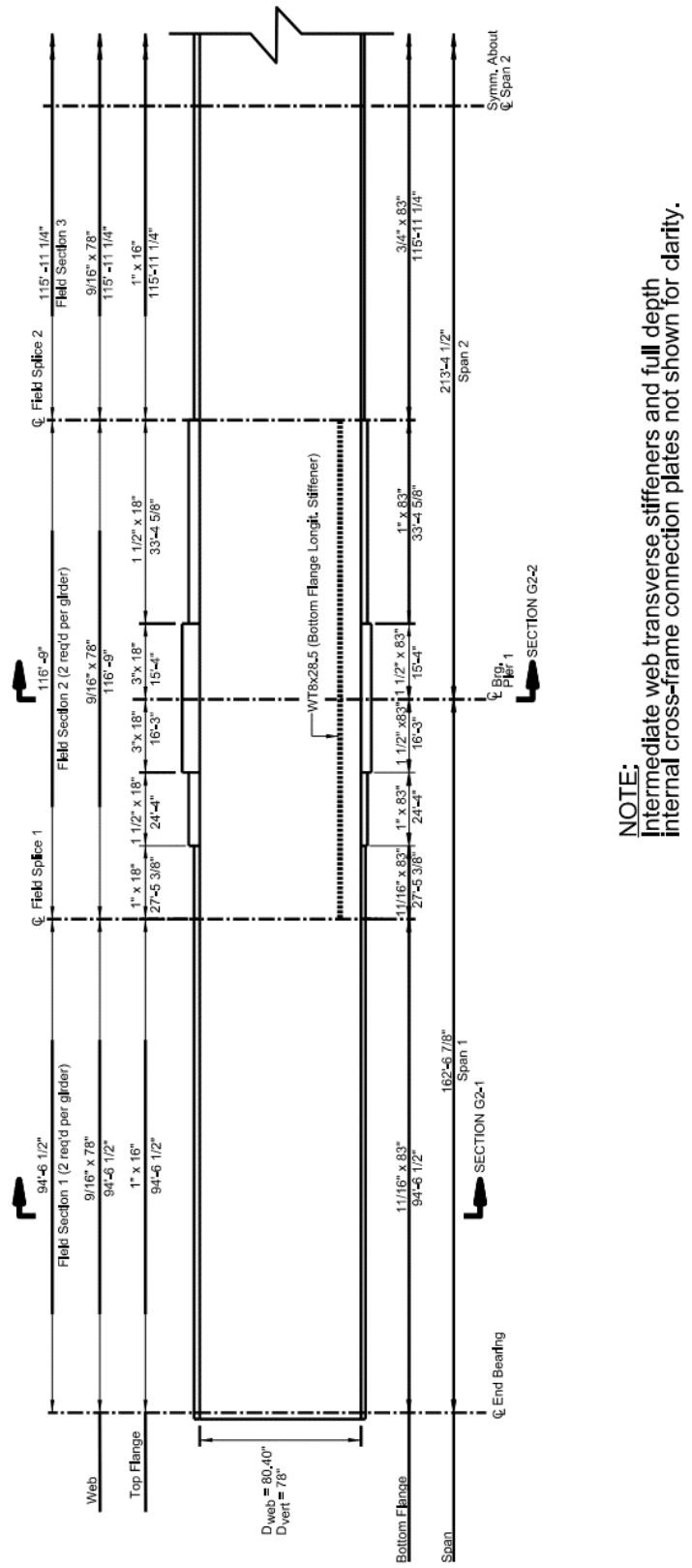

Figure 9 Girder G2 elevation

7.1.1 Girder Web Depth

Proper proportioning of tub girders involves a study of various girder depths versus girder weight to arrive at the least weight solution that meets all performance and handling requirements. The overall weight of the tub girder can vary dramatically based on web depth. Establishing a sound optimum depth for tub girders is particularly important because the sizes of the bottom flange plates can typically be varied less over the bridge length, Also, boxes that are overly shallow may potentially be subject to larger torsional shears. Therefore, selection of the proper depth is an extremely important consideration affecting the economy of the design. From a practical standpoint, tub girder web depths should not be less than about 5 feet to facilitate fabrication and inspection.

The NSBA Publication, *Practical Steel Tub Girder Design* [1] points out that a traditional rule of thumb for steel tub girder bridge depths is L/25, however designers should not be reluctant to exceed this ratio. Tangent steel tub girders have approached L/35 while meeting all code requirements for strength and deflection. Furthermore, tub girders are generally stiffer than I-girders because an individual tub nearly acts as two I-girders for major-axis bending. For torsion, an individual tub girder is significantly stiffer than two-I-girders.

Article 2.5.2.6.3 provides suggested minimum span-to-depth ratios for I-girders, but does not specifically address tub girder sections. The suggested minimum total depth of a composite I-girder in a continuous span is given as 0.032L, where L is the span length in feet. This criterion, which is based on the traditional span-to-depth ratio of L/25 for simple-span I-girders multiplied by a factor of 0.8 to account for double-end continuity in a continuous span, is applied herein to determine a starting depth of the tub girder for the depth studies. The length of the center span of the outside girder, Girder G2, is 213.38 feet (measured along the centerline of the tub section), which is the longest effective span in this design example. Therefore, the suggested minimum depth of the composite section is:

$$0.032(213.38) = 6.828 \text{ ft} = 81.9 \text{ in.}$$

Considering that 81.9 inches is the suggested minimum depth of the composite section including the depth of the concrete deck, a vertical web depth of 78.0 inches is chosen in this design example.

Note: The optimum depth for a box section will typically be slightly less than the optimum depth of an I-section for the same span because of the inherent torsional stiffness of a box section. It should be noted that given the relatively low performance ratios determined in the calculations that follow, a somewhat shallower vertical web depth could probably have been utilized in this example to provide a more efficient design. However, since the primary intent of this example is simply to illustrate the proper application of the AASHTO LRFD provisions to the design of a continuous horizontally curved steel tub-girder bridge, the calculations that follow are based on the originally selected vertical web depth of 78.0 inches.

Tub girders typically employ inclined webs, as they are advantageous in reducing the width of the bottom flange. Article 6.11.2.1 specifies that the web inclination should not exceed 1:4 (horizontal:vertical). Because progressively deeper webs may result in a narrower and potentially

thicker bottom flange plate (at location of maximum flexure), it is generally necessary for the Engineer to explore a wide range of web depths and web spacing options in conjunction with bottom flange requirements to determine the optimal solution.

The maximum recommended web inclination of 1:4 is used for this design example so as to minimize the bottom flange width. Based on the previously mentioned web depth study, a vertical web depth of 78.0 inches is selected, resulting in a distance of 81 inches between the centerline of the webs at the bottom flange. The actual bottom flange width is 83 inches in order to provide a minimum 1.0-inch flange extension on the outside of each web, which provides access for welding of the webs to the bottom flange. However, it should be noted, according to the AASHTO/NSBA Steel Bridge Collaboration Document *G1.4: Guidelines for Design Details* [10], most fabricators prefer a bottom flange extension of 1.5 inches, and 1.0 inch is the minimum. The 1.5-inch flange extensions shown in Figure 10 and Figure 12 are measured from the centerline of the web.

7.1.2 Cross-section Proportions

Proportion limits for webs of tub girders are specified in Article 6.11.2.1. Provisions for webs with and without longitudinal stiffeners are presented. For this example a longitudinally stiffened web is not anticipated. Therefore, the web plate must be proportioned such that the web plate thickness (t_w) meets the requirement:

$$\frac{D}{t_w} \le 150 \qquad \text{Eq. (6.11.2.1.2-1)}$$

where D is the distance along the web. For inclined webs, Article 6.11.2.1.1 states that the distance along the web is to be used for all design checks. The web thickness used along the entire length of both girders in this design example is 0.5625 inches. Determine the web depth along the incline:

$$D = 78\left(\frac{4.123}{4.0}\right) = 80.40 \text{ in.}$$

Checking Eq. (6.11.2.1.2-1):

$$\frac{D}{t_w} = \frac{80.40}{0.5625} = 142.9 < 150 \qquad \text{OK}$$

Cross-section proportion limits for top flanges of tub girders are specified in Article 6.11.2.2. The smallest top flange employed in this design example is 1.0 in. x 16.0 in. The minimum width of flanges is specified as:

$$b_f \ge \frac{D}{6} = \frac{80.40}{6} = 13.4 \text{ in.} \qquad \text{Eq. (6.11.2.2-2)}$$

Therefore, the minimum top flange width of 16.0 in. satisfies the requirements of Eq. (6.11.2.2-2). The minimum thickness of the top flange must satisfy the following two provisions:

$$\frac{b_f}{2t_f} \le 12.0 \qquad \text{Eq. (6.11.2.2-1)}$$

$$\frac{b_f}{2t_f} = \frac{16.0}{2(1.0)} = 8.0 < 12.0 \qquad \text{OK}$$

and,

$$t_f \ge 1.1\, t_w \qquad \text{Eq. (6.11.2.2-3)}$$

$$t_f = 1.0 \text{ in.} > 1.1\, t_w = 1.1(0.5625) = 0.62 \text{ in.} \quad \text{OK}$$

It should be noted that the AASHTO/NSBA Steel Bridge Collaboration document *G12.1: Guidelines to Design for Constructability and Fabrication* [12] recommends a minimum flange thickness of 0.75 inches to enhance girder stability during handling and erection.

The *AASHTO LRFD BDS* currently imposes no limitation on the b/t ratio of bottom flanges of composite tub girders in tension. Past and current industry guidance has suggested "rules of thumb" for the maximum b/t ratio ranging from as slender as 120 to as stocky as 80. White et al. (2019) [18] developed guidance (described below) which has been adopted in the *AASHTO LRFD BDS* for noncomposite steel box girder members, and which White et al. suggested should also be considered for composite steel tub girder bottom flanges. These limits are intended to address several fabrication concerns, including waviness and warping effects during welding of the bottom flange to the webs. Furthermore, the Engineer should be aware that it is possible that the bottom flange in tension in the final condition may be in compression during lifting of the tub girder during erection, possibly causing buckling of the slender bottom flange.

Article 6.12.2.2.2b suggests a limit on the b/t ratio, based on the inside width of the flanges, of 90 for longitudinally unstiffened compression and tension flanges in noncomposite box-section members to address similar concerns. Compression flanges exceeding this value must include longitudinal stiffeners. Tension flanges in these members with a b/t ratio exceeding 130 must include longitudinal stiffeners to prevent noticeable out-of-plane deflections of the flange under self-weight or under self-weight with a small concentrated transverse load. Unless otherwise specified by the Owner, a minimum thickness of 0.5 inches is also specified for compression and tension flanges in these members to limit potential local deformation or distortion of box section flanges during fabrication, transportation, erection, and service conditions. Additional information on these limits may be found in White et al. (2019) [18]. Additional discussion concerning this issue can also be found in the NSBA publication *Practical Steel Tub Girder Design* [1].

If it is desired to exceed the suggested b/t limit of 90 for tension flanges, the Engineer should consult with fabricators to verify that a tub girder with the selected bottom flange thickness in regions of positive flexure can be fabricated without causing any significant handling and/or distortion concerns without providing any flange longitudinal stiffeners. For this example, tension flanges in regions of positive flexure with thicknesses exceeding 0.5 inches and with a maximum

b/t ratio (based on the inside width of the flanges) of approximately 120 or less are utilized (maximum b/t = 79.4375/0.6875 = 115.5). This represents a reduction in the b/t ratios from the original design for this example, which was completed before the preceding guidance was available. In an actual design, consideration should probably be given to using a somewhat lower b/t for these flanges.

The AASHTO/NSBA Steel Bridge Collaboration document G1.4, *Guidelines for Design Details* [10] (Page 116) suggests preferred bottom flange extensions of 1-1/2 inches for welding access. Therefore, bottom flange extensions of 1-1/2 inches (measured from the centerline of the webs) were assumed in this design example.

7.2 Section Properties

The calculation of the section properties for Sections G2-1 and G2-2 is illustrated below. In computing the composite section properties, the structural slab thickness, or total thickness minus the thickness of the integral wearing surface, should be used. However, in the case of this design example, there is no integral wearing surface assumed, therefore the total structural thickness of the deck slab is 9.5 in.

For all section property calculations, the deck haunch depth of 4.00 in. is considered in computing the section properties, but the area of the deck haunch is not included. Since the actual depth of the haunch concrete may vary from its theoretical value to account for construction tolerances, some designers ignore the haunch concrete depth in all calculations. For composite section properties including only longitudinal reinforcement, the deck haunch depth is considered when determining the vertical position of the reinforcement relative to the steel girder. For the purposes of the section property calculations in this example, the longitudinal reinforcement steel area is assumed to be equal to 20.0 $in.^2$ per girder, and is assumed to be placed at the mid-depth of the effective structural deck thickness (see Section 7.2.3).

The section properties calculated herein also include the longitudinal component of the top flange lateral bracing area, the longitudinal bottom flange stiffener (where present), and the 1.5 in. bottom-flange extensions. A single top flange lateral bracing member of 8.0 $in.^2$ placed at an angle of 30 degrees from the girder tangent is assumed in this design example in the computation of the section properties. The inclusion of the longitudinal component of the top flange lateral bracing area is not required and may conservatively be neglected if desired.

The composite section consists of the steel section and the transformed area of the effective width of the concrete deck. Therefore, compute the modular ratio, *n* (Article 6.10.1.1.1b):

$$n = \frac{E}{E_c} \qquad \text{Eq. (6.10.1.1.1b-1)}$$

where E_c is the modulus of elasticity of the concrete determined as specified in Article 5.4.2.4. A unit weight of 0.150 kcf is used for the concrete in the calculation of the modular ratio, which is more conservative than the value given in Table 3.5.1-1 since it includes an additional 0.005 kcf to account for the weight of the reinforcement. The correction factor for source of aggregate, K_1,

is taken as 1.0. The traditional equation for E_c for normal-weight concrete given in Article C5.4.2.4 is used in this example.

$$E_c = 33,000\, K_1\, w_c^{1.5} \sqrt{f'_c} \qquad \text{Eq. (C5.4.2.4-2)}$$

$$E_c = 33,000\,(1.0)\,(0.150)^{1.5}\sqrt{4.0} = 3,834 \text{ ksi}$$

$$n = \frac{29,000}{3,834} = 7.56$$

n = 7.56 will be used in all subsequent computations in this design example.

7.2.1 Section G2-1: Span 1 Positive Moment Section Properties

Section G2-1 is located in Span 1, approximately 57 feet from the centerline of the bearing at Abutment 1. The cross-section for Section G2-1 is shown in Figure 10. For this section, the longitudinal reinforcement is conservatively neglected in computing the composite section properties as is typically assumed in design.

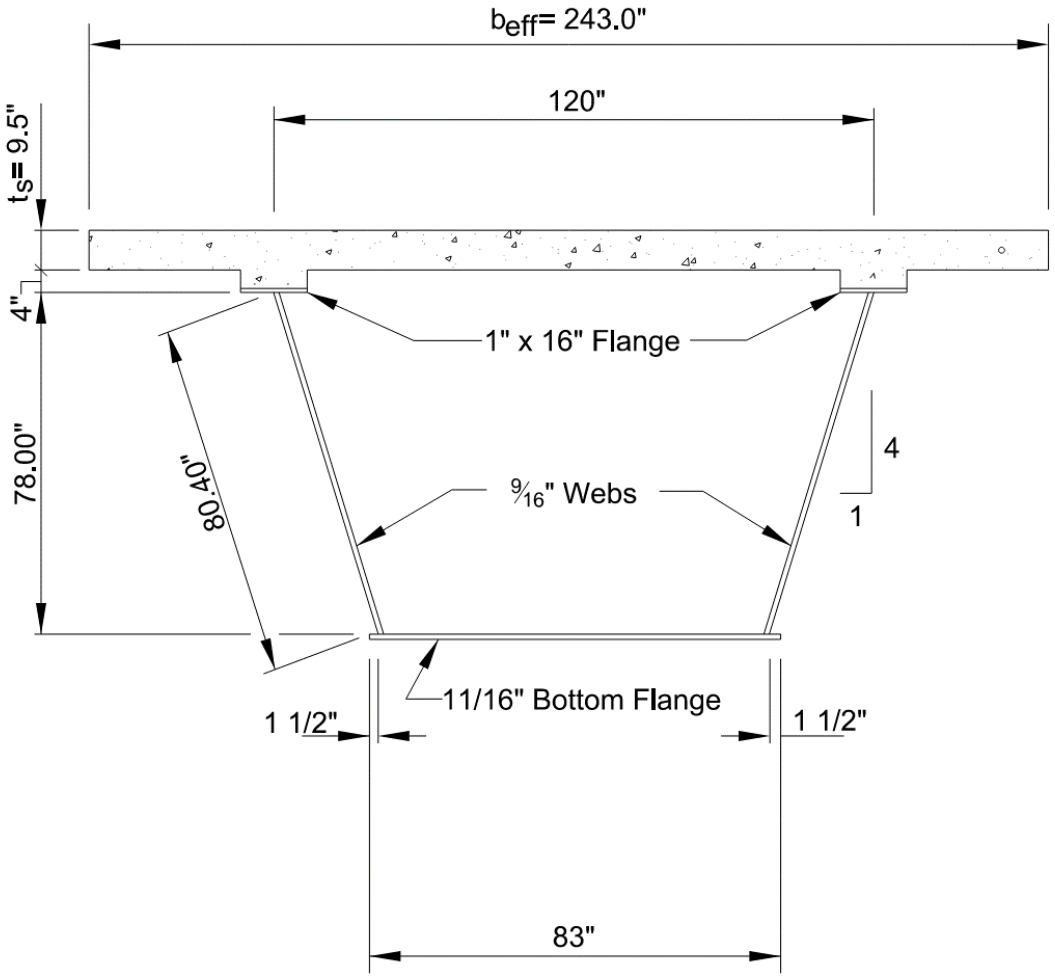

Figure 10 Tub-Girder Cross–Section at Section G2-1

7.2.1.1 Effective Width of Concrete Deck

As specified in Article 6.10.1.1.1e, the effective flange width is to be determined as specified in Article 4.6.2.6. According to Article 4.6.2.6, the deck slab effective width may be taken as the tributary width perpendicular to the axis of the member for determining the cross-section stiffnesses for analysis and for determining flexural resistances. In a typical two tub girder cross-section, the tributary width of the deck slab over each girder is taken as the distance between the two webs of the girder, plus half the distance from one web to the adjacent web of the adjacent girder plus the full overhang width. Therefore, the deck slab effective width, b_{eff}, for Girder G2 is:

$$b_{eff} = 4.00 + 10.00 + \frac{12.50}{2} = 20.25 \text{ ft} = 243 \text{ in.}$$

7.2.1.2 Elastic Section Properties: Section G2-1

For tub sections with inclined webs, the area of the inclined webs should be used in computing all section properties. As shown in Figure 11, the moment of inertia of a single inclined web, I_{ow}, with respect to a horizontal axis at mid-depth of the web is computed as:

$$I_{ow} = \frac{S^2}{S^2 + 1} I_w$$

where: S = web slope with respect to the horizontal (equal to 4.00 in this example)
I_w = moment of inertia of each inclined web with respect to an axis normal to the web

$$I_{ow} = \left(\frac{4.0^2}{4.0^2 + 1} \right) \frac{1}{12} (0.5625)(80.4)^3 = 22{,}929 \text{ in.}^4$$

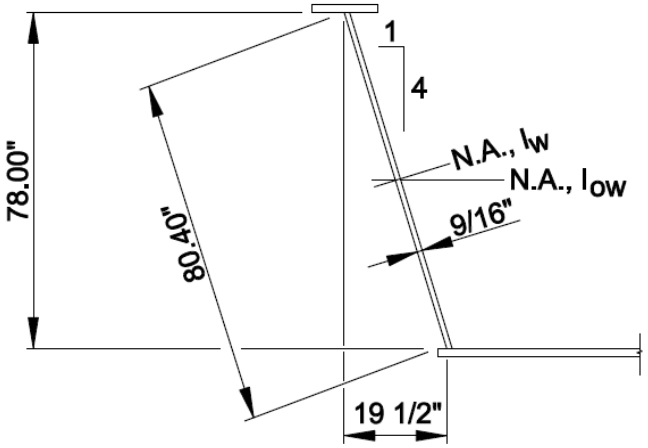

Figure 11 Moment of Inertia of an Inclined Web

In the calculations of the section properties that follow in Table 8 to Table 10, d is measured vertically from a horizontal axis through the mid-depth of the web to the centroid of each element of the tub girder.

Table 8 **Section G2-1: Steel Only Section Properties**

Component	A	d	Ad	Ad^2	I_o	I
2 Top Flanges 1" x 16"	32.00	39.50	1,264	49,928	2.67	49,931
2 Webs 9/16" x 80.40"	90.45				45,858	45,858
Bottom Flange 11/16" x 83"	57.06	-39.34	-2,245	88,308	2.25	88,310
Top Flange Lat. Bracing 8.0 $in.^2$ @ 30°	6.93	39.50	273.7	10,813		10,813
Σ	186.44		-707.3			194,912

-3.79(707.3) = -2,681

I_{NA} = 192,231 $in.^4$

$$d_s = \frac{-707.3}{186.44} = -3.79 \text{ in.}$$

$d_{\text{Top of Steel}} = 40.00 + 3.79 = 43.79 \text{ in.}$ $d_{\text{Bot of Steel}} = 39.69 - 3.79 = 35.90 \text{ in.}$

$S_{\text{Top of Steel}} = \frac{192,231}{43.79} = 4,390 \text{ in.}^3$ $S_{\text{Bot of Steel}} = \frac{192,231}{35.90} = 5,355 \text{ in.}^3$

Table 9 **Section G2-1: 3*n*=22.68 Composite Section Properties**

Component	A	d	Ad	Ad^2	I_o	I
Steel Section	186.44		-707.3			194,912
Concrete Slab 9½″ x 243″/22.68	101.8	47.75	4,861	232,110	765.5	232,876
Σ	288.24		4,154			427,788

-14.41(4,154) = -59,859

I_{NA} = 367,929 in.^{4}

$d_{3n} = \frac{4,154}{288.24} = 14.41 \text{ in.}$

$d_{\text{Top of Steel}} = 40.00 - 14.41 = 25.59 \text{ in.}$ $d_{\text{Bot of Steel}} = 39.69 + 14.41 = 54.10 \text{ in.}$

$S_{\text{Top of Steel}} = \frac{367,929}{22.59} = 14,378 \text{ in.}^3$ $S_{\text{Bot of Steel}} = \frac{367,929}{54.10} = 6,801 \text{ in.}^3$

Table 10 **Section G2-1: *n*=7.56 Composite Section Properties**

Component	A	d	Ad	Ad^2	I_o	I
Steel Section	186.44		-707.3			194,912
Concrete Slab 9½″ x 243″/7.56	305.4	47.75	14,583	696,331	2,297	698,628
Σ	491.84		13,876			893,540

-28.21(13,876) = -391,442

I_{NA} = 502,098 in.^{4}

$d_n = \frac{13,876}{491.84} = 28.21 \text{ in.}$

$d_{\text{Top of Steel}} = 40.00 - 28.21 = 11.79 \text{ in.}$ $d_{\text{Bot of Steel}} = 39.69 + 28.21 = 67.90 \text{ in.}$

$S_{\text{Top of Steel}} = \frac{502,098}{11.79} = 42,587 \text{ in.}^3$ $S_{\text{Bot of Steel}} = \frac{502,098}{67.90} = 7,395 \text{ in.}^3$

7.2.1.3 Plastic Moment Neutral Axis: Section G2-1

As specified in Article 6.11.6.2.2 for sections in positive flexure, the ductility requirement of Article 6.10.7.3 must be satisfied for compact and noncompact sections to protect the concrete deck from premature crushing. This requires the computation of the plastic neutral axis in

accordance with Article D6.1. The longitudinal deck reinforcement is conservatively neglected. The location of the plastic neutral axis for the entire tub girder is computed as follows:

$P_t = F_{yt}b_t t_t$ = (50)(83.00)(0.6875) = 2,853 kips
$P_w = 2F_{yw}Dt_w$ = (2)(50)(80.40)(0.5625) = 4,523 kips
$P_c = 2F_{yc}b_c t_c$ = (2)(50)(16.00)(1.00) = 1,600 kips
$P_s = 0.85f'_c b_{eff} t_s$ = (0.85)(4.0)(243)(9.5) = 7,849 kips
$P_{rb} = P_{rt} = 0$ kips

$P_t + P_w + P_c > P_s + P_{rb} + P_{rt}$
2,853 + 4,523 + 1,600 = 8,976 kips > 7,849 kips

Therefore, the plastic neutral axis (PNA) is in the top flange according to Case II of Table D6.1-1. Compute the PNA in accordance with Case II:

$$\overline{Y} = \frac{t_c}{2}\left[\frac{P_w + P_t - P_s - P_{rt} - P_{rb}}{P_c} + 1\right] = \frac{1.00}{2}\left[\frac{4,523 + 2,853 - 7,849 - 0 - 0}{1,600} + 1\right]$$

$\overline{Y}$ = 0.35 in. downward from the top of the top flange (PNA location)

7.2.2 Section G2-2: Support 2 Negative Moment Section Properties

Section G2-2 is located at Support 2, and is as shown in Figure 12. The effective width of concrete deck is the same for Section G2-2 as calculated for Section G2-1, b_{eff} = 243.0 in.

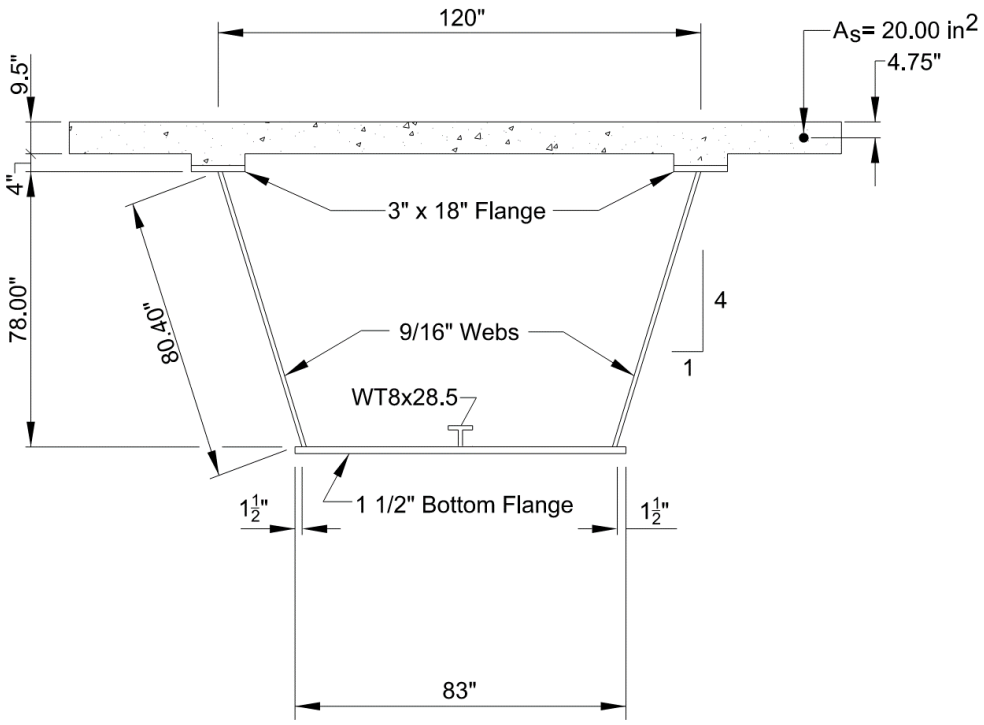

Figure 12 Tub-Girder Cross–Section at Section G2-2

7.2.2.1 Elastic Section Properties: Section G2-2

For members with shear connectors provided throughout their entire length that also satisfy the provisions of Article 6.10.1.7, Articles 6.6.1.2.1 and 6.10.4.2.1 permit the concrete deck to also be considered effective for negative flexure when computing stress ranges and flexural stresses acting on the composite section at all sections in the member at the fatigue and service limit states, respectively. Therefore, section properties for the short-term and long-term composite section, including the concrete deck but neglecting the longitudinal reinforcement, are also determined for later use in the calculations of Section G2-2 at these limit states.

Although not required by the *AASHTO LRFD BDS*, for stress calculations involving the application of long-term loads to the composite section in regions of negative flexure in this example, the area of the longitudinal reinforcement is conservatively adjusted for the effects of concrete creep by dividing the area by 3 (i.e. 20.00 $in.^2/3 = 6.67$ $in.^2$). The concrete is assumed to transfer the force from the longitudinal deck reinforcement to the rest of the cross-section and concrete creep acts to reduce that force over time.

As shown in Figure 12, a single WT 8x28.5 is utilized as a bottom flange longitudinal stiffener with the stem welded to the bottom flange and is placed at the centerline of the bottom flange. The WT 8x28.5 is considered in the section property computations.

In the calculation of the section properties that follow in Table 11 to Table 15, d is measured vertically from a horizontal axis through the mid-depth of the web to the centroid of each element of the tub girder.

Table 11 Section G2-2: Steel Only Section Properties

Component	A	d	Ad	Ad^2	I_o	I
2 Top Flanges (3" x 18")	108.0	40.50	4,374	177,147	81.0	177,228
2 Webs (9/16" x 80.40")	90.45	0.00			45,858	45,858
Bottom Flange (1.50" x 83")	124.5	-39.75	-4,949	196,718	23.3	196,741
Top Flange Lat. Bracing (8 $in.^2$ @ 30°)	6.93	40.50	280.7	11,367	0	11,367
Bottom Flange Stiffener WT 8x28.5	8.39	-32.72	-274.5	8,982	48.7	9,031
	338.3		-568.8			440,225
					$-(-1.68)(-568.8) =$	-956
					$I_{NA} =$	439,269 $in.^4$

$$d_s = \frac{-568.8}{338.3} = -1.68 \text{ in.}$$

$$d_{TOP OF STEEL} = 42.00 + 1.68 = 43.68 \text{ in.}$$

$$S_{TOP OF STEEL} = \frac{439,269}{43.68} = 10,057 \text{ in.}^3$$

$$d_{BOT OF STEEL} = 40.50 - 1.68 = 38.82 \text{ in.}$$

$$S_{BOT OF STEEL} = \frac{439,269}{38.82} = 11,316 \text{ in.}^3$$

Table 12 Section G2-2: 3*n*=22.68 Composite Section Properties with Transformed Deck

Component	A	d	Ad	Ad^2	I_o	I
Steel Section	338.3		-568.8			440,225
Concrete Slab (9½" x 243")/22.68	101.8	47.75	4,861	232,110	765.5	232,876
	440.1		4,292			673,101
					$-9.75(4,292) =$	-41,847
					$I_{NA} =$	631,254 $in.^4$

$$d_{3n} = \frac{4,292}{440.1} = 9.75 \text{ in.}$$

$$d_{TOP OF STEEL} = 42.00 - 9.75 = 32.25 \text{ in.}$$

$$S_{TOP OF STEEL} = \frac{631,254}{32.25} = 19,574 \text{ in.}^3$$

$$d_{BOT OF STEEL} = 40.50 + 9.75 = 50.25 \text{ in.}$$

$$S_{BOT OF STEEL} = \frac{631,254}{50.25} = 12,562 \text{ in.}^3$$

Table 13 Section G2-2: *n*=7.56 Composite Section Properties with Transformed Deck

Component	A	d	Ad	Ad^2	I_o	I
Steel Section	338.3		-568.8			440,225
Concrete Slab (9½" x 243")/7.56	305.4	47.75	14,583	696,331	2,297	698,628
	643.7		14,014			1,139,372
					$-21.77(14{,}014) =$	-305,085
					$I_{NA} =$	833,768 in.^{4}

$$d_n = \frac{14{,}014}{643.7} = 21.77 \text{ in.}$$

$$d_{TOP\,OF\,STEEL} = 42.00 - 21.77 = 20.23 \text{ in.} \qquad d_{BOT\,OF\,STEEL} = 40.50 + 21.77 = 62.27 \text{ in.}$$

$$S_{TOP\,OF\,STEEL} = \frac{833{,}768}{20.23} = 41{,}234 \text{ in.}^3 \qquad S_{BOT\,OF\,STEEL} = \frac{833{,}768}{62.27} = 13{,}390 \text{ in.}^3$$

Table 14 Section G2-2: 3*n* Composite Section Properties with Longitudinal Steel Reinforcement

Component	A	d	Ad	Ad^2	I_o	I
Steel Section	338.3		--568.8			440,225
Longitudinal Reinforcement	6.67	47.75	318.5	15,208		15,208
	345.0		-250.3			455,940
					$-(-0.73)(-250.3) =$	-183
					$I_{NA} =$	455,250 in.^{4}

$$d_{3n} = \frac{-250.3}{345.0} = -0.73 \text{ in.}$$

$$d_{TOP\,OF\,STEEL} = 42.00 + 0.73 = 42.73 \text{ in.} \qquad d_{BOT\,OF\,STEEL} = 40.50 - 0.73 = 39.77 \text{ in.}$$

$$S_{TOP\,OF\,STEEL} = \frac{455{,}250}{42.73} = 10{,}654 \text{ in.}^3 \qquad S_{BOT\,OF\,STEEL} = \frac{455{,}250}{39.77} = 11{,}447 \text{ in.}^3$$

Table 15 Section G2-2: *n* Composite Section Properties with Longitudinal Steel Reinforcement

Component	A	d	Ad	Ad^2	I_o	I
Steel Section	338.3		-568.8			440,225
Longitudinal Reinforcement	20.0	47.75	955.0	45,601		45,601
	358.3		386.2			486,333
					$-1.06(378.5) =$	-417
					$I_{NA} =$	485,409 in.^{4}

$$d_n = \frac{386.2}{358.3} = 1.08 \text{ in.}$$

$$d_{TOP\,OF\,STEEL} = 42.00 - 1.08 = 40.94 \text{ in.} \qquad d_{BOT\,OF\,STEEL} = 40.50 + 1.08 = 41.58 \text{ in.}$$

$$S_{TOP\,OF\,STEEL} = \frac{485{,}409}{40.92} = 11{,}862 \text{ in.}^3 \qquad S_{BOT\,OF\,STEEL} = \frac{485{,}409}{41.58} = 11{,}674 \text{ in.}^3$$

7.2.3 Check of Minimum Negative Flexure Concrete Deck Reinforcement (Article 6.10.1.7)

To control concrete deck cracking in regions of negative flexure, Article 6.10.1.7 specifies that the total cross-sectional area of the longitudinal reinforcement must not be less than 1 percent of the total cross-sectional area of the deck. The minimum longitudinal reinforcement must be provided wherever the longitudinal tensile stress in the concrete deck due to either the factored construction loads or Load Combination Service II exceeds ϕf_r. ϕ is to be taken as 0.9 and f_r is to be taken as the modulus of rupture of the concrete determined as follows:

- For normal weight concrete: $f_r = 0.24\sqrt{f_c'}$
- For lightweight concrete: f_r is calculated as specified in Article 5.4.2.6.

It is further specified that the reinforcement is to have a specified minimum yield strength not less than 60 ksi and a size that should not exceed No. 6 bars. The reinforcement should be placed in two layers uniformly distributed across the deck width, and two-thirds should be placed in the top layer. The individual bars should be spaced at intervals not exceeding 12 inches.

Article 6.10.1.1.1c states that for calculating stresses in composite sections subjected to negative flexure at the strength limit state, the composite section for both short-term and long-term moments is to consist of the steel section and the longitudinal reinforcement within the effective width of the concrete deck. Referring to the cross-section shown in Figure 2:

$$A_{deck} = (\text{entire width of 9.5"-thick deck}) + (\text{triangular portion of overhang})$$

$$A_{deck} = \frac{9.5}{12}(40.5) + 2\left[\frac{1}{2}\left(\frac{4.0}{12}\right)\left(4.0 - \frac{16.0/2}{12}\right)\right] = 33.17 \text{ ft}^2 = 4{,}777 \text{ in.}^2$$

$$0.01(4{,}777) = 47.77 \text{ in.}^2$$

$$\frac{47.77}{40.5} = 1.18 \text{ in.}^2/\text{ft} = 0.098 \text{ in.}^2/\text{in.}$$

$$0.098(243.0) = 23.81 \text{ in.}^2 \text{ per tub girder}$$

Therefore, the assumption of 20.00 in.^{2} for the longitudinal deck reinforcement used in the calculation of the section properties for Section G2-1 (Table 14 and Table 15), which was assumed in the original design example, is conservative as the longitudinal deck reinforcement to be used is more than that assumed in the section property calculations. In the actual deck, the longitudinal reinforcement should have a minimum cross-sectional area of 23.81 in.^{2} per tub girder. If the reinforcement is detailed, #6 bars at 6 inches are placed in the top layer, and #4 bars at 6 inches are placed in the bottom layer. Therefore, the total area of deck reinforcement steel in the given effective width of concrete deck is:

$$A_S = \left(0.44 + 0.44 + 0.20 \ + \ 0.20\right)\left(\frac{243.0}{12}\right) = 25.92 \text{ in.}^2 > 23.81 \text{ in.}^2$$

Also, approximately two-thirds of the reinforcement is in the top layer: $\frac{0.44 + 0.44}{1.28} = 0.69 \approx \frac{2}{3}$

7.3 Girder Check: Section G2-1, Constructability (Article 6.11.3)

Article 6.11.3 directs the engineer to Article 6.10.3 for discussion regarding the constructability checks of tub girders. For critical stages of construction, the provisions of Articles 6.10.3.2.1 through 6.10.3.2.3 are to be applied to the top flanges of the tub girder. The noncomposite bottom tub flange in compression or tension is to satisfy the requirements specified in Article 6.11.3.2. Web shear is to be checked in accordance with Article 6.10.3.3, with the shear to be taken along the slope of the web in accordance with the provisions of Article 6.11.6.

As specified in Article 6.10.3.4.1, sections in positive flexure that are composite in the final condition, but noncomposite during construction, are to be investigated during the various stages of deck placement. The effects of forces from deck overhang brackets acting on the fascia girders are also to be considered. Wind load effects on the noncomposite structure prior to and during casting are also an important consideration during construction. The presence of construction equipment may also need to be considered. Lastly, the potential for uplift at bearings should be investigated at each critical construction stage. For this design example, the effects of wind load on the structure and the presence of construction equipment are not considered.

Calculate the maximum flexural stresses in the flanges of the steel section due to the factored loads resulting from the application of steel self-weight and Cast #1 of the deck placement sequence. Cast #1 yields the maximum positive moment in the noncomposite Section G2-1. As specified in Article 6.10.1.6, for design checks where the flexural resistance is based on lateral torsional buckling, f_{bu} is to be determined as the largest value of the compressive stress throughout the unbraced length in the flange under consideration, calculated without consideration of flange lateral bending. For design checks where the flexural resistance is based on yielding, flange local buckling or web bend-buckling, f_{bu} may be determined as the stress at the section under consideration. From Figure 1, brace points adjacent to Section G2-1 are located at intervals of approximately 16.3 feet, and the largest stress occurs within this unbraced length.

In accordance with Article 3.4.2.1, when investigating Strength I during construction, load factors for the weight of the structure and appurtenances, DC and DW, are not to be taken to be less than 1.25. Also, as discussed previously, the η factor is taken equal to 1.0 in this example. As shown in Table 7 the unfactored moments due to steel self-weight and Cast #1 are 1,144 k-ft and 2,979 k-ft, respectively. Therefore,

For Construction Strength I:

General: $$f_{bu} = \frac{\eta \, \gamma \, M_{DC}}{S_{nc}}$$

Top Flanges: $f_{bu} = \frac{1.0(1.25)(1{,}144 + 2{,}979)(12)}{4{,}390} = -14.09 \text{ ksi}$

Bot. Flange: $f_{bu} = \frac{1.0(1.25)(1{,}144 + 2{,}979)(12)}{5{,}355} = 11.55 \text{ ksi}$

Although not included in this example in the interest of brevity, the special load combination specified in Article 3.4.2.1 must also be considered in the design checks for the DC loads and construction loads, C, applied to the fully erected steelwork during the deck placement sequence (see Section 5.4).

7.3.1 Deck Overhang Bracket Load

During construction, the weight of the deck overhang wet concrete is resisted by the deck overhang brackets. Other loads supported by the overhang brackets during construction include the formwork, screed rail, railing, worker walkway, and possibly the deck finishing machine.

The deck overhang construction loads are typically applied to the noncomposite section and are removed once the concrete deck has become composite with the steel girders. The deck overhang bracket imparts a lateral force on the top and bottom flanges resulting in lateral bending of the flanges. The lateral bending of the top flange must be considered as part of the constructability check, however in a tub girder bridge, the flange lateral bending of the bottom flange is typically ignored due to the large section modulus of the bottom flange in the lateral direction. Also, it should be noted that if the bottom of the bracket does not bear on the web near the junction of the web and bottom flange, additional support and/or stiffening of the web may be warranted.

Since G2 is a fascia girder, one-half of the deck overhang weight is assumed to be carried by the girder and one-half is assumed placed on the overhang brackets, as shown in Figure 13.

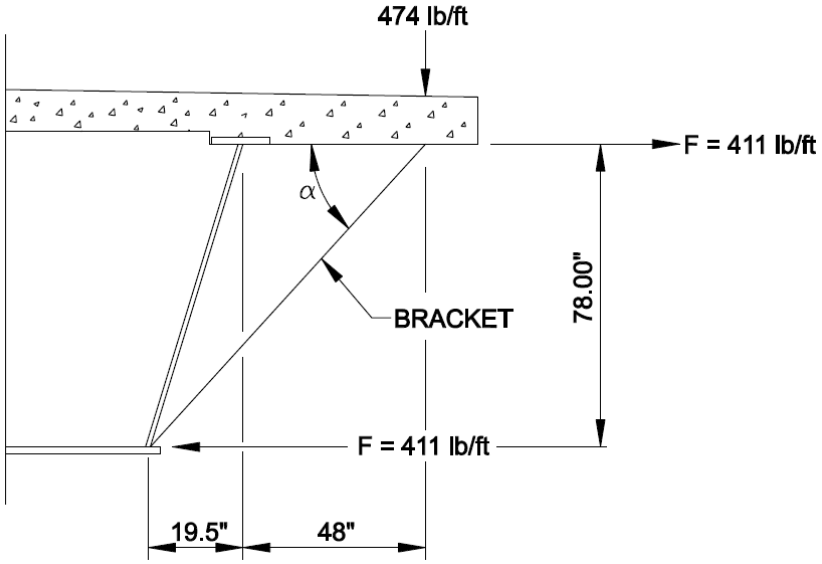

Figure 13 Deck Overhang Bracket Loading

The deck overhang bracket loads are assumed to be applied uniformly to the top flange, even though the brackets are actually spaced at approximately 3 feet along the length of the girder.

The unbraced length of the top flange is approximately 16.3 ft in Span 1. The deck thickness in the overhang area is assumed to be 10 inches, and the weight of the deck finishing machine is not considered in these calculations. Therefore, the vertical load on the deck overhang brackets is computed as:

Deck Overhang: $\left(\frac{1}{2}\right)(4.0)\left(\frac{10}{12}\right)(150)$ = 250 lbs/ft

Deck Forms + Screed Rail = 224 lbs/ft (assumed)

Total Uniform Load on Brackets = 474 lbs/ft

According to Article 3.4.2.1, the load factor for construction loads is to be taken as 1.50 for the Strength I load combination. The factored Strength I lateral force on the top flange is therefore computed as:

$$\alpha = \tan^{-1}\left(\frac{78.0}{67.5}\right) = 49.1°$$

$$F_\ell = \frac{1.25(250)+1.50(224)}{\tan(49.1°)} = 562 \text{ lb/ft} = 0.562 \text{ kip/ft}$$

The flange lateral bending moment on the exterior web top flange due to the deck overhang bracket is computed. The flange lateral moment at the brace points due to the overhang forces is negative in the top flange of Girder G2 on the outside of the curve in regions of positive flexure because the stress due to the lateral moment is compressive on the convex side of the flange at the brace points. The opposite would be true on the convex side of the Girder G1 top flange on the inside of the curve in regions of positive flexure at the brace points. In the absence of a more refined analysis, the equations given in Article C6.10.3.4.1 may be used to estimate the maximum flange lateral bending moments in the discretely braced compression flange due to the lateral bracket forces. Assuming the flange is continuous with the adjacent unbraced lengths and that the adjacent unbraced lengths are approximately equal, the factored Strength I lateral bending moment due to a statically equivalent uniformly distributed lateral bracket force may be estimated as:

$$M_\ell = \frac{F_\ell L_b^2}{12} = -\left[\frac{0.562(16.3)^2}{12}\right] = -12.4 \text{ kip-ft} \qquad \text{Eq. (C6.10.3.4.1-1)}$$

7.3.2 Flange Lateral Bending Due to Horizontal Component of Web Shear

In addition to the lateral bending moment due to the overhang brackets, the inclined webs of the tub girder cause a lateral force on the top flanges. However, in this example this force and subsequent lateral bending effects are relatively small and are ignored in these computations. Refer to NSBA's *Steel Bridge Design Handbook: Example 4: Three-Span Continuous Straight Composite Steel Tub-Girder Bridge* [8] for a sample calculation of these lateral bending effects.

7.3.3 Flange Lateral Bending Due to Curvature

Another source of lateral bending is due to curvature, which can either be taken from the analysis results (if the curvature of the tub girder top flanges between the top flange lateral bracing struts is captured with sufficient discretization, i.e., if the top flanges are not modeled using a single beam element chorded between the top flange lateral bracing strut nodes), or estimated by the approximate V-load equation given in Article C4.6.1.2.4b. The V-load equation assumes the presence of a cross-frame at the point under investigation and a constant major-axis moment over the distance between the brace points. Although the V-load equation is intended for application to I-girders and is not theoretically pure for tub girders or at locations in-between brace points, it may conservatively be used to estimate the flange lateral bending moments at the cross-frames in the top flanges of a tub.

The top flange size is constant between brace points in this region under investigation. In positive moment regions, the largest value of the major-axis bending stress (f_{bu}) may not necessarily be at either brace point. Generally, in positive moment regions, f_{bu} will not be significantly larger than the value at adjacent brace points, which is the case in this example. Therefore, the computed value of f_{bu} at Section G2-1 and the lateral bending moment at the brace points are conservatively combined for this constructability check.

For this example, and illustration purposes, the V-load equation is used to compute the flange lateral bending moment due to curvature. For a single tub girder flange, consider only one-half of the girder major-axis moment due to steel self-weight and Cast #1 of the deck placement sequence.

$$M = \frac{(1{,}144 + 2{,}979)}{2} = 2{,}062 \text{ kip-ft}$$

$$M_{LAT} = \frac{M\ell^2}{NRD} = -\left[\frac{(2{,}062)(16.3)^2}{(12)(716.25)(6.5)}\right] = -9.8 \text{ kip-ft} \qquad \text{Eq. (C4.6.1.2.4b-1)}$$

where:

M_{LAT} = flange lateral bending moment (kip-ft)
M = major-axis bending moment (kip-ft)
ℓ = unbraced length (ft)
N = a constant taken as 10 or 12 in past practice; 12 is recommended for use herein
R = girder radius (ft)
D = web depth (ft)

The flange lateral moment at the brace points due to curvature is negative when the top flanges are subjected to compression because the stress due to the lateral moment is in compression on the convex side of the flange at the brace points. The opposite is true whenever the top flanges are subjected to tension. Thus, the flange lateral moments due to the overhang loads in the top flange of Girder G2 on the outside of the curve in regions of positive flexure are additive to those due to curvature (see below); the opposite is true in the top flange of Girder G1 on the inside of the curve in regions of positive flexure. The total factored Strength I lateral moment and stress in the top flange of Girder G2, including the factored lateral moment from the overhang bracket is:

$$M_{TOT\_LAT} = (1.25)(-9.8) + (-12.4) = -24.7 \text{ kip-ft}$$

$$f_\ell = \frac{M_{TOT\_LAT}}{S_\ell} = \frac{-24.7(12)}{(1.00)(16)^2/6} = -6.95 \text{ ksi}$$

It should be noted that another significant source of flange lateral bending results from forces that develop in single-diagonal top flange bracing members resulting from major-axis bending of the tub girder. This effect is recognized in flange lateral moments that are taken directly from a finite element analysis. In the absence of a refined analysis, equations have been developed to evaluate bracing member forces and the forces imparted on the top flange in tub girders due to major-axis bending [13 and 17]. The flange lateral bending due to the forces in the top lateral bracing is not considered in these computations.

7.3.4 Top Flange Lateral Bending Amplification

According to Article 6.10.1.6, lateral bending stresses determined from a first-order analysis may be used in discretely braced compression flanges for which:

$$L_b \le 1.2 L_p \sqrt{\frac{C_b R_b}{f_{bu}/F_{yc}}} \qquad \text{Eq. (6.10.1.6-2)}$$

L_p is the limiting unbraced length specified in Article 6.10.8.2.3 determined as:

$$L_p = 1.0 r_t \sqrt{\frac{E}{F_{yc}}} \qquad \text{Eq. (6.10.8.2.3-4)}$$

where r_t is the effective radius of gyration for lateral torsional buckling specified in Article 6.10.8.2.3 determined as:

$$r_t = \frac{b_{fc}}{\sqrt{12\left(1 + \frac{1}{3}\frac{D_c t_w}{b_{fc} t_{fc}}\right)}} \qquad \text{Eq. (6.10.8.2.3-9)}$$

For the steel section, the depth of the web in compression in the elastic range, D_c, at Section G2-1 is computed along the web (not vertical) as follows:

Note that for the steel section only: $d_{TOP\ OF\ STEEL} = 43.79$ in.

$$D_c = (d_{TOP\ OF\ STEEL} - t_f)\sqrt{\frac{S^2+1}{S^2}}$$

$$D_c = (43.79 - 1.00)\sqrt{\frac{4^2+1}{4^2}} = 44.11 \text{ in.}$$

It should be noted that values of D_c and D are taken as distances along the web in accordance with Article 6.11.2.1.1. Therefore,

$$r_t = \frac{16}{\sqrt{12\left(1+\frac{1}{3}\frac{44.11(0.5625)}{16(1.00)}\right)}} = 3.75 \text{ in.}$$

$$L_p = \frac{1.0(3.75)}{12}\sqrt{\frac{29{,}000}{50}} = 7.53 \text{ ft}$$

C_b is the moment gradient modifier specified in Article 6.10.8.2.3 and may conservatively be taken equal to 1.0 in regions of positive flexure. According to Article 6.10.1.10.2, the web load-shedding factor, R_b, is to be taken equal to 1.0 when checking constructability. Finally, f_{bu} is the largest value of the compressive stress due to the factored loads throughout the unbraced length in the flange under consideration, calculated without consideration of flange lateral bending. In this case, use f_{bu} = -14.09 ksi, as computed earlier for the Construction Strength I load combination. Therefore:

$$1.2(7.53)\sqrt{\frac{1.0(1.0)}{\frac{|-14.09|}{50}}} = 17.02 \text{ ft} > L_b = 16.3 \text{ ft} \qquad \text{Eq. (6.10.1.6-2)}$$

Therefore, Eq. 6.10.1.6-2 is satisfied, and amplification of the first-order elastic compression-flange lateral bending stresses is not required. The flange lateral bending stress, f_ℓ, determined from the first-order elastic analysis is sufficient; thus f_ℓ = -6.95 ksi. The factored flange lateral bending stress is less than the limit of $0.6F_{yf} = 0.6(50) = 30.0$ ksi specified in Article 6.10.1.6.

7.3.5 Flexure (Article 6.11.3.2)

For critical stages of construction, Article 6.11.3.2 directs the engineer to the provisions of Article 6.10.3.2 to compute the resistance of top flanges of tub sections. The unbraced length should be taken as the distance between interior cross-frames or diaphragms. However as stated in the

commentary to Article 6.11.3.2, top lateral bracing attached to the flanges at points where only struts exist between the flanges may be considered as brace points at the discretion of the Engineer. In the case of this design example, which features a full-length top flange lateral bracing system, it is reasonable to consider both the struts with internal cross-frames and the alternating struts without internal cross-frames as brace points for the top flanges.

Article 6.10.3.2.1 requires that discretely braced flanges in compression satisfy the following:

$$f_{bu} + f_{\ell} \le \phi_f R_h F_{yc} \qquad \text{Eq. (6.10.3.2.1-1)}$$

$$f_{bu} + \frac{1}{3} f_{\ell} \le \phi_f F_{nc} \qquad \text{Eq. (6.10.3.2.1-2)}$$

$$f_{bu} \le \phi_f F_{crw} \qquad \text{Eq. (6.10.3.2.1-3)}$$

Article 6.11.3.2 requires that the noncomposite box flange (bottom flange) in tension satisfy:

$$f_{bu} \le \phi_f R_h F_{yf} \ \Delta \qquad \text{Eq. (6.11.3.2-3)}$$

where: ϕ_f = resistance factor for flexure from Article 6.5.4.2 ($\phi_f = 1.0$)
R_h = hybrid factor specified in Article 6.10.1.10.1 (1.0 at homogeneous Section G2-1)
F_{crw} = nominal elastic bend-buckling resistance for webs determined as specified in Article 6.10.1.9
F_{nc} = nominal flexural resistance of the compression flange determined as specified in Article 6.10.8.2 (i.e. local or lateral torsional buckling resistance, as applicable). The provisions of Article A6.3.3 are not to be used to determine the lateral torsional buckling resistance of top flanges of tub girders with compact or noncompact webs, as specified in Article 6.11.3.2.
Δ = a factor dependent on the St. Venant torsional shear stress in the bottom flange. St. Venant torsional shear stress will be addressed later in this example.

7.3.5.1 Top Flange

7.3.5.1.1 Top Flange: Yielding

First, determine if the noncomposite Section G2-1 is a compact or noncompact web section according to Eq. (6.10.6.2.3-1), or alternatively, see Table C6.10.1.10.2-2:

$$\frac{2D_c}{t_w} \le \lambda_{rw} \qquad \text{Eq. (6.10.6.2.3-1)}$$

where:

$$4.6\sqrt{\frac{E}{F_{yc}}} \le \lambda_{rw} = \left(3.1+\frac{5.0}{a_{wc}}\right)\sqrt{\frac{E}{F_{yc}}} \le 5.7\sqrt{\frac{E}{F_{yc}}} \qquad \text{Eq. (6.10.6.2.3-3)}$$

$$a_{wc} = \frac{2D_c t_w}{b_{fc} t_{fc}} \qquad \text{Eq. (6.10.6.2.3-4)}$$

$$\frac{2D_c}{t_w} = \frac{2(44.11)}{0.5625} = 156.8$$

$$4.6\sqrt{\frac{E}{F_{yc}}} = 4.6\sqrt{\frac{29,000}{50}} = 111$$

$$5.7\sqrt{\frac{E}{F_{yc}}} = 5.7\sqrt{\frac{29,000}{50}} = 137$$

$$a_{wc} = \frac{2(44.11)(0.5625)}{16(1.0)} = 3.10$$

$$111 < \lambda_{rw} = \left(3.1+\frac{5.0}{3.10}\right)\sqrt{\frac{29,000}{50}} = 113.5 < 137$$

$$\therefore \lambda_{rw} = 113.5 < \frac{2D_c}{t_w} = 156.8$$

Therefore, the noncomposite Section G2-1 is a slender-web section. As a result, for the top flanges, Eq. (6.10.3.2.1-1) must be checked since f_ℓ is not zero. Check that the top flanges satisfy Eq. 6.10.3.2.1-1 as follows:

$$f_{bu} + f_\ell \le \phi_f R_h F_{yc} \qquad \text{Eq. (6.10.3.2.1-1)}$$

$$f_{bu} + f_\ell = |-14.09| + |-6.95| = 21.04 \text{ ksi}$$

$$\phi_f R_h F_{yc} = 1.0(1.0)(50) = 50.0 \text{ ksi} > 21.04 \text{ ksi} \qquad \text{OK} \quad (\text{Ratio} = 0.421)$$

7.3.5.1.2 Top Flange: Local Buckling Resistance (Article 6.10.8.2.2)

Determine the slenderness ratio of the top flange:

$$\lambda_f = \frac{b_{fc}}{2t_{fc}} \qquad \text{Eq. (6.10.8.2.2-3)}$$

$$\lambda_f = \frac{16}{2(1.00)} = 8.00$$

Determine the limiting slenderness ratio for a compact flange (alternatively see Table C6.10.8.2.2-1):

$$\lambda_{pf} = 0.38\sqrt{\frac{E}{F_{yc}}} \qquad \text{Eq. (6.10.8.2.2-3)}$$

$$\lambda_{pf} = 0.38\sqrt{\frac{29{,}000}{50}} = 9.15$$

Since $\lambda_f < \lambda_{pf}$,

$$F_{nc} = R_b R_h F_{yc} \qquad \text{Eq. (6.10.8.2.2-1)}$$

Since R_b is taken as 1.0 for constructability,

$$F_{nc} = (1.0)(1.0)(50) = 50 \text{ ksi}$$

Check Eq. 6.10.3.2.1-2 as follows:

$$|-14.09| + \frac{1}{3}|-6.95| = 16.41 \text{ ksi} \le (1.0)(50.0) = 50.0 \text{ ksi} \qquad \text{OK} \qquad \text{(Ratio = 0.328)}$$

7.3.5.1.3 Top Flange: Lateral Torsional Buckling Resistance (Article 6.10.8.2.3)

The limiting unbraced length, L_p, was computed earlier to be 7.53 feet. The effective radius of gyration for lateral torsional buckling, r_t, for the noncomposite Section G2-1 was also computed earlier to be 3.75 inches. The computations for L_p and r_t are shown in Section 7.3.4.

Determine the limiting unbraced length, L_r:

$$L_r = \pi r_t \sqrt{\frac{E}{F_{yr}}} \qquad \text{Eq. (6.10.8.2.3-5)}$$

where F_{yr} is the compression flange stress at the onset on nominal yielding, including residual stress effects, and is to be taken as the smaller of $0.7F_{yc}$ and F_{yw}, but not less than $0.5F_{yc}$. Since F_{yc} and F_{yw} are both equal to 50 ksi,

$F_{yr} = 0.7(50) = 35$ ksi

$$L_r = \frac{\pi\,(3.75)}{12}\sqrt{\frac{29{,}000}{35}} = 28.26 \text{ ft}$$

Since $L_p = 7.53$ feet < $L_b = 16.30$ feet < $L_r = 28.26$ feet, Eq. (6.10.8.2.3-2) is used to compute the lateral torsional buckling resistance.

$$F_{nc} = C_b\left[1-\left(1-\frac{F_{yr}}{R_h F_{yc}}\right)\left(\frac{L_b - L_p}{L_r - L_p}\right)\right]R_b R_h F_{yc} \le R_b R_h F_{yc} \qquad \text{Eq. (6.10.8.2.3-2)}$$

Compute the moment-gradient modifier, C_b, to be used in Eq. (6.10.8.2.3-2), where

$C_b = 1.0$ for members where $f_{mid}/f_2 > 1$ or $f_2 = 0$ Eq. (6.10.8.2.3-6)

Otherwise: $C_b = 1.75 - 1.05\left(\frac{f_1}{f_2}\right) + 0.3\left(\frac{f_1}{f_2}\right)^2 \le 2.3$ Eq. (6.10.8.2.3-7)

where:

f_{mid} = flange stress without the consideration of lateral bending at the middle of the unbraced length of the flange under consideration. f_{mid} shall be due to factored loads and shall be taken as positive in compression and negative in tension.

f_2 = largest compressive flange stress without consideration of lateral bending at either end of the unbraced length of the flange under consideration. f_2 shall be due to factored loads and shall be taken as positive. If the flange stress is zero or tensile in the flange under consideration at both ends of the unbraced length, f_2 shall be taken as zero.

f_1 = in the case of Section G2-1, the moment diagram along the entire length between brace points is concave in shape, and therefore, $f_1 = f_0$, and is the stress without consideration of lateral bending at the brace point opposite to the one corresponding to f_2.

Refer to the sample cases shown in Article C6.4.10 for further interpretation of the preceding stress definitions for different types of moment-gradient conditions.

The largest compressive stress at the end of the unbraced length under consideration is at the brace point 65.04 ft into Span 1. From calculations not shown herein, the unfactored moments at 65.04 ft due to steel self-weight and Cast #1 are 1,115 k-ft and 3,361 k-ft, respectively. Therefore, f_2 is calculated as:

$$f_2 = \frac{1.0(1.25)(1{,}115 + 3{,}361)(12)}{4{,}390} = 15.29 \text{ ksi}$$

f_{mid} is the compressive stress at the location under investigation, previously computed as 1409 ksi in compression. Check the f_{mid}/f_2 ratio:

$$\frac{f_{mid}}{f_2} = \frac{14.09}{15.29} = 0.92 < 1.0$$

Therefore, C_b can be calculated using Eq. (6.10.8.2.3-7). First, it is necessary to compute f_1, which is the flange stress at the opposite brace point from f_2. From calculations not shown herein, the unfactored moments at 48.77 ft due to steel self-weight and Cast #1 are 1,116 k-ft and 2,588 k-ft, respectively. Therefore, f_1 is calculated as:

$$f_1 = \frac{1.0(1.25)(1{,}116 + 2{,}588)(12)}{4{,}390} = 12.66 \text{ ksi}$$

C_b is computed as:

$$C_b = 1.75 - 1.05\left(\frac{12.66}{15.29}\right) + 0.3\left(\frac{12.66}{15.29}\right)^2 = 1.09 \le 2.3$$

Therefore, the lateral torsional buckling resistance is:

$$F_{nc} = (1.09)\left[1 - \left(1 - \frac{0.7(50)}{(1.0)(50)}\right)\left(\frac{16.30 - 7.53}{28.26 - 7.53}\right)\right](1.0)(1.0)(50) = 47.6 \text{ ksi} \quad \le (1.0)(1.0)(50) = 50 \text{ ksi}$$

Check Eq. 6.10.3.2.1-2 as follows:

$$|-14.09| + \frac{1}{3}|-6.95| = 16.41 \text{ ksi} \quad \le (1.0)(47.6) = 47.6 \text{ ksi} \qquad \text{OK} \qquad \text{(Ratio = 0.345)}$$

Although not necessary in this case, if a larger lateral torsional buckling resistance had been required, then the equations of Article D6.4.1 could have alternatively been used to potentially obtain a larger resistance since C_b is greater than 1.0.

7.3.5.1.4 Top Flange: Web Bend-Buckling Resistance (Article 6.10.1.9)

Determine the nominal elastic web bend-buckling resistance at Section G2-1 according to the provisions of Article 6.10.1.9.1 as follows:

$$F_{crw} = \frac{0.9Ek}{\left(\frac{D}{t_w}\right)^2} \le \min\left(R_h F_{yc},\ \frac{F_{yw}}{0.7}\right) \qquad \text{Eq. (6.10.1.9.1-1)}$$

where:

$$k = \frac{9}{\left(D_c/D\right)^2} \qquad \text{Eq. (6.10.1.9.1-2)}$$

In earlier calculations, D_c was computed as 44.11 in. along the inclined web.

$$k = \frac{9}{\left(\frac{44.11}{80.40}\right)^2} = 29.9$$

Therefore,

$$F_{crw} = \frac{0.9(29{,}000)(29.9)}{\left(\frac{80.40}{0.5625}\right)^2} = 38.20 \text{ ksi} < R_h F_{yc} = 50 \text{ ksi}$$

Check Eq. (6.10.3.2.1-3),

$$\left|-14.09\right| = 14.09 \text{ ksi} \quad \le (1.0)(38.20) = 38.20 \text{ ksi} \qquad \text{OK} \qquad \text{(Ratio = 0.369)}$$

It should be noted that the web bend-buckling resistance is generally checked against the maximum compression flange stress due factored loads, without consideration of flange lateral bending, as shown in the previous calculation. Since web-bend buckling is a check of the web, the maximum flexural compression stress in the web could be calculated and used for comparison against the bend-buckling resistance. However, the precision associated with making the distinction between the stress in the compression flange and the maximum compressive stress in the web is typically not warranted.

7.3.5.2 Bottom Flange

Noncomposite tub flanges in tension, in this particular case the bottom flange, must satisfy the following requirement:

$$f_{bu} \le \phi_f R_h F_{yf} \ \Delta \qquad \text{Eq. (6.11.3.2-3)}$$

where:

$$\Delta = \sqrt{1 - 3\left(\frac{f_v}{F_{yf}}\right)^2} \qquad \text{Eq. (6.11.3.2-4)}$$

The term f_v is the factored St. Venant torsional shear stress in the flange at the section under consideration, and is taken as:

$$f_v = \frac{T}{2\,A_o\,t_f} \qquad \text{Eq. (6.11.3.2-5)}$$

where:

T = internal torque due to factored loads (kip-in.)
A_o = enclosed area within the box section (in.^{2})
t_f = bottom flange thickness (in.)

Compute the enclosed area of the noncomposite box section, A_o.

$$A_o = \frac{\left[120+\left(83-2(1.5)\right)\right]}{2}\left(\frac{1.00}{2}+78+\frac{0.6875}{2}\right) = 7{,}884 \text{ in.}^2$$

As shown in Table 7, the unfactored torques due to steel self-weight and Cast #1 are 59 kip-ft and 464 kip-ft, respectively. Therefore,

$$f_v = \frac{(1.25)(59+464)(12)}{2(7{,}884)(0.6875)} = 0.72 \text{ ksi}$$

$$\Delta = \sqrt{1-3\left(\frac{f_v}{F_{yf}}\right)^2} = \sqrt{1-3\left(\frac{0.72}{50}\right)^2} = 1.0$$

The factored bottom flange major-axis bending stress, calculated previously, is 11.55 ksi. Check Eq. 6.11.3.2-3 as follows:

$$f_{bu} = 11.55 \text{ ksi} < \phi_f R_h F_{yf} \Delta = (1.0)(1.0)(50)(1.0) = 50.0 \text{ ksi} \quad \text{OK} \quad (\text{Ratio} = 0.231)$$

Although the check here of the bottom flange is illustrated for completeness, the bottom flange will typically not govern the constructability check in regions of positive flexure.

7.3.6 Shear (Article 6.10.3.3)

Article 6.10.3.3 requires that interior panels of stiffened webs satisfy the following requirement:

$$V_u \le \phi_v V_{cr} \qquad \text{Eq. (6.10.3.3-1)}$$

where:

ϕ_v = resistance factor for shear = 1.0 (Article 6.5.4.2)
V_u = shear in the web at the section under consideration due to the factored permanent loads and factored construction loads applied to the noncomposite section
V_{cr} = shear-yield or shear-buckling resistance determined from Eq. (6.10.9.3.3-1)

Only the interior panels of stiffened webs are checked because the shear resistance of the end panel of stiffened webs and the shear resistance of unstiffened webs are already limited to the shear-yield or shear-buckling resistance at the strength limit state.

For this example, the web is unstiffened in the positive moment regions. Therefore, the constructability check for shear is not required at this section.

7.3.7 Concrete Deck (Article 6.10.3.2.4)

Generally, the entire deck is not placed in a single pour. Typically, for continuous span bridges, the positive flexure regions are placed first. Thus, positive flexure regions may become composite prior to placing the other sections of the deck. As the deck placement operation progresses, tensile stresses can develop in previously placed regions that will exceed the allowable modulus of rupture (ϕf_r) of the hardened deck. When cracking is predicted, longitudinal deck reinforcing as specified in Article 6.10.1.7 is required to control cracking. Otherwise, alternative deck casting sequences must be employed to minimize the anticipated stresses to acceptable levels. This check is illustrated in NSBA's *Steel Bridge Design Handbook: Example 1: Three-Span Continuous Straight Composite Steel I-Girder Bridge* [3].

7.4 Girder Check: Section G2-1, Service Limit State (Article 6.11.4)

Article 6.11.4 directs the Engineer to Article 6.10.4, which contains provisions related to the control of elastic and permanent deformations at the service limit state.

7.4.1 Permanent Deformations (Article 6.10.4.2)

Article 6.10.4.2 contains criteria intended to control permanent deformations that would impair rideability. As specified in Article 6.10.4.2.1, these checks are to be made under the Service II load combination.

Article 6.10.4.2.2 requires that flanges of composite sections satisfy the following:

Top flange of composite sections: $f_f \le 0.95 R_h F_{yf}$ Eq. (6.10.4.2.2-1)

Bottom flange of composite sections: $f_f + \frac{f_\ell}{2} \le 0.95 R_h F_{yf}$ Eq. (6.10.4.2.2-2)

The term f_f is the flange stress at the section under consideration due to the Service II loads calculated without consideration of flange lateral bending. The f_ℓ term, the flange lateral bending stress, in Eq. 6.10.4.2.2-2 is to be taken equal to zero in accordance with Article 6.11.4, for tub

girder bottom flanges. A resistance factor is not included in these equations because Article 1.3.2.1 specifies that the resistance factor be taken equal to 1.0 at the service limit state.

It should be noted that in accordance with Article 6.11.4 redistribution of negative moment due to the Service II loads at the interior-pier sections in continuous-span flexural members using the procedures specified in Appendix B6 is not to be applied to tub girder sections. The applicability of the Appendix B6 provisions to tub-girder sections has not been demonstrated; hence, the procedures are not permitted for the design of tub-girder sections.

Furthermore, according to Article C6.11.4, under the load combinations specified in Table 3.4.1-1, Eqs. 6.10.4.2.2-1 and 6.10.4.2.2-2 need only be checked for compact sections in positive flexure. For sections in negative flexure and noncompact sections in positive flexure, these two equations do not control and need not be checked. Composite sections in all horizontally curved girder systems are to be treated as noncompact sections at the strength limit state in accordance with Article 6.11.6.2.2. Therefore, for Section G2-1, Eqs. 6.10.4.2.2-1 and 6.10.4.2.2-2 do not need to be checked, and are not checked in this example.

7.4.2 Web Bend-Buckling

With the exception of composite sections in positive flexure in which the web satisfies the requirement of Articles 6.11.2.1.2 and 6.10.2.1.1 (i.e., $D/t_w \leq 150$), web bend-buckling of all sections under the Service II load combination is to be checked as follows:

$$f_c \leq F_{crw} \qquad \text{Eq. (6.10.4.2.2-4)}$$

The term f_c is the compression-flange stress at the section under consideration due to the Service II loads calculated without consideration of flange lateral bending, and F_{crw} is the nominal elastic bend-buckling resistance for webs determined as specified in Article 6.10.1.9. Because Section G2-1 is a composite section subject to positive flexure satisfying Article 6.11.2.1.2, Eq. (6.10.4.2.2-4) need not be checked as $D/t_w = 142.9$, which is less than 150. An explanation as to why these particular sections are exempt from the above web bend-buckling check is given in Article C6.10.1.9.1.

7.5 Girder Check: Section G2-1, Fatigue and Fracture Limit State (Article 6.11.5)

Article 6.11.5 directs the designer to Article 6.10.5, where details in tub girder section flexural members must be investigated for fatigue as specified in Article 6.6.1. As appropriate, the Fatigue I and Fatigue II load combinations specified in Table 3.4.1-1 and the fatigue live load specified in Article 3.6.1.4 are to be employed for checking load-induced fatigue in tub girder sections. The Fatigue I load combination is to be used in combination with design checks for infinite fatigue life. The Fatigue II load combination is to be used in combination with design checks for finite fatigue life.

As specified in Article 6.11.5, one additional requirement specified for tub-girder sections deals with the consideration of longitudinal warping and transverse bending stresses due to cross-section distortion. When tub girders are subjected to torsion, their cross-section becomes distorted

resulting in secondary bending stresses. Therefore, longitudinal warping stresses and transverse bending stresses due to cross-section distortion are to be considered in the fatigue checks for:

- Single tub girders in straight or horizontally curved bridges;
- Multiple tub girders in straight bridges that do not satisfy requirements of Article 6.11.2.3;
- Multiple tub girders in horizontally curved bridges; or
- Any single or multiple tub girder with a bottom flange that is not fully effective according to the provisions of Article 6.11.1.1.

Therefore, in this design example at Section G2-1, the stress range due to longitudinal warping resulting from cross-section distortion in the girders is considered in checking the fatigue resistance of the base metal. For simplicity in this design example, in lieu of determining the distortional warping stresses resulting from cross-section distortion at Section G2-1 based on the beam-on-elastic foundation analogy (BEF) discussed in the next paragraph, it is assumed that the longitudinal warping stresses are approximately (and conservatively) equal to 10 percent of the longitudinal stresses caused by the major-axis bending moment. Thus, for the calculations contained herein at Section G2-1, the fatigue live load major-axis bending moments are conservatively increased by 10 percent in computing the stress range for checking load-induced fatigue. If the nominal fatigue resistance had been exceeded, more detailed calculations utilizing the BEF analogy could be performed to provide more accurate values of the stress range due to longitudinal warping.

The transverse bending stress range is considered separately from the longitudinal warping stress range for evaluating the fatigue resistance of the base metal adjacent to flange-to-web fillet welds and adjacent to the termination of fillet welds connecting transverse elements to webs and box flanges. The transverse bending stress range is not computed in this design example for Section G2-1. More exact calculations to determine the stress range from longitudinal warping and transverse bending due to cross-section distortion can be carried out using the beam-on-elastic-foundation analogy (BEF) presented by Wright and Abdel-Samad [9]. Sample calculations for determining these distortional stresses based on the BEF analogy are presented in the 2003 AASHTO *Guide Specification for Horizontally Curved Steel Girder Highway Bridges* [19], which is superseded by the current AASHTO specifications. Calculations demonstrating the use of the BEF analogy to compute the longitudinal warping stress and transverse bending stress ranges are included as part of the fatigue check for Section G2-2 in Section 7.9.1.

At Section G2-1, it is necessary to check the bottom flange for the fatigue limit state. The base metal at the transverse stiffener weld terminations and internal cross-frame connection-plate welds at locations subject to a net tensile stress must be checked as a Category C′ fatigue detail (refer to Table 6.6.1.2.3-1). Only the bottom flange is checked herein, as a net tensile stress is not induced in the top flange by the fatigue loading at this location (refer to Article 6.6.1.2.1).

According to Table 3.6.2.1-1, the dynamic load allowance for the fatigue live load is 15%. Centrifugal force effects are considered and included in the fatigue live load moments. As discussed previously, the projected 75-year single lane ADTT in one direction is assumed to be 1,000 trucks per day.

According to Eq. (6.6.1.2.2-1), $\gamma(\Delta f)$ must not exceed the nominal fatigue resistance, $(\Delta F)_n$. In accordance with Article C6.6.1.2.2, the resistance factor, ϕ, and the load modifier, η, are taken as 1.0 for the fatigue limit state.

$$\gamma\left(\Delta f\right) \le \left(\Delta F\right)_n \qquad \text{Eq. (6.6.1.2.2-1)}$$

From Table 6.6.1.2.3-2, the 75-year $(ADTT)_{SL}$ Equivalent to Infinite Life for a Category C′ fatigue detail is 975 trucks per day. Therefore, since the assumed $(ADTT)_{SL}$ for this design example is 1,000 trucks per day, the detail must be checked for infinite fatigue life using the Fatigue I load combination. In accordance with Article 6.6.1.2.5, the nominal fatigue resistance for infinite fatigue life is equal to the constant-amplitude fatigue threshold:

$$\left(\Delta F\right)_n = \left(\Delta F\right)_{TH} \qquad \text{Eq. (6.6.1.2.5-1)}$$

where $(\Delta F)_{TH}$ is the constant-amplitude fatigue threshold taken from Table 6.6.1.2.5-3. For a Category C′ fatigue detail, $(\Delta F)_{TH}$ = 12.0 ksi, and therefore:

$$\left(\Delta F\right)_n = 12.0 \text{ ksi}$$

As shown in Table 7 the unfactored negative and positive moments due to the fatigue live load, including centrifugal force effects and the 15 percent dynamic load allowance, at Section G2-1 are -290 kip-ft and 1,525 kip-ft, respectively. The short-term composite section properties (n = 7.56) used to compute the stress at the bottom of the web (top of the bottom flange) are:

$I_{NA(n)}$ = 502,098 in.^{4}

$d_{BOT\ OF\ WEB} = d_{BOT\ OF\ STEEL} - t_{f\_BOT\ FLANGE}$ = 67.90 in. – 0.6875 in. = 67.21 in.

As specified in Table 3.4.1-1, the load factor, γ, for the Fatigue I load combination is 1.75. The total factored stress range at the bottom of the web, including the 10 percent increase estimated for the longitudinal warping stress, is computed as follows:

$$\gamma\left(\Delta f\right) = \left(1.75\right)\left(\frac{\left(1.10\right)\left(\left|-290\right| + 1{,}525\right)\left(12\right)\left(67.21\right)}{502{,}098}\right) = 5.61 \text{ ksi}$$

Check Eq. (6.6.1.2.2-1) as follows:

$$\gamma\left(\Delta f\right) = 5.61 \text{ ksi} \le \left(\Delta F\right)_n = 12.00 \text{ ksi} \quad \text{OK} \quad (\text{Ratio} = 0.468)$$

7.5.1 Special Fatigue Requirements for Webs

In accordance with Article 6.10.5.3, interior panels of stiffened webs must satisfy:

$$V_u \leq V_{cr} \qquad \text{Eq. (6.10.5.3-1)}$$

where:

V_u = shear in the web at the section under consideration, due to unfactored permanent loads plus the factored fatigue load (Fatigue I)
V_{cr} = shear-yield or shear-buckling resistance determined from Eq. (6.10.9.3.3-1).

Satisfaction of Eq. (6.10.5.3-1) is intended to control elastic flexing of the web, such that the member is assumed to be able to sustain an infinite number of smaller loadings without fatigue cracking due to this effect. The live load shear in the special requirement is intended to represent the heaviest truck expected to cross the bridge in 75 years.

Only interior panels of stiffened webs are investigated because the shear resistance of end panels of stiffened webs and the shear resistance of unstiffened webs are limited to the shear-yield or shear-buckling resistance at the strength limit state.

The detailed check of this special fatigue requirement for webs is not illustrated in this example; however, similar checks are illustrated in NSBA's *Steel Bridge Design Handbook: Example 1: Three-Span Continuous Straight Composite Steel I-Girder Bridge* [3].

7.5.2 Fracture (Article 6.6.2)

As specified in Article 6.10.5.2, fracture toughness requirements in the contract drawings must be in conformance with the provisions of Article 6.6.2.1. Material for main load-carrying components subject to tensile stress under the Strength I load combination is assumed for this example to be ordered to meet the appropriate Charpy V-notch fracture toughness requirements (Table C6.6.2.1-1) specified for Temperature Zone 2 (Table 6.6.2.1-2).

Article 6.6.2.2 provides provisions for Fracture-Critical Members (FCMs). A FCM is defined as a steel primary member or portion thereof subject to tension whose failure would probably cause a portion of or the entire bridge to collapse. Article 6.6.2.2 specifies that the Engineer is to have the responsibility for identifying and designating on the contract plans which primary members or portions thereof are fracture-critical members (FCMs). The tension components of tub girders in single- and twin-tub girder systems have typically been designated as FCMs.

The designation of a particular member, or member component, as a FCM entails additional and more stringent fabrication requirements given in Clause 12 of the AASHTO/AWS D1.5M/D1.5 *Bridge Welding Code* (D1.5) [20], and hands-on inspections every two years. The additional fabrication requirements are an initial cost premium in the design of new bridges that has been proven to be effective in preventing fracture. However, the hands-on inspection requirements give rise to considerably larger expenses that take place throughout the service life of the bridge, which involve risks to the safety of the inspectors and bridge users.

Article 6.6.2.2 further indicates that a primary member or portion thereof subject to tension, for which the redundancy is not known by engineering judgment, but which is demonstrated to have redundancy in the presence of a simulated fracture in that member through the use of a refined

analysis, is to be designated as a System Redundant Member (SRM) in the contract documents. SRMs are to be fabricated in accordance with Clause 12 of D1.5 and are to have routine inspections performed but need not be subject to the hands-on in-service inspection requirements.

One acceptable detailed finite element analysis and evaluation procedure for classification of SRMs [21] is provided in the AASHTO *Guide Specifications for Analysis and Identification of Fracture Critical Members and System Redundant Members* [22]. The Guide Specification is intended to provide Engineers and Owners with an analytical framework to evaluate the redundancy of typical steel bridges and designate primary steel members as FCMs or SRMs. This framework is composed of the finite element analysis procedure, techniques, and inputs needed to create a reliable model of the steel bridge; as well as the minimum required primary steel member failure scenarios, load combinations, and performance criteria used to evaluate the redundancy of a steel bridge. Connor et al. (2020) [23] also provides a suggested alternative simplified approach for classifying SRMs in continuous composite twin tub-girder bridges.

7.6 Girder Check: Section G2-1, Strength Limit State (Article 6.11.6)

7.6.1 Flexure (Article 6.11.6.2)

According to Article 6.11.6.2.2, sections in horizontally curved steel tub girder bridges are to be considered noncompact sections and are to satisfy the requirements of Article 6.11.7.2. Furthermore, compact and noncompact sections in positive flexure must satisfy the ductility requirement specified in Article 6.10.7.3. The ductility requirement is intended to protect the concrete deck from premature crushing. The section must satisfy:

$$D_p \le 0.42\, D_t \qquad \text{Eq. (6.10.7.3-1)}$$

where D_p is the distance from the top of the concrete deck to the neutral axis of the composite section at the plastic moment, and D_t is the total depth of the composite section. Refer the section property computations for the location of the neutral axis of the composite section at the plastic moment (Section 7.2.1.3). At Section G2-1:

$$D_p = 9.5 + 4.0 - 1.0 + 0.35 = 12.85 \text{ in.}$$

$$D_t = 0.6875 + 78.0 + 4.0 + 9.5 = 92.19 \text{ in.}$$

$$0.42D_t = 0.42(92.19) = 38.72 \text{ in.} > 12.85 \text{ in.} \qquad \text{OK} \qquad (\text{Ratio} = 0.332)$$

For a horizontally curved steel tub girder at the strength limit state, noncompact sections in positive flexure must satisfy the provisions of Article 6.11.7.2. At the strength limit state, the compression flanges of tub sections must satisfy:

$$f_{bu} \le \phi_f F_{nc} \qquad \text{Eq. (6.11.7.2.1-1)}$$

where:

f_{bu} = longitudinal flange stress at the section under consideration calculated without consideration of flange lateral bending or longitudinal warping
ϕ_f = resistance factor for flexure as specified in Article 6.5.4.2 ($\phi_f = 1.0$)
F_{nc} = nominal flexural resistance of the compression flange determined as specified in Article 6.11.7.2.2

Flange lateral bending is not considered for the compression flanges in positive bending at the strength limit state because the flanges are continuously supported by the concrete deck. In accordance with Article 6.11.1.1, longitudinal warping stresses may be ignored at the strength limit state. However, St. Venant torsion and cross-section distortion stresses in the bottom flange must be considered for noncompact sections.

At the strength limit state, the tension flange must satisfy:

$$f_{bu} \le \phi_f F_{nt} \qquad \text{Eq. (6.11.7.2.1-2)}$$

where:

F_{nt} = nominal flexural resistance of the tension flange determined as specified in Article 6.11.7.2.2

Lateral bending does not need to be considered for the tension flange, in this case the bottom flange, as lateral bending is typically negligible in bottom flanges of tub girders.

Furthermore, the maximum longitudinal compressive stress in the concrete deck at the strength limit state is not to exceed $0.6f'_c$. The longitudinal compressive stress in the deck is to be determined in accordance with Article 6.10.1.1d, which allows the permanent and transient load stresses in the concrete deck to be computed using the short-term section properties (i.e., with the modular ratio taken as *n*).

The unfactored bending moments at Section G2-1 are taken directly from the analysis and are shown below (see Table 7). The live load moment includes the centrifugal force and dynamic load allowance effects.

Noncomposite Dead Load:	M_{DC1}	= 5,891 kip-ft
Composite Dead Load:	M_{DC2}	= 765 kip-ft
Future Wearing Surface Dead Load:	M_{DW}	= 1,006 kip-ft
Live Load (incl. IM and CF):	M_{LL+IM}	= 5,920 kip-ft

Compute the factored flange flexural stresses at Section G2-1 for the Strength I load combination, without consideration of flange lateral bending. As discussed previously, the η factor is taken equal to 1.0 in this example. Therefore:

For Strength I:

Top Flange:

$$f_{bu} = -1.0\left[\frac{1.25(5{,}891)}{4{,}390} + \frac{1.25(765)}{14{,}378} + \frac{1.5(1{,}006)}{14{,}378} + \frac{1.75(5{,}920)}{42{,}587}\right]12 = -25.11\,\text{ksi}$$

Bottom Flange:

$$f_{bu} = 1.0\left[\frac{1.25(5{,}891)}{5{,}355} + \frac{1.25(765)}{6{,}801} + \frac{1.5(1{,}006)}{6{,}801} + \frac{1.75(5{,}920)}{7{,}395}\right]12 = 37.66\,\text{ksi}$$

In accordance with Article 6.11.1.1, the effects of both flexural and St. Venant torsional shear are to be considered in horizontally curved tub girder bridges. Therefore, compute the factored St. Venant torsional shear stress, f_v, in the bottom flange for the Strength I load combination. f_v is determined by dividing the St. Venant torsional shear flow [$f = T/(2A_o)$] by the thickness of the bottom flange:

$$f_v = \frac{T}{2A_o t_f} \qquad \text{Eq. (6.11.3.2-5)}$$

where:

T = internal torque due to factored loads (kip-in.)
A_o = enclosed area within the box section (in.^{2})
t_f = bottom flange thickness (in.)

The unfactored torques at Section G2-1 obtained directly from the analysis are shown below (see Table 7). The live load torque includes the centrifugal force and dynamic load allowance effects.

Noncomposite Dead Load:	T_{DC1}	= 264 kip-ft
Composite Dead Load:	T_{DC2}	= 41 kip-ft
Future Wearing Surface Dead Load:	T_{DW}	= 54 kip-ft
Live Load (incl. IM and CF):	T_{LL+IM}	= 525 kip-ft

Article C6.11.1.1 indicates that for torques applied to the noncomposite section, A_o is to be computed for the noncomposite section. Since the top lateral bracing in this example is attached to the top flange, the vertical depth can be calculated as the distance between the mid-thicknesses of the top and bottom flanges. Furthermore, for torques applied to the composite section, A_o is to be computed for the composite section, using the depth from the mid-thickness of the bottom flange to the mid-thickness of the concrete deck. In this example, the height of the deck haunch is considered.

Compute the enclosed area of the noncomposite tub section, A_{o_NC}.

$$A_{o\_NC} = \frac{\left[120 + \left(83 - 2\left(1.5\right)\right)\right]}{2}\left(\frac{1.00}{2} + 78 + \frac{0.6875}{2}\right) = 7{,}884 \text{ in.}^2$$

Compute the enclosed area of the composite tub section, A_{o_C}.

$$A_{o\_C} = \frac{\left[120 + \left(83 - 2\left(1.5\right)\right)\right]}{2}\left(78 + \frac{0.6875}{2} + 4.00 + \frac{9.50}{2}\right) = 8{,}709 \text{ in.}^2$$

Compute the factored Strength I St. Venant torsional shear stress on the noncomposite section:

$$f_{v\_NC} = \left(1.0\right)\frac{\left(1.25\right)\left(264\right)\left(12\right)}{2\left(7{,}884\right)\left(0.6875\right)} = 0.37 \text{ ksi}$$

Compute the factored Strength I St. Venant torsional shear stress on the composite section:

$$f_{v\_C} = \left(1.0\right)\frac{\left[\left(1.25\right)\left(41\right) + \left(1.50\right)\left(54\right) + \left(1.75\right)\left(525\right)\right]\left(12\right)}{2\left(8{,}709\right)\left(0.6875\right)} = 1.05 \text{ ksi}$$

Therefore the total factored Strength I St. Venant torsional shear stress is computed as:

$$f_v = 0.37 + 1.05 = 1.42 \text{ ksi}$$

According to Article 6.11.1.1, the factored St. Venant torsional shear stress in box flanges at the strength limit state is not to exceed the factored torsional shear resistance of flange, F_{vr}, taken as:

$$F_{vr} = 0.75\phi_v \frac{F_{yf}}{\sqrt{3}} \qquad \text{Eq. (6.11.1.1-1)}$$

where:

ϕ_v = resistance factor for shear specified in Article 6.5.4.2

Therefore:

$$F_{vr} = 0.75\left(1.0\right)\frac{50}{\sqrt{3}} = 21.65 \text{ ksi} > f_v = 1.42 \text{ ksi} \qquad \text{OK}$$

7.6.1.1 Top Flange Flexural Resistance in Compression

In accordance with Article 6.11.7.2.2, the nominal flexural resistance of the compression flanges of noncompact composite tub sections is to be taken as:

$$F_{nc} = R_b R_h F_{yc} \qquad \text{Eq. (6.11.7.2.2-1)}$$

where:

R_b = web load-shedding factor determined as specified in Article 6.10.1.10.2
R_h = hybrid factor determined as specified in Article 6.10.1.10.1.

For a homogenous girder, the hybrid factor, R_h, is equal to 1.0. In accordance with Article 6.10.1.10.2, the web load-shedding factor, R_b, is equal to 1.0 for composite sections in which the web satisfies the requirement of Article 6.11.2.1.2 such that $D/t_w \leq 150$.

$$\frac{D}{t_w} = \frac{80.40}{0.5625} = 142.9 < 150$$

Therefore:

$$F_{nc} = (1.0)(1.0)(50.0) = 50.00 \text{ ksi}$$

For Strength I:

$$f_{bu} \leq \phi_f F_{nc} \qquad \text{Eq. (6.11.7.2.1-1)}$$

$$f_{bu} = |-25.11| \text{ ksi} \leq \phi_f F_{nc} = (1.0)(50.00) = 50.00 \text{ ksi} \qquad \text{OK} \qquad \text{(Ratio = 0.502)}$$

7.6.1.2 Bottom Flange Flexural Resistance in Tension

Article 6.11.7.2.2 states that the nominal flexural resistance of the tension flange of a noncompact tub section is to be taken as:

$$F_{nt} = R_h F_{yt} \Delta \qquad \text{Eq. (6.11.7.2.2-5)}$$

in which:

$$\Delta = \sqrt{1 - 3\left(\frac{f_v}{F_{yt}}\right)^2} \qquad \text{Eq. (6.11.7.2.2-6)}$$

$$\Delta = \sqrt{1 - 3\left(\frac{1.42}{50.0}\right)^2} = 0.999$$

Therefore:

$$F_{nt} = (1.0)(50.0)(0.999) = 49.93 \text{ ksi}$$

For Strength I:

$$f_{bu} \le \phi_f F_{nt} \qquad \text{Eq. (6.11.7.2.1-2)}$$

$$f_{bu} = 37.66 \text{ ksi} \le \phi_f F_{nt} = (1.0)(49.93) = 49.93 \text{ ksi} \quad \text{OK} \quad (\text{Ratio} = 0.754)$$

Note that longitudinal warping stresses due to cross-section distortion do not need to be considered at the strength limit state. However, transverse bending stresses due to cross-section distortion do need to be considered at the strength limit state and are not to exceed 20.0 ksi as specified in Article 6.11.1.1. However, in this design example for Section G2-1, it is assumed that the transverse bending stresses at the strength limit state do not exceed 20.0 ksi. For more detailed calculations of the transverse bending stress due to cross-section distortion at the strength limit state, see the computations for Section G2-2 in this design example.

7.6.1.3 Concrete Deck Stresses

According to Article 6.11.7.2.1, the maximum longitudinal compressive stress in the concrete deck at the strength limit state is not to exceed $0.6f'_c$. This limit is to verify linear behavior of the concrete, which is assumed in the calculation of steel flange stresses. The longitudinal compressive stress in the deck is to be determined in accordance with Article 6.10.1.1.1d, which allows the permanent and transient load stresses in the concrete deck to be computed using the short-term

composite section properties (n = 7.56). Referring to Table 10 of the section property calculations, the section modulus to the top of the concrete deck is:

$$S_{deck} = \frac{502{,}098}{92.19 - 67.90} = 20{,}671 \text{ in.}^3$$

Calculate the Strength I factored longitudinal compressive stress in the deck at this section, noting that the concrete deck is not subjected to noncomposite dead loads. The stress in the concrete deck is obtained by dividing the stress acting on the transformed section by the modular ration, n.

$$f_{deck} = 1.0\left[\frac{1.25(765) + 1.5(1{,}006) + 1.75(5{,}920)}{(20{,}671)(7.56)}\right]12 = -0.99 \text{ ksi}$$

$$f_{deck} = |-0.99 \text{ ksi}| < 0.6f'_c = 0.6(4.0) = 2.40 \text{ ksi} \qquad \text{OK} \qquad \text{(Ratio = 0.413)}$$

7.7 Girder Check: Section G2-2, Constructability (Article 6.11.3)

7.7.1 Flexure (Article 6.11.3.2)

The bottom flange in regions of negative flexure is to satisfy the requirements of Eqs. (6.11.3.2-1) and (6.11.3.2-2) for critical stages of construction. Generally, these provisions will not control because the size of the bottom flange in negative flexure regions is normally governed by the strength limit state. With regard to construction loads, the maximum negative moment reached during the deck placement analysis, plus the moment due to the self-weight, typically does not significantly exceed the calculated noncomposite negative moments assuming a single stage deck pour. Nonetheless, the constructability check is performed herein for completeness and to illustrate the constructability checks for a negative moment region. For this constructability check, it is assumed that the concrete deck has not yet hardened at Section G2-2.

$$f_{bu} \le \phi_f F_{nc} \qquad \text{Eq. (6.11.3.2-1)}$$

$$f_{bu} \le \phi_f F_{crw} \qquad \text{Eq. (6.11.3.2-2)}$$

Additionally, the top flanges, which are considered discretely braced for constructability (i.e., the deck is not hardened), must satisfy the requirement specified in Article 6.10.3.2.2. Because the top flange is discretely braced, flange lateral bending must be considered, as shown in Eq. 6.10.3.2.2-1.

$$f_{bu} + f_\ell \le \phi_f R_h F_{yt} \qquad \text{Eq. (6.10.3.2.2-1)}$$

To illustrate this constructability check, from separate analysis results not shown, the unfactored major-axis bending moment due to the deck pour sequence is -12,272 kip-ft. As shown in Table 4, the unfactored major-axis moment due to steel self-weight is -3,154 kip-ft.

Calculate the factored major-axis flexural stresses in the flanges of the steel section resulting from the steel self-weight and the assumed deck pour sequence.

For Construction Strength I:

$$\text{Top Flange:} \quad f_{bu} = -\frac{1.0(1.25)[(-3{,}154) + (-12{,}272)](12)}{10{,}057} = 23.01 \text{ ksi}$$

$$\text{Bot. Flange:} \quad f_{bu} = \frac{1.0(1.25)[(-3{,}154) + (-12{,}272)](12)}{11{,}316} = -20.45 \text{ ksi}$$

For this example, and illustration purposes, the V-load equation is used to compute the top flange lateral bending moment due to curvature. For a single flange, consider only one-half of the girder major-axis moment due to steel self-weight and the deck placement sequence.

$$M = \frac{\left[(-3{,}154) + (-12{,}272)\right]}{2} = -7{,}713 \text{ kip-ft}$$

$$M_{LAT} = \frac{M\ell^2}{NRD} = \left|\frac{(-7{,}713)(16.3)^2}{(12)(716.25)(6.5)}\right| = 36.7 \text{ kip-ft} \qquad \text{Eq. (C4.6.1.2.4b-1)}$$

Combine the flange lateral bending moment computed using the V-load equation with the factored lateral moment due to the overhang brackets, which was computed previously in the Section G2-1 calculations. Noting that the factored flange lateral bending moment due to the deck overhang bracket loads is 12.4 kip-ft, the factored flange lateral bending moment and flange lateral bending stress are computed as:

$$M_{TOT\_LAT} = (1.25)(36.7) + 12.4 = 58.3 \text{ kip-ft}$$

$$f_\ell = \frac{M_{TOT\_LAT}}{S_\ell} = \frac{(58.3)(12)}{(3.00)(18)^2/6} = 4.32 \text{ ksi}$$

Because the top flanges are subject to tension at Section G2-2, amplification of the first-order flange lateral bending stress is not required. The factored flange lateral bending stress is less than the limit of $0.6F_{yf} = 0.6(50) = 30.0$ ksi specified in Article 6.10.1.6.

It should be noted that another significant source of flange lateral bending results from forces that develop in the single-diagonal top flange bracing members resulting from the major-axis bending of the tub girder. This effect is recognized in flange lateral moments taken directly from a finite element analysis. In the absence of a refined analysis, Fan and Helwig [24] have developed equations to evaluate bracing member forces and the forces imparted on the top flanges of tub girders resulting from major-axis bending of the girder. The flange lateral bending due to the top lateral bracing is not considered in these computations. However, in an actual bridge design the

top-flange lateral bending moments due to the forces in the top lateral bracing members resulting from major-axis bending should be considered, and can be computed using the procedures suggested by Fan and Helwig [24].

Compute the factored St. Venant torsional shear stress, f_v, in the bottom flange for the Strength I load combination.

$$f_v = \frac{T}{2A_o t_f} \qquad \text{Eq. (6.11.3.2-5)}$$

Compute the enclosed area of the noncomposite tub section, A_o.

$$A_o = \frac{\left[120 + \left(83 - 2\left(1.5\right)\right)\right]}{2}\left(\frac{3.00}{2} + 78 + \frac{1.50}{2}\right) = 8{,}025 \text{ in.}^2$$

The unfactored torques due to steel self-weight and Cast #1 are -22 kip-ft and -33 kip-ft, respectively (note that results for Cast #1 at this location are not provided in the analysis results table). Therefore,

$$f_v = \left(1.0\right)\frac{\left(1.25\right)\left(22 + 33\right)\left(12\right)}{2\left(8{,}025\right)\left(1.50\right)} = \text{ 0.034 ksi}$$

7.7.1.1 Top Flange

Check that the top flange tension stress is in compliance with Article 6.10.3.2.2:

$$f_{bu} + f_\ell \le \phi_f R_h F_{yt} \qquad \text{Eq. (6.10.3.2.2-1)}$$

For Construction Strength I:

$$f_{bu} + f_\ell = 23.01 \text{ ksi} + 4.32 \text{ ksi} = 27.33 \text{ ksi}$$

$$\phi_f R_h F_{yt} = \left(1.0\right)\left(1.0\right)\left(50.0\right) = 50.0 \text{ ksi}$$

$$f_{bu} + f_\ell = 27.33 \text{ ksi} \; < \; \phi_f R_h F_{yt} = 50.0 \text{ ksi} \qquad \text{OK} \qquad \text{(Ratio = 0.547)}$$

7.7.1.2 Bottom Flange

7.7.1.2.1 Bottom Flange: Flexural Resistance in Compression – Stiffened Flange

Calculate the nominal flexural resistance of the bottom flange in compression, F_{nc}, in accordance with Article 6.11.8.2. Per Article 6.11.3.2, in computing F_{nc} for constructability, the web load-shedding factor, R_b, is to be taken as 1.0. The bottom flange is longitudinally stiffened at this

location with a single WT 8x28.5 stiffener placed at the center of the bottom flange. Therefore, Article 6.11.8.2.3 applies.

Determine the slenderness ratio of the bottom flange:

$$\lambda_f = \frac{b_{fc}}{t_{fc}} \qquad \text{Eq. (6.11.8.2.2-8)}$$

where, in this case:

b_{fc} = w = larger of the width of the flange between the longitudinal flange stiffeners or the distance from a web to the nearest longitudinal flange stiffener.

Since the longitudinal stiffener is at the center of the bottom flange, w is the distance from the longitudinal stiffener to the inside face of the web.

$$\lambda_f = \frac{\left(\frac{79.4375}{2}\right)}{1.50} = 26.48$$

Calculate the limiting slenderness ratio, λ_p:

$$\lambda_p = 0.57\sqrt{\frac{Ek}{F_{yc}\Delta}} \qquad \text{Eq. (6.11.8.2.2-9)}$$

where k is computed in accordance with Article 6.11.8.2.3 for longitudinally stiffened flanges, and Δ is computed as specified in Article 6.11.8.2.2.

As specified in Article 6.11.8.2.3, since a single bottom flange stiffener is used, n = 1 and the plate-buckling coefficient for uniform normal stress, k, is to be taken as:

$$k = \left(\frac{8I_S}{wt_{fc}^{\ 3}}\right)^{\frac{1}{3}} \qquad \text{Eq. (6.11.8.2.3-1)}$$

and:

$$\Delta = \sqrt{1-3\left(\frac{f_v}{F_{yc}}\right)^2} \qquad \text{Eq. (6.11.8.2.2-11)}$$

where:

f_v = factored St. Venant torsional shear stress in the flange (ksi)

n = number of equally spaced longitudinal flange stiffeners
k = plate-buckling coefficient for uniform normal stress, $1.0 \le k \le 4.0$
I_S = moment of inertia of a single longitudinal flange stiffener about an axis parallel to the flange and taken at the base of the stiffener (in.^{4})

Structural tees are efficient shapes for longitudinal stiffeners because they provide a high ratio of stiffness to cross-sectional area. For the WT 8x28.5 stiffener, I_x = 48.7 in.^{4}, A = 8.39 in.^{2}, and the elastic neutral axis (N.A.) is 6.28 in. from the tip of the stem. Therefore, I_s is computed as:

$$I_S = 48.7 + (8.39)(6.28)^2 = 379.6 \text{ in.}^4$$

Compute the plate-buckling coefficient k:

$$k = \left(\frac{8(379.6)}{\left(\frac{79.4375}{2}\right)(1.50^3)} \right)^{\frac{1}{3}} = 2.83 < 4.0$$

Compute the Δ term:

$$\Delta = \sqrt{1 - 3\left(\frac{0.034}{50.0}\right)^2} = 1.0$$

Compute λ_p:

$$\lambda_p = 0.57\sqrt{\frac{(29{,}000)(2.83)}{(50.0)(1.0)}} = 23.09$$

Since λ_f is greater than 23.09 (λ_f = 26.48), it is necessary to compute the limiting slenderness ratio, λ_r:

$$\lambda_r = 0.95\sqrt{\frac{Ek}{F_{yr}}} \qquad \text{Eq. (6.11.8.2.2-10)}$$

where:

$$F_{yr} = (\Delta - 0.3)F_{yc} \le F_{yw} \qquad \text{Eq. (6.11.8.2.2-13)}$$

$$F_{yr} = (1.0 - 0.3)(50) = 35.0 \text{ ksi} < F_{yw} = 50 \text{ ksi}$$

Compute λ_r:

$$\lambda_r = 0.95\sqrt{\frac{(29{,}000)(2.83)}{35.0}} = 46.00$$

Since $\lambda_p < \lambda_f = 26.48 < \lambda_r$, then the nominal axial compression buckling resistance of the flange under compression alone, F_{cb}, is calculated as follows:

$$F_{cb} = R_b R_h F_{yc}\left[\Delta - \left(\Delta - \frac{\Delta - 0.3}{R_h}\right)\left(\frac{\lambda_f - \lambda_p}{\lambda_r - \lambda_p}\right)\right] \qquad \text{Eq. (6.11.8.2.2-3)}$$

$$F_{cb} = (1.0)(1.0)(50)\left[1.0 - \left(1.0 - \frac{1.0 - 0.3}{1.0}\right)\left(\frac{26.48 - 23.09}{46.00 - 23.09}\right)\right]$$

$$F_{cb} = 47.78 \text{ ksi}$$

Compute the nominal flexural resistance of the compression flange:

$$F_{nc} = F_{cb}\sqrt{1 - \left(\frac{f_v}{\phi_v F_{cv}}\right)^2} \qquad \text{Eq. (6.11.8.2.2-1)}$$

where:

F_{cv} = nominal shear buckling resistance of the flange under shear alone (ksi)

In order to compute F_{cv}, first calculate k_s, the plate-buckling coefficient for shear stress as specified in Article 6.11.8.2.3:

$$k_S = \frac{5.34 + 2.84\left(\frac{I_S}{wt_{fc}^{\,3}}\right)^{\frac{1}{3}}}{(n+1)^2} \le 5.34 \qquad \text{Eq. (6.11.8.2.3-3)}$$

$$k_S = \frac{5.34 + 2.84\left(\frac{379.6}{(79.4375/2)(1.50^3)}\right)^{\frac{1}{3}}}{(1+1)^2} = 2.34 < 5.34$$

As specified in Article 6.11.8.2.2, if $\lambda_f \le 1.12\sqrt{\frac{Ek_s}{F_{yc}}}$, then:

$$F_{cv} = 0.58F_{yc} \qquad \text{Eq. (6.11.8.2.2-5)}$$

$$\lambda_f = 26.48 < 1.12\sqrt{\frac{(29{,}000)(2.34)}{50}} = 41.26$$

Therefore:

$$F_{cv} = 0.58(50) = 29.0 \text{ ksi}$$

Compute F_{nc}:

$$F_{nc} = 47.78\sqrt{1-\left(\frac{0.034}{(1.0)(29.0)}\right)^2} = 47.78 \text{ ksi}$$

Checking compliance with Eq. 6.11.3.2-1:

$$f_{bu} \le \phi_f F_{nc} \qquad \text{Eq. (6.11.3.2-1)}$$

For Construction Strength I:

$$f_{bu} = |\text{-}20.45 \text{ ksi}| \; < \; \phi_f F_{nc} = (1.00)(47.78) \; = \; 47.78 \text{ ksi} \qquad \text{OK} \qquad \text{(Ratio = 0.428)}$$

7.7.1.2.2 Bottom Flange: Flexural Resistance in Compression – Web Bend-Buckling

According to Article 6.11.3.2, for sections with compact or noncompact (i.e., nonslender) webs, the web bend-buckling check of Eq. 6.11.3.2-2 is not necessary. Therefore, check if the web satisfies the noncompact slenderness limit given in Article 6.10.6.2.3.

$$\frac{2D_c}{t_w} \le \lambda_{rw} \qquad \text{Eq. (6.10.6.2.3-1)}$$

where:

$$4.6\sqrt{\frac{E}{F_{yc}}} \le \lambda_{rw} = \left(3.1+\frac{5.0}{a_{wc}}\right)\sqrt{\frac{E}{F_{yc}}} \le 5.7\sqrt{\frac{E}{F_{yc}}} \qquad \text{Eq. (6.10.6.2.3-3)}$$

$$a_{wc} = \frac{2D_c t_w}{b_{fc} t_{fc}}$$ Eq. (6.10.6.2.3-4)

For a tub girder with inclined webs, the depth of the web in compression, D_c, must be taken along the inclined web. Therefore:

$$D_c = (38.82 - 1.5) / \cos 14.04^\circ = 38.47 \text{ in.}$$

$$\frac{2D_c}{t_w} = \frac{2(38.47)}{0.5625} = 136.8$$

$$4.6\sqrt{\frac{E}{F_{yc}}} = 4.6\sqrt{\frac{29,000}{50}} = 111$$

$$5.7\sqrt{\frac{E}{F_{yc}}} = 5.7\sqrt{\frac{29,000}{50}} = 137$$

$$a_{wc} = \frac{2(38.47)(0.5625)}{(79.4375/2)(1.5)} = 0.73$$

$$111 < \lambda_{rw} = \left(3.1 + \frac{5.0}{0.73}\right)\sqrt{\frac{29,000}{50}} = 240 > 137$$

$$\therefore \lambda_{rw} = 137 > \frac{2D_c}{t_w} = 136.8$$

Since Eq. 6.10.6.2.3-1 is satisfied, the web is nonslender and the web bend-buckling check of Eq. 6.11.3.2.-2 does not need to be investigated for constructability.

7.7.1.3 Shear (Article 6.11.3.3)

For constructability, Article 6.10.3.3 requires that interior panels of stiffened webs satisfy the following requirement:

$$V_u \le \phi_v V_{cr}$$ Eq. (6.10.3.3-1)

where:

ϕ_v = resistance factor for shear specified in Article 6.5.4.2 (ϕ_v = 1.0)
V_u = shear in the web at the section under consideration due to the factored permanent loads and factored construction loads applied to the noncomposite section.

V_{cr} = shear-yield or shear-buckling resistance determined from Eq. (6.10.9.3.3-1).

The panel on the Span 2 side of Section G2-2 will be investigated herein. The transverse stiffener spacing at this location is 62 inches. The total factored shear will include the contribution of the noncomposite dead load, and should not only include the vertical shear due to flexure but also shear in the web due to torsion. The shears used in the computations below are for flexure plus the torsional shear in the critical web. The critical web shear due to steel self-weight is 47 kips (see Table 2), and the critical web shear for Cast #1 is taken as 185 kips (analysis results are not explicitly provided for Cast #1).

For Construction Strength I:

$$V_u = 1.0(1.25)(47+185) = 265 \text{ kips}$$

However, it is required that the shear be taken along the inclined web, in accordance with Article 6.11.9:

$$V_{ui} = \frac{V_u}{\cos(\theta_{WEB})} \qquad \text{Eq. (6.11.9-1)}$$

$$V_{ui} = \frac{265}{\cos(14.04°)} = 273 \text{ kips}$$

The shear-buckling resistance of the 62 inch panel is determined as:

$$V_n = V_{cr} = CV_p \qquad \text{Eq. (6.10.9.3.3-1)}$$

C is the ratio of the shear-buckling resistance to the shear yield strength determined as specified in Article 6.10.9.3.2. First, compute the shear-buckling coefficient, k:

$$k = 5 + \frac{5}{\left(\frac{d_o}{D}\right)^2} = 5 + \frac{5}{\left(\frac{62}{80.4}\right)^2} = 13.41 \qquad \text{Eq. (6.10.9.3.2-7)}$$

Since:

$$\frac{D}{t_w} = \frac{80.4}{0.5625} = 142.9 > 1.40\sqrt{\frac{Ek}{F_{yw}}} = 1.40\sqrt{\frac{29{,}000(13.41)}{50}} = 123.5$$

$$C = \frac{1.57}{\left(\frac{D}{t_w}\right)^2}\left(\frac{Ek}{F_{yw}}\right) \qquad \text{Eq. (6.10.9.3.2-6)}$$

$$C = \frac{1.57}{(142.9)^2}\left(\frac{29{,}000(13.41)}{50}\right) = 0.598$$

V_p is the plastic shear force and is calculated as follows:

$$V_p = 0.58F_{yw}Dt_w \qquad \text{Eq. (6.10.9.3.3-2)}$$

$$V_p = 0.58\ (50.0)(80.40)(0.5625) = 1{,}311 \text{ kips}$$

Therefore,

$$V_n = V_{cr} = CV_p = (0.598)(1{,}311) = 784 \text{ kips}$$

$$\phi_v V_{cr} = 1.0(784) = 784 \text{ kips}$$

$V_{ui} = 273$ kips $< \phi_v V_{cr} = 784$ kips OK (Ratio = 0.348)

7.8 Girder Check: Section G2-2, Service Limit State (Article 6.11.4)

Article 6.11.4 directs the Engineer to Article 6.10.4, which contains provisions related to the control of elastic and permanent deformations at the service limit state.

7.8.1 Permanent Deformations (Article 6.10.4.2)

Article 6.10.4.2 contains criteria intended to control permanent deformations that would impair rideability. As specified in Article 6.10.4.2.1, these checks are to be made under the Service II load combination.

As stated previously for the service limit state check of Section G2-1, Article 6.10.4.2.2 requires that flanges of composite sections satisfy the following:

Top flange of composite sections: $f_f \le 0.95R_hF_{yf}$ Eq. (6.10.4.2.2-1)

Bottom flange of composite sections: $f_f + \frac{f_\ell}{2} \le 0.95R_hF_{yf}$ Eq. (6.10.4.2.2-2)

However, according to Article C6.11.4, under the load combinations specified in Table 3.4.1-1, Eqs. 6.10.4.2.2-1 and 6.10.4.2.2-2 need only be checked for compact sections in positive flexure. For sections in negative flexure and noncompact sections in positive flexure, these two equations do not control and need not be checked. Therefore, for Section G2-2, Eqs. 6.10.4.2.2-1 and 6.10.4.2.2-2 do not need to be checked, and are not checked in this example.

7.8.2 Web Bend-Buckling

With the exception of composite sections in positive flexure in which the web satisfies the requirement of Articles 6.11.2.1.2 and 6.10.2.1.1 (i.e., $D/t_w \leq 150$), web bend-buckling of all sections under the Service II load combination is to be checked as follows:

$$f_c \leq F_{crw} \qquad \text{Eq. (6.10.4.2.2-4)}$$

The term f_c is the compression-flange stress at the section under consideration due to the Service II loads calculated without consideration of flange lateral bending, and F_{crw} is the nominal elastic bend-buckling resistance for webs determined as specified in Article 6.10.1.9. Because Section G2-2 is a section in negative flexure, Eq. 6.10.4.2.2-4 must be checked.

Determine the nominal web bend-buckling resistance, F_{crw}, for Section G2-2 in accordance with Article 6.10.1.9.1, as follows:

$$F_{crw} = \frac{0.9Ek}{\left(\frac{D}{t_w}\right)^2} \qquad \text{Eq. (6.10.1.9.1-1)}$$

However, F_{crw} is not to exceed the smaller of R_hF_{yc} and $F_{yw}/0.7$. The bend-buckling coefficient, k, is computed as:

$$k = \frac{9}{\left(D_c / D\right)^2} \qquad \text{Eq. (6.10.1.9.1-2)}$$

where:

D_c = depth of the web in compression in the elastic range (in.). For composite sections, D_c is to be determined as specified in Article D6.3.1.

In accordance with Article 6.10.4.2.1, for members with shear connectors provided throughout the entire length of the girder that also satisfy Article 6.10.1.7, the concrete deck may be assumed to be effective for both positive and negative flexure for loads applied to the composite section, provided that the corresponding longitudinal stresses in the concrete deck at the section under consideration under the Service II loads are smaller than $2f_r$, where f_r is the modulus of rupture of concrete specified in Article 6.10.1.7. The requirements of Article 6.10.1.7 related to the minimum one percent longitudinal reinforcement required in the concrete deck are satisfied for Section G2-2 in this design example.

$$f_r = 0.24\sqrt{f'_c} \qquad \text{Article 6.10.1.7}$$

Therefore,

$$2f_r = 2\left(0.24\sqrt{4}\right) = 0.960 \text{ ksi}$$

In accordance with Article 6.10.1.1.1d, the longitudinal flexural stresses in the concrete deck due to all permanent and transient loads are to be computed using the short-term modular ratio, *n*. The calculated stress on the transformed section is divided by *n* to obtain the longitudinal stress in the concrete deck. Since the deck is not subjected to noncomposite dead loads, the longitudinal stress in the deck at Section G2-2 is due to DC2, DW, and LL+I moments only. The unfactored major-axis bending moments at Section G2-2 are (see Table 4):

Noncomposite Dead Load:	M_{DC1}	= -15,426 kip-ft
Composite Dead Load:	M_{DC2}	= -1,923 kip-ft
Future Wearing Surface Dead Load:	M_{DW}	= -2,550 kip-ft
Live Load (incl. IM and CF):	M_{LL+IM}	= -8,127 kip-ft

The longitudinal compressive stress in the deck is to be determined in accordance with Article 6.10.1.1.1d, which allows the permanent and transient load stresses to be computed using the short-term composite section properties (*n* = 7.56). Referring to Table 13 of the section property calculations, the section modulus to the top of the concrete deck is:

$$S_{deck} = \frac{833{,}768}{93.00 - 62.27} = 27{,}132 \text{ in.}^3$$

Calculate the Service II factored longitudinal compressive stress in the deck at this section, noting that the concrete deck is not subjected to noncomposite dead loads. The stress in the concrete deck is obtained by dividing the stress acting on the transformed section by the modular ratio, *n*.

$$f_{deck} = -1.0\left[\frac{1.00(-1{,}923) + 1.00\left(-2{,}550\right) + 1.30\left(-8{,}127\right)}{\left(27{,}132\right)\left(7.56\right)}\right]12 = 0.880 \text{ ksi}$$

$$f_{deck} = 0.880 \text{ ksi} \; < \; 2f_r = 0.960 \text{ ksi}$$

Since f_{deck} is less than $2f_r$, for this Service limit state check, the flexural stresses in the composite section caused by the Service II loads acting on the composite section may be computed assuming that the concrete deck is effective in tension. Refer to Table 12 and Table 13 for the section properties assuming that the concrete deck is effective. The major-axis bending stresses in the top and bottom flanges for the Service II load combination are computed as follows (f_t = tension flange, f_c = compression flange):

For Service II:

Top Flange:

$$f_t = -1.0\left[\frac{1.00(\text{-}15{,}426)}{10{,}057} + \frac{1.00(\text{-}1{,}923)}{19{,}574} + \frac{1.00(\text{-}2{,}550)}{19{,}574} + \frac{1.30(\text{-}8{,}127)}{41{,}234}\right]12 = 24.22 \text{ ksi}$$

Bottom Flange:

$$f_c = 1.0\left[\frac{1.00(\text{-}15{,}426)}{11{,}316} + \frac{1.00(\text{-}1{,}923)}{12{,}562} + \frac{1.00(\text{-}2{,}550)}{12{,}562} + \frac{1.30(\text{-}8{,}127)}{13{,}390}\right]12 = -30.10 \text{ ksi}$$

In order to compute F_{crw}, it is first necessary to determine D_c, the depth of the web in compression, in accordance with Eq. D6.3.1-1, as required in Article D6.3.1 for composite sections in negative flexure whenever the deck is considered effective in tension at the service limit state:

$$D_c = \left(\frac{-f_c}{|f_c| + f_t}\right)d - t_{fc} \geq 0 \qquad \text{Eq. (D6.3.1-1)}$$

where:

f_c = sum of the compression flange stresses caused by DC1, DC2, DW, and LL+I; acting on their respective sections (ksi). Flange lateral bending is disregarded.
f_t = sum of the tension flange stresses caused by DC1, DC2, DW, and LL+I; acting on their respective sections (ksi). Flange lateral bending is disregarded.
d = depth of steel section (in.)
t_{fc} = thickness of compression flange (in.)

Therefore:

$$D_c = \left(\frac{-(-30.10)}{|-30.10| + 24.22}\right)(82.50) - 1.50 = 44.22 \text{ in. } > 0$$

However, the depth of the web in compression, D_c, should be taken along the inclined web for computing the web bend-buckling resistance. Therefore:

$$D_{ci} = \frac{44.22}{\cos\left(14.04°\right)} = 45.58 \text{ in.}$$

Compute the bend-buckling coefficient, k:

$$k = \frac{9}{\left(D_c / D\right)^2} = \frac{9}{\left(45.58 / 80.40\right)^2} = 28.00$$

Therefore, the nominal web bend-buckling resistance, F_{crw}, is computed as:

$$F_{crw} = \frac{0.9Ek}{\left(\frac{D}{t_w}\right)^2} = \frac{0.9\ (29{,}000)\ (28.00)}{\left(\frac{80.40}{0.5625}\right)^2} = 35.77 \text{ ksi} \ < \ \min\left(R_h F_{yc}, F_{yw}/0.7\right) = 50.0 \text{ ksi}$$

Verify Eq. (6.10.4.2.2-4):

$$f_c = \left|-30.10\right| \text{ ksi} < F_{crw} = 35.77 \text{ ksi} \qquad \text{OK} \qquad \text{(Ratio = 0.841)}$$

7.8.3 Concrete Deck (Article 6.10.1.7)

Article 6.10.1.7 requires the minimum one-percent longitudinal reinforcement in the concrete deck wherever the longitudinal tensile stress in the deck due to the factored construction loads or due to the Service II load combination exceeds ϕf_r. This check is illustrated for the negative moment region in NSBA's *Steel Bridge Design Handbook: Example 4: Three-Span Continuous Straight Composite Steel Tub-Girder Bridge* [8].

7.9 Girder Check: Section G2-2, Fatigue Limit State (Article 6.11.5)

Article 6.11.5 directs the designer to Article 6.10.5, where details in tub girder flexural members must be investigated for fatigue as specified in Article 6.6.1. The Fatigue I load combination specified in Table 3.4.1-1 and the fatigue live load specified in Article 3.6.1.4 are employed for checking load-induced fatigue at Section G2-2.

At Section G2-2, it is necessary to check the top flange for the fatigue limit state for major-axis bending. The base metal at the transverse stiffener weld terminations and internal cross-frame connection-plate welds at locations subject to a net tensile stress must be checked as a Category C′ fatigue detail (refer to Table 6.6.1.2.3-1). Additional consideration must be given to cross-section distortion stresses, as discussed in more detail later in this section.

According to Table 3.6.2.1-1, the dynamic load allowance for the fatigue live load is 15%. Centrifugal force effects are considered and included in the fatigue live load moments. As discussed previously, the projected 75-year single lane ADTT in one direction is assumed to be 1,000 trucks per day.

According to Eq. (6.6.1.2.2-1), $\gamma(\Delta f)$ must not exceed the nominal fatigue resistance, $(\Delta F)_n$. In accordance with Article C6.6.1.2.2, the resistance factor, ϕ, and the load modifier, η, are taken as 1.0 for the fatigue limit state.

$$\gamma\left(\Delta f\right) \le \left(\Delta F\right)_n \qquad \text{Eq. (6.6.1.2.2-1)}$$

From Table 6.6.1.2.3-2, the 75-year $(ADTT)_{SL}$ Equivalent to Infinite Life for a Category C′ fatigue detail is 975 trucks per day. Therefore, since the assumed $(ADTT)_{SL}$ for this design example is

1,000 trucks per day, the detail must be checked for infinite fatigue life using the Fatigue I load combination. Per Article 6.6.1.2.5, the nominal fatigue resistance for infinite fatigue life is equal to the constant-amplitude fatigue threshold:

$$(\Delta F)_n = (\Delta F)_{TH} \qquad \text{Eq. (6.6.1.2.5-1)}$$

where $(\Delta F)_{TH}$ is the constant-amplitude fatigue threshold taken from Table 6.6.1.2.5-3. For a Category C′ fatigue detail, $(\Delta F)_{TH}$ = 12.0 ksi, and therefore:

$$(\Delta F)_n = 12.0 \text{ ksi}$$

As shown in Table 4 the unfactored negative and positive moments due to fatigue, including the 15 percent dynamic load allowance, at Section G2-2 are -1,384 kip-ft and 256 kip-ft, respectively.

In accordance with Article 6.6.1.2.1, for flexural members that utilize shear connectors throughout the entire length that also have concrete deck reinforcement satisfying the provisions of Article 6.10.1.7, it is permissible to compute the flexural stresses and stress ranges assuming the concrete deck to be effective for both positive and negative flexure at the fatigue limit state.

As required by Articles 6.10.10.1 and 6.11.10, shear connectors are necessary along the entire length of horizontally curved tub girder bridges. Also, earlier calculations in this design example show that the deck reinforcement is in compliance with Article 6.10.1.7. Therefore, the concrete deck is assumed effective in computing the major-axis bending stresses for the fatigue limit state at Section G2-2. The short-term composite section properties (n = 7.56) used to compute the stress at the top of the web (bottom of the top flange) are:

$I_{NA(n)}$ = 833,768 in.^{4}

$d_{TOP\ OF\ WEB} = d_{TOP\ OF\ STEEL} - t_{f\_TOP\ FLANGE}$ = 20.23 in. – 3.00 in. = 17.23 in.

As specified in Table 3.4.1-1, the load factor, γ, for the Fatigue I load combination is 1.75. The factored stress range at the top of the web, without consideration of the flange lateral bending stress and distortional longitudinal warping stress since the top flange is continuously braced by the concrete deck, is computed as follows:

$$\gamma(\Delta f) = (1.75)\left(\frac{(|-1,384| + 256)(12)(17.23)}{833,768}\right) = 0.71 \text{ ksi} < (\Delta F)_{TH} = 12.0 \text{ ksi} \quad \text{ok}$$

(Ratio = 0.059)

7.9.1 Cross-section Distortion Stresses

As stated previously for the fatigue limit state check of Section G2-1, additional requirements are placed on computing stresses due to fatigue loads for tub sections. In particular, Article 6.11.5 requires the consideration of longitudinal warping stresses and transverse bending stresses due to

cross-section distortion in tub sections. When a tub section is subjected to torsion, the cross-section becomes distorted, resulting in these secondary stresses.

In accordance with Article 6.11.5, the stress range due to longitudinal warping resulting from cross-section distortion should be considered when investigating the load-induced fatigue resistance of the base metal at all details in a horizontally curved tub section. For simplicity, the longitudinal warping stresses are added to the longitudinal major-axis bending stresses.

Also, as specified in Article 6.11.5, the stress range due to the transverse bending stresses is to be considered in the base metal adjacent to the termination of fillet welds connecting transverse elements to webs and box flanges. The transverse bending stresses are considered separately from the longitudinal warping stresses. Article C6.11.5 states that as a result of the transverse bending, a stress concentration occurs at the termination of the fillet welds connecting transverse elements to webs and box flanges. According to Article C6.11.5, the fatigue resistance of this detail, when subject to transverse bending, is not currently quantified but is anticipated to be as low as a Category E detail.

Calculations to determine the stress range from longitudinal warping and transverse bending can be carried out using the beam-on-elastic-foundation (BEF) analogy presented by Wright and Abdel-Samad [9]. The *Designers Guide to Box Girder Bridges* by Bethlehem Steel Corporation [25] also presents the method developed by Wright and Abdel-Samad to estimate the transverse bending stresses using the BEF analogy. In this method, the moment in the BEF is analogous to the longitudinal warping stress and the deflection of the BEF is analogous to the transverse bending stress.

The BEF analogy for computing the distortional stresses is demonstrated for Section G2-2 in the calculations that follow. Equation and figure references relate to those shown in the *Designers Guide to Box Girder Bridges* (DGBGB) [25]. The calculations that follow are intended to simply illustrate the procedure for computing these stresses using the BEF analogy. These stresses are typically of greater concern in boxes subject to much larger torques; e.g., single box sections, sharply curved boxes and boxes resting on skewed supports. Also, at Section G2-2, the bottom flange is not subject to a net tensile stress by inspection, and the top flanges are continuously braced by the concrete deck. Thus, the effect of the distortional stresses may be ignored at Section G2-2 for fatigue. However, in an actual design of a horizontally curved tub girder, these stresses should at least be considered in the base metal adjacent to welded details at or near the bottom flange at locations where the flange is subject to a net tensile stress.

From a separate analysis (all results not shown) the unfactored negative and positive torques due to fatigue loading, including the 15 percent dynamic load allowance, at Section G2-2 are -309 kip-ft and 339 kip-ft, respectively. Where force effects in the cross-frames or diaphragms are computed from a refined analysis, stress ranges for checking load-induced fatigue and torque ranges for checking fatigue due to cross-section distortion in cross-frame and diaphragm members should be based on the single fatigue truck positioned as specified in Article 3.6.1.4.3a, but with the truck confined to a single transverse position during each passage of the truck along the bridge (per Article C6.6.1.2.1).

For continuous spans, the number of stress cycles per truck passage, n, is equal to 1.5 at sections near the interior pier and 1.0 elsewhere (Table 6.6.1.2.5-2). Sections 'near the interior pier' are defined as sections within a distance of one-tenth of the span on each side of the interior support. As indicated in Article C6.6.1.2.3, for values of n other than 1.0, the values of the 75-year $(ADTT)_{SL}$ Equivalent to Infinite Life given in Table 6.6.1.2.3-2 are to be modified by dividing by the appropriate value of n taken from Table 6.6.1.2.5-2.

The projected 75-year single lane Average Daily Truck Traffic $(ADTT)_{SL}$ is assumed to be 1,000 trucks per day for this example. From Table 6.6.1.2.3-2, the 75-year $(ADTT)_{SL}$ Equivalent to Infinite Life for a Category E detail is 4,615/1.5 = 3,077 trucks per day, adjusted for n = 1.5, which is greater than 1,000 trucks per day. Therefore, the detail must be checked for finite fatigue life using the Fatigue II load combination. Applying the load factor for the Fatigue II load combination ($\gamma = 0.80$), the factored fatigue torque range, T_{FAT}, is:

$$T_{FAT} = (0.80)\left[|-309| + 339\right] = 518 \text{ kip-ft}$$

Other required constants that will be used in the calculations that follow are:

$I_{NA(n)}$ = 833,768 in.^{4}.
t_c = web thickness = 0.5625 in.
t_b = bottom flange thickness = 1.50 in.
t_a = slab thickness = 9.5 in.
E_c = 3,834 ksi
E_s = 29,000 ksi
μ_c = Possion's ratio for concrete = 0.20 (Article 5.4.2.5)
μ_s = Possion's ratio for steel = 0.30
ℓ = cross-frame spacing = 16.30 ft = 196 in.
Transverse stiffener spacing at Section G2-2 = 62 in.
Transverse stiffener is 0.5 in. x 5.5 in.

Calculate the transverse flexural rigidities, D_a and D_b, of the concrete deck and the bottom box flange, respectively.

$$D_a = \frac{E_c t_a^3}{12\left(1-\mu_c^2\right)} = \frac{(3{,}834)(9.5)^3}{12\left(1-0.20^2\right)} = 285{,}345 \ \frac{\text{k}-\text{in.}^2}{\text{in.}} \qquad \text{DGBGB Eq. (A3a)}$$

$$D_b = \frac{E_s t_b^3}{12\left(1-\mu_s^2\right)} = \frac{(29{,}000)(1.50)^3}{12\left(1-0.30^2\right)} = 8{,}963 \ \frac{\text{k}-\text{in.}^2}{\text{in.}} \qquad \text{DGBGB Eq. (A3b)}$$

Article 6.11.1.1 permits transverse stiffeners to be considered effective in resisting transverse bending. Therefore, the transverse flexural rigidity of the web, D_c, is computed considering the stiffness of the transverse stiffener. Calculate the effective width of the web plate, d_o, that acts with the transverse stiffener (see Figure 14):

$$d_o = \frac{d \tanh\left(5.6\frac{d}{h}\right)}{5.6\frac{d}{h}\left(1-\mu_s^2\right)}$$ DGBGB Eq. (A4)

where:

d = spacing of transverse stiffeners = 62 in.
h = web plate depth along the inclined web = 80.40 in.

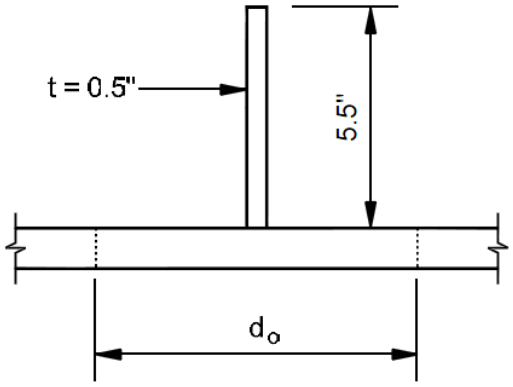

Figure 14 Effective Width of Web Plate, d_o, Acting with the Transverse Stiffener

Therefore,

$$d_o = \frac{(62)\ \tanh\left(5.6\left(\frac{62}{80.40}\right)\right)}{5.6\left(\frac{62}{80.40}\right)\left(1-0.30^2\right)} = 15.8 \text{ in.}$$

The transverse flexural rigidity of the web, D_c, considering the stiffness of the transverse stiffener is computed as:

$$D_c = \frac{E_s I_s}{d}$$ DGBGB Eq. (A3d)

where:

I_s = moment of inertia of the effective stiffened web plate for transverse bending, including the transverse stiffener.

To compute I_s, first compute the location of the neutral axis of the effective section from the outer web face:

Area of stiffener = (5.5)(0.5) = 2.75 in.^{2}

Area of effective web = (15.8)(0.5625) $= 8.89 \text{ in.}^2$
Total Area $= 11.64 \text{ in.}^2$

$$\text{N.A.} = \frac{2.75\left(0.5625 + \frac{5.5}{2}\right) + 8.89\left(\frac{0.5625}{2}\right)}{11.64} = 1.0 \text{ in.}$$

Calculate the moment of inertia, I_s:

$$I_s = \left(\frac{1}{12}\right)(0.5)(5.5)^3 + 2.75\left(\frac{5.5}{2} + 0.5625 - 1.0\right)^2 + \left(\frac{1}{12}\right)(15.8)(0.5625)^3 + 8.89\left(\frac{0.5625}{2} - 1.0\right)^2$$

$I_s = 26.5 \text{ in.}^4$

Therefore,

$$D_c = \frac{(29{,}000)(26.5)}{62} = 12{,}395 \ \frac{\text{kip-in.}^2}{\text{in.}}$$

The stiffness of the transverse stiffener is assumed to be distributed evenly along the web.

Compute the compatibility shear, v, at the center of the bottom (box) flange for unit loads applied at the top corners of a box section of a unit length:

$$v = \frac{\frac{1}{D_c}\left[(2a + b)abc\right] + \frac{1}{D_a}ba^3}{(a + b)\left(\frac{a^3}{D_a} + \frac{2c\left(a^2 + ab + b^2\right)}{D_c} + \frac{b^3}{D_b}\right)} \qquad \text{DGBGB Eq. (A2)}$$

where a, b, and c are dimensional parameters of the tub section:

a = distance between centerline of webs at top of tub section = 120 in.
b = distance between centerline of webs at bottom of tub section = 80 in.
c = height of web, along the incline = 80.40 in.

$$v = \frac{\frac{1}{12,395}\left[\left(2(120)+80\right)(120)(80)(80.40)\right] + \frac{1}{285,345}(80)\left(120^3\right)}{(120+80)\left(\frac{120^3}{285,345} + \frac{2(80.40)\left(120^2+(120)(80)+80^2\right)}{12,395} + \frac{80^3}{8,963}\right)} = 0.22$$

Compute the box distortion per kip of load, δ_1, assuming no cross-bracing or diaphragms are present:

$$\delta_1 = \frac{ab}{24(a+b)}\left[\frac{c}{D_c}\left(\frac{2ab}{a+b} - v(2a+b)\right) + \frac{a^2}{D_a}\left(\frac{b}{a+b} - v\right)\right] \qquad \text{DGBGB Eq. (A1)}$$

$$\delta_1 = \frac{(120)(80)}{24(120+80)}\left[\frac{80.40}{12,395}\left(\frac{2(120)(80)}{120+80} - (0.22)\left(2(120)+80\right)\right) + \frac{120^2}{285,345}\left(\frac{80}{120+80} - 0.22\right)\right]$$

$$\delta_1 = 0.35 \ \frac{\text{in.}^2}{\text{kip}}$$

The BEF stiffness parameter, β, is a measure of the torsional stiffness of the beam, and is analogous to the beam-foundation parameter in the BEF derivation. The BEF stiffness parameter, β, is calculated as:

$$\beta = \left(\frac{1}{E\ I_c\ \delta_1}\right)^{\frac{1}{4}} \qquad \text{DGBGB Eq. (A5)}$$

$$\beta = \left(\frac{1}{(29,000)(833,768)(0.35)}\right)^{\frac{1}{4}} = 0.00330 \text{ in.}^{-1}$$

Multiplying the BEF stiffness parameter by the length between internal cross-frames yields:

$$\beta\ \ell = (0.00330)(196.0) = 0.65$$

The transverse bending stress range at the top or bottom corners of the tub section may be determined as:

$$\sigma_t = C_t\ F_d\ \beta\ \frac{1}{2a}\ T_{range} \qquad \text{DGBGB Eq. (A8)}$$

where:

C_t = BEF factor for determining the transverse distortional bending stress from DGBGB Figure A6 (see Figure 15)

T_{range} = range of concentrated torque = T_{FAT} (computed previously)

a = distance between webs at the top of tub section

F_d = $\frac{bv}{2S}$ for the bottom corner of tub section [DGBGB Eq. (A9a)]

= $\left(\frac{a}{2S}\right)\left(\frac{b}{a+b}-v\right)$ for top corner of tub section [DGBGB Eq. (A9b)]

S = section modulus of the transverse member (per inch)

Calculate the section modulus, S, per unit length of the stiffened portion of the web. S is taken at the top of the transverse member. In the following equation, the section modulus is divided by the stiffener spacing, d; and the distance from neutral axis of the stiffened web to the tip of the stiffener is c_S.

$$S_{STIFFENED} = \left(\frac{I}{c_S}\right)\left(\frac{1}{d}\right) = \left(\frac{26.5}{5.5+0.5625-1.0}\right)\left(\frac{1}{62}\right) = 0.084 \ \frac{\text{in.}^3}{\text{in.}}$$

Calculate the section modulus, S, per unit length of the unstiffened portion of the web taken at the mid-thickness of the web. In the equation that follows, b_{US} is taken as a unit 1.0 inch, so that the section modulus is computed per unit length.

$$S_{UNSTIFFENED} = \left(\frac{b_{US}h^2}{6}\right) = \left(\frac{(1.0)(0.5625)^2}{6}\right) = 0.0527 \ \frac{\text{in.}^3}{\text{in.}}$$

Compute the term F_d at the bottom corner of the tub section for the stiffened and unstiffened portions of the web:

Stiffened Web: $F_d = \frac{bv}{2S} = \frac{(80)(0.22)}{2(0.084)} = 105 \ \text{in.}^{-1}$

Unstiffened Web: $F_d = \frac{bv}{2S} = \frac{(80)(0.22)}{2(0.0527)} = 167 \ \text{in.}^{-1}$

Compute the term F_d at the top corner of the tub section for the stiffened and unstiffened portions of the web:

Stiffened Web: $F_d = \left(\frac{a}{2S}\right)\left(\frac{b}{a+b}-v\right) = \left(\frac{120}{2(0.084)}\right)\left(\frac{80}{120+80}-0.22\right) = 129 \ \text{in.}^{-1}$

Unstiffened Web: $$F_d = \left(\frac{a}{2S}\right)\left(\frac{b}{a+b} - v\right) = \left(\frac{120}{2(0.0527)}\right)\left(\frac{80}{120+80} - 0.22\right) = 205 \text{ in.}^{-1}$$

It is conservatively assumed that the transverse stiffeners are not attached to the top or bottom flanges. Therefore, F_d is equal to 205 in.$^{-1}$, as the larger value governs so as to produce a larger transverse bending stress.

In order to read C_t from Figure 15 (DGBGB Figure A6), the dimensionless ratio, q, must be calculated. The quantity q represents the ratio of cross-frame / diaphragm brace stiffness to the tub section stiffness per unit length and is computed as:

$$q = \left[\frac{E_b\ A_b}{L_b\ \ell\ \delta_1}\right] \delta_b^2 \qquad \text{DGBGB Eq. (A6)}$$

where:

E_b = Young's modulus of the internal cross-frame / diaphragm material
A_b = cross-sectional area of one cross-frame / diaphragm bracing member
ℓ = internal cross-frame / diaphragm spacing
L_b = length of cross-frame / diaphragm bracing member
δ_b = deformation of the bracing member due to the applied torque and is calculated in accordance with DGBGB Eq. (A7)

$$= \frac{2\left(1+\frac{a}{b}\right)}{\sqrt{1+\left[\frac{a+b}{2h}\right]^2}}(\delta_1) \qquad \text{DGBGB Eq. (A7)}$$

h = vertical web depth of the tub section.

First, compute δ_b:

$$\delta_b = \frac{2\left(1+\frac{120}{80}\right)}{\sqrt{1+\left[\frac{120+80}{2(78)}\right]^2}}(0.35) = 1.08 \ \frac{\text{in.}^2}{\text{kip}}$$

Calculate the cross-frame stiffness ratio, q. The area of one diagonal, A_b, in the internal cross-frame is assumed to be equal to 5.0 in.^{2}, and the length of the diagonal, L_b, is equal to 87.9 in.

$$q = \left[\frac{(29{,}000)(5.0)}{(87.9)(196)(0.35)}\right] (1.08)^2 = 28.0$$

From Figure 15, for q = 28.0 and $\beta\ell$ = 0.65, C_t is approximately equal to 0.12. Therefore, the transverse bending stress range at the top or bottom corners of the tub section is:

$$\sigma_t = (0.12)(205)(0.00330)\frac{1}{2(120)}\ (518(12)) = 2.10 \text{ ksi}$$

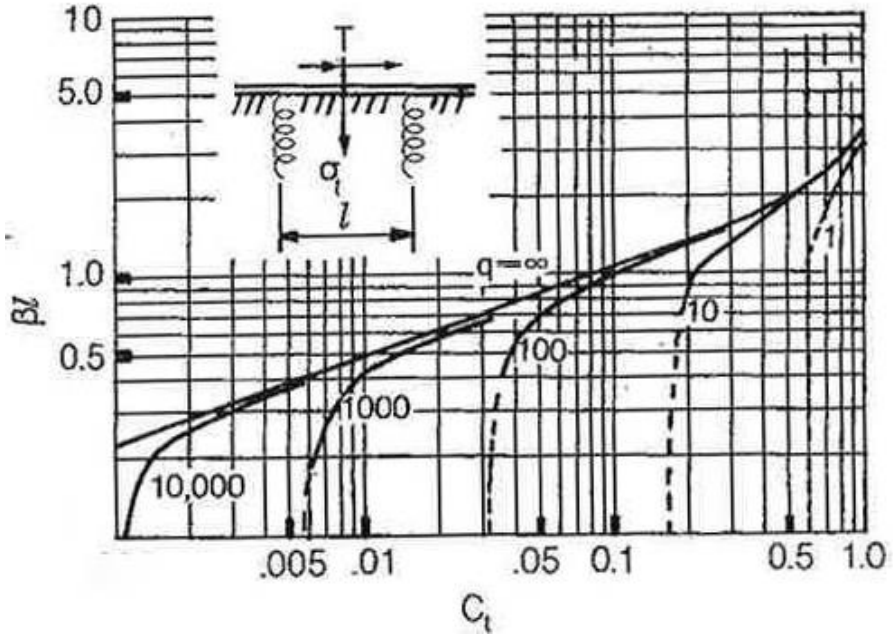

Figure 15 Concentrated Torque at Mid-panel on Continuous Beam - Distortional Bending Stress at Load (DGBGB Figure A6 [25])

As discussed previously, the base metal adjacent to the termination of fillet welds connecting transverse elements to webs and box flanges is assumed to be a Category E detail for transverse bending. Thus, the transverse bending stress range would be compared to the appropriate nominal fatigue resistance for a Category E detail computed according to the provisions of Article 6.6.1.2.5. The finite life fatigue resistance is determined from Eq. 6.6.1.2.5-2 as follows:

$$(\Delta F)_n = \left(\frac{A}{N}\right)^{\frac{1}{3}} \qquad \text{Eq. (6.6.1.2.5-2)}$$

in which:

$$N = (365)(75)n(ADTT)_{SL} \qquad \text{Eq. (6.6.1.2.5-3)}$$

$$N = (365)(75)(1.5)(1000) = 41.06 \times 10^6 \text{ cycles}$$

From Table 6.6.1.2.5-1, the detail category constant, A, for a Category E detail is 11 x 10^8 ksi^3. Therefore,

$$(\Delta F)_n = \left(\frac{11 \times 10^8}{41.06 \times 10^6} \right)^{\frac{1}{3}} = 2.99 \text{ ksi} > \sigma_t = 2.10 \text{ ksi}$$

The fatigue longitudinal warping stress range at the top and bottom corners of the tub section due to cross section distortion can be computed as follows:

$$\sigma_{dw} = \frac{C_w \, y}{I \, \beta \, a} \, T_{range} \qquad \text{DGBGB Eq. (A10)}$$

where:

C_w = BEF factor for determining the distortional longitudinal stress from DGBGB Figure A9 (see Figure 16)
y = distance along the transverse vertical axis of the tub section from the neutral axis to the point under consideration

The distortional longitudinal warping stress range at the bottom of the tub section would be considered in checking the load-induced fatigue resistance of the base metal at the connection plate welds to the bottom flange at locations where the flange is subject to a net tensile stress.

From Table 6.6.1.2.3-2, the 75-year $(ADTT)_{SL}$ Equivalent to Infinite Life for a Category C' detail is 975/1.5 = 650 trucks per day, adjusted for n = 1.5, which is less than 1,000 trucks per day. Therefore, the detail must be checked for infinite fatigue life using the Fatigue I load combination. Applying the load factor for the Fatigue I load combination ($\gamma = 1.75$), the factored fatigue torque range, T_{FAT}, is:

$$T_{FAT} = (1.75)\left[\left|-309\right| + 339\right] = 1{,}134 \text{ kip-ft}$$

Obtain C_w from the graph shown in Figure 16, where q = 28.0 and $\beta\ell = 0.65$. C_w is approximately 0.55. Therefore, using the short-term composite section properties with the transformed deck at Section G2-2 (see Table 13), the factored distortional longitudinal stresses are:

$$\sigma_{dw\_TOP} = \frac{(0.55)(17.23)}{(833{,}768)(0.00330)(120)} \left(1{,}134(12)\right) = 0.39 \text{ ksi}$$

$$\sigma_{dw\_BOT} = \frac{(0.55)(60.77)}{(833{,}768)(0.00330)(120)} \left(1{,}134(12)\right) = 1.38 \text{ ksi}$$

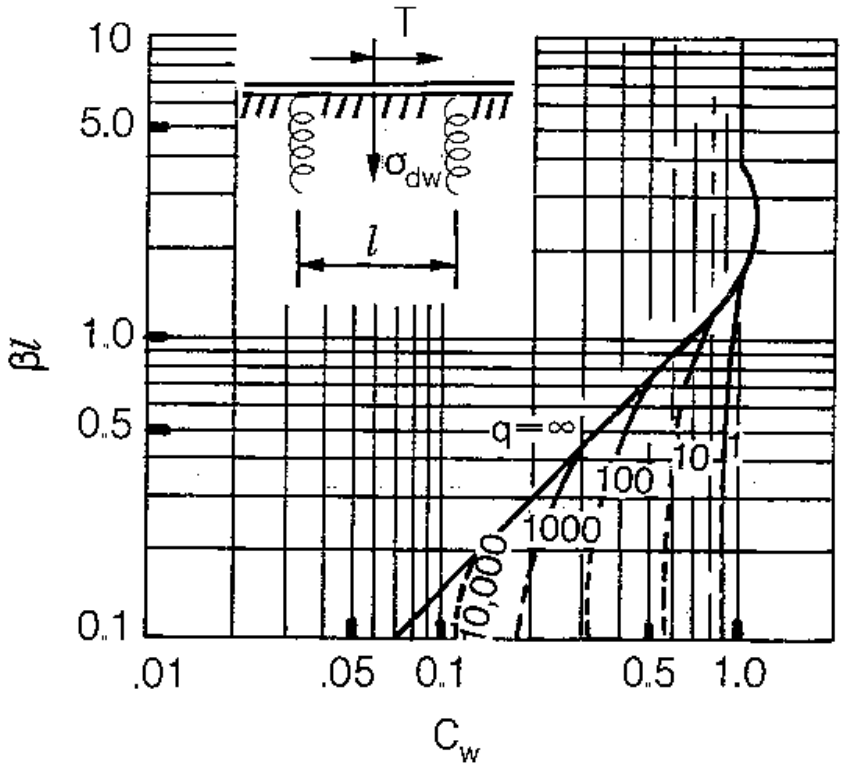

Figure 16 Concentrated Torque at Mid-panel on Continuous Beam – Normal Distortional Warping Stress at Mid-panel (DGBGB Table A9 [25])

The distortional longitudinal warping stress range would simply be added to the major-axis bending stress range at the detail. The distortional longitudinal warping stress at the top of the tub section may be ignored since the top flanges are continuously braced by the concrete deck. As mentioned previously, the preceding calculations were simply intended to illustrate the procedure for computing cross-section distortional stresses using the BEF analogy. These stresses are of greater concern in boxes subjected to much larger torques. Also, at Section G2-2, the bottom flange is not subject to a net tensile stress by inspection, and the top flanges are continuously braced by the concrete deck. However, these stresses should at least be considered in the base metal adjacent to welded details at or near the bottom flange in horizontally curved tub girder bridges at locations where the flange is subject to a net tensile stress.

7.10 Girder Check: Section G2-2, Strength Limit State (Article 6.11.6)

7.10.1 Flexure (Article 6.11.6.2)

For composite sections in negative flexure at the strength limit state, Article 6.11.6.2.3 directs the Engineer to Article 6.11.8. Furthermore, Article 6.11.6.2.3 states that the provisions of Appendix A6 do not apply to tub girders, nor is redistribution of negative moment in accordance with Appendix B6 permitted.

At the strength limit state, the top flanges in tension are continuously braced by the concrete deck, and are to satisfy:

$$f_{bu} \le \phi_f F_{nt} \qquad \text{Eq. (6.11.8.1.2-1)}$$

where F_{nt} is the nominal flexural resistance of the tension flanges determined as specified in Article 6.11.8.3.

At the strength limit state, tub flanges (bottom flanges) in compression are to satisfy:

$$f_{bu} \le \phi_f F_{nc} \qquad \text{Eq. (6.11.8.1.1-1)}$$

where F_{nc} is the nominal flexural resistance of the bottom flange determined as specified in Article 6.11.8.2.

The unfactored bending moments at Section G2-2 from the analysis are shown below (see Table 4). The live load moment includes the centrifugal force and dynamic load allowance effects.

Noncomposite Dead Load:	M_{DC1}	= -15,426 kip-ft
Composite Dead Load:	M_{DC2}	= -1,923 kip-ft
Future Wearing Surface Dead Load:	M_{DW}	= -2,550 kip-ft
Live Load (incl. IM and CF):	M_{LL+IM}	= -8,127 kip-ft

Compute the factored flange flexural stresses at Section G2-2 for the Strength I load combination, without consideration of flange lateral bending. For loads applied to the composite section, cracked section properties are used to compute the major-axis bending stresses at the strength limit state in accordance with Article 4.5.2.2. Shear lag need not be considered since the box flange (bottom flange) does not exceed one-fifth of the span of the bridge (Article C6.11.1.1). Therefore, the major-axis bending stress is assumed to be uniform across the flange because shear lag need not be considered. Also, the longitudinal warping stress due to cross- section distortion does not need to be considered at the strength limit state, in accordance with Article 6.11.1.1. As discussed previously, the η factor is taken equal to 1.0 in this example. Therefore:

For Strength I:

Top Flange:

$$f_{bu} = -1.0\left[\frac{1.25(-15{,}426)}{10{,}057} + \frac{1.25(-1{,}9232)}{10{,}654} + \frac{1.5(-2{,}550)}{10{,}654} + \frac{1.75(-8{,}127)}{11{,}862}\right]12 = 44.41 \text{ ksi}$$

Bottom Flange:

$$f_{bu} = 1.0\left[\frac{1.25(-15{,}426)}{11{,}316} + \frac{1.25(-1{,}923)}{11{,}447} + \frac{1.5(-2{,}550)}{11{,}447} + \frac{1.75(-8{,}127)}{11{,}674}\right]12 = -41.60 \text{ ksi}$$

In accordance with Article 6.11.1.1, the effects of both flexural and St. Venant torsional shear are to be considered for horizontally curved bridges. Therefore, compute the factored St. Venant torsional shear stress, f_v, in the bottom flange for the Strength I load combination. f_v is determined by dividing the St. Venant torsional shear flow [$f = T/(2A_o)$] by the thickness of the bottom flange:

$$f_v = \frac{T}{2A_o t_f} \qquad \text{Eq. (6.11.3.2-5)}$$

where:

T = internal torque due to factored loads (kip-in.)
A_o = enclosed area within the box section (in.^{2})
t_f = bottom flange thickness (in.)

The unfactored torques at Section G2-2 obtained from the analysis are shown below (see Table 6). The live load torque includes the centrifugal force and dynamic load allowance effects. The positive torques are used in the calculations that follow as the total of the positive torques governs over the absolute value of the total of the negative torques.

Noncomposite Dead Load:	T_{DC1}	= 36 kip-ft + (-33 kip-ft) = 3 kip-ft
Composite Dead Load:	T_{DC2}	= 192 kip-ft
Future Wearing Surface Dead Load:	T_{DW}	= 255 kip-ft
Live Load (incl. IM and CF):	T_{LL+IM}	= 980 kip-ft

Article C6.11.1.1 indicates that for torques applied to the noncomposite section, A_o is to be computed for the noncomposite section. Since the top lateral bracing in this example is attached to the top flange, the vertical depth can be calculated as the distance between the mid-thicknesses of the top and bottom flanges. Furthermore, for torques applied to the composite section, A_o is to be computed for the composite section using the depth from the mid-thickness of the bottom flange to the mid-thickness of the concrete deck. In this example, the height of the deck haunch is considered.

Compute the enclosed area of the noncomposite tub section, A_{o_NC}.

$$A_{o\_NC} = \frac{\left[120 + \left(83 - 2(1.5)\right)\right]}{2}\left(\frac{3.00}{2} + 78 + \frac{1.50}{2}\right) = 8{,}025 \text{ in.}^2$$

Compute the enclosed area of the composite tub section, A_{o_C}.

$$f_{v\_C} = (1.0)\frac{\left[(1.25)(192) + (1.50)(255) + (1.75)(980)\right](12)}{2(8{,}750)(1.50)} = 1.069 \text{ ksi}$$

$$A_{o\_C} = \frac{\left[120 + \left(83 - 2(1.5)\right)\right]}{2}\left(78 + \frac{1.50}{2} + 4.00 + \frac{9.50}{2}\right) = 8{,}750 \text{ in.}^2$$

Compute the factored Strength I St. Venant torsional shear stress in the bottom flange of the noncomposite section:

$$f_{v\_NC} = (1.0)\frac{(1.25)(3)(12)}{2(8{,}025)(1.50)} = 0.002 \text{ ksi}$$

Compute the factored Strength I St. Venant torsional shear stress in the bottom flange of the composite section:

Therefore the total factored Strength I St. Venant torsional shear stress is computed as:

$$f_v = 0.002 + 1.069 = 1.071 \text{ ksi}$$

According to Article 6.11.1.1, the factored St. Venant torsional shear stress in box flanges (bottom flange in this tub girder) at the strength limit state is not to exceed the factored torsional shear resistance of the flange, F_{vr}, taken as:

$$F_{vr} = 0.75\phi_v \frac{F_{yf}}{\sqrt{3}} \qquad \text{Eq. (6.11.1.1-1)}$$

where:

ϕ_v = resistance factor for shear specified in Article 6.5.4.2

Therefore:

$$F_{vr} = 0.75(1.0)\frac{50}{\sqrt{3}} = 21.65 \text{ ksi} > f_v = 1.071 \text{ ksi} \qquad \text{OK}$$

7.10.2 Top Flange

Calculate the nominal flexural resistance of the top flanges in tension, F_{nt}, in accordance with Article 6.11.8.3.

$$F_{nt} = R_h F_{yt} \qquad \text{Eq. (6.11.8.3-1)}$$

For a homogenous girder, R_h, is equal to 1.0 (Article 6.10.1.10.1). Therefore:

$$F_{nt} = (1.0)(50.0) = 50.0 \text{ ksi}$$

For Strength I:

$$f_{bu} \le \phi_f F_{nt} \qquad \text{Eq. (6.11.8.1.2-1)}$$

$$f_{bu} = 44.41 \text{ ksi} < \phi_f F_{nt} = (1.0)(50.00) = 50.00 \text{ ksi} \qquad \text{OK} \qquad (\text{Ratio} = 0.888)$$

7.10.3 Bottom Flange

Calculate the nominal flexural resistance of the bottom flange in compression, F_{nc}, in accordance with Article 6.11.8.2. The bottom flange is longitudinally stiffened at this location, with a single WT 8x28.5 stiffener placed at the center of the bottom flange.

$$\lambda_f = \frac{b_{fc}}{t_{fc}} \qquad \text{Eq. (6.11.8.2.2-8)}$$

where, in this case:

b_{fc} = w = larger of the width of the flange between the longitudinal flange stiffeners or the distance from a web to the nearest longitudinal flange stiffener.

Since the longitudinal stiffener is at the center of the bottom flange, w is the distance from the longitudinal stiffener to the inside face of the web.

$$\lambda_f = \frac{\left(\frac{79.4375}{2}\right)}{1.50} = 26.48$$

Calculate the first limiting slenderness ratio:

$$\lambda_p = 0.57\sqrt{\frac{Ek}{F_{yc}\Delta}} \qquad \text{Eq. (6.11.8.2.2-9)}$$

where k is computed as specified in Article 6.11.8.2.3 for longitudinally stiffened flanges, and Δ is computed in accordance with Article 6.11.8.2.2.

As specified in Article 6.11.8.2.3, since a single bottom flange stiffener is used, n = 1 and the plate-buckling coefficient for uniform normal stress, k, is to be taken as:

$$k = \left(\frac{8I_S}{wt_{fc}^{\ 3}}\right)^{\frac{1}{3}} \qquad \text{Eq. (6.11.8.2.3-1)}$$

and:

$$\Delta = \sqrt{1 - 3\left(\frac{f_v}{F_{yc}}\right)^2} \qquad \text{Eq. (6.11.8.2.2-11)}$$

where:

f_v = factored St. Venant torsional shear stress in the flange (ksi)
n = number of equally spaced longitudinal flange stiffeners
k = plate-buckling coefficient for uniform normal stress, $1.0 \le k \le 4.0$
I_S = moment of inertia of a single longitudinal flange stiffener about an axis parallel to the flange and taken at the base of the stiffener (in.^{4})

Structural tees are efficient shapes for longitudinal stiffeners because they provide a high ratio of stiffness to cross-sectional area. For the WT 8x28.5 stiffener, I_x = 48.7 in.^{4}, A = 8.39 in.^{2}, and the elastic neutral axis (N.A.) is 6.28 in. from the tip of the stem. Therefore, I_s is computed as:

$$I_S = 48.7 + (8.39)(6.28)^2 = 379.6 \text{ in.}^4$$

Compute the plate-buckling coefficient k:

$$k = \left(\frac{8(379.6)}{\left(\frac{79.4375}{2}\right)(1.50^3)}\right)^{\frac{1}{3}} = 2.83 < 4.0$$

Compute the Δ term:

$$\Delta = \sqrt{1 - 3\left(\frac{1.071}{50.0}\right)^2} = 0.999$$

Compute λ_p:

$$\lambda_p = 0.57\sqrt{\frac{(29{,}000)(2.83)}{(50.0)(0.999)}} = 23.10$$

Since λ_f is greater than 23.10 (λ_f = 26.48), it is necessary to compute the second limiting slenderness ratio:

$$\lambda_r = 0.95\sqrt{\frac{Ek}{F_{yr}}} \qquad \text{Eq. (6.11.8.2.2-10)}$$

where:

$$F_{yr} = (\Delta - 0.3)F_{yc} \le F_{yw} \qquad \text{Eq. (6.11.8.2.2-13)}$$

$$F_{yr} = (0.999 - 0.3)(50) = 35.0 \text{ ksi} < F_{yw} = 50 \text{ ksi}$$

Compute λ_r:

$$\lambda_r = 0.95\sqrt{\frac{(29{,}000)(2.83)}{35.0}} = 46.00$$

Since $\lambda_p < \lambda_f = 26.48 < \lambda_r$, then the nominal axial compression buckling resistance of the flange under compression alone, F_{cb}, is calculated as follows:

$$F_{cb} = R_b R_h F_{yc}\left[\Delta - \left(\Delta - \frac{\Delta - 0.3}{R_h}\right)\left(\frac{\lambda_f - \lambda_p}{\lambda_r - \lambda_p}\right)\right] \qquad \text{Eq. (6.11.8.2.2-3)}$$

The hybrid factor, R_h, is equal to 1.0, as specified in Article 6.10.1.10.1.

Determine the web load-shedding factor, R_b. First, compute the depth of the web in compression, D_c, in accordance with the provisions of Article D6.3.1. These provisions state that for composite sections in negative flexure at the strength limit state, D_c is to be computed for the section consisting of the steel girder plus the longitudinal deck reinforcement. For this example, D_c is calculated using the short-term (n) section property computations for the steel section plus the longitudinal reinforcement shown in Table 15. As indicated in Article C6.11.8.2.2, in calculating R_b for a tub section, use one-half of the effective box (bottom) flange width in conjunction with one top flange and a single web.

Therefore, compute D_c along the inclined web:

$$D_c = (41.58 - 1.50)\sqrt{\frac{4^2 + 1}{4^2}} = 41.31 \text{ in.}$$

$$\frac{2D_c}{t_w} = \frac{2(41.31)}{0.5625} = 146.9$$

According to the provisions of Article 6.10.1.10.2:

$$\text{If } \frac{2D_c}{t_w} \le \lambda_{rw}, \text{ then } R_b = 1.0 \qquad \text{Eq. (6.10.1.10.2-1)}$$

where:

$$4.6\sqrt{\frac{E}{F_{yc}}} \le \lambda_{rw} = \left(3.1 + \frac{5.0}{a_{wc}}\right)\sqrt{\frac{E}{F_{yc}}} \le 5.7\sqrt{\frac{E}{F_{yc}}} \qquad \text{Eq. (6.10.1.10.2-5)}$$

$$a_{wc} = \frac{2D_c t_w}{b_{fc} t_{fc}} \qquad \text{Eq. (6.10.1.10.2-8)}$$

$$4.6\sqrt{\frac{E}{F_{yc}}} = 4.6\sqrt{\frac{29{,}000}{50}} = 111$$

$$5.7\sqrt{\frac{E}{F_{yc}}} = 5.7\sqrt{\frac{29{,}000}{50}} = 137$$

$$a_{wc} = \frac{2(41.31)(0.5625)}{(79.4375/2)(1.5)} = 0.78$$

$$111 < \lambda_{rw} = \left(3.1 + \frac{5.0}{0.78}\right)\sqrt{\frac{29{,}000}{50}} = 229.0 > 137$$

$$\therefore \lambda_{rw} = 137 < \frac{2D_c}{t_w} = 146.9$$

Since $\frac{2D_c}{t_w} > \lambda_{rw}$, calculate R_b as follows:

$$R_b = 1 - \left(\frac{a_{wc}}{1200 + 300a_{wc}}\right)\left(\frac{2D_c}{t_w} - \lambda_{rw}\right) \le 1.0 \qquad \text{Eq. (6.10.1.10.2-3)}$$

$$R_b = 1 - \left(\frac{0.78}{1200 + 300(0.78)}\right)\left(\frac{2(41.31)}{0.5625} - 137\right) = 0.995 \le 1.0$$

Compute the nominal axial compression buckling resistance:

$$F_{cb} = (0.995)(1.0)(50)\left[0.999 - \left(0.999 - \frac{0.999 - 0.3}{1.0}\right)\left(\frac{26.48 - 23.10}{46.00 - 23.10}\right)\right]$$

$$F_{cb} = 47.50 \text{ ksi}$$

Compute the nominal flexural resistance of the compression flange:

$$F_{nc} = F_{cb}\sqrt{1 - \left(\frac{f_v}{\phi_v F_{cv}}\right)^2} \qquad \text{Eq. (6.11.8.2.2-1)}$$

where:

F_{cv} = nominal shear buckling resistance of the flange under shear alone (ksi)

In order to compute F_{cv}, first calculate k_s, the plate-buckling coefficient for shear stress in accordance with Article 6.11.8.2.3:

$$k_S = \frac{5.34 + 2.84\left(\frac{I_S}{w\, t_{fc}^{\,3}}\right)^{\frac{1}{3}}}{(n+1)^2} \le 5.34 \qquad \text{Eq. (6.11.8.2.3-3)}$$

$$k_S = \frac{5.34 + 2.84\left(\frac{379.6}{(79.4375/2)(1.50^3)}\right)^{\frac{1}{3}}}{(1+1)^2} = 2.34 < 5.34$$

As specified in Article 6.11.8.2.2, if $\lambda_f \le 1.12\sqrt{\frac{Ek_s}{F_{yc}}}$, then:

$$F_{cv} = 0.58\, F_{yc} \qquad \text{Eq. (6.11.8.2.2-5)}$$

$$\lambda_f = 26.48 < 1.12\sqrt{\frac{(29{,}000)(2.34)}{50}} = 41.26$$

Therefore:

$$F_{cv} = 0.58(50) = 29.0 \text{ ksi}$$

Compute F_{nc}:

$$F_{nc} = 47.50\sqrt{1-\left(\frac{1.071}{(1.0)(29.0)}\right)^2} = 47.47 \text{ ksi}$$

Checking compliance with Eq. 6.11.8.1.1-1:

$$f_{bu} \le \phi_f F_{nc} \qquad \text{Eq. (6.11.8.1.1-1)}$$

For Strength I:

$$f_{bu} = |\text{-}41.60 \text{ ksi}| \; < \; \phi_f F_{nc} = (1.00)(47.47) \; = \; 47.47 \text{ ksi} \qquad \text{OK} \qquad \text{(Ratio = 0.876)}$$

Article C6.11.8.1.1 states that in general, bottom box flanges at interior pier sections are subjected to biaxial stresses due to major-axis bending of the tub section and major-axis bending of the internal diaphragm over the bearing sole plate. The bottom flange is also subject to shear stresses due to the internal diaphragm vertical shear and, in cases where it needs to be considered, the St. Venant torsional shear. For cases where the shear stresses and/or bending of the internal diaphragm are deemed significant, Article C6.11.8.1.1 suggests that the following equation be used to check the combined stress state in the box flange at the strength limit state:

$$\sqrt{f_{bu}^2 - f_{bu}f_{by} + f_{by}^2 + 3(f_d + f_v)^2} \le \phi_f R_b R_h F_{yc} \qquad \text{Eq. (C6.11.8.1.1-1)}$$

where:

f_{bu} = factored longitudinal stress at the section under consideration calculated without consideration of longitudinal warping (ksi)
f_{by} = factored stress in the flange caused by major-axis bending of the internal diaphragm over the bearing sole plate (ksi)
f_d = factored shear stress in the flange caused by the internal diaphragm vertical shear (ksi)
f_v = factored St. Venant torsional shear stress in the flange (ksi)
R_b = web load-shedding factor determined as specified in Article 6.10.1.10.2
R_h = hybrid factor determined as specified in Article 6.10.1.10.1

In this example, each tub girder is supported on two bearings at each support. Therefore, the bottom flange bending stresses due to major-axis bending of the diaphragm over the bearing sole plates are relatively small and are neglected in this example (f_{by} = 0.0 ksi). The effect of these forces in a tub section supported on a single bearing is likely to be more significant and should be considered. As specified in Article C6.11.8.1.1 an effective flange width of 6 times the thickness of the tub girder bottom flange may be considered effective with the internal diaphragm for computing the stress in the box flange (bottom flange in this tub girder) caused by major-axis bending of the internal diaphragm over the bearing sole plate. Furthermore, if an access hole is

provided within the internal diaphragm, the hole should be considered in calculating the section properties of the effective diaphragm section.

From previous calculations, the total factored St. Venant torsional shear stress in the bottom flange, f_v, is equal to 1.071 ksi.

To estimate the shear stress in the bottom flange due to the internal diaphragm shear, a 1 in. by 12 in. top flange for the diaphragm is assumed. The diaphragm web is assumed to be 78 inches deep and 1 inch thick, and for simplicity in this example, an access hole is assumed not to be provided in the web. As specified in Article C6.11.8.1.1, a box flange width equal to 6 times its thickness may be considered effective with the internal diaphragm. Therefore:

$$b_{bf\_EFF} = 6\ (1.50) = 9.0 \text{ in.}$$

Therefore, the effective bottom flange of the internal diaphragm is 9.0 inches wide and has a thickness of 1.50 inches. The thickness of the effective bottom flange of the internal diaphragm is the same as the thickness of the tub girder bottom flange.

From separate calculations not shown here, the moment of inertia of the effective internal diaphragm is 79,565 in.^{4}, and the neutral axis is located 39.89 in. above the bottom of the bottom flange. Calculations associated with the design of the internal diaphragm, shown later, indicate that the total factored vertical component of the diaphragm shear is 1,406 kips. The shear stress in the tub girder bottom flange, f_d, caused by the internal diaphragm vertical shear due to factored loads is approximated as:

$$f_d = \frac{VQ}{It_{fc}} \qquad \text{Eq. (C6.11.8.1.1-2)}$$

where:

V = vertical shear in the internal diaphragm due to flexure plus St. Venant torsion (kip)
Q = first moment of inertia of one-half the effective box-flange area about the neutral axis of the effective internal diaphragm (in.^{3})
I = moment of inertia of the effective internal diaphragm section (in.^{4})

The first moment of inertia of one-half the effective box-flange area about the neutral axis of the effective internal diaphragm, Q, is computed as:

$$Q = \frac{1}{2}(9.0)(1.50)\left(39.89 - \frac{1.50}{2}\right) = 264.2 \text{ in.}^3$$

Therefore,

$$f_d = \frac{VQ}{It_{fc}} = \frac{(1{,}406)(264.2)}{(79{,}565)(1.50)} = 3.11 \text{ ksi}$$

Only one-half of the effective flange area is used in computing the first moment of inertia, Q, used in this calculation since the shear stress in the flange is a maximum at the diaphragm and assumed to be zero at each edge of the effective flange (with a linear distribution assumed in-between).

The factored longitudinal stress in the tub girder bottom flange, f_{bu}, resulting from major-axis bending was computed previously as -41.60 ksi. Also, R_h is equal to 1.0, and R_b was computed in previous computations and is equal to 0.995.

Checking compliance with Eq. C6.11.8.1.1-1:

$$\sqrt{(-41.60)^2 - (-41.60)(0) + (0)^2 + 3(3.11+1.07)^2} = 42.23 \text{ ksi}$$

$$42.23 \text{ ksi} < \phi_f R_b R_h F_{yc} = (1.0)(0.995)(1.0)(50) = 49.75 \text{ ksi} \quad \text{OK} \qquad (\text{Ratio} = 0.849)$$

7.10.3.1 Cross-section Distortion Stresses

In accordance with Article 6.11.1.1, transverse bending stress due to cross-section distortion are to be considered at the strength limit state. The factored transverse bending stresses are not to exceed 20.0 ksi at the strength limit state. Longitudinal warping stresses due to cross-section distortion may be ignored at the strength limit state.

As shown previously in the fatigue computations for Section G2-2, the transverse bending stress range at the top or bottom corners of the tub section may be determined as:

$$\sigma_t = C_t \; F_d \; \beta \; \frac{1}{2a} \; T \qquad \text{DGBGB Eq. (A8)}$$

The same values computed under the fatigue computations may be used at the strength limit state, thus C_t is equal to 0.12, F_d is equal to 205 in.$^{-1}$, β is equal to 0.00330 in.$^{-1}$, and *a* is equal to 120 in. T represents the total factored concentrated torque and is computed as follows:

For Strength I:

$$T = 1.25(3) + 1.25(192) + 1.50(255) + 1.75(980) = 2{,}341 \text{ kip-ft}$$

Therefore, the factored transverse bending stress due to cross-section distortion is computed as:

$$\sigma_t = (0.12)(205)(0.00330)\ \frac{1}{2(120)}\ (2{,}341(12)) = 9.50 \text{ ksi} < 20.0 \text{ ksi} \quad \text{OK (Ratio = 0.475)}$$

7.10.4 Shear (Article 6.11.6.3)

Article 6.11.6.3 invokes the provision of Article 6.11.9 to determine the shear resistance at the strength limit state. Article 6.11.9 further directs the Engineer to the provision of Article 6.10.9 for determining the factored shear resistance of a single web. For the case of inclined webs, D, is to be taken as the depth of the web measured along the slope. The factored shear load in the inclined web is to be taken as:

$$V_{ui} = \frac{V_u}{\cos(\theta)} \qquad \text{Eq. (6.11.9-1)}$$

where V_u is the factored shear on one inclined web, and θ is the angle of inclination of the web plate. For tub sections, especially those in horizontally curved bridges, St. Venant torsional shear must be considered in the design of the webs. The total shear in one web is greater than the shear in the other web at the same section since the torsional shear is of opposite sign in the two webs. The critical shear should be the maximum combination of factored shear due to major-axis bending and the St. Venant torsional shear. For practicality, both webs are designed for the critical shear.

At the strength limit state, webs must satisfy the following:

$$V_u \le \phi_v V_n \qquad \text{Eq. (6.10.9.1-1)}$$

where:

ϕ_v = resistance factor for shear = 1.0 (Article 6.5.4.2)
V_n = nominal shear resistance determined as specified in Articles 6.10.9.2 and 6.10.9.3 for unstiffened and stiffened webs, respectively (kip)
V_u = V_{ui} = shear in a single web at the section under consideration due to factored loads (kip)

The unfactored shears at Section G2-2 obtained from the analysis are shown below (see Table 2). The unfactored shears are vertical shears and are the summation of the shears due to major-axis bending and St. Venant torsion in the critical web. The live load moment includes the centrifugal force and dynamic load allowance effects. The positive shears are used in the calculations that follow as the total of the positive shears governs over the absolute value of the total of the negative shears.

Noncomposite Dead Load:	V_{DC1}	= 232 kip
Composite Dead Load:	V_{DC2}	= 44 kip
Future Wearing Surface Dead Load:	V_{DW}	= 58 kip

Live Load (incl. IM and CF): V_{LL+IM} = 160 kip

The η factor is again taken equal to 1.0 in this example at the strength limit state. The total factored shear at the interior pier in the inclined web is:

$$V_{ui} = \frac{1.0\left[1.25(232+44)+1.5(58)+1.75(160)\right]}{\cos\left(14.036°\right)} = 734 \text{ kips}$$

7.10.4.1 Interior Panel (Article 6.10.9.3.2)

Article 6.10.9.1 stipulates that the transverse stiffener spacing for interior panels without a longitudinal stiffener is not to exceed 3D = 3(80.40) = 241.2 inches. For the first panel on each side of the interior support, a transverse stiffener spacing of 62 inches is assumed for this design example, satisfying the 3D requirement.

For interior panels of girders with the section along the entire panel proportioned such that:

$$\frac{2Dt_w}{\left(b_{fc}t_{fc}+b_{ft}t_{ft}\right)} \le 2.5 \qquad \text{Eq. (6.10.9.3.2-1)}$$

the nominal shear resistance is to be taken as the sum of the shear-buckling resistance and the post-buckling resistance due to tension-field action, which is to be computed according to:

$$V_n = V_p\left[C+\frac{0.87(1-C)}{\sqrt{1+\left(\frac{d_o}{D}\right)^2}}\right] \qquad \text{Eq. (6.10.9.3.2-2)}$$

in which:

$$V_p = 0.58F_{yw}Dt_w \qquad \text{Eq. (6.10.9.3.2-3)}$$

where:

d_o = transverse stiffener spacing (in.)
V_n = nominal shear resistance of the web panel (kip)
V_p = plastic shear force (kip)
C = ratio of the shear-buckling resistance to the shear yield strength.

According to Article 6.11.9, for box flanges, b_{fc} (in this case) is to be taken as one-half the effective flange width between webs in checking Eq. 6.10.9.3.2-1, but not to exceed 18 times the thickness of the box flange. Therefore, (79.4375/2) = 39.7 in. > 18(1.50) = 27.0 in. Use b_{fc} = 27.0 in. to check Eq. 6.10.9.3.2-1. For the interior web panel under consideration, check Eq. 6.10.9.3.2-1 as follows:

$$\frac{2(80.40)(0.5625)}{((27.0)(1.50)+(18)(3.00))}=0.96<2.5$$

Therefore, Eq. (6.10.9.3.2-2) is applicable. First, compute the shear-buckling coefficient, k:

$$k=5+\frac{5}{\left(\frac{d_o}{D}\right)^2}=5+\frac{5}{\left(\frac{62}{80.40}\right)^2}=13.41 \qquad \text{Eq. (6.10.9.3.2-7)}$$

Since:

$$\frac{D}{t_w}=\frac{80.4}{0.5625}=142.9>1.40\sqrt{\frac{Ek}{F_{yw}}}=1.40\sqrt{\frac{29{,}000(13.41)}{50}}=123.5$$

$$C=\frac{1.57}{\left(\frac{D}{t_w}\right)^2}\left(\frac{Ek}{F_{yw}}\right) \qquad \text{Eq. (6.10.9.3.2-6)}$$

$$C=\frac{1.57}{(142.9)^2}\left(\frac{29{,}000(13.41)}{50}\right)=0.598$$

V_p is the plastic shear force and is calculated as follows:

$$V_p=0.58\,F_{yw}D\,t_w \qquad \text{Eq. (6.10.9.3.3-2)}$$

$$V_p=0.58\,(50.0)(80.40)(0.5625)=1{,}312 \text{ kips}$$

Therefore,

$$V_n=(1{,}312)\left[0.598+\frac{0.87(1-0.598)}{\sqrt{1+\left(\frac{62.0}{80.40}\right)^2}}\right]=1{,}148 \text{ kips}$$

Checking compliance with Eq. (6.10.9.1-1):

$V_u = 734$ kips $< \phi_v V_n = (1.0)(1{,}148) = 1{,}148$ kips OK (Ratio = 0.639)

7.11 Bottom Flange Longitudinal Stiffener

A single longitudinal flange stiffener is used on the bottom flange of the tub girders in the negative moment regions. The longitudinal stiffeners are terminated at the bolted field splices at each end of Field Sections 2 and 4. By terminating the longitudinal stiffener at the bolted field splices, it is not necessary to consider fatigue at the terminus of the stiffener. Otherwise, the base metal at the stiffener termination would need to be checked as a fatigue Category E or E' detail depending on the stiffener thickness, unless a transition radius is provided at the termination (refer to Condition 4.3 in Table 6.6.1.2.3-1). The bottom flange splice plates inside the tub girder must be designed and fabricated to permit the longitudinal stiffener to extend to the free edge of the flange, where the longitudinal stress is zero (refer to Figure 20). Refer to NSBA's *Steel Bridge Design Handbook: Example 4: Three-Span Continuous Straight Composite Steel Tub-Girder Bridge* [8] for further discussion regarding the fatigue design of bottom flange longitudinal stiffeners.

A single WT 8x28.5 is utilized for the longitudinal stiffener with the stem welded to the bottom flange and is placed at the centerline of the bottom flange. As specified in Article 6.11.11.2, longitudinal compression flange stiffeners on tub girder bottom flanges are to be equally spaced across the width of the flange. Furthermore, the yield strength of the longitudinal stiffeners must not be less than the yield strength of the flanges to which they are attached.

The projecting width, b_l, of the longitudinal flange stiffener must satisfy Eq. (6.11.11.2-1):

$$b_\ell \le 0.48\, t_s \sqrt{\frac{E}{F_{yc}}} \qquad \text{Eq. (6.11.11.2-1)}$$

where:

t_s = thickness of the projecting longitudinal stiffener element (in.)

In the case of a structural tee, t_s is taken as the flange thickness of the structural tee since each half-flange would buckle similarly to a single plate connected to the web. Furthermore, the projecting width, b_l, of structural tees is to be taken as one-half the width of the tee flange. Therefore,

$$b_l \le 0.48\,(0.715)\sqrt{\frac{29{,}000}{50}} = 8.27 \text{ in.}$$

$$b_l = \frac{7.12}{2} = 3.56 \text{ in.} < 8.27 \text{ in.} \qquad \text{WT 8x28.5 flange is OK}$$

The moment of inertia, I_ℓ, of each stiffener about an axis parallel to the flange and taken at the base of the stiffener must satisfy:

$$I_\ell \ge \psi\, w\, t_{fc}^3 \qquad \text{Eq. (6.11.11.2-2)}$$

where:

ψ = $0.125k^3$ for n = 1
= $1.120k^3$ for n = 2
k = plate buckling coefficient for uniform stress, $1.0 \le k \le 4.0$
n = number of equally spaced longitudinal flange stiffeners
w = larger of the width of the flange between longitudinal flange stiffeners or the distance from a web to the nearest longitudinal flange stiffener (in.)
t_{fc} = thickness of the tub girder compression flange (in.)

Calculate the moment of inertia of the stiffener, I_ℓ, about the base of the stiffener:

$$I_\ell = I_o + Ad^2 = 48.7 + (8.39)\,(8.22 - 1.94)^2 = 379.6 \text{ in}^4$$

As specified in Article C6.11.11.2, the actual longitudinal flange stiffener moment of inertia, I_s, used in determining the plate-buckling coefficient for uniform normal stress, k, from either Eq. 6.11.8.2.3-1 or Eq. 6.11.8.2.3-2, as applicable, automatically satisfies Eq. 6.11.11.2-2. Alternatively, for preliminary sizing of the stiffener for example, a value of k can be assumed in lieu of using Eq. 6.11.8.2.3-1 or Eq. 6.11.8.2.3-2, as applicable, but a range of 2.0 to 4.0 should generally apply. For completeness, check Eq. 6.11.11.2-2, where k was previously calculated as 2.83:

$$379.6 \text{ in.}^4 \cong 0.125(2.83)^3\left(\frac{79.4375}{2}\right)(1.5)^3 \cong 379.8 \text{ in.}^4 \qquad \text{OK}$$

The slight difference between the two values is due to rounding. Since Eq. 6.11.11.2-1 and Eq. 6.11.11.2-2 are satisfied, the WT 8x25 is acceptable for the bottom flange longitudinal stiffener.

7.12 Internal Pier Diaphragm Design

Article 6.11.1 directs the designer to the provision of Article 6.7.4 for general design considerations for internal and external cross-frames and diaphragms (specifically Article 6.7.4.3). The internal diaphragms are subject to major-axis bending over the bearing sole plates in addition to shear. Article C6.11.8.1.1 requires that the principal stresses in the internal support diaphragm at the strength limit state not exceed the compressive resistance given by Eq. C6.11.8.1.1-1, which is a yield criterion for combined stress. In this example, each tub girder is supported by two bearings, therefore, as specified in Article C6.11.8.1.1, the major-axis bending stress in the internal diaphragms, f_{by}, is typically small and can be neglected.

Example calculations are demonstrated for the Girder G2 internal diaphragms at the Pier 1 supports (Girder Section G2-2). A 1.0 inch thick Grade 50 steel plate is assumed for the internal diaphragm web at this location. Figure 17 shows a sketch of the internal diaphragm. For simplicity, the access hole in the web for inspection purposes is not considered in this example.

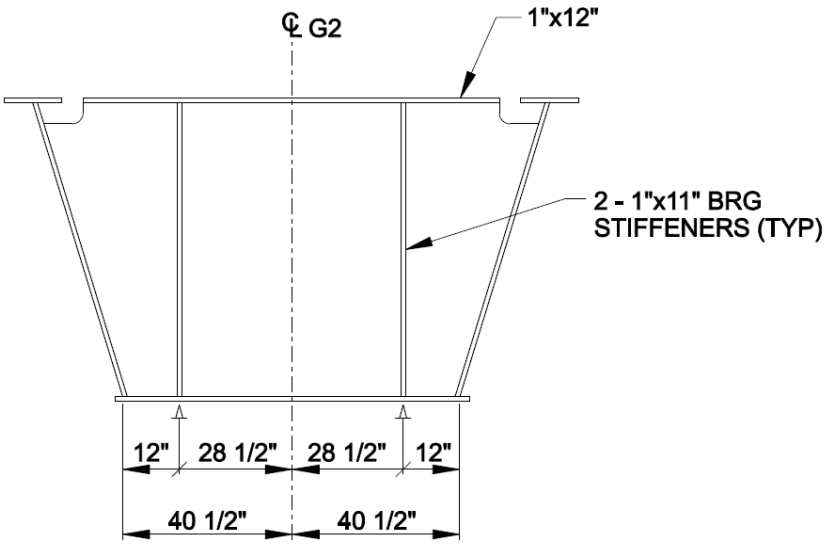

Figure 17 Internal Pier Diaphragm and Bearing Locations

First, summarize the maximum vertical shears and torsional moments acting on the internal diaphragm. The unfactored shears are taken from Table 2, and most of the unfactored torques are taken from Table 6.

The maximum unfactored vertical shears acting on the internal diaphragm, using the critical tub girder web are shown below. The unfactored vertical shears are due to the combined effects of bending and St. Venant torsion in the critical tub girder web. Therefore, it is necessary to separate out the shears due to bending and St. Venant torsion in computations that follow later in this section.

The maximum unfactored vertical shears in the critical tub girder web due to tub girder flexure and St. Venant torsion are:

Steel Dead Load:	$V_{DC1\text{-}STEEL} = 47 + \lvert -46 \rvert = 93$ kips
Concrete Deck Dead Load:	$V_{DC1\text{-}CONC} = 185 + \lvert -185 \rvert = 370$ kips
Composite Dead Load:	$V_{DC2} = 44 + \lvert -41 \rvert = 85$ kips
Future Wearing Surface Dead Load:	$V_{DW} = 58 + \lvert -55 \rvert = 113$ kips
Live Load (incl. IM and CF):	$V_{LL+IM} = 160 + \lvert -155 \rvert = 315$ kips

The maximum unfactored torques acting on the internal diaphragm, are:

Steel Dead Load:	$T_{DC1\text{-}STEEL} = \lvert -22 \rvert + 36 = 58$ kip-ft
Concrete Dead Load:	$T_{DC1\text{-}CONC} = 48 + \lvert -33 \rvert = 81$ kip-ft
Composite Dead Load:	$T_{DC2} = \lvert -149 \rvert + 192 = 341$ kip-ft
Future Wearing Surface Dead Load:	$T_{DW} = \lvert -197 \rvert + 255 = 452$ kip-ft
Live Load (incl. IM and CF):	$T_{LL+IM} = 980 + \lvert -425 \rvert = 1405$ kip-ft

For computing the above live load torque, assumed concurrent torques are used that produce the largest torsional reaction at the support, and thus the largest torque acting on the internal diaphragm.

Compute the maximum factored shear stress in the diaphragm web. The vertical shear acting on the critical tub girder web is equal to the maximum shear in the internal diaphragm. First, it is necessary to separate out the shears due to tub girder flexure (bending), V_b, and the shears due to St. Venant torsion, V_T, as the maximum unfactored vertical shears above include the web shear due to torsion.

7.12.1 Web Shear Check

The calculations in this section check the combined principal stresses in the internal diaphragm web and the shear in the internal diaphragm web. To perform these checks, it is necessary to separately consider the shear in the internal diaphragm for tub girder flexure (bending) and the shear due to torsion.

7.12.1.1 Noncomposite Shear Force

The sum of the total noncomposite Strength I factored shears is:

$V_{DC1} = 1.25(93 + 370) = 579$ kips

To compute the shear due to torsion, it is necessary to compute the shear flow in the noncomposite tub girder section. The enclosed area of the noncomposite tub section, A_{o_NC}, was computed previously as 8,025 in^2. The factored shear flow in the noncomposite section is computed as:

$$f_v = \frac{T}{2\,A_o} \qquad \text{Eq. (C6.11.1.1-1)}$$

where:

T = internal torque due to factored loads (kip-in.)
A_o = enclosed area within the box section ($in.^2$)

$$f_v = \frac{T}{2A_o} = \frac{1.25(58+81)(12)}{2(8{,}025)} = 0.130 \text{ kip/in.}$$

Note that the internal factored noncomposite dead load torque is equal to 173.8 kip-ft.

To obtain the factored noncomposite dead load St. Venant torsional shear, V_T, multiply the factored shear flow by the depth of the tub girder web along the incline:

$V_T = 0.130(80.40) = 10.45$ kips

The vertical component of V_T is computed as:

$$(V_T)_{Vert} = 10.45\left(\frac{78.0}{80.40}\right) = 10.14 \text{ kips}$$

The factored vertical shear in the diaphragm web due to tub girder flexure alone and noncomposite dead loads is then computed by subtracting the vertical component of the factored noncomposite dead load St. Venant torsional shear from the total noncomposite dead load shear:

$V_b = 579 - 10.14 = 569$ kips

Figure 18 provides an illustration of the above calculation.

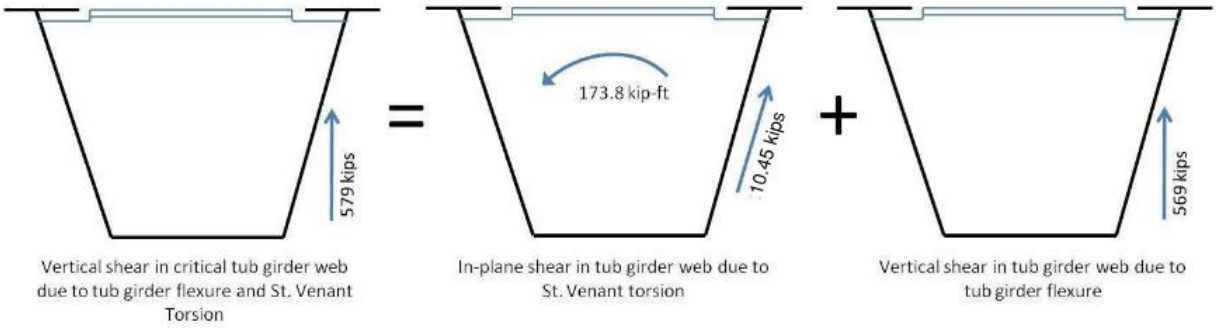

Figure 18 Computation of the Shear in the Internal Pier Diaphragm due to St. Venant Torsion and Tub Girder Flexure

7.12.1.2 Composite Shear Force

The sum of the total composite Strength I factored shears is:

$V_{DC2+DW+(LL+I)} = 1.25(85) + 1.5(113) + 1.75(315) = 827$ kips

The enclosed area of the composite tub section, A_{o_C}, was computed previously as 8,750 in^2. The factored shear flow in the composite section is computed as:

$$f_v = \frac{T}{2A_o} = \frac{[1.25(341) + 1.5(452) + 1.75(1{,}405)](12)}{2(8{,}750)} = 2.44 \text{ kip/in.}$$

To obtain the factored composite St. Venant torsional shear, V_T, multiply the factored shear flow by the depth of the web along the incline:

$V_T = 2.44(80.40) = 196.2$ kips

The vertical component of V_T is computed as:

$$(V_T)_{Vert} = 196.2\left(\frac{78.0}{80.40}\right) = 190 \text{ kips}$$

The factored vertical shear in the diaphragm web due to tub girder flexure alone and composite loads is then computed by subtracting the vertical component of the factored composite St. Venant torsional shear from the total factored composite shear:

$V_b = 827 - 190 = 637$ kips

7.12.1.3 Total Factored Shear Force

The total factored shear stress in the diaphragm web due to torsion is calculated by dividing the shear flows by the thickness of the web:

$$(f_v)_T = \frac{0.130}{1.0 \text{ in.}} + \frac{2.44}{1.0 \text{ in.}} = 2.57 \text{ ksi}$$

The average Strength I factored shear stress in the diaphragm web due to tub girder flexure (bending) is calculated by dividing the total factored shear by the area of the web:

$$(f_v)_b = \frac{569 + 637}{78(1.0)} = 15.46 \text{ ksi}$$

7.12.1.4 Check of Internal Diaphragm Web

As discussed previously, for a tub girder supported on two bearings, the bending stresses in the plane of the internal diaphragm due to vertical bending of the diaphragm over the bearing sole plates are relatively small and will be neglected in this example. For a tub girder supported on a single bearing, the effects of the bending stresses in the plane of the diaphragm are likely to be more significant and should be considered. As specified in Article C6.11.8.1.1, a width of the bottom (box) flange equal to 6 times the thickness may be considered effective with the diaphragm in resisting in-plane bending.

Therefore, for this example, since bending in the plane of the diaphragm is ignored, the maximum principal stress is simply equal to the total factored shear stress:

$f_v = (f_v)_T + (f_v)_b = 2.57 + 15.46 = 18.03$ ksi

The combined factored principal stresses in the diaphragm are checked using the general form of the Huber-von Mises-Hencky yield criterion, which is similar to Eq. C6.11.8.1.1-1. The general form of the Huber-von Mises-Hencky yield criterion is:

$$\sqrt{\sigma_1^2 - \sigma_1\sigma_2 + \sigma_2^2} \le F_y$$

where σ_1 and σ_2 are the maximum and minimum principal stresses in the diaphragm web, and:

$$\sigma_1, \sigma_2 = \left(\frac{\sigma_y + \sigma_z}{2} \right) \pm \sqrt{\left(\frac{\sigma_y - \sigma_z}{2} \right)^2 + f_v^2}$$

There is a major-axis bending moment that must be carried by the internal diaphragm, resulting from the fact that the web is cantilevered out from the bearing (see Figure 17). Assuming that the vertical shear force acts at the mid-depth of the web, the internal diaphragm moment at the centerline of the bearing is computed as:

M_{ID} = (569 kips + 637 kips) (12.0 in. + 9.75 in.) = 26,231 kip-in.

It was stated earlier in these calculations (Section 7.10.3) that the moment of inertia of the effective internal diaphragm is 79,565 in.^{4}, and the neutral axis is located 39.89 in. above the bottom of the bottom flange. The bottom flange thickness is equal to the bottom flange thickness of the tub girder, which is 1.50 inches. Therefore, the major-axis bending stress, σ_y in the internal diaphragm web is computed as:

$$\sigma_y = \frac{M_{ID} c}{I} = \frac{(26{,}231)(39.89 - 1.50)}{79{,}565} = 12.66 \text{ ksi}$$

σ_z is equal to zero because there are no loads applied that cause stress in vertical direction in the internal diaphragm web.

Therefore, the principal stresses are computed as:

$$\sigma_{1,2} = \left(\frac{12.66 + 0}{2} \right) \pm \sqrt{\left(\frac{12.66 - 0}{2} \right)^2 + 18.02^2} = \pm 25.43 \text{ ksi}$$

Check the combined principal stress using the Huber-von Mises-Hencky yield criterion:

$$\sqrt{25.43^2 - (25.43)(-25.43) + (-25.43)^2} = 44.05 \text{ ksi} < F_y = 50.0 \text{ ksi}$$ OK (Ratio= 0.881)

Next, check the shear resistance of the internal diaphragm and compare the computed resistance to the factored diaphragm shear force. Compute the shear resistance according to Article 6.11.9, which refers to the provisions of Article 6.10.9 for I-girders. Article 6.7.4.3 specifies that the nominal shear resistance of internal diaphragm webs is to be computed from Eq. (6.10.9.3.3-1). Calculations not shown here indicate that C = 1.0.

$$V_u \le \phi_v V_n$$ Eq. (6.10.9.1-1)

$$V_n = V_{cr} = CV_p \qquad \text{Eq. (6.10.9.3.3-1)}$$

$$V_p = 0.58F_{yw}Dt_w = 0.58(50.0)(78)(1.0) = 2,262 \text{ kips} \qquad \text{Eq. (6.10.9.2-2)}$$

$$V_n = (1.0)(2{,}262) = 2,262 \text{ kips}$$

Check Eq. 6.10.9.1-1:

$$V_u = 569 + 639 = 1{,}208 \text{ kips} < \phi_v V_n = (1.0)(2{,}262) = 2,262 \text{ kips} \qquad \text{OK (Ratio 0.534)}$$

Article 6.7.4.3 further specifies that webs of internal diaphragms are to satisfy Eq. (6.10.1.10.2-1) to verify that the webs are nonslender and not subject to web bend-buckling.

$$D_c = 39.89 - 1.5 = 38.39 \text{ in.}$$

$$\frac{2D_c}{t_w} = \frac{2(38.39)}{1.0} = 76.8$$

$$\frac{2D_c}{t_w} \le \lambda_{rw} \qquad \text{Eq. (6.10.1.10.2-1)}$$

where:

$$4.6\sqrt{\frac{E}{F_{yc}}} \le \lambda_{rw} = \left(3.1 + \frac{5.0}{a_{wc}}\right)\sqrt{\frac{E}{F_{yc}}} \le 5.7\sqrt{\frac{E}{F_{yc}}} \qquad \text{Eq. (6.10.1.10.2-5)}$$

$$a_{wc} = \frac{2D_c t_w}{b_{fc} t_{fc}} \qquad \text{Eq. (6.10.1.10.2-8)}$$

$$4.6\sqrt{\frac{E}{F_{yc}}} = 4.6\sqrt{\frac{29{,}000}{50}} = 111$$

$$5.7\sqrt{\frac{E}{F_{yc}}} = 5.7\sqrt{\frac{29{,}000}{50}} = 137$$

$$a_{wc} = \frac{2(38.39)(1.0)}{(9.0)(1.5)} = 5.69$$

$$111 > \lambda_{rw} = \left(3.1 + \frac{5.0}{5.69}\right)\sqrt{\frac{29{,}000}{50}} = 95.8 < 137$$

$$\therefore \lambda_{rw} = 111 > \frac{2D_c}{t_w} = 76.8 \quad \text{OK}$$

7.12.2 Bearing Stiffeners

Bearing stiffeners are placed on each side of the web of the internal diaphragm at each bearing location. The design of the Girder G2 bearing stiffeners at Pier 1 (Section G2-2) is illustrated in this section. It is assumed that the bearings at Pier 1 are fixed, thus there is no expansion causing eccentric loading on the bearing stiffeners that are attached to the internal diaphragm. According to Article 6.11.11.1, bearing stiffeners attached to the internal diaphragms are to be designed using the provisions of Article 6.10.11.2.4b applied to the diaphragm rather than the girder web.

Bearing stiffeners must extend the full depth of the web and as closely as practical to the outer edges of the flanges. Each stiffener is to be either finished-to-bear against the flange through which it receives its load and attached with fillet welds (which is required if the stiffener also serves as a connection plate which is not the case here) or attached to that flange by a full penetration groove weld. Using finish-to-bear plus fillet welds to connect the bearing stiffeners to the appropriate flange, allowing the option to use fillet welds even if not required for the connection, is recommended [12]. For connection to the top flange, finish-to-bear is not necessary, and fillet welding of the stiffener to the top flange is only necessary if the stiffener also serves as a connection plate. Full penetration groove welds are costly and often result in welding deformation of the flange.

The unfactored reactions are as shown below for the left and right bearings at Pier 1, Girder G2. These results are taken directly from the three-dimensional analysis.

Left Bearing:

Steel Dead Load:	$R_{DC1\text{-}STEEL}$ = 79 kips
Concrete Deck Dead Load:	$R_{DC1\text{-}CONC}$ = 238 kips
Composite Dead Load:	R_{DC2} = 85 kips
Future Wearing Surface Dead Load:	R_{DW} = 113 kips
Live Load (incl. IM and CF):	R_{LL+IM} = 294 kips

Right Bearing:

Steel Dead Load:	$R_{DC1\text{-}STEEL}$ = 93 kips
Concrete Deck Dead Load:	$R_{DC1\text{-}CONC}$ = 370 kips
Composite Dead Load:	R_{DC2} = 11 kips
Future Wearing Surface Dead Load:	R_{DW} = 15 kips
Live Load (incl. IM and CF):	R_{LL+IM} = 287 kips

The maximum Strength I factored reactions for each bearing are computed as:

$R_{LEFT} = 1.25(79 + 238 + 85) + 1.5(113) + 1.75(294) = 1{,}187$ kips

$R_{RIGHT} = 1.25(93 + 370 + 11) + 1.5(15) + 1.75(287) = 1{,}117$ kips

The factored reaction at the left bearing is larger, and therefore controls. The bearing stiffeners are assumed to have a yield stress of 50 ksi, and are 1 in. by 11 in. plates. As shown in Figure 17, there is one bearing stiffener on each side of the internal diaphragm web, and therefore two at each bearing location.

The thickness, t_p, of each projecting stiffener element must satisfy:

$$t_p \geq \frac{b_t}{0.48\sqrt{\frac{E}{F_{ys}}}} \qquad \text{Eq. (6.10.11.2.2-1)}$$

$$t_p = 1.0 \text{ in.} > \frac{11}{0.48\sqrt{\frac{29{,}000}{50}}} = 0.95 \text{ in.} \qquad \text{OK}$$

7.12.2.1 Bearing Resistance

According to Article 6.10.11.2.3, the factored bearing resistance for the fitted ends of bearing stiffeners is taken as:

$$\left(R_{sb}\right)_r = \phi_b \left(R_{sb}\right)_n \qquad \text{Eq. (6.10.11.2.3-1)}$$

where:

ϕ_b = resistance factor for bearing specified in Article 6.5.4.2 (ϕ_b = 1.0)
$(R_{sb})_n$ = nominal bearing resistance for fitted ends of bearing stiffeners (kip)

and:

$$\left(R_{sb}\right)_n = 1.4 A_{pn} F_{ys} \qquad \text{Eq. (6.10.11.2.3-2)}$$

where:

A_{pn} = area of the projecting elements of the stiffener outside of the web-to-flange fillet welds but not beyond the edge of the flange (in.^{2})
F_{ys} = specified minimum yield strength of the stiffener (ksi)

Assuming a 1 inch stiffener clip, compute A_{pn} as follows:

$$A_{pn} = 2(11-1)(1.00) = 20.0 \text{ in}^2$$

The nominal bearing resistance of the stiffeners at a single bearing is computed as:

$$\left(R_{sb}\right)_n = 1.4\left(20.0\right)\left(50\right) = 1{,}400 \text{ kips}$$

The factored bearing resistance of the stiffeners at a single bearing is computed as:

$$\left(R_{sb}\right)_r = 1.0\left(1{,}400\right) = 1{,}400 \text{ kips} > R_u = 1{,}187 \text{ kips} \qquad \text{OK}$$

7.12.2.2 Axial Resistance

Determine the axial resistance of the bearing stiffener according to Article 6.10.11.2.4. This article directs the Engineer to Article 6.9.2.1 for calculation of the factored axial resistance, P_r. The yield strength is F_{ys}, the radius of gyration is computed about the midthickness of the web, and the effective length is 0.75 times the web depth ($K\ell = 0.75D$).

$$P_r = \phi_c P_n \qquad \text{Eq. (6.9.2.1-1)}$$

where: P_n = nominal compressive resistance determined using the provisions of Article 6.9.4 (kip)
ϕ_c = resistance factor for compression as specified in Article 6.5.4.2 (ϕ_c = 0.95)

As indicated in Article C6.9.4.1.1, only the limit state of flexural buckling is applicable for bearing stiffeners. Based on the above width-to-thickness ratio limit, bearing stiffeners are also composed only of nonslender elements; therefore, local buckling effects on the overall compressive resistance of the stiffeners need not be considered.

To compute P_n, first compute P_e and P_o. P_e is the elastic critical buckling resistance determined as specified in Article 6.9.4.1.2 for flexural buckling. P_o is the nominal yield resistance equal to F_yA_g:

$$P_e = \frac{\pi^2 E}{\left(\frac{K\ell}{r_s}\right)^2} A_g \qquad \text{Eq. (6.9.4.1.2-1)}$$

In accordance with Article 6.10.11.2.4, the effective length, $K\ell$, is to be taken as 0.75D:

$K\ell = 0.75D = 0.75(80.40) = 60.3$ in.

Compute the radius of gyration about the midthickness of the web.

$$r_s = \sqrt{\frac{I_s}{A_s}}$$

According to the provisions of Article 6.10.11.2.4b, for stiffeners welded to the web, a portion of the web is to be included as part of the effective column section. For stiffeners consisting of two

plates welded to the web, the effective column section is to consist of the two stiffener elements, plus a centrally located strip of web extending $9t_w$ on each side of the outer projecting elements of the group. The area of the web that is part of the effective section is computed as follows:

$$A_w = 2(9)(1.0)(1.0) = 18.0 \text{ in.}^2$$

The total area of the effective section is therefore:

$$A_s = 18.0 + 2(1.00)(11.00) = 40.0 \text{ in.}^2$$

Next, compute the moment of inertia of the effective section about the centerline of the diaphragm of the web, conservatively using the stiffeners only:

$$I = 2\left[\frac{1}{12}(1.0)(11.0)^3 + 11.0\left(\frac{11.0}{2} + \frac{1.0}{2}\right)^2\right] = 1,014 \text{ in.}^4$$

Compute the radius of gyration:

$$r_s = \sqrt{\frac{1,014}{40.0}} = 5.03 \text{ in.}$$

The elastic critical buckling resistance is computed as follows:

$$P_e = \frac{\pi^2(29,000)}{\left(\frac{60.3}{5.03}\right)^2}(40.0) = 79,663 \text{ kips}$$

The nominal yield resistance is computed as follows, with A_s used for A_g:

$$P_o = F_y A_g = (50)(40.0) = 2,000 \text{ kips}$$

Since

$$\frac{P_o}{P_e} = \frac{2,000}{79,663} = 0.025 < 2.25,$$

the nominal compressive resistance is computed as:

$$P_n = \left[0.658^{\left(\frac{P_o}{P_e}\right)}\right] P_o \qquad \text{Eq. (6.9.4.1.1-1)}$$

$$P_n = \left[0.658^{\left(\frac{1}{39.8}\right)} \right] (2{,}000) = 1{,}979 \text{ kips}$$

The factored compressive resistance of the bearing stiffeners is computed as follows:

$$P_r = \phi_c P_n = 0.95(1{,}979) = 1{,}880 \text{ kips}$$

$$P_u = 1{,}187 \text{ kips} < P_r = 1{,}880 \text{ kips} \qquad \text{OK} \quad (\text{Ratio} = 0.631)$$

The 1.0 in. by 11.0 in. bearing stiffeners selected satisfy the requirements for design.

7.13 Top Flange Lateral Bracing Design

Top flanges of tub girders should be braced so that the section acts as a pseudo-box for noncomposite loads applied before the concrete deck hardens or is made composite. The calculations herein demonstrate the design of the top flange single diagonal bracing member in Span 1 of Girder G2 in the first bay adjacent to the abutment for constructability. Top flange bracing must also be designed to satisfy the strength limit state for the final condition as well as for constructability. Since the bracing is permanent, composite dead load force effects (i.e., due to DC_2 and DW) and live load force effects are considered at the strength limit state, although these effects are relatively small in this case since the bracing is located at the top of the tub section. In many cases, the factored forces during construction will govern over the factored forces in the final condition.

Article 6.11.1 specifies that the top lateral bracing for tub girders must satisfy the provisions of Article 6.7.5. The bracing is designed according to the provision of Articles 6.8 and 6.9 for tension and compression, respectively. The effects of lateral loading due to wind and the lateral force caused by deck overhang brackets are neglected in this design example.

The unfactored axial forces in the diagonal bracing member in the first bay of Span 1 of Girder G2 are obtained from the three-dimensional analysis and are as follows:

Steel Dead Load:	P_{STEEL} = -13 kip
Deck Cast #1 Dead Load:	P_{CONC} = -100 kip

In accordance with Article 3.4.2.1, when investigating the Strength I and Strength III load combinations for maximum force effects during construction, load factors for the weight of the structure and appurtenances, DC and DW, are not to be taken to be less than 1.25. Therefore, the factored axial load is computed as:

$$P_u = P_{axial} = 1.25[-13 + (-100)] = -141 \text{ kips I}$$

Although not included in this example in the interest of brevity, the special load combination specified in Article 3.4.2.1 must also be considered in the design checks for the DC loads and

construction loads, C, applied to the fully erected steelwork during the deck placement sequence (see Section 5.4).

Compute the unbraced length of the top flange lateral bracing member, L_b:

Tub width at the top flanges = 120 in.
Top flange width = 16 in.
Clear distance between top flanges = 120 – 16 = 104 in.
Spacing of top flange lateral bracing = 16.3 ft = 196 in.

$$L_b = \sqrt{104^2 + 196^2} = 222 \text{ in.}$$

A structural tee is used for the top flange lateral bracing, with the stem down and its flange bolted to the bottom of the top flanges, which is the preferable method of connection. A WT 9x48.5 is selected for the top flange lateral bracing. From the AISC *Steel Construction Manual* [26], the section properties for a WT 9x48.5 are:

Area = 14.2 in.^{2}; y = 1.91 in.; S_x = 12.7 in.^{3}; r_x = 2.56 in.; r_y = 2.65 in.; J = 2.92 in.^{4}; d = 9.30 in.; b_f = 11.1 in.; t_f = 0.870 in.; I_x = 93.8 in.^{4}; I_y = 100 in.^{4}; Z_x = 22.6 in.^{3}; t_w = 0.535 in.

The thickness of the tee stem exceeds the minimum permissible thickness of 5/16″ specified for structural steel in Article 6.7.3.

Check buckling about the x-axis as this is the governing condition. The eccentricity of the connection to the center of gravity of the structural tee causes a moment on the member. The top flanges of the tub girder at this location are 1.0-inch thick. The moment due to eccentricity is computed as:

$$M_{ux} = P_{axial}\,(y + 1.0/2) = (141)(1.91 + 1.0/2) = 340 \text{ kip-in.}$$

Since the structural tee is subjected to axial compression and flexure, it is necessary to check the combined effects of axial compression and flexure in accordance with Article 6.9.2.2.

First, check the limiting slenderness ratio for secondary members in compression (see Table 6.6.2.1-1), as specified in Article 6.9.3. Article 4.6.2.5 allows the effective length factor, K, to be taken as 0.75 for members with bolted or welded connections at both ends. Assume K_y = 0.75. However, since only the tub flanges are providing restraint for buckling about the x-axis, K_x will conservatively be taken equal to 1.0. The slenderness ratios about each axis in this case are therefore:

$$\frac{K_y \ell_y}{r_y} = \frac{0.75(222)}{2.65} = 62.8 < 140 \quad \text{ok}$$

$$\frac{K_x \ell_x}{r_x} = \frac{1.0(222)}{2.56} = 86.7 < 140 \quad \text{ok}$$

To determine if the effects of local buckling of the tee stem on the nominal compressive resistance of the member need to be considered, check the width-to-thickness ratio provision of Article 6.9.4.2.1 for the lateral bracing member:

$$\frac{b}{t} \le \lambda_r \qquad \text{Eq. (6.9.4.2.1-1)}$$

where:

λ_r = width-to-thickness ratio limit specified in Table 6.9.4.2.1-1
b = full depth of the tee section (in.)
t = element thickness (in.)

$$\frac{b}{t} = \frac{9.30}{0.535} = 17.4 < \lambda_r = 0.75\sqrt{\frac{29{,}000}{50}} = 18.1 \quad \text{OK} \quad \text{Tee stem is nonslender}$$

Similar calculations, not shown, indicate that the flange of the tee section is also a nonslender element. If the tee stem or flange were slender, local buckling effects would need to be considered according to the provisions of Article 6.9.4.2.2.

Compute the compressive resistance in accordance with Article 6.9.2.1, where the factored compressive resistance, P_r, is taken as:

$$P_r = \phi_c P_n \qquad \text{Eq. (6.9.2.1-1)}$$

where:

ϕ_c = resistance factor for compression as specified in Article 6.5.4.2 (ϕ_c = 0.95)
P_n = nominal compressive resistance as specified in Article 6.9.4 or 6.9.5, as applicable (kip)

Compute the nominal compressive resistance, P_n, in accordance with Article 6.9.4.1.1. In order to determine which equation to use to compute the nominal compressive resistance, it is necessary to compute the elastic critical buckling resistance, P_e, and the nominal yield resistance, P_o.

The elastic critical buckling resistance, P_e, is specified in Article 6.9.4.1.2 for flexural buckling, and specified in Article 6.9.4.1.3 for flexural-torsional buckling. In accordance with Table 6.9.4.1.1-1, flexural buckling and flexural-torsional buckling must be considered to determine the compressive resistance of structural tees. Separate calculations, not provided here, show that flexural buckling governs in this particular case. The computation of P_e for the flexural buckling resistance is illustrated herein.

Compute the elastic critical buckling resistance, P_e, based on flexural buckling in accordance with Article 6.9.4.1.2:

$$P_e = \frac{\pi^2 E}{\left(\frac{K\ell}{r_s}\right)^2} A_g \qquad \text{Eq. (6.9.4.1.2-1)}$$

where:

A_g = gross cross-sectional area of the member (in.^{2})
K = effective length factor in the plane of buckling determined as specified in Article 4.6.2.5
ℓ = unbraced length in the plane of buckling (in.)
r_s = radius of gyration about the axis normal to the plane of buckling (in.)

The elastic critical buckling resistance is then computed as:

$$P_e = \frac{\pi^2 (29{,}000)}{(65.0)^2}(14.2) = 962 \text{ kips}$$

The nominal yield resistance, P_o, is computed in accordance with Article 6.9.4.1.1 as follows:

$$P_o = F_y A_g$$

Therefore, the nominal yield resistance, P_o, is computed as:

$$P_o = (50)(14.2) = 710 \text{ kips}$$

As specified in Article 6.9.4.1.1, check the result of P_o/P_e:

$$\frac{P_o}{P_e} = \frac{710}{962} = 0.74$$

Since P_o/P_e is less than 2.25, the nominal compressive resistance, P_n, is computed in accordance with Eq. 6.9.4.1.1-1.

$$P_n = \left[0.658^{\left(\frac{P_o}{P_e}\right)}\right] P_o \qquad \text{Eq. (6.9.4.1.1-1)}$$

$$P_n = \left[0.658^{\left(\frac{710}{962}\right)}\right](710) = 521 \text{ kips}$$

Compute the factored compressive resistance, P_r, in accordance with Article 6.9.2.1:

$$P_r = \phi_c P_n = (0.95)(521) = 495 \text{ kips} \qquad \text{Eq. (6.9.2.1-1)}$$

Determine the factored flexural resistance about the x-axis using the provisions of Article 6.12.1.2 for miscellaneous flexural members, and specifically Article 6.12.2.2.4 for structural tees. The factored flexural resistance, M_r, is to be taken as:

$$M_r = \phi_f M_n \qquad \text{Eq. (6.12.1.2.1-1)}$$

where:

ϕ_f = resistance factor for flexure as specified in Article 6.5.4.2 ($\phi_f = 1.0$)
M_n = nominal flexural resistance specified in Articles 6.12.2.2 or 6.12.2.3, as applicable (kip-in.)

In accordance with Article 6.12.2.2.4a, the nominal flexural resistance is to be taken as the smallest value based on yielding, lateral torsional buckling, flange local buckling, and local buckling of the tee stem, as applicable.

For yielding of tee stems subject to tension, the nominal flexural resistance is given as:

$$M_n = F_y Z_x \le 1.6 M_y \qquad \text{Eq. (6.12.2.2.4b-1)}$$

where:

F_y = specified minimum yield strength (ksi)
M_y = yield moment = $F_y S_x$ (kip-in.)
S_x = elastic section modulus about the *x*-axis with respect to the tip of the tee stem (in.^{3})
Z_x = plastic section modulus about the x-axis (in.^{3})

For yielding of tee stems subject to compression, M_n is equal to M_y according to Eq. (6.12.2.2.4b-2). Determine if the tip of the stem is in compression or tension:

$$f_{tip,\,stem} = \frac{P_{axial}}{A_g} + \frac{M_{ux}}{S_x} = \frac{-141}{14.2} + \frac{340}{12.7} = 16.8 \text{ ksi} \qquad \text{(tension)}$$

Therefore, the nominal flexural resistance for yielding is limited to $1.6M_y$. The nominal flexural resistance for yielding is computed as:

$$M_n = F_y Z_x = (50)(22.6) = 1{,}130 \text{ kip} - \text{in.}$$

$$1.6M_y = 1.6F_y S_x = 1.6(50)(12.7) = 1{,}016 \text{ kip} - \text{in.} \qquad \text{(governs)}$$

$$M_n = 1{,}016 \text{ kip} - \text{in.} \quad \text{(for yielding)}$$

For tee stems subject to tension, the nominal flexural resistance based on lateral torsional buckling is to be taken as:

- If $L_b \le L_p$, then lateral–torsional buckling does not apply.
- If $L_p < L_b \le L_r$, then:

$$M_n = M_p - \left(M_p - M_y\right)\left(\frac{L_b - L_p}{L_r - L_p}\right) \qquad (6.12.2.2.4c\text{-}1)$$

- If $L_b > \underline{L_r}$, then:

$$M_n = M_{cr} \qquad (6.12.2.2.4c\text{-}2)$$

in which:

$$L_p = 1.76 r_y \sqrt{\frac{E}{F_y}} \qquad (6.12.2.2.4c\text{-}3)$$

$$L_r = 1.95\left(\frac{E}{F_y}\right)\frac{\sqrt{I_y J}}{S_x}\sqrt{2.36\left(\frac{F_y}{E}\right)\frac{dS_x}{J} + 1} \qquad (6.12.2.2.4c\text{-}4)$$

$$M_{cr} = \frac{1.95E}{L_b}\sqrt{I_y J}\left(B + \sqrt{1 + B^2}\right) \qquad (6.12.2.2.4c\text{-}5)$$

$$B = 2.3\left(\frac{d}{L_b}\right)\sqrt{\frac{I_y}{J}} \qquad (6.12.2.2.4c\text{-}6)$$

where:

d = depth of the tee in tension (in.)
I_y = moment of inertia about the *y*-axis (in.^{4})
J = St. Venant torsional constant (in.^{4})
L_b = unbraced length (in.)
r_y = radius of gyration about the y-axis (in.)
S_x = elastic section modulus about the *x*-axis with respect to the tip of the tee stem (in.^{3})

Determine L_p:

$$L_p = 1.76 r_y \sqrt{\frac{E}{F_y}} = 1.76(2.65)\sqrt{\frac{29{,}000}{50}} = 112.3 \text{ in.}$$

Determine L_r:

$$L_r = 1.95\left(\frac{E}{F_y}\right)\frac{\sqrt{I_y J}}{S_x}\sqrt{2.36\left(\frac{F_y}{E}\right)\frac{dS_x}{J}+1}$$

$$= 1.95\left(\frac{29{,}000}{50}\right)\frac{\sqrt{(100)(2.92)}}{12.7}\sqrt{2.36\left(\frac{50}{29{,}000}\right)\frac{(9.30-1.91)(12.7)}{2.92}+1} = 1{,}618 \text{ in.}$$

Since L_b = 222 in. is greater than L_p = 112.3 in. but less than L_r = 1,618 in., the nominal lateral torsional buckling resistance is computed from Eq. (6.12.2.2.4c-1) as follows:

$$M_n = M_p - \left(M_p - M_y\right)\left(\frac{L_b - L_p}{L_r - L_p}\right)$$

$M_p = M_n$ for yielding = 1,016 kip-in.

(*Note: there is an error in the 9th Edition AASHTO LRFD BDS. M_p for checking lateral-torsional buckling should be taken as the value of M_n determined for yielding – see AISC Specification Article F9*).

$M_y = F_y S_x = (50)(12.7) = 635$ kip-in.

$$M_n = 1{,}016 - (1{,}016 - 635)\left(\frac{222 - 112.3}{1{,}618 - 112.3}\right) = 988 \text{ kip} - \text{in.}$$

Since the flange is in compression, flange local buckling must also be considered in accordance with Article 6.12.2.2.4d. First check if the flange slenderness, λ_f, exceeds the limiting slenderness for a compact flange for tees, λ_{pf}. If λ_{pf} is not exceeded, flange local buckling does not need to be checked.

$$\lambda_f = \frac{b_f}{2t_f} = \frac{11.1}{2\ (0.870)} = 6.38$$

$$\lambda_{pf} = 0.38\sqrt{\frac{E}{F_y}} = 0.38\sqrt{\frac{29{,}000}{50}} = 9.15 \qquad \text{Eq. (6.12.2.2.4d-6)}$$

$$\lambda_f = 6.38 < \lambda_{pf} = 9.15$$

Given that $\lambda_f < \lambda_{pf}$, local flange buckling does not need to be checked. Also, because the stem is in tension, local buckling of the stem does not need to be investigated.

Thus, the nominal flexural resistance, M_n, of the tee section is governed by lateral torsional buckling, and is equal to 988 kip-in. Compute the factored flexural resistance, M_r, as follows:

$$M_r = \phi_f M_n = (1.0)(988) = 988 \text{ kip} - \text{in.} \qquad \text{Eq. (6.12.1.2.1-1)}$$

Check the combined axial compression and flexure as specified in Article 6.9.2.2.1. First, it is necessary to determine the value of the factored axial compressive load, P_u, divided by the factored compressive resistance, P_r.

$$\frac{P_u}{P_r} = \frac{|-141|}{495} = 0.285 > 0.2$$

Since the above ratio is greater than 0.2, Eq. 6.9.2.2.1-2 is to be used to check the combined axial compression and flexure, noting that there is no bending about the y-axis. Article C6.9.2.2.1 discusses the fact that Eqs. (6.9.2.2.1-1) and (6.9.2.2.1-2) may significantly underestimate the resistance of tees subject to combined axial compression and flexure in which the axial and flexural stresses in the flange of the tee are additive in compression. However, it is recommended that these equations be conservatively applied in such cases unless significant additional resistance is required.

$$\frac{P_u}{P_r} + \frac{8}{9}\left(\frac{M_{ux}}{M_{rx}}\right) \le 1.0 \qquad \text{Eq. (6.9.2.2.1-2)}$$

where:

M_{ux} = factored flexural moment about the x-axis (kip-in.)
M_{rx} = factored flexural resistance (kip-in.)

Second-order effects arise from the additional secondary moment caused by the axial force acting through the member deflection. Article 6.9.2.2.1 permits the single-step adjustment or moment magnification method specified in Article 4.5.3.3.2b to be used to determine the second-order elastic moment in lieu of a second-order elastic analysis as follows:

$$(M_{ux})_2 = \delta_b (M_{ux})_1 \qquad \text{Eq. (4.5.3.2.2b-1)}$$

The magnification factor, δ_b, is computed as follows:

$$\delta_b = \frac{C_m}{1-\frac{P_u}{\varphi_K P_e}} \geq 1.0 \qquad \text{Eq. (4.5.3.2.2b-3)}$$

ϕ_K is a stiffness reduction factor taken equal to 1.0 for steel members. C_m is the equivalent uniform moment factor, which for members braced against sidesway and without transverse loading (other than the self-weight of the member) between supports in the plane of bending, is to be taken as:

$$C_m = 0.6 + 0.4\frac{M_1}{M_2} \qquad \text{Eq. (4.5.3.2.2b-6)}$$

The tee section is bent in single curvature by equal moments at the end of the member due to the eccentricity. For single curvature, the ratio of the end moments $M_1/M_2 = 1.0$ is to be taken as positive. Therefore, from the preceding equation, $C_m = 1.0$.

P_e is the Euler buckling load for buckling about the x-axis (i.e. the plane of bending), which is to be taken as follows:

$$P_e = \frac{\pi^2 EI}{\left(K_x \ell_x\right)^2} \qquad \text{Eq. (4.5.3.2.2b-5)}$$

K_x is the effective length factor for buckling about the x-axis, and ℓ_x is the unbraced length for buckling about the x-axis. For this case, K_x is equal to 1.0 and I is equal to $I_x = 93.8$ in.^{4}. Therefore:

$$P_e = \frac{\pi^2 (29,000)(93.8)}{\left(1.0 * 222\right)^2} = 545 \text{ kips}$$

$$\delta_b = \frac{1.0}{1-\frac{|-141|}{1.0(545)}} = 1.35$$

Thus:

$$\left(M_{ux}\right)_2 = 1.35(340) = 459 \text{ kip} - \text{in.}$$

Check Eq. 6.9.2.2.1-2 as follows:

$$\frac{P_u}{P_r} + \frac{8.0}{9.0}\left(\frac{M_{ux}}{M_{rx}}\right) = \frac{|-141|}{495} + \frac{8}{9}\left(\frac{459}{988}\right) = 0.70 < 1.0 \qquad \text{OK}$$

The WT 9x48.5 serving as the top flange diagonal bracing member in Span 1 of Girder G2 in the first bay adjacent to the abutment satisfies the interaction ratio for combined axial compression

and flexure for constructability loading. Design checks would be performed for all top flange lateral bracing members, investigating both tension and compression constructability forces.

7.14 Bolted Field Splice Design

This section will show the design of a bolted field splice, in accordance with the provisions of Article 6.13.6. The design computations will be illustrated for the Field Splice #1 on Girder G2 (see Figure 9). First, single bolt capacities are computed for slip resistance (Article 6.13.2.8) and shear resistance (Article 6.13.2.7), and the bearing resistance on the connected material (Article 6.13.2.9). The field splice is then checked for constructability, the service limit state, and the strength limit state. For further information on bolted field splice design, refer to the NSBA document *Bolted Field Splices for Steel Bridge Flexural Members – Overview and Design Examples* [27], which is available on the NSBA website (www.aisc.org/nsba), and also NSBA's *Steel Bridge Design Handbook: Splice Design* [28].

All bolts used in the field splice are 0.875 inch diameter ASTM F3125 Grade 325 bolts. Table 6.13.2.4.2-1 shows that a standard hole diameter size for a 0.875 inch diameter bolt is 0.9375 inch. The connection is designed assuming a Class B surface condition is provided and that the faying surface is unpainted and blast cleaned. The threads are assumed excluded from the shear planes in the flange splices and included in the shear planes in the web splice. This will be checked later on in Sections 7.14.3.4 and 7.14.4.3.

Article 6.13.6.1.3a requires at least two rows of bolts on each side of the connection. Oversize or slotted holes in either the member or the splice plates are not permitted. In continuous spans, bolted splices preferably should be located in regions of lower moment at or near points of dead load contraflexure to reduce the major-axis bending moments acting on the splice. This may not always be possible in certain situations, such as in longer-span bridges or in cases where additional field splices may be needed to reduce the size of a shipping piece; for example, in a sharply curved member or where shipping lengths start to exceed a practical upper limit. Web and flange splices in areas of stress reversal are to be investigated for both positive and negative flexure to determine the governing condition.

The bolt pattern for the top flange splices is shown in Figure 19, the bolt pattern for the bottom flange splice is shown in Figure 20, and the bolt pattern for the web splice is shown in Figure 21. It should be noted that a 0.5 inch gap is assumed between the edges of the field pieces at this splice location. Note in Figure 20 that the bottom flange longitudinal stiffener is terminated at the end of the field section. By including a gap in the splice plate and terminating the longitudinal stiffener at the end of the section where the stress is zero, it is not necessary to consider fatigue at the terminus of the stiffener, as discussed further in Section 7.11.

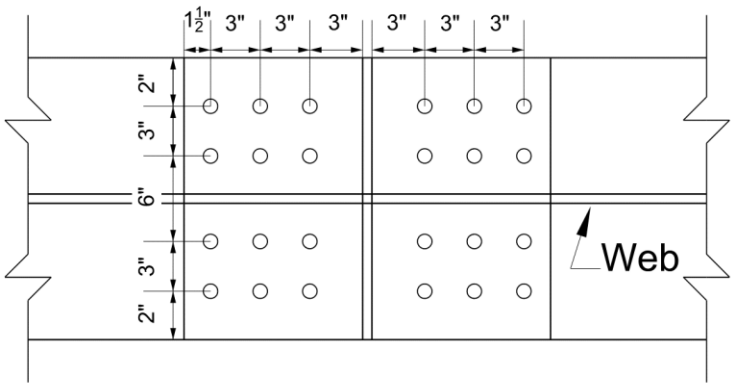

Figure 19 Bolt Pattern for the Top Flange Field Splices

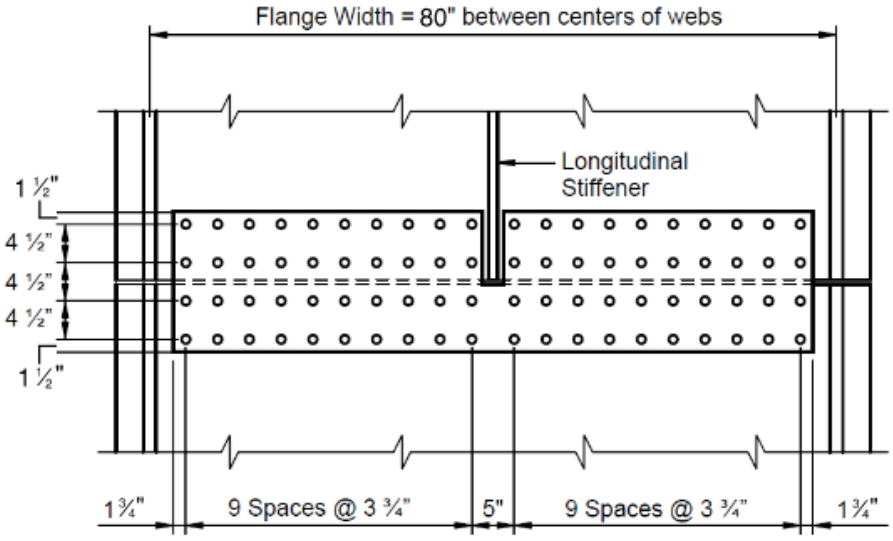

Figure 20 Bolt Pattern for the Bottom Flange Field Splice, shown inside the tub girder looking down at the bottom flange

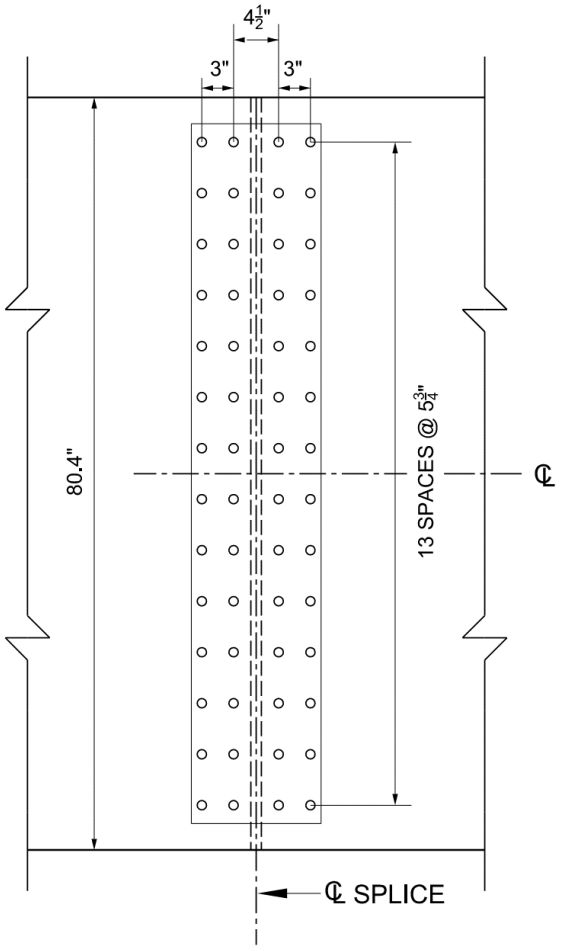

Figure 21 Bolt Pattern for the Web Field Splice, dimensions shown along the web slope

Unfactored analysis results for the girder major-axis bending moments, torques, shears, and top flange lateral bending moments at Field Splice #1 on Girder G2 are summarized in Table 16.

Table 16 Unfactored Analysis Results for the Design of Field Splice #1 on Girder G2

Unfactored Demands at G2 Field Splice 1							
Demand	Dead Load					LL+I	
	$DC1_{STEEL}$	$DC1_{CONC}$	$DC1_{CAST1}$	DC2	DW	Pos.	Neg.
Moment (kip-ft)	462	1941	2749	326	428	5221	-3080
Torque (kip-ft)	-36	-125	-188	-58	-76	346	-517
Top Flange Lateral Moment (kip-ft)	-1	-7	-15	n/a	n/a	n/a	n/a
Shear (kips)	-17	-69	-61	-12	-16	36	-85

Note: Reported shears are the vertical shears and are for major-axis bending plus torsion in the critical tub girder web.

Referring to Table 16, the factored Strength I design major-axis bending moments at the point of splice are computed as follows:

Positive Moment = 1.25[(462 + 1,941) + (326)] + 1.5(428) + 1.75(5,221) = +13,190 kip-ft

Negative Moment = 0.90[(462 + 1,941) + (326)] + 0.65(428) + 1.75(-3,080) = -2,656 kip-ft

7.14.1 Bolt Resistance for the Service Limit State and Constructability

Article 6.13.6.1.3a specifies that bolted splices for flexural members are to be designed using slip-critical connections (Article 6.13.2.1.1). The connections are to be proportioned to prevent slip under load combination Service II and during the placement of the concrete deck. For slip-critical connections, the factored resistance, R_r, of a bolt for the Service II load combination and for constructability is taken as:

$$R_r = R_n \qquad \text{Eq. (6.13.2.2-1)}$$

where:

R_n = the nominal slip resistance as specified in Article 6.13.2.8 (kip)

The nominal slip resistance of a bolt in a slip-critical connection is to be taken as:

$$R_n = K_h K_s N_s P_t \qquad \text{Eq. (6.13.2.8-1)}$$

where:

N_s = number of slip planes per bolt
P_t = minimum required bolt tension specified in Table 6.13.2.8-1(kip)
K_h = hole size factor specified in Table 6.13.2.8-2
K_s = surface condition factor specified in Table 6.13.2.8-3

For this design example:

- 2 slip planes are provided as there are two splice plates on each side of the girder element, thus N_s equals 2;
- As specified in Table 6.13.2.8-1, for 0.875 inch diameter ASTM F3125 Grade 325 bolt, P_t is equal to 39 kips;
- As specified in Table 6.13.2.8-2, for a standard size hole, K_h is equal to 1.00; and
- As specified in Table 6.13.2.8-3, for Class B surface conditions, K_s is equal to 0.50.

Therefore, the factored slip resistance for service and constructability checks is:

$$R_r = R_n = (1.0)(0.50)(2)(39) = 39 \text{ kips/bolt}$$

7.14.2 Bolt Resistance for the Strength Limit State

The factored resistance, R_r, of a bolted connection at the strength limit state is to be taken as:

$$R_r = \phi R_n \qquad \text{Eq. (6.13.2.2-2)}$$

where:

ϕ = applicable resistance factor for bolts specified in Article 6.5.4.2

The nominal resistance of the bolted connection at the strength limit state must be computed for shear, bearing, and tension, where applicable.

Article 6.13.6.1.3a states that the factored flexural resistance of the flanges at the point of the splice at the strength limit state must satisfy the applicable provisions of Article 6.10.6.2, which relates to flexure. The girder satisfies the applicable provisions of Article 6.10.6.2 at the splice location; however, the checks at this location are not included in this example.

7.14.2.1 Bolt Shear Resistance (Article 6.13.2.7)

The nominal shear resistance, R_n, of a high-strength bolt at the strength limit state in joints whose length between extreme fasteners measured parallel to the line of action of the force is less than or equal to 38.0 in. (which will be assumed in this design example) and where threads are excluded from the shear plane is computed as follows:

$$R_n = 0.56 A_b F_{ub} N_s \qquad \text{Eq. (6.13.2.7-1)}$$

where:

A_b = area of bolt corresponding to the nominal diameter ($in.^2$)
F_{ub} = specified minimum tensile strength of the bolt in accordance with Article 6.4.3(ksi)
N_s = number of shear planes

In accordance with Article 6.4.3, the specified minimum tensile strength of a 0.875-inch diameter ASTM F3125 Grade 325 bolt is 120 ksi. Two shear planes exist for all field splice connections. Therefore, the nominal shear resistance is computed as:

$R_n = 0.56(0.601)(120)(2) = 80.8$ kips/bolt

The factored shear resistance, R_r, of a high-strength bolt at the strength limit state is computed as follows:

$$R_r = \phi_s R_n \qquad \text{Eq. (6.13.2.2-2)}$$

where:

ϕ_s = shear resistance factor for bolts in shear from Article 6.5.4.2 (ϕ_s = 0.80)

Therefore, the factored shear resistance is:

$R_r = (0.80)(80.8) = 64.6$ kips/bolt

The nominal shear resistance in similar joints where threads are included in the shear plane is computed as:

$$R_n = 0.45 A_b F_{ub} N_s \qquad \text{Eq. (6.13.2.7-2)}$$

$$R_n = 0.45(0.601)(120)(2) = 64.9 \text{ kips / bolt}$$

The factored shear resistance at the strength limit state is taken as:

$R_r = 0.80(64.9) = 51.9$ kips/bolt

The nominal shear resistance of a bolt in lap splice tension connections greater than 38.0 in. in length is to be taken as 0.83 times the preceding values.

7.14.2.2 Bearing Resistance of the Connected Material (Article 6.13.2.9)

The nominal bearing resistance of interior and end bolt holes at the strength limit, R_n, is taken as one of the following two terms, depending on the bolt clear distance and the clear end distance.

(1) With bolts spaced at a clear distance between holes not less than 2.0d and with a clear end distance not less than 2.0d:

$$R_n = 2.4 dt F_u \qquad \text{Eq. (6.13.2.9-1)}$$

(2) If either the clear distance between holes is less than 2.0d or the clear end distance is less than 2.0d:

$$R_n = 1.2 L_c t F_u \qquad \text{Eq. (6.13.2.9-2)}$$

where:

d = nominal diameter of the bolt (in.)
t = thickness of the connected material (in.)
F_u = tensile strength of the connected material specified in Table 6.4.1-1 (ksi)
L_c = clear distance between holes or between the hole and the end of the member in the direction of the applied force

For example, in the case of the web splice plates, the end distance is 2.0 inches. According to Article 6.8.3, the width of each standard bolt hole for design is to be taken as the nominal diameter of the hole = 0.9375 in., creating a clear end distance of 1.53 inches, which is less than 2.0d. Therefore, Eq. (6.13.2.9-2) applies. The specified minimum tensile strength of the girder and splice plates in this design example is 65 ksi. The bearing resistance of the web controls in this case since the web thickness is assumed to be less than the sum of the two web splice plate thicknesses. The nominal bearing resistance for the end row of bolts in the web splice plates is therefore:

$R_n = 1.2(1.53)(0.5625)(65) = 67.13$ kips/bolt

The factored bearing resistance, R_r, is computed as:

$$R_r = \phi_{bb} R_n \qquad \text{Eq. (6.13.2.2-2)}$$

where:

ϕ_{bb} = resistance factor for bolts bearing on material from Article 6.5.4.2 ($\phi_{bb} = 0.80$)

Therefore, the factored bearing resistance is:

$R_r = \phi_{bb} R_n = (0.80)(67.13) = 53.70$ kips/bolt

7.14.3 Flange Splice Design

7.14.3.1 General

Article 6.13.6.1.3b states that flange splice plates and their connections are to be designed to develop the smaller design yield resistance of the flanges on either side of the splice. The design yield resistance of each flange, P_{fy}, at the point of splice is taken as:

$$P_{fy} = F_{yf} A_e \qquad (6.13.6.1.3b\text{-}1)$$

in which: A_e = effective area of the flange under consideration (in.^{2}). A_e is to be taken as:

$$A_e = \left(\frac{\phi_u F_u}{\phi_y F_{yf}} \right) A_n \le A_g \qquad (6.13.6.1.3b\text{-}2)$$

where:

ϕ_u = resistance factor for fracture of tension members = 0.80 (Article 6.5.4.2)
ϕ_y = resistance factor for yielding of tension members = 0.95 (Article 6.5.4.2)
A_n = net area of the flange under consideration determined as specified in Article 6.8.3 (in.^{2})
A_g = gross area of the flange under consideration (in.^{2})

F_u = specified minimum tensile strength of the flange under consideration determined as specified in Table 6.4.1-1 (ksi)
F_{yf} = specified minimum yield strength of the flange under consideration (ksi)

The use of the effective flange area in the computation of P_{fy} accounts for the loss in section causing a reduction in the fracture resistance of the net section at the connection for loading conditions in which the flange is subject to tension. The effective flange area is conservatively used for both tension and compression flanges.

7.14.3.2 Flange Splice Bolts

For each flange, the smaller design yield resistance at the point of splice, P_{fy}, is to be divided by the factored shear resistance of the bolts, determined in Section 7.14.2.1, to determine the total number of flange splice bolts required on one side of the splice at the strength limit state. Where filler plates are required, the provisions of Article 6.13.6.1.4 apply.

Top Flanges

The left side of the splice has the smaller design yield resistance (i.e., the top flange on the left side has a smaller area). Assume 4 rows of bolts across the width of a single top flange

$$A_e = \left(\frac{0.80(65)}{0.95(50)}\right)\left[16 - 4(0.9375)\right](1.0) = 13.4 \text{ in.}^2 < (1.0)(16) = 16.0 \text{ in.}^2$$

$$P_{fy} = 50(13.4) = 670 \text{ kips}$$

Since the flange thicknesses are the same on either side of the splice, a filler plate is not required in this case.

Therefore:

$$N = \frac{670}{64.6} = 10.4 \text{ bolts}$$

Use 4 rows with 3 bolts per row = 12 bolts on each side of the splice.

For flanges with one web in horizontally curved girders, the effects of flange lateral bending need not be considered in the design of the bolted flange splices since the combined areas of the flange splice plates will typically equal or exceed the area of the smaller flange to which they are attached. The girder flanges are designed so that the yield stress of the flange is not exceeded at the flange tips under combined major-axis and lateral bending for constructability and at the strength limit state. Flange lateral bending is also less critical at locations in-between the cross-frames or diaphragms where bolted splices are located. The rows of bolts provided in the flange splice on each side of the web provide the necessary couple to resist the lateral bending. Flange lateral bending will increase the flange slip force on one side of the splice and decrease the slip force on the other side of the splice; slip cannot occur unless it occurs on both sides of the splice.

St. Venant torsional shears and longitudinal warping stresses due to cross-section distortion are typically neglected in top flanges of tub-girder sections once the flanges are continuously braced.

Bottom Flange

The size of the bottom flange is the same on either side of the splice. A filler plate is not required. Assume 20 rows of bolts across the width of the flange.

$$A_e = \left(\frac{0.80(65)}{0.95(50)}\right)\left[83 - 20(0.9375)\right](0.6875) = 48.4 \text{ in.}^2 < (0.6875)(83) = 57.1 \text{ in.}^2$$

$$P_{fy} = 50(48.4) = 2,420 \text{ kips}$$

For box sections in horizontally curved bridges, the vector sum of the St. Venant torsional shear and the design yield resistance is to be considered in the design of the bottom flange splice at the strength limit state (Article 6.13.6.1.3b). Longitudinal warping stresses due to cross-section distortion may be ignored at the strength limit state since the bottom flange splices are designed to develop the full design yield capacity of the flanges. Flange lateral bending due to curvature is not a consideration for bottom flanges of box girders.

Calculate the factored St. Venant torsional shear flow, f, in the bottom flange at the point of splice for the Strength I load combination. The negative live load plus impact torque controls by inspection (refer to Table 16).

For the DC_1 torque, which is applied to the non-composite section, the enclosed area, A_o, is computed for the non-composite box section. The vertical depth, D, between the mid-thickness of the flanges, which is equal to 78.84 in., is used. The bottom-flange width between the mid-thickness of the tub-girder webs is 80.0 in. Therefore:

$$A_o = \frac{(120 + 80)}{2} * (78.0 + 0.5 + \frac{0.6875}{2}) * \frac{1 \text{ ft}^2}{144 \text{ in.}^2} = 54.8 \text{ ft}^2$$

From Eq. C6.11.1.1-1, the St. Venant torsional shear flow is calculated as:

$$f = \frac{T}{2A_o}$$

$$f = \frac{1.0(1.25)(-36 + -125)}{2(54.8)} = -1.84 \text{ kips/ft}$$

For the torques applied to the composite section (i.e. the DC_2, DW and LL+IM torques), calculate A_o for the composite section from the mid-thickness of the bottom flange to the mid-thickness of the concrete deck (considering the deck haunch):

$$A_o = \frac{(120+80)}{2} * (78.0 + \frac{0.6875}{2} + 4.0 + \frac{9.5}{2}) * \frac{1\,\text{ft}^2}{144\,\text{in.}^2} = 60.5\,\text{ft}^2$$

$$f = \frac{1.0\left|1.25(-58)+1.5(-76)+1.75(-517)\right|}{2(60.5)} = -9.02\ \text{kips/ft}$$

$$f_{total} = -1.84 + -9.02 = -10.86\ \text{kips/ft}$$

The factored St. Venant torsional shear at the strength limit state, V_{SV}, at the point of splice is computed as:

$$V_{SV} = f_{total} b_f = \left|-10.86\right| \frac{80.0}{12} = 72.4\ \text{kips}$$

The resultant bolt shear force is computed as:

$$R = \sqrt{\left(P_{fy}\right)^2 + \left(V_{sv}\right)^2} = \sqrt{\left(2,420\right)^2 + \left(72.4\right)^2} = 2,421\ \text{kips}$$

$$N = \frac{2,421}{64.6} = 37.5\ \text{bolts}$$

Use 20 rows with 2 bolts per row = 40 bolts on each side of the splice.

7.14.3.3 Moment Resistance

The moment resistance provided by the flanges at the point of splice is next to be checked against the factored moment at the strength limit state. Should the factored moment exceed the moment resistance provided by the flanges, the additional moment is to be resisted by the web as specified in Article 6.13.6.1.3c.

For composite sections subject to positive flexure, the moment resistance provided by the flanges at the strength limit state is computed as P_{fy} for the bottom flange times the moment arm taken as the vertical distance from the mid-thickness of the bottom flange to the mid-thickness of the concrete deck including the concrete haunch (Figure C6.13.6.1.3b-1). For composite sections subject to negative flexure and noncomposite sections subject to positive or negative flexure, the moment resistance provided by the flanges is computed as P_{fy} for the top or bottom flange, whichever is smaller, times the moment arm taken as the vertical distance between the mid-thickness of the top and bottom flanges (Figure C6.13.6.1.3b-2). If necessary, the moment resistance provided by the flanges can potentially be increased by staggering the flange bolts.

Positive Flexure (refer to Figure C6.13.6.1.3b-1)

Use P_{fy} for the bottom flange = 2,420 kips

Flange moment arm: $A = D + t_{ft}/2 + t_{haunch} + t_s/2 = 78 + (0.6875/2) + 4.0 + (9.5/2) = 87.09$ in.

$M_{flange} = 2{,}420 \times (87.09/12) = 17{,}653$ kip-ft > 13,190 kip-ft OK

Negative Flexure (refer to Figure C6.13.6.1.3b-2)

Use the smaller value of P_{fy} for the top and bottom flanges. In this case, the top flanges have the smaller value of $P_{fy} = 2 \times 670$ kips = 1,340 kips.

Flange Moment Arm: $A = D + (t_{ft} + t_{fc})/2 = 78 + (1.0 + 0.6875)/2 = 78.84$ in.

$M_{flange} = 1{,}340 \times (78.84/12) = 8{,}804$ kip-ft > |-2,656| kip-ft

Therefore, the flanges have adequate capacity to resist the Strength I moment requirements at the splice. No moment contribution from the web is required.

7.14.3.4 Flange Splice Plates

The design of the top-flange splice plates is illustrated first. The width of the outside splice plate should be at least as wide as the width of the narrowest flange at the splice. The thickness of the outside splice plate should be at least one-half the thickness of the thinner flange at the splice plus 1/16 of an inch [27]. As a result, the flange will control the bearing and block shear rupture resistance, which is checked later on in this design example.

$$t_o \geq \frac{1.0}{2} + 0.0625 = 0.5625 \text{ in.} \quad \text{Use } t_o = \frac{5}{8} \text{ in.}$$

The width of the inside splice plates should be such that the plates clear the flange-to-web weld on each side of the web by a minimum of ⅛ in [27]. Assuming 5/16-inch flange-to-web welds are used, the minimum clearance distance, C, between the two inner splice plates is computed as follows:

$$C \geq t_{web} + 2\left[\text{weld size} + \frac{1}{8}^{"}\right] = 0.5625 + 2\left[0.3125 + \frac{1}{8}^{"}\right] = 1.4375 \text{ in.}$$

$$b_i = \frac{(b_f - C)}{2} = \frac{(16 - 1.4375)}{2} = 7.28 \text{ in.}$$

At the strength limit state, P_{fy} may be assumed equally divided to the inner and outer flange splice plates when the areas of the inner and outer plates do not differ by more than 10 percent (Article C6.13.6.1.3b). In this case, P_{fy} may be assumed equally divided to the inner and outer plates and the shear resistance of the bolted connection may be checked for P_{fy} acting in double shear. Applying the above 10 percent guideline gives:

$$0.9b_f t_o \le 2b_i t_i \le 1.1b_f t_o$$

Substituting the equation for b_i given above into the preceding equation and rearranging gives:

$$0.9t_o \le \left(1-\frac{C}{b_f}\right)t_i \le 1.1t_o$$

$$0.9(0.625) \le \left(1-\frac{1.4375}{16.0}\right)t_i \le 1.1(0.625)$$

$$0.5625 \le (0.91)t_i \le 0.6875$$

$$0.62 \le t_i \le 0.76 \quad \text{Use } t_i = \frac{3}{4}"$$

Therefore, for the top-flange splices, try a 5/8 in. x 16 in. outside splice plate and two ¾ in. x 7¼ in. inside splice plates. A filler plate is not required. All plates are ASTM A709 Grade 50 steel.

At the strength limit state, the design force in the splice plates is not exceed the factored resistance in tension specified in Article 6.13.5.2. The factored resistance, R_r, in tension is to be taken as the least of the values given by either Eqs. 6.8.2.1-1 and 6.8.2.1-2 for yielding and fracture, respectively, or the block shear rupture resistance specified in Article 6.13.4.

Check the factored yield resistance of the splice plates in tension:

$$R_r = \phi_y F_y A_g \qquad \text{Eq. (6.8.2.1-1)}$$

where:

ϕ_y = resistance factor for yielding of tension members = 0.95 (Article 6.5.4.2)
A_g = gross cross-sectional area of the connected element (in.^{2})

Outside splice plate:

$$R_r = 0.95(50)(16.0)(0.625) = 475 \text{ kips} > 670/2 = 335 \text{ kips} \quad \text{ok}$$

Inside splice plates:

$$R_r = 0.95(50)(2)(7.25)(0.75) = 517 \text{ kips} > 670/2 = 335 \text{ kips} \quad \text{ok}$$

Check the net section fracture resistance of the splice plates in tension. As specified in Article 6.8.3, for design calculations, the width of standard-size bolt holes is taken as the nominal diameter of the holes, or $^{15}/_{16}$ in. for a ⅞-in.-diameter bolt. According to Article 6.13.5.2, for splice plates subject to tension, the design net area, A_n, must not exceed $0.85A_g$.

Outside plate:

$$0.85(16.0)(0.625) = 8.50 \text{ in.}^2 > A_n = \left[16.0 - 4(0.9375)\right](0.625) = 7.66 \text{ in.}^2$$

Inside plates:

$$0.85(2)(7.25)(0.75) = 9.24 \text{ in.}^2 > A_n = \left[2(7.25) - 4(0.9375)\right](0.75) = 8.06 \text{ in.}^2$$

Therefore, use the lesser net area to check the net section fracture resistance of the splice plates. If A_n had been greater than or equal to $0.85A_g$, then $0.85A_g$ should be substituted for A_n to check the net section fracture resistance.

$$R_r = \phi_u F_u A_n R_p U \qquad \text{Eq. (6.8.2.1-2)}$$

where:

ϕ_u = resistance factor for fracture of tension members = 0.80 (Article 6.5.4.2)
F_u = tensile strength of the connected element specified in Table 6.4.1-1 (ksi)
A_n = net cross-sectional area of the connected element determined as specified in Article 6.8.3 (in.^{2})
R_p = reduction factor for holes taken equal to 0.90 for bolt holes punched full size, and 1.0 for bolt holes drilled full size or subpunched and reamed to size (use 1.0 for splice plates since the holes in field splices are not allowed to be punched full size)
U = reduction factor to account for shear lag (use 1.0 for splice plates since all elements are connected)

Outside plate:

$$R_r = 0.80(65)[16.0 - 4(0.9375)](0.625)(1.0)(1.0) = 398 \text{ kips} > 670/2 = 335 \text{ kips} \quad \text{ok}$$

Inside plates:

$$R_r = 0.80(65)[2(7.25) - 4(0.9375)](0.75)(1.0)(1.0) = 419 \text{ kips} > 670/2 = 335 \text{ kips} \quad \text{ok}$$

To check the block shear rupture resistance of the splice plates and the flange (and later on the factored bearing resistance of the bolt holes in Section 7.14.3.5), the bolt spacings and bolt edge and end distances must first be established and checked. Refer to the bolt pattern shown in Figure 19.

As specified in Article 6.13.2.6.1, the minimum spacing between centers of bolts in standard holes is not to be less than 3.0d, where d is the diameter of the bolt. For ⅞-in.-diameter bolts:

$$s_{min} = 3d = 3(0.875) = 2.63 \text{ in.} \quad \text{use } 3.0 \text{ in.}$$

Since the length between the extreme bolts (on one side of the splice) in this lap-splice tension connection measured parallel to the line of action of the force is less than 38.0 in., no reduction in the factored shear resistance of the bolts is required, as originally assumed.

As specified in Article 6.13.2.6.2, to seal against the penetration of moisture in joints, the spacing, *s*, of a single line of bolts adjacent to a free edge of an outside plate or shape (when the bolts are not staggered) must satisfy the following requirement:

$$s \le \left(4.0 + 4.0t\right) \le 7.0 \text{ in.}$$

where *t* is the thickness of the thinner outside plate or shape. First, check for sealing along the edges of the outer splice plate (the thinner plate) parallel to the direction of the applied force. The bolt lines closest to the edges of the flanges are assumed to be 3.0 in. from the edges of the flanges. A ½-in. gap is assumed between the girder flanges at the splice to allow the splice to provide drainage and allow for fit-up:

$$s_{max} = 4.0 + 4.0(0.625) = 6.5 \text{ in.} < 7.0 \text{ in.}$$
$$s_{max} = 6.5 \text{ in.} = 6.5 \text{ in.} \quad \text{OK}$$

Check for sealing along the free edge at the end of the splice plate:

$$s_{max} = 4.0 + 4.0(0.625) = 6.5 \text{ in.} < 7.0 \text{ in.}$$
$$s_{max} = 6.5 \text{ in.} > 6.0 \text{ in.} \quad \text{OK}$$

Note that the maximum pitch requirements for stitch bolts specified in Article 6.13.2.6.3 apply only to the connection of plates in mechanically fastened built-up members and are not to be applied here in the design of the splice.

The edge distance of bolts is defined as the distance perpendicular to the line of force between the center of a hole and the edge of the component. In this example, the edge distance of 2.0 in. satisfies the minimum edge distance requirement of 1⅛ in. specified for ⅞-in.-diameter bolts in Table 6.13.2.6.6-1. This distance also satisfies the maximum edge distance requirement of 8.0*t* (not to exceed 5.0 in.) = 8.0(0.625) = 5.0 in. specified in Article 6.13.2.6.6.

The end distance of bolts is defined as the distance along the line of force between the center of a hole and the end of the component. In this example, the end distance of 1.5 in. satisfies the minimum end distance requirement of 1⅛ in. specified for ⅞-in.-diameter bolts. The maximum end distance requirement of 5.0 in. is also satisfied. Although not specifically required, note that the distance from the corner bolts to the corner of the splice plate, equal to $\sqrt{(2.0)^2 + (1.5)^2} = 2.5$ in., also satisfies the maximum end distance requirement. If desired, the corners of the plate can be clipped to meet this requirement. Although not done in this example, fabricators generally prefer that the end distance on the girder flanges at the point of splice be increased a minimum of ¼ in. from the design value to allow for girder trim.

Check the block shear rupture resistance of the splice plates in tension.

$$R_r = \phi_{bs} R_p \left(0.58 F_u A_{vn} + U_{bs} F_u A_{tn}\right) \leq \phi_{bs} R_p \left(0.58 F_y A_{vg} + U_{bs} F_u A_{tn}\right) \qquad \text{Eq. (6.13.4-1)}$$

where:

ϕ_{bs} = resistance factor for block shear rupture = 0.80 (Article 6.5.4.2)
A_{vg} = gross area along the plane resisting shear stress (in.^{2})
A_{vn} = net area along the plane resisting shear stress (in.^{2})
A_{tn} = net area along the plane resisting tension stress (in.^{2})
U_{bs} = reduction factor for block shear rupture resistance taken equal to 0.50 when the tension stress is non-uniform and 1.0 when the tension stress is uniform (use 1.0 for splice plates)

Assume the potential block shear failure planes on the outside and inside splice plates shown in Figure 22.

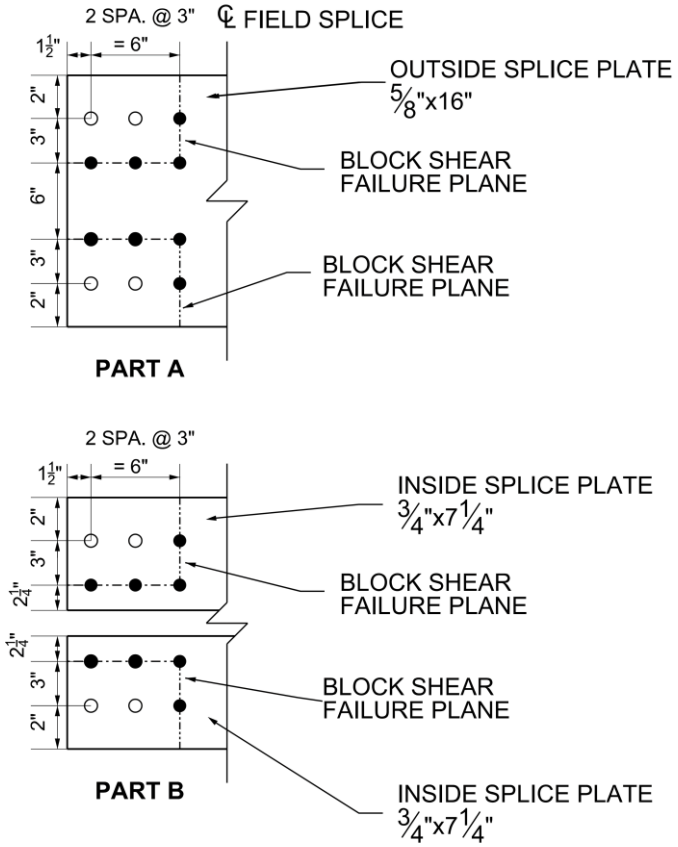

Figure 22 Assumed Block Shear Failure Planes for Top Flange Splice Plates

A) Outside Splice Plate; B) Inside Splice Plates

Check the outside splice plate. A_{tn} is the net area along the place resisting the tensile stress.

$$A_{tn} = 2\left[3.0 + 2.0 - 1.5(0.9375)\right](0.625) = 4.49 \text{ in.}^2$$

A_{vn} is the net area along the place resisting the shear stress.

$$A_{vn} = 2\left[2(3.0) + 1.5 - 2.5(0.9375)\right](0.625) = 6.45 \text{ in.}^2$$

A_{vg} is the gross area along the plane resisting the shear stress.

$$A_{vg} = 2\left[2(3.0) + 1.5\right](0.625) = 9.38 \text{ in.}^2$$

Therefore:

$$\begin{aligned} R_r &= 0.80(1.0)\left[0.58(65)(6.45) + 1.0(65)(4.49)\right] = 428 \text{ kips} \\ &< 0.80(1.0)\left[0.58(50)\left(9.38\right) + 1.0(65)(4.49)\right] = 451 \text{ kips} \\ &\therefore R_r = 428 \text{ kips} > \frac{670}{2} = 335 \text{ kips} \quad \text{OK} \end{aligned}$$

Since the inside splice plates are thicker than the outside splice plate in this case, the block shear rupture resistance of the inside splice plates is satisfactory by inspection.

Check the block shear rupture resistance in tension of the critical girder top flange at the splice. Only the calculations for the flange on the left-hand side of the splice, which is the critical flange for this check, are shown below. Two potential failure modes are investigated for the flange as shown in Figure 23.

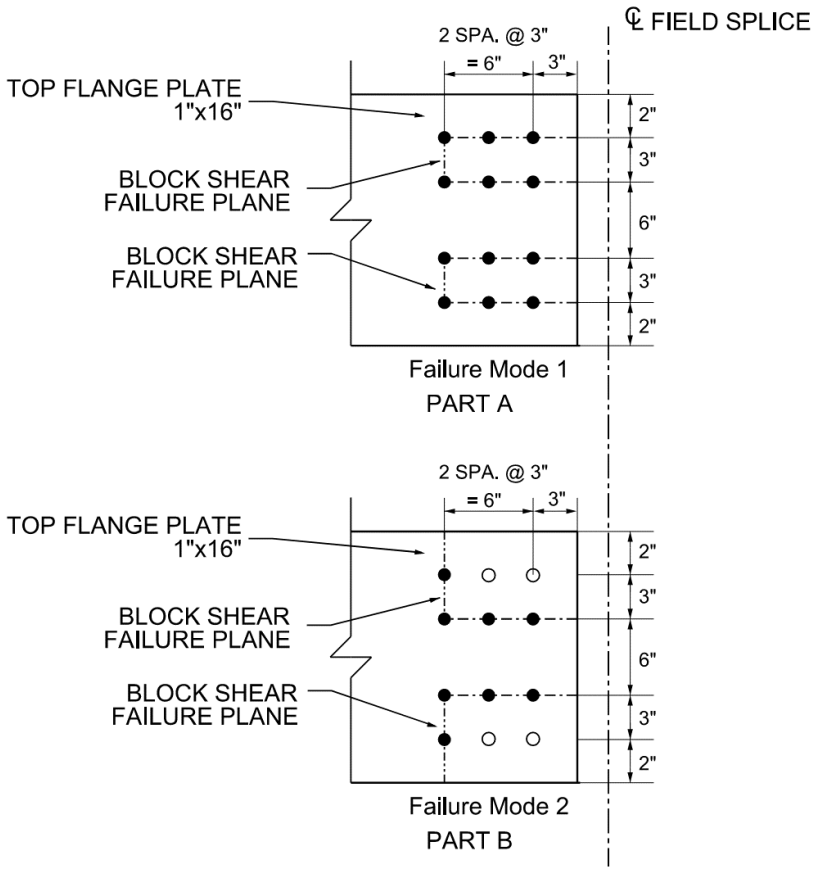

Figure 23 Assumed Block Shear Failure Planes for Critical Top Flange at the Splice

A) Assumed Failure Mode 1; B) Assumed Failure Mode 2

For Failure Mode 1:

$$A_{tn} = 2\left[3.0 - 0.9375\right](1.0) = 4.13\ \text{in.}^2$$

$$A_{vn} = 4\left[2(3.0) + 3.0 - 2.5(0.9375)\right](1.0) = 26.63\ \text{in.}^2$$

$$A_{vg} = 4\left[2(3.0) + 3.0\right](1.0) = 36.00\ \text{in.}^2$$

$$R_r = 0.80(1.0)\left[0.58(65)(26.63) + 1.0(65)(4.13)\right] = 1,018\ \text{kips}$$
$$< 0.80(1.0)\left[0.58(50)\left(36.00\right) + 1.0(65)(4.13)\right] = 1,050\ \text{kips}$$
$$\therefore R_r = 1,018\ \text{kips} > 670\ \text{kips} \quad \text{OK}$$

For Failure Mode 2:

$$A_{tn} = 2\left[3.0 + 2.0 - 1.5(0.9375)\right](1.0) = 7.19\ \text{in.}^2$$

$$A_{vn} = 2\left[2(3.0) + 3.0 - 2.5(0.9375)\right](1.0) = 13.31\,\text{in.}^2$$

$$A_{vg} = 2\left[2(3.0) + 3.0\right](1.0) = 18.00\,\text{in.}^2$$

$$\begin{aligned} R_r &= 0.80(1.0)\left[0.58(65)(13.31) + 1.0(65)(7.19)\right] = 775\,\text{kips} \\ &< 0.80(1.0)\left[0.58(50)(18.00) + 1.0(65)(7.19)\right] = 791\,\text{kips} \\ &\therefore R_r = 775\,\text{kips} > 670\,\text{kips} \quad \text{OK} \end{aligned}$$

The factored yield resistance of the splice plates in compression is the same as the factored yield resistance of the splice plates in tension given by Eq. (6.8.2.1-1), and therefore, need not be checked. Buckling of the splice plates in compression is not a concern since the unsupported length of the plates is limited by the maximum bolt spacing and end distance requirements.

Next, the design of the bottom flange splice plates will be illustrated. The thickness of the splice plates should be at least one-half the thickness of the thinner flange at the splice plus 1/16 of an inch [27]. As a result, the flange will control the bearing and block shear rupture resistance, which is checked later on in this design example.

$$t_o \geq \frac{0.6875}{2} + 0.0625 = 0.4063\,\text{in.} \quad \text{Use } t_o = \frac{3}{4}\,\text{in.}$$

The splice-plate thickness satisfies the minimum thickness requirement for steel specified in Article 6.7.3.

The width of the inside splice plate should be such that the plate clears the flange-to-web weld on each side of the web by a minimum of ⅛ in [27]. Assuming 5/16-inch flange-to-web welds are used, the minimum clearance distance, C, on each side is computed as:

$$C \geq \left[\text{weld size} + \frac{1}{8}^{"}\right] = \left[0.3125 + \frac{1}{8}^{"}\right] = 0.4375\,\text{in.}$$

The maximum width of the inside splice plate is therefore computed as:

$$80.0 - 0.5625 - 2(0.4375) = 78.56\,\text{in.}$$

Therefore, for the bottom-flange splice, try ¾ in. x 76 in. outside and inside splice plates. A filler plate is not required. All plates are again ASTM A709 Grade 50 steel.

Check the factored yield resistance of the splice plates in tension. Use the resultant force, R, which includes the St. Venant torsional shear in the bottom flange:

$$R_r = 0.95(50)(76.0)(0.75) = 2,708 \text{ kips} > 2,421/2 = 1,211 \text{ kips} \quad \text{ok}$$

Check the net section fracture resistance of the splice plates in tension. According to Article 6.13.5.2, for splice plates subject to tension, the design net area, A_n, must not exceed $0.85A_g$.

$$0.85(76.0)(0.75) = 48.45 \text{ in.}^2 > A_n = \left[76.0 - 20(0.9375)\right](0.75) = 42.94 \text{ in.}^2$$

Therefore, use the lesser net area to check the net section fracture resistance of the splice plates. If A_n had been greater than or equal to $0.85A_g$, then $0.85A_g$ should be substituted for A_n to check the net section fracture resistance.

$$R_r = 0.80(65)[76.0 - 20(0.9375)](0.75)(1.0)(1.0) = 2,233 \text{ kips} > 2,421/2 = 1,211 \text{ kips} \qquad \text{OK}$$

To check the block shear rupture resistance of the splice plates and the flange (and later on the factored bearing resistance of the bolt holes in Section 7.14.3.5), the bolt spacings and bolt edge and end distances must first be established and checked. Refer to the bolt pattern shown in Figure 20.

Since the length between the extreme bolts (on one side of the splice) in this lap-splice tension connection measured parallel to the line of action of the force is less than 38.0 in., no reduction in the factored shear resistance of the bolts is required, as originally assumed.

Check for sealing along the edges of the outer splice plate parallel to the direction of the applied force. The bolt lines closest to the edges of the flanges are assumed to be 2.0 in. from the edges of the flanges. A ½-in. gap is assumed between the girder flanges at the splice to allow the splice to provide drainage and allow for fit-up:

$$s_{max} = 4.0 + 4.0(0.75) = 7.0 \text{ in.}$$
$$s_{max} = 7.0 \text{ in.} > 4.5 \text{ in.} \quad \text{OK}$$

Check for sealing along the free edge at the end of the splice plate:

$$s_{max} = 4.0 + 4.0(0.75) = 7.0 \text{ in.}$$
$$s_{max} = 7.0 \text{ in.} > 5.0 \text{ in.} \quad \text{OK}$$

The edge distance of bolts is defined as the distance perpendicular to the line of force between the center of a hole and the edge of the component. In this example, the edge distance of 1.75 in. satisfies the minimum edge distance requirement of 1⅛ in. specified for ⅞-in.-diameter bolts in Table 6.13.2.6.6-1. This distance also satisfies the maximum edge distance requirement of 8.0*t* (not to exceed 5.0 in.) = 8.0(0.75) = 6.0 in. > 5.0 in. (i.e., use 5.0 in.) specified in Article 6.13.2.6.6.

The end distance of bolts is defined as the distance along the line of force between the center of a hole and the end of the component. In this example, the end distance of 1.5 in. satisfies the minimum end distance requirement of 1⅛ in. specified for ⅞-in.-diameter bolts. The maximum

end distance requirement of 4.0 in. is also satisfied. Although not specifically required, note that the distance from the corner bolts to the corner of the splice plate, equal to $\sqrt{(1.75)^2 + (1.5)^2} = 2.3\,\text{in.}$, also satisfies the maximum end distance requirement. If desired, the corners of the plate can be clipped to meet this requirement. Although not done in this example, fabricators generally prefer that the end distance on the girder flanges at the point of splice be increased a minimum of ¼ in. from the design value to allow for girder trim.

Check the block shear rupture resistance of the splice plates in tension.

Assume the potential block shear failure planes on the splice plates shown in Figure 24. The failure planes are shown on one splice plate only; the same failure planes apply to both the outside and inside plates.

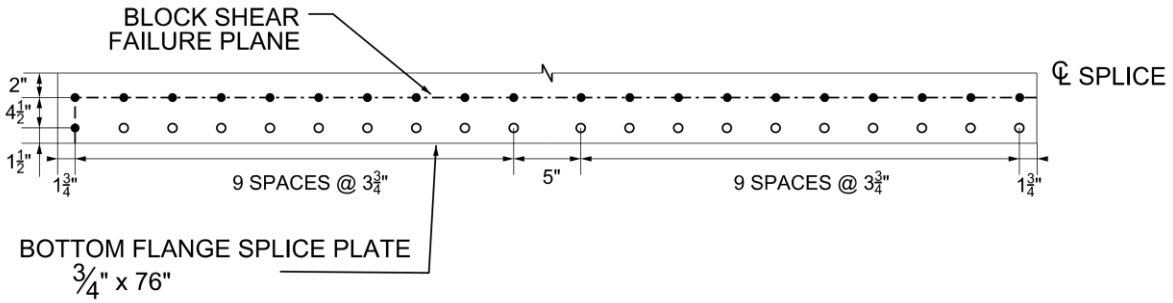

Figure 24 Assumed Block Shear Failure Planes for Bottom Flange Splice Plates

A_{tn} is the net area along the place resisting the tensile stress.

$$A_{tn} = \left[1.75 + 18(3.75) + 5.0 - 19.5(0.9375)\right](0.75) = 41.98\,\text{in.}^2$$

A_{vn} is the net area along the place resisting the shear stress.

$$A_{vn} = \left[1.5 + 4.5 - 1.5(0.9375)\right](0.75) = 3.45\,\text{in.}^2$$

A_{vg} is the gross area along the plane resisting the shear stress.

$$A_{vg} = \left[1.5 + 4.5\right](0.75) = 4.50\,\text{in.}^2$$

Therefore:

$$R_r = 0.80(1.0)\left[0.58(65)(3.45) + 1.0(65)(41.98)\right] = 2,287\ \text{kips}$$
$$\cong 0.80(1.0)\left[0.58(50)\left(4.50\right) + 1.0(65)(41.98)\right] = 2,287\ \text{kips}$$
$$\therefore R_r = 2,287\ \text{kips} > \frac{2,421}{2} = 1,211\,\text{kips} \quad \text{OK}$$

The block shear rupture resistance of the critical bottom flange at the splice is satisfactory by inspection since the end distance for the flange of 2.0 in. is larger than for the splice plates and a similar block shear failure plane would be assumed.

The factored yield resistance of the splice plates in compression is the same as the factored yield resistance of the splice plates in tension given by Eq. (6.8.2.1-1), and therefore, need not be checked. Buckling of the splice plates in compression is not a concern since the unsupported length of the plates is limited by the maximum bolt spacing and end distance requirements.

Check that the threads are excluded from the shear planes as originally assumed. According to the 2020 RCSC Specification [29], shear planes located in the transition length of high-strength bolts should be considered shear planes with the threads included. Unless the use and position of washers and DTIs are clearly identified in the contract documents, a conservative assumption to determine whether threads are excluded from or included in the shear plane is to position one washer and one DTI under the bolt head located adjacent to the thicker outer ply. Refer to ASTM F436/F436M for washer thicknesses; the nominal thickness of the typical standard washer is 5/32 inches (the dimension "T" in the calculations below). Refer to ASME B18.2.6 [30] or manufacturer data for the appropriate DTI dimensions (for a 7/8" diameter bolt, use a DTI thickness of 0.260 inches – the dimension "F" in the calculations below). Sum the grip length of the connection, i.e., the total nominal thicknesses of the connection plies, the thicknesses of the assumed washer and DTI, plus an additional value specified in Table C-2.2 of the 2020 RCSC Specification [29] to allow for manufacturing tolerances and sufficient thread engagement with a heavy hex nut. Round up the sum to the next ¼-inch increment up to a bolt length of 6 inches and to the next ½-inch increment for longer bolts to determine the minimum nominal bolt length (the dimension "L_{NOM}" in the calculations below). Next, determine the minimum bolt body length, i.e., the distance from the head of the bolt to the beginning of the transition length (the dimension "$L_{B\,MIN}$" in the calculations below) and compare that length to the location of the furthest shear plane measured from the bolt head (the dimension "L_{SP}" in the calculations below) to determine whether the threads are excluded or included. The minimum bolt body length can either be determined directly from Table 2.1.9.2-1 of ASME B18.2.6 [30] using the calculated minimum nominal bolt length and the nominal bolt diameter or calculated indirectly by subtracting the appropriate thread length, L_T, and transition thread length, Y, found in Table C-2.1 of the 2020 RCSC Specification [29] from the calculated minimum nominal bolt length.

Short high-strength bolts with lengths indicated in Table 2.5 of the 2020 RCSC Specification [29] are fully threaded in accordance with ASME B18.2.6 [30] and thus should be designed for threads included in the shear plane. The thicknesses of the assumed washer and DTI should conservatively be subtracted from the calculated minimum nominal bolt length before making this determination.

<u>Bottom Flange Splice:</u>

7/8" diameter bolt

$$L_{PLY} = 0.75" + 0.6875" + 0.75" = 2.1875"$$

$$L_{MIN} = L_{PLY} + F + T + 1.125" \text{ (RCSC Table C-2.2)}$$

$$= 2.1875" + 0.260" + 5/32" + 1.125" = 3.73"$$

$L_{NOM} = 3.75"$ (round up to nearest $1/4"$ per RCSC 2.7 Commentary)

$L_{NOM} - F - T$

$= 3.75" - 0.260" - 5/32" = 3.33" > L = 2"$ (RCSC Table 2.5)

Therefore, bolt is not fully threaded.

$L_{B\,MIN} = L_{NOM} - L_T - Y$ (RCSC Table C-2.1)

$= 3.75" - 1.5" - 9/32" = 1.97"$

(Note: agrees with value of $L_{B\,MIN}$ from Table 2.1.9.2-1 of ASME B18.2.6)

$L_{SP} = 0.260" + 5/32" + 0.75" + 0.6875" = 1.85" < L_{B\,MIN} = 1.97"$

Therefore, threads are *excluded* from the shear planes.

Top Flange Splice:

7/8" diameter bolt

$L_{PLY} = 0.625" + 1.0" + 0.75" = 2.375"$

$L_{MIN} = L_{PLY} + F + T + 1.125"$ (RCSC Table C-2.2)

$= 2.375" + 0.260" + 5/32" + 1.125" = 3.92"$

$L_{NOM} = 4.00"$ (round up to nearest $1/4"$ per RCSC 2.7 Commentary)

$L_{NOM} - F - T$

$= 4.00" - 0.260" - 5/32" = 3.58" > L = 2"$ (RCSC Table 2.5)

Therefore, bolt is not fully threaded.

$L_{B\,MIN} = L_{NOM} - L_T - Y$ (RCSC Table C-2.1)

$= 4.00" - 1.5" - 9/32" = 2.22"$

(Note: agrees with value of $L_{B\,MIN}$ from Table 2.1.9.2-1 of ASME B18.2.6)

$L_{SP} = 0.260" + 5/32" + 0.75" + 1.00" = 2.17" < L_{B\,MIN} = 2.22"$

Therefore, threads are *excluded* from the shear planes.

If the threads had been included in the shear planes in either case, check with the Owner to see if the use of DTIs is permitted. If not, the DTI may be removed from the above calculations.

7.14.3.5 Bearing Resistance Check

The bearing resistance of the connection at the strength limit state is taken as the sum of the smaller of the shear resistance of the individual bolts and the bearing resistance of the individual bolt holes parallel to the line of the design force.

The bearing resistance of connected material in the top-flange splice will be checked herein. The sum of the inner and outer splice plate thicknesses exceeds the thickness of the thinner flange at the point of splice, and the splice plate areas satisfy the 10 percent rule described previously. Therefore, the smaller flange on the left-hand side of the splice controls the bearing resistance of the connection.

For standard-size holes, the nominal bearing resistance, R_n, parallel to the applied bearing force is given by Eq. (6.13.2.9-1) or (6.13.2.9-2), as applicable.

For the four bolt holes adjacent to the end of the flange, the end distance is 3.0 in. Therefore, the clear distance, L_c, between the edge of the hole and the end of the flange is:

$$L_c = 3.0 - \frac{0.9375}{2} = 2.53 \text{ in.} > 2.0d = 2.0(0.875) = 1.75 \text{ in.}$$

Therefore, use Eq. (6.13.2.9-1):

$$R_n = 4(2.4dtF_u) = 4\left[2.4(0.875)(1.0)(65)\right] = 546 \text{ kips}$$

Since:

$$R_r = \phi_{bb} R_n$$

$$R_r = 0.80(546) = 437 \text{ kips}$$

The total factored shear resistance of the bolts in the four holes adjacent to the end of the flange, acting in double shear is 4(64.6) = 258 kips < 437 kips. Therefore, the factored shear resistance of the bolts controls and bearing does not control for the four end holes.

For the other eight bolt holes, the center-to-center distance between the bolt holes in the direction of the applied force is 3.0 in. Therefore, the clear distance, L_c, between the edges of the adjacent holes is:

$$L_c = 3.0 - 0.9375 = 2.0625 \text{ in.} > 2.0d = 1.75 \text{ in.}$$

Therefore, use Eq. (6.13.2.9-1):

$$R_n = 8(2.4dtF_u) = 8\left[2.4(0.875)(1.0)(65)\right] = 1{,}092 \text{ kips}$$

Since:

$$R_r = \phi_{bb} R_n$$

$R_r = 0.80(1{,}092) = 874$ kips

The total factored shear resistance of the bolts in the eight interior bolt holes is 8(64.6) = 517 kips < 874 kips. Therefore, the factored shear resistance of the bolts controls and bearing does not control for the eight interior bolt holes.

The total factored shear resistance of the bolts in the twelve holes is:

$R_r = 258 + 517 = 775$ kips $> P_{fy} = 670$ kips OK

Calculations similar to the above show that the bearing resistance of the connected material in the bottom flange splice does not control, and that the total factored shear resistance of the bolts in the forty bolt holes in the bottom flange splice is sufficient.

7.14.3.6 Slip Resistance Check

The moment resistance provided by the nominal slip resistance of the flange splice bolts that are required to satisfy the strength limit state is to be checked against the factored moment for checking slip. The nominal slip resistance of the flange splice bolts was determined previously in Section 7.14.1. The nominal slip resistance of a bolt need not be adjusted for the effect of a filler (if present); the resistance to slip between either connected part and the filler is comparable to that which would exist between the connected parts if the filler were not present.

Should the factored moment exceed the moment resistance provided by the nominal slip resistance of the flange splice bolts, the additional moment is to be resisted by the web as specified in Article 6.13.6.1.3c. The factored moments for checking slip are to be taken as the moment at the point of splice under Load Combination Service II, as specified in Table 3.4.1-1, and also the factored moment at the point of splice due to the deck placement sequence as specified in Article 3.4.2.1.

St. Venant torsional shears and longitudinal warping stresses due to cross-section distortion are typically neglected in top flanges of tub sections once the flanges are continuously braced. Longitudinal warping stresses due to cross-section distortion are typically relatively small in the bottom flange at the service limit state and for constructability and may be neglected when checking bottom flange splices for slip. As discussed in Section 7.14.3.2, the effects of flange lateral bending also need not be considered in checking the bolted connections of the flange splices for slip.

The moment resistance provided by the nominal slip resistance of the flange splice bolts is calculated as shown in Figures C6.13.6.1.3b-1 and C6.13.6.1.3b-2, with the appropriate nominal

slip resistance of the flange splice bolts substituted for P_{fy}. For checking slip due to the factored deck casting moment, the moment resistance of the noncomposite section is used.

Service II Positive Moment (refer to Figure C6.13.6.1.3b-1)

Referring to Table 16, the factored Service II positive moment at the point of splice is computed as:

Service II Positive Moment = 1.0(462 + 1,941) + 1.0(326) + 1.0(428) + 1.3(+5,221) = +9,944 kip-ft

Use the nominal slip resistance of the bottom flange splice bolts. For box sections in horizontally curved bridges, for checking slip, the St. Venant torsional shear in the bottom flange is conservatively subtracted from the slip resistance provided by the bottom flange bolts (Article 6.13.6.1.3b)

Calculate the factored St. Venant torsional shear flow, f, in the bottom flange at the point of splice for the Service II load combination. The negative live load plus impact torque controls by inspection (refer to Table 16).

For the DC_1 torque, which is applied to the non-composite section, the enclosed area, A_o, for the non-composite box section was computed previously to be 54.8 ft^2 (Section 7.14.3.2).

From Eq. (C6.11.1.1-1), the St. Venant torsional shear flow is calculated as:

$$f = \frac{T}{2A_o}$$

$$f = \frac{1.0(-36 + -125)}{2(54.8)} = -1.47 \text{ kips/ft}$$

For the torques applied to the composite section (i.e. the DC_2, DW and LL+IM torques), A_o for the composite section was computed previously to be 60.5 ft^2 (Section 7.14.3.2). Therefore:

$$f = \frac{|1.0(-58) + 1.0(-76) + 1.3(-517)|}{2(60.5)} = -6.66 \text{ kips/ft}$$

$$f_{total} = -1.47 + -6.66 = -8.13 \text{ kips/ft}$$

The bottom-flange width between the mid-thickness of the tub-girder webs is 80.0 in. The factored St. Venant torsional shear for the Service II load combination, V_{SV}, at the point of splice is computed as:

$$V_{SV} = f_{total} b_f = |-8.13| \frac{80.0}{12} = 54.2 \text{ kips}$$

Nominal slip resistance of the bottom flange splice with 40 bolts:

P_t = 40(39.0 kips/bolt) = 1,560 kips – 54.2 kips = 1,506 kips

Flange Moment Arm: $A = D + t_{ft}/2 + t_{haunch} + t_s/2 = 78 + 0.6875/2 + 4.0 + 9.5/2 = 87.09$ in.

M_{flange} = 1,506 kips x (87.09/12) = 10,930 kip-ft > 9,944 kip-ft OK

Service II Negative Moment (refer to Figure C6.13.6.1.3b-2)

Referring to Table 16, the factored Service II negative moment at the point of splice is computed as:

Service II Negative Moment = 1.0(462 + 1,941) + 1.0(326) + 1.0(428) + 1.3(-3,080) = -847 kip-ft

Use the nominal slip resistance of the top or bottom flange splice bolts, whichever is smaller.

Nominal slip resistance of the top flange splices with 12 bolts each: P_t = 2 x 12(39.0 kips/bolt) = 936 kips < 1,506 kips

Flange moment arm: $A = D + (t_{ft} + t_{fc})/2 = 78 + (1.0 + 0.6875)/2 = 78.84$ in.

M_{flange} = 936 x (78.84/12) = 6,150 kip-ft > |-847| kip-ft

Deck Placement (refer to Figure C6.13.6.1.3b-2)

Referring to Table 16, the factored moment due to the self-weight of the steel plus the moment due to the deck placement at the point of splice is computed as:

$M_{deck\ placement}$ = 1.25(462 + 2,749) = 4,014 kip-ft

The deck-placement moment is applied to the noncomposite section. Use the nominal slip resistance of the top or bottom flange splice bolts, whichever is smaller.

Nominal slip resistance of the top flange splices with 12 bolts each: P_t = 2 x 12(39.0 kips/bolt) = 936 kips < 1,506 kips

Flange moment arm: $A = D + (t_{ft} + t_{fc})/2 = 78 + (0.6875 + 1.0)/2 = 78.84$ in.

M_{flange} = 936 x (78.84/12) = 6,150 kip-ft > 4,014 kip-ft OK

Although not included in this example in the interest of brevity, the special load combination specified in Article 3.4.2.1 must also be considered in this check for the deck placement sequence. Separate calculations show that the slip resistance of the flange splice bolts is also satisfactory for this load combination.

Therefore, the flanges have adequate slip resistance to resist the Service II and deck casting moment requirements at the splice. No moment contribution from the web is required.

In cases where the moment resistance provided by the flange splice bolts is sufficient at the strength limit state (which is the case in this design example), but a moment contribution from the web is required to resist slip, the number of flange splice bolts may be increased to increase the moment resistance provided by the nominal slip resistance of the flange splice bolts to prevent having to add an additional row of web splice bolts to resist the resultant web slip force.

Since the combined area of the inside and outside flange splice plates is greater than the area of the smaller top flange at the point of splice, fatigue of the base metal of the top flange splice plates adjacent to the slip-critical bolted connections (if subject to a net tensile stress as specified in Article 6.6.1.2.1) does not need to be checked. Similarly, the flexural stresses in the splice plates at the service limit state under the Service II load combination need not be checked.

7.14.3.7 Article 6.10.1.8 – Tension Flanges with Holes

When checking flexural members at the strength limit state or for constructability, the following additional requirement shall be satisfied at all cross-sections containing holes in the tension flange:

$$f_t \le 0.84\left(\frac{A_n}{A_g}\right)F_u \le F_{yt} \qquad \text{Eq. (6.10.1.8-1)}$$

where:

A_n = net area of the tension flange determined as specified in Article 6.8.3 (in.^{2})
A_g = gross area of the tension flange (in.^{2})
f_t = stress on the gross area of the tension flange due to the factored loads calculated without consideration of flange lateral bending (ksi)
F_u = specified minimum tensile strength of the tension flange determined as specified in Table 6.4.1-1 (ksi)

Separate calculations show that the tensile stress in the bottom flange at the strength limit state controls. Calculate the factored Strength I tensile stress in the bottom flange at the point of splice:

$$f_t \text{ (bot. flange)} = 1.0\left[\frac{1.25(462+1{,}941)}{5{,}355}+\frac{1.25(326)+1.5(428)}{6{,}801}+\frac{1.75(5{,}221)}{7{,}395}\right](12) = 23.41 \text{ ksi (T)}$$

$$A_n = [83.0 - 20(0.9375)](0.6875) = 44.17 \text{ in.}^2$$

$$A_g = (83.0)(0.6875) = 57.06 \text{ in.}^2$$

$$0.84\left(\frac{A_n}{A_g}\right)F_u = 0.84\left(\frac{44.17}{57.06}\right)(65) = 42.27 \text{ ksi} < F_{yt} = 50 \text{ ksi}$$

$f_t = 23.41 \text{ ksi} < 42.27 \text{ ksi}$ OK

7.14.4 Web Splice Design

7.14.4.1 General

As a minimum, web splice plates and their connections are to be designed at the strength limit state for a design web force taken equal to the smaller factored shear resistance of the web, $V_r = \phi_v V_n$, on either side of the splice determined according to the provisions of Article 6.10.9 or 6.11.9, as applicable. Since the web splice is being designed to develop the full factored shear resistance of the web at the strength limit state, the effect of the additional St. Venant torsional shear in the web may be ignored at the strength limit state.

Should the moment resistance provided by the flanges at the point of splice, determined as specified in Article 6.13.6.1.3b, not be sufficient to resist the factored moment at the strength limit state (which is not the case in this design example), the web splice connections are to instead be designed for a design web force taken equal to the vector sum of the smaller factored shear resistance and a horizontal force in the web that provides the necessary moment resistance in conjunction with the flanges.

The horizontal force in the web is to be computed as the portion of the factored moment at the strength limit state at the point of splice that exceeds the moment resistance provided by the flanges divided by the appropriate moment arm. For composite sections subject to positive flexure, the moment arm is taken as the vertical distance from the mid-depth of the web to the mid-thickness of the concrete deck including the concrete haunch (Figure C6.13.6.1.3c-1). For composite sections subject to negative flexure and noncomposite sections subject to positive or negative flexure, the moment arm is taken as one-quarter of the web depth (Figure C6.13.6.1.3c-2).

7.14.4.2 Web Splice Bolts

The computed design web force is to be divided by the factored shear resistance of the bolts, determined in Section 7.14.2.1, to determine the total number of web splice bolts required on one side of the splice at the strength limit state. The factored shear resistance of the bolts should be based on threads included in the shear planes, unless the web splice-plate thickness exceeds 0.5 in. As a minimum, two vertical rows of bolts spaced at the maximum spacing for sealing bolts specified in Article 6.13.2.6.2 should be provided, with a closer spacing and/or additional rows provided only as needed. For bolted web splices with thickness differences of 1/16 in. or less, filler plates should not be provided.

Since the moment resistance provided by the flange splices is sufficient to resist the factored moment at the strength limit state at the point of splice in this case, the web splice bolts are

designed at the strength limit state for a design web force taken equal to the smaller factored shear resistance of the web on either side of the splice.

Compute the nominal shear resistance of the 0.5625-inch-thick web at the splice according to the provisions of Articles 6.10.9.2 and 6.10.9.3 for unstiffened and stiffened webs, respectively. For this design example, separate calculations indicate that transverse stiffeners are required at the splice, therefore Article 6.10.9.3 is employed. A stiffener spacing equal to the internal cross-frame spacing used on Girder G2 is assumed, where d_o = 196 inches.

The nominal shear resistance of an interior web panel is computed in accordance with Article 6.10.9.3.2. First, determine if Eq. 6.10.9.3.2-1 is satisfied. According to Article 6.11.9, for box flanges, b_{fc} (in this case) is to be taken as one-half the effective flange width between webs in checking Eq. 6.10.9.3.2-1, but not to exceed 18 times the thickness of the box flange. Therefore, (79.4375/2) = 39.72 in. > 18(0.6875) = 12.38 in. Use b_{fc} = 12.38 in. to check Eq. 6.10.9.3.2-1 as follows:

$$\frac{2Dt_w}{\left(b_{fc}t_{fc}+b_{ft}t_{ft}\right)} \le 2.5 \qquad \text{Eq. (6.10.9.3.2-1)}$$

$$\frac{2Dt_w}{\left(b_{fc}t_{fc}+b_{ft}t_{ft}\right)} = \frac{2\left(80.40\right)\left(0.5625\right)}{\left(\left(16\right)\left(1.0\right)+\left(12.38\right)\left(0.6875\right)\right)} = 3.69 > 2.5$$

Since Eq. 6.10.9.3.2-1 is not satisfied, the nominal shear resistance, V_n, is computed in accordance with Eq. (6.10.9.3.2-8).

$$V_n = V_p\left[C+\frac{0.87\left(1-C\right)}{\left(\sqrt{1+\left(\frac{d_o}{D}\right)^2}+\frac{d_o}{D}\right)}\right] \qquad \text{Eq. (6.10.9.3.2-8)}$$

where:

V_n = nominal shear resistance of the web panel (kip)
V_p = plastic shear force (kip)
C = ratio of shear-buckling resistance to the shear yield strength
d_o = transverse stiffener spacing (in.)

The plastic shear force, V_p, is computed according to Eq. 6.10.9.3.2-3 as follows:

$$V_p = 0.58F_{yw}Dt_w \qquad \text{Eq. (6.10.9.3.2-3)}$$

Determine which equation is to be used to compute the ratio of shear-buckling resistance to the shear yield strength, C.

$$k = 5 + \frac{5}{\left(\frac{d_o}{D}\right)^2} = 5 + \frac{5}{\left(\frac{196}{80.40}\right)^2} = 5.84$$ Eq. (6.10.9.3.2-7)

Since:

$$\frac{D}{t_w} = \frac{80.4}{0.5625} = 142.9 > 1.40\sqrt{\frac{Ek}{F_{yw}}} = 1.40\sqrt{\frac{29{,}000(5.84)}{50}} = 81$$

$$C = \frac{1.57}{\left(\frac{D}{t_w}\right)^2}\left(\frac{Ek}{F_{yw}}\right)$$ Eq. (6.10.9.3.2-6)

$$C = \frac{1.57}{(142.9)^2}\left(\frac{29{,}000(5.84)}{50}\right) = 0.260$$

V_p is the plastic shear force and is calculated as follows:

$$V_p = 0.58\, F_{yw} D\, t_w$$ Eq. (6.10.9.3.2-3)

$$V_p = 0.58\,(50.0)(80.40)(0.5625) = 1{,}312 \text{ kips}$$

Therefore,

$$V_n = (1{,}312)\left[0.260 + \frac{0.87(1-0.260)}{\sqrt{1+\left(\frac{196.0}{80.40}\right)^2} + \frac{196}{80.40}}\right] = 508 \text{ kips}$$

$$V_r = \phi_v V_n = 1.0(508) = 508 \text{ kips}$$

Number of Bolts Required (threads included in the shear plane): N = 508/51.9 = 9.8 bolts

Note that the greater than 38.0 in. length reduction for the shear resistance of the bolts only applies to lap-splice tension connections (Article 6.13.2.7) and is not to be applied in the design of the web splice.

The *AASHTO LRFD BDS* requires at least two rows of bolts in the web over the depth of the web (Article 6.13.6.1.3a). The maximum permitted spacing of the bolts for sealing is $s \leq (4.0 + 4.0t) \leq 7.0$ in., where t is the thickness of the splice plate (Article 6.13.2.6.2). Assuming the splice plate thickness will be one-half the smaller web thickness at the point of splice plus 1/16 in. gives a splice plate thickness of:

$$t = \frac{1}{2} \text{ x } \frac{9}{16} + \frac{1}{16} = 0.34 \text{ in. Use } t = \frac{7}{16} \text{ in.}$$

The splice-plate thickness satisfies the minimum thickness requirement for steel specified in Article 6.7.3. A filler plate is not required since the webs are the same thickness on both sides of the splice.

The maximum bolt spacing for the $^{7}/_{16}$ in. splice plate is:

$$s \leq 4.0 + (4.0 \text{ x } 0.4375) = 5.75 \text{ in.} < 7.0 \text{ in.}$$

The minimum bolt spacing is 3d = 3(0.875) = 2.625 in.

Using approximately a 2.825 in. gap from the top and bottom of the web to the top and bottom web splice bolts so as to not impinge on bolt assembly clearances [refer to Table 7-15 of the AISC *Manual of Steel Construction* – use H2 + max(C1, C2) = 2¾ in. minimum clearance for a 7/8-in. diameter bolt] [26], the available web depth for the bolt pattern is 80.40 – (2 x 2.825) = 74.75 in. The number of bolts required to meet the maximum bolt spacing is:

$$\text{Number of bolts} = 1 + \frac{74.75}{5.75} = 14 \text{ bolts in two vertical rows on each side of splice}$$

= 28 bolts > N = 9.8 bolts OK

Use 28 bolts in two vertical rows (14 bolts per row) on each side of the splice.

7.14.4.3 Web Splice Plates

The web splice plates are $^{7}/_{16}$ in. x 78¾ in. The plates are ASTM A709 Grade 50 steel.

The factored shear resistance of the web at the strength limit state, V_r, is not to exceed the factored shear yielding or factored shear rupture resistance of the web splice plates (Article 6.13.6.1.3c).

For shear yielding, the factored resistance of the web splice plates is determined as specified in Article 6.13.5.3 as follows:

$$R_r = \phi_v 0.58 F_y A_{vg} \qquad \text{Eq. (6.13.5.3-1)}$$

where:

A_{vg} = gross area of the connection element subject to shear (in.^{2})
F_y = specified minimum yield strength of the connection element (ksi)
ϕ_v = resistance factor for shear = 1.0 (Article 6.5.4.2)

$$R_r = 1.0(0.58)(50)2(0.4375)(78.75) = 1{,}998 \text{ kips}$$

$$R_r = 1{,}998 \text{ kips} > V_r = 508 \text{ kips} \quad \text{OK}$$

For shear rupture, the factored resistance of the web splice plates is determined as specified in Article 6.13.5.3 as follows:

$$R_r = \phi_{vu} 0.58 R_p F_u A_{vn} \qquad \text{Eq. (6.13.5.3-2)}$$

where:

A_{vn} = net area of the connection element subject to shear (in.^{2})
F_u = tensile strength of the connection element (ksi)
R_p = reduction factor for holes taken equal to 0.90 for bolt holes punched full size and 1.0 for bolt holes drilled full size or subpunched and reamed to size (use 1.0 for splice plates since the holes in field splices are not allowed to be punched full size)
ϕ_{vu} = resistance factor for shear rupture of connection elements = 0.80 (Article 6.5.4.2)

$$R_r = 0.80(0.58)(1.0)(65)(2)\left[78.75 - 14(0.9375)\right](0.4375) = 1{,}732 \text{ kips}$$

$$R_r = 1{,}732 \text{ kips} > V_r = 508 \text{ kips} \quad \text{OK}$$

The factored shear resistance of the web, V_r, is also not to exceed the block shear rupture resistance of the web splice plates. To check the block shear rupture resistance of the web splice plates (and the factored bearing resistance of the bolt holes in Section 7.14.4.4), the bolt edge and end distances must first be established and checked.

The edge distance of bolts is defined as the distance perpendicular to the line of force between the center of a hole and the edge of the component. In this example, the edge distance from the center of the vertical line of holes in the web plate to the edge of the field piece of 2.0 in. satisfies the minimum edge distance requirement of 1⅛ in. specified for ⅞-in.-diameter bolts in Table 6.13.2.6.6-1. This distance also satisfies the maximum edge distance requirement of 8.0*t* (not to exceed 5.0 in.) = 8.0(0.4375) = 3.5 in. specified in Article 6.13.2.6.6. The edge distance for the outermost vertical row of holes on the web splice plates is set at 2.0 in. Although not done in this example, fabricators generally prefer that the edge distance on the web at the point of splice be increased a minimum of ¼ in. from the design value to allow for girder trim.

The end distance of bolts is defined as the distance along the line of force between the center of a hole and the end of the component. In this example, the end distance of 2.0 in. at the top and bottom of the web splice plates satisfies the minimum end distance requirement of 1⅛ in. specified for ⅞-

in.-diameter bolts. The maximum end distance requirement of 3.5 in. is also satisfied. Although not specifically required, note that the distance from the corner bolts to the corner of the web splice plate, equal to $\sqrt{(2.0)^2 + (2.0)^2} = 2.8\,\text{in.}$, also satisfies the maximum end distance requirement.

Block shear rupture resistance normally does not govern for typical web splice plates, but the check is illustrated here for completeness. The assumed block shear failure plane for the web splice plate is shown in **Error! Reference source not found.**25.

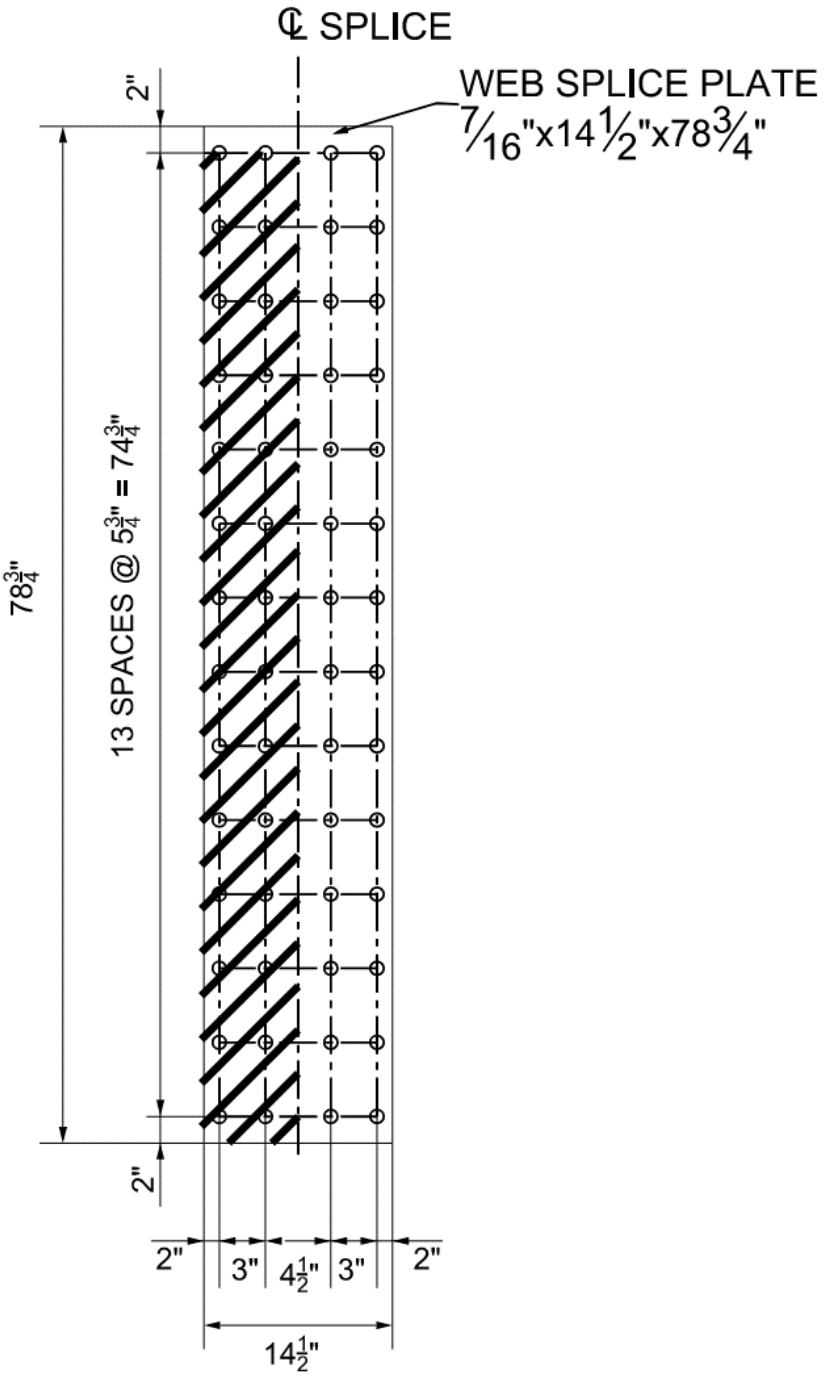

Figure 25 Assumed Block Shear Failure Planes for the Web Splice Plates

(Note: the indicated vertical distances are measured along the web slope.)

According to Article 6.13.4, the factored resistance of the combination of parallel and perpendicular planes is to be taken as:

$$R_r = \phi_{bs} R_p \left(0.58 F_u A_{vn} + U_{bs} F_u A_{tn}\right) \le \phi_{bs} R_p \left(0.58 F_y A_{vg} + U_{bs} F_u A_{tn}\right) \qquad \text{Eq. (6.13.4-1)}$$

where:

R_p = reduction factor for holes taken equal to 1.0 for bolt holes drilled full size
A_{vg} = gross area along the plane resisting shear stress (in.^{2})
A_{vn} = net area along the plane resisting shear stress (in.^{2})
U_{bs} = reduction factor for block shear rupture resistance taken equal to 1.0 when the tension stress is uniform
A_{tn} = net area along the plane resisting tension stress (in.^{2})
ϕ_{bs} = resistance factor for block shear = 0.80 (Article 6.5.4.2)

First, compute the area terms, based on the assumed block shear failure planes shown in **Error! R eference source not found.**:

$$A_{vg} = 2\left[78.75 - 2.0\right](0.4375) = 67.16 \text{ in.}^2$$

$$A_{vn} = 2\left[78.75 - 2.0 - 13.5(0.9375)\right](0.4375) = 56.08 \text{ in.}^2$$

$$A_{tn} = 2\left[3.0 + 2.0 - 1.5(0.9375)\right](0.4375) = 3.14 \text{ in.}^2$$

Compute the factored resistance as follows:

$$R_{r1} = 0.80(1.0)\left[0.58(65)(56.08) + (1.0)(65)(3.14)\right] = 1{,}855 \text{ kips}$$

$$R_{r2} = 0.80(1.0)\left[0.58(50)(67.16) + 1.0(65)(3.14)\right] = 1{,}721 \text{ kips (controls)}$$

$$R_r = 1{,}721 \text{ kips} > V_r = 508 \text{ kips} \quad \text{OK}$$

Since the combined area of the web splice plates is greater than the area of the web at the point of splice, the fatigue stresses in the base metal of the web splice plates adjacent to the slip-critical bolted connections (if subject to a net tensile stress as specified in Article 6.6.1.2.1) need not be checked. Also, the flexural stresses in the splice plates at the service limit state under the Service II load combination need not be checked.

Check that the threads are included in the shear planes as originally assumed. Refer to the discussion near the end of Section 7.14.3.4 regarding this check.

Web Splice:

7/8" diameter bolt

$L_{PLY} = 0.4375" + 0.5625" + 0.4375" = 1.4375"$

$L_{MIN} = L_{PLY} + F + T + 1.125"$ (RCSC Table C-2.2)

$= 1.4375" + 0.260" + 5/32" + 1.125" = 2.98"$

$L_{NOM} = 3.00"$ (round up to nearest $1/4"$ per RCSC 2.7 Commentary)

$L_{NOM} - F - T$

$= 3.00" - 0.260" - 5/32" = 2.58" > L = 2"$ (RCSC Table 2.5)

Therefore, bolt is not fully threaded.

$L_{B\,MIN} = L_{NOM} - L_T - Y$ (RCSC Table C-2.1)

$= 3.00" - 1.5" - 9/32" = 1.22"$

(Note: agrees with value of $L_{B\,MIN}$ from Table 2.1.9.2-1 of ASME B18.2.6)

$L_{SP} = 0.260" + 5/32" + 0.4375" + 0.5625" = 1.42" > L_{B\,MIN} = 1.22"$

Therefore, threads are *included* in the shear planes.

7.14.4.4 Bearing Resistance

Check the bearing resistance of the web splice bolt holes at the strength limit state. The assumption is that at the strength limit state, the bolts have slipped and gone into bearing. The bearing resistance of the smaller web controls in this case since the web thickness is less than the sum of the two splice plate thicknesses.

When a moment contribution from the web is required at the strength limit state (which is not the case in this example), the resultant forces causing bearing on the web bolt holes are inclined. The bearing resistance of each bolt hole in the web can conservatively be calculated in this case using the clear edge distance, as shown on the left of Figure C6.13.6.1.3c-3. This calculation is conservative since the resultant forces act in the direction of inclined distances that are larger than the clear edge distance. This calculation is also likely to be a conservative calculation for the bolt holes in the adjacent rows. Should the bearing resistance be exceeded, it is recommended that the edge distance be increased slightly in lieu of increasing the number of bolts or thickening the web. Another option would be to calculate the bearing strength based on the inclined distance or resolve the resultant force in the direction parallel to the edge distance. In cases where the bearing strength of the web splice plate controls, the smaller of the clear edge or end distance on the splice plates can be used to compute the bearing strength of the outermost hole.

For the two bolt holes at the bottom of the web splice, the clear distance, L_c, between the edge of the hole and the end of the web in the direction of the applied force is:

$$L_c = 2.825 - \frac{0.9375}{2} = 2.36 \text{ in.} > 2.0d = 2.0(0.875) = 1.75 \text{ in.}$$

Therefore, use Eq. (6.13.2.9-1):

$$R_n = 2(2.4dtF_u) = 2\left[2.4(0.875)(0.5625)(65)\right] = 154 \text{ kips}$$

Since:

$$R_r = \phi_{bb} R_n$$

$R_r = 0.80(154) = 123$ kips

The total factored shear resistance of the bolts in the two holes at the bottom of the web splice, acting in double shear, is 2(51.9) = 104 kips < 123 kips. Therefore, the factored shear resistance of the bolts controls and bearing does not control for these two bolt holes.

The center-to-center distance between the other twenty-six bolt holes in the direction of the applied force is 5¾ in. Therefore, the clear distance, L_c, between the edges of the adjacent holes is:

$$L_c = 5.75 - 0.9375 = 4.8125 \text{ in.} > 2.0d = 2.0(0.875) = 1.75 \text{ in.}$$

Therefore, use Eq. (6.13.2.9-1):

$$R_n = 26(2.4dtF_u) = 26\left[2.4(0.875)(0.5625)(65)\right] = 1{,}996 \text{ kips}$$

Since:

$$R_r = \phi_{bb} R_n$$

$R_r = 0.80(1{,}996) = 1{,}597$ kips

The total factored shear resistance of the other twenty-six bolts in the web splice is 26(51.9) = 1,349 kips < 1,597 kips. Therefore, the factored shear resistance of the bolts controls and bearing does not control for other twenty-six bolt holes.

The total factored shear resistance of the bolts in the twenty-eight holes is:

$R_r = 104 + 1{,}349 = 1{,}453$ kips > $V_r = 508$ kips ok

7.14.4.5 Slip Resistance

At a minimum, bolted connections for web splices are to be checked for slip under a web slip force taken equal to the factored shear in the web at the point of splice.

Should the moment resistance provided by the nominal slip resistance of the flange splice bolts, determined as specified in Article 6.13.6.1.3b, not be sufficient to resist the factored moment for checking slip at the point of splice (which is not the case in this example), the web splice bolts are instead to be checked for slip under a web slip force taken equal to the vector sum of the factored shear and a horizontal force in the web that provides the necessary slip resistance in conjunction with the flange splices. The horizontal force in the web is computed as the portion of the factored moment for checking slip at the point of splice that exceeds the moment resistance provided by the nominal slip resistance of the flange splice bolts divided by the appropriate moment arm (see Figure C6.13.6.1.3c-1 or C6.13.6.1.3c-2, as applicable).

The factored shear for checking slip is taken as the shear in the web at the point of splice under Load Combination Service II, as specified in Table 3.4.1-1, or the factored shear in the web at the point of splice due to the deck placement sequence as specified in Article 3.4.2.1, whichever governs. For tub girders in horizontally curved bridges (and since slip is a serviceability requirement), the shear is taken as the sum of the factored flexural and St. Venant torsional shears in the web subjected to additive shears when checking slip (Article 6.13.6.1.3c). Since the tub girder has inclined webs, the factored shear is taken as the component of the factored vertical shear in the plane of the web.

The unfactored shears at the point of splice in the web subject to additive shears are as follows (Table 16):

V_{DC1} = -17 + -69 = -86 kips
V_{DC2} = -12 kips
V_{DW} = -16 kips
V_{-LL+IM} = -85 kips
$V_{deck\ placement}$ = -61 kips

Service II Shear = 1.0(-86 + -12) + 1.0(-16) + 1.3(-85) = -225 kips

$|-225|$ kips > $V_{deck\ placement}$ = 1.25 x $|-61|$ kips = 76 kips

Although not included in this example in the interest of brevity, the special load combination specified in Article 3.4.2.1 must also be considered in this check for the deck placement sequence. Separate calculations show that this load combination also does not control for the web slip-resistance check.

The factored shear in the plane of the inclined web is computed as:

$$V_i = \frac{V}{\cos\theta} = \frac{-225}{\cos 14^\circ} = -232 \text{ kips}$$

Slip resistance of web splice w/ 28 bolts: P_t = 28(39.0 kips/bolt) = 1,092 kips > $|-232$ kips$|$ OK

8.0 SUMMARY OF DESIGN CHECKS AND PERFORMANCE RATIOS

The results for this design example at each limit state are summarized below for the maximum positive moment and maximum negative moment locations. The results for each limit state are expressed in terms of a performance ratio, defined as the ratio of the calculated value due to the applied loads to the corresponding resistance.

Maximum Positive Moment Region, Span 1 (Section G2-1)

Constructability	
Flexure (Strength I)	
Eq. (6.10.3.2.1-1) – Top Flange Yielding	0.421
Eq. (6.10.3.2.1-2) – Top Flange Local Buckling	0.328
Eq. (6.10.3.2.1-2) – Top Flange Lateral Torsional Buck.	0.345
Eq. (6.10.3.2.1-3) – Top Flange Web Bend Buckling	0.369
Eq. (6.11.3.2-3) – Bottom Flange Yielding	0.231
Service Limit State	
No checks required in this design example	
Fatigue Limit State	
Flexure (Fatigue I)	
Eq. (6.6.1.2.2-1) – Bottom Flange	0.468
Strength Limit State	
Ductility Requirement – Eq. (6.10.7.3-1)	0.332
Flexure (Strength I)	
Eq. (6.11.7.2.1-1) – Top Flange	0.502
Eq. (6.11.7.2.2-5) – Bottom Flange	0.754
Article 6.11.7.2.1 – Concrete Deck Stresses	0.413

Interior Support, Maximum Negative Moment (Section G2-2)

Constructability	
Flexure (Strength I)	
Eq. (6.10.3.2.2-1) – Top Flange Yielding	0.547
Eq. (6.11.3.2-1) – Bottom Flange Local Buckling	0.428
Shear (Strength I)	
Eq. (6.10.3.3-1)	0.348
Service Limit State (Service II)	
Web Bend-Buckling - Eq. (6.10.4.2.2-4)	0.841
Fatigue Limit State	
Flexure (Fatigue I)	
Eq. (6.6.1.2.2-1) – Top Flange	0.059

Strength Limit State

- Flexure (Strength I)
  - Eq. (6.11.8.1.2-1) – Top Flange Yielding 0.888
  - Eq. (6.11.8.1.1-1) – Bottom Flange Local Buckling 0.876
  - Eq. (C6.11.8.1.1-1) – Bottom Flange 0.849
  - Article 6.11.1.1
    - Bottom Flange cross-section distortional stresses 0.475
- Shear (Strength I) – Eq. (6.10.9.1-1) 0.639

9.0 REFERENCES

1. Coletti, D.A., Fan, Z., Holt, J., Vogel, J., Gatti, W. *Practical Steel Tub Girder Design*, National Steel Bridge Alliance (NSBA), 2005.

2. AASHTO. *LRFD Bridge Design Specifications, 9th Edition*, American Association of State Highway and Transportation Officials, Washington, DC, 2020.

3. NSBA. *Steel Bridge Design Handbook: Design Example 1: Three-Span Continuous Straight Composite Steel I-Girder Bridge.* National Steel Bridge Alliance, 2022.

4. Kulicki, J., Wassef, W., Smith, C, and Johns, K. "AASHTO-LRFD Design Example: Horizontally Curved Steel Box Girder Bridge, Final Report," National Cooperative Highway Research Project 12-52, Transportation Research Board, Washington, DC, 2005.

5. NSBA. *Steel Bridge Design Handbook: Design Example 2A: Two-Span Continuous Straight Composite Steel I-Girder Bridge.* National Steel Bridge Alliance, 2022.

6. NSBA. *Steel Bridge Design Handbook: Design Example 2B: Two-Span Continuous Straight Composite Steel Wide-Flange Beam Bridge.* National Steel Bridge Alliance, 2022.

7. NSBA. *Steel Bridge Design Handbook: Design Example 3: Three-Span Continuous Horizontally Curved Composite Steel I-Girder Bridge.* National Steel Bridge Alliance, 2022.

8. NSBA. *Steel Bridge Design Handbook: Design Example 4: Three-Span Continuous Straight Composite Steel Tub-Girder Bridge.* National Steel Bridge Alliance, 2022.

9. Wright, R.N. and Abdel-Samad, S.R. "BEF Analogy for Analysis of Box Girders," *Journal of the Structural Divisi*on, ASCE, Vol. 94, No. ST7, 1968.

10. AASHTO/NSBA. *G1.4: Guidelines for Design Details, 1st Edition*, NSBAGDD-1-OL, American Association of State Highway and Transportation Officials, Washington, DC, 2006.

11. Texas Department of Transportation (TxDOT). *Preferred Practices for Steel Bridge Design, Fabrication, and Erection*, Texas Steel Quality Council, 2009.

12. AASHTO/NSBA, *G12.1: Guidelines to Design for Constructability and Fabrication, 4th Edition*, NSBAGDC-4-OL, American Association of State Highway and Transportation Officials, Washington, DC, 2020.

13. Helwig, T., Yura, J., Herman, R., Williamson, E., and Li, D. "Design Guidelines for Trapezoidal Box Girder Systems," Report No. FHWA/TX-07/0-4307-1, Center for Transportation Research, University of Texas at Austin, 2007.

14. NSBA. *Steel Bridge Design Handbook: Bracing System Design.* National Steel Bridge Alliance, 2022.

15. NSBA. *Steel Bridge Design Handbook: Limit States.* National Steel Bridge Alliance, 2022.

16. NSBA. *Steel Bridge Design Handbook: Structural Analysis.* National Steel Bridge Alliance, 2022.

17. FHWA. *Manual for Refined Analysis in Bridge Design and Evaluation*. Federal Highway Administration, Washington, DC, 2019.

18. White, D. W., Grubb, M. A., King, C. M., and Slein, R. "Proposed AASHTO Guidelines for Bottom Flange Limits of Steel Box Girders". Final Report for NCHRP Project 20-07, Task 415, National Cooperative Highway Research Program, Transportation Research Board, Washington, DC, 2019.

19. AASHTO. *AASHTO Guide Specification for Horizontally Curved Steel Girder Highway Bridges*. American Association of State Highway and Transportation Officials, Washington, DC, 2003.

20. AASHTO/AWS. *Bridge Welding Code*, BWC-8 (AASHTO/AWS D1.5M/D1.5:2020). American Association of State Highway and Transportation Officials and American Welding Society, Washington, DC, 2020.

21. NCHRP. *National Cooperative Highway Research Project Report 883: Fracture-Critical System Analysis for Steel Bridges*. National Cooperative Highway Research Program, Transportation Research Board, Washington, DC, 2018.

22. AASHTO. *Guide Specifications for Analysis and Identification of Fracture Critical Members and System Redundant Members. 1st Edition*, American Association of State Highway and Transportation Officials, Washington, DC, 2018.

23. Connor, R. J., Korkmaz, C., Campbell, L. E., Bonachera Martin, F. J., and Lloyd, J. B. A *Simplified Approach to Design Composite Continuous Twin Tub-Girder Bridges as Redundant Structures*. Purdue University, West Lafayette, IN, 2020.

24. Fan, Z. and Helwig, T. "Behavior of Steel Box Girders with Top Flange Bracing," *Journal of Structural Engineering*, ASCE, Vol. 125, No. 8, pp. 829-837, 1999.

25. Heins, C.P. and Hall, D.H. *Designers Guide to Steel Box Girder Bridges*, Booklet No. 3500, Bethlehem Steel Corporation, contact the National Steel Bridge Alliance, Chicago, IL, 1981.

26. AISC. *Steel Construction Manual, 15th Edition*, American Institute of Steel Construction, Chicago, IL, 2017.

27. NSBA. *Bolted Field Splices for Steel Bridge Flexural Members – Overview and Design Examples*, National Steel Bridge Alliance, Chicago, IL, 2020.

28. NSBA. *Steel Bridge Design Handbook: Structural Analysis*. National Steel Bridge Alliance, 2022.

29. RCSC. *Specification for Structural Joints Using High-strength Bolts*. Research Council on Structural Connections, Chicago, IL, 2020.

30. ASME. *Fasteners for Use in Structural Applications*, ASME B18.2.6. American Society of Mechanical Engineers, New York, NY, 2019.

Smarter. Stronger. Steel.

National Steel Bridge Alliance
312.670.2400 | aisc.org/nsba

B956-22